

Energy Levels of Light Nuclei ($Z=11$ to $Z=20$). II.

P. M. ENDT, *Fysisch Laboratorium der Rijksuniversiteit, Utrecht, Netherlands*

AND

C. M. BRAAMS, *Stichting voor Fundamenteel Onderzoek der Materie, Utrecht, Netherlands*

INTRODUCTION

THE present compilation is a modernized version of the paper on the same subject¹ which appeared in 1954. It contains the experimental material published in the period from December 1, 1953, up to about February 1, 1957, and together with En 54a provides a fairly complete bibliography for the years prior to 1957. In a few cases, reference was made to papers which appeared after February 1, 1957, either because the authors had sent preprints, or because the importance of the paper made it desirable to add a note in the proof.

Presentation of some subjects which were treated in more detail in En 54a has been shortened. Little attention is given to cross-section measurements. For neutron cross sections the reader is referred to the compilation by Hughes and Harvey.² Many-particle reactions, as ($n,2n$) or spallation reactions, are omitted altogether. Theoretical papers are quoted only briefly, and the bibliography is certainly incomplete on theoretical subjects.

The situation regarding nuclear masses has much improved since the appearance of the 1954 review because of the accurate mass-spectroscopic measurement of the S^{32} mass by Quisenberry, Scolman, and Nier,³ and of the recent extension of Q -value chains into the $A > 32$ region,⁴ connecting nuclides up to $A = 45$ to S^{32} through precision Q -value measurements. In Table LXV the masses are listed which were used to compute the Q_m values quoted after the heading of each specific reaction. The procedure followed in arriving at the values listed, is outlined in the text preceding the table.

Rules adopted for construction of the level diagrams and the systematics of arrangement of the material in the text are not significantly different from those in En 54a.

(a) Levels known with an accuracy of 15 kev or better, and found preferably from two or more reactions, are marked by heavy lines, doubtful levels by broken lines. Three-decimal figures are reserved for levels known with an accuracy of 5 kev or better.

(b) Resonance energies indicated in the level diagrams are given in the laboratory system.

¹ P. M. Endt and J. C. Kluyver, Revs. Modern Phys. **26**, 95 (1954) (quoted as En 54a).

² D. J. Hughes and J. A. Harvey, "Neutron cross sections," Brookhaven National Laboratory BNL 325 (1955).

³ Quisenberry, Scolman, and Nier, Phys. Rev. **102**, 1071 (1956).

⁴ Endt, Buechner, Braams, Paris, and Sperduto, Phys. Rev. **106**, 764 (1957).

(c) Nuclides are presented in order of increasing A , and nuclides of the same A in order of increasing Z .

(d) Generally each nuclear reaction is treated under the heading of the final nucleus, exceptions are reactions where resonances are observed, which are treated under the compound nucleus, and the β decay of unstable nuclei, treated under the parent nucleus, and then as the first reaction. The order of the other reactions is determined by the initial nucleus starting with the lowest- Z element and within that element with the lowest- A isotope.

ACKNOWLEDGMENT

We are particularly grateful to the many physicists who sent results before publication.

Na²⁰

(not illustrated)

I. Na²⁰(β^+)Ne²⁰ $Q_m = 15.3^*$

Positron decay proceeds at least partly to states of Ne²⁰ between 6.8 and 10.8 Mev which decay by α emission. Half-life, 0.25 sec, as measured by α detection (Al 50a), and 0.23 ± 0.08 sec as measured by β^+ detection (Sh 51b). Another value, 0.385 ± 0.01 sec, is reported (Aj 52). Energy of α 's is > 2 Mev (Al 50a).

Theoretical prediction of Na²⁰ spin, De 53a.

Discussion of possibility that positron decay is super-allowed, Bo 55.

II. Ne²⁰(p,n)Na²⁰ $Q_m = -16.1$

Threshold 16.9 Mev, Al 50a.

Na²¹

(Fig. 1)

I. Na²¹(β^+)Ne²¹ $Q_m = 3.52$

Half-life, 23 ± 2 sec (Cr 40) and 22.8 ± 0.5 sec (Sc 52); also Bo 53. The β^+ end point is 2.50 ± 0.03 Mev determined with a 180° spectrometer (Sc 52); also Bo 53. A γ ray reported (Po 40), but recent work shows no γ ray of $E_\gamma > 0.5$ Mev (Sc 52). Log $ft = 3.6$, confirming that spin of Na²¹ is same as that of mirror nucleus Ne²¹, namely $3/2^+$.

* For each reaction the Q value calculated from the masses is designated Q_m .

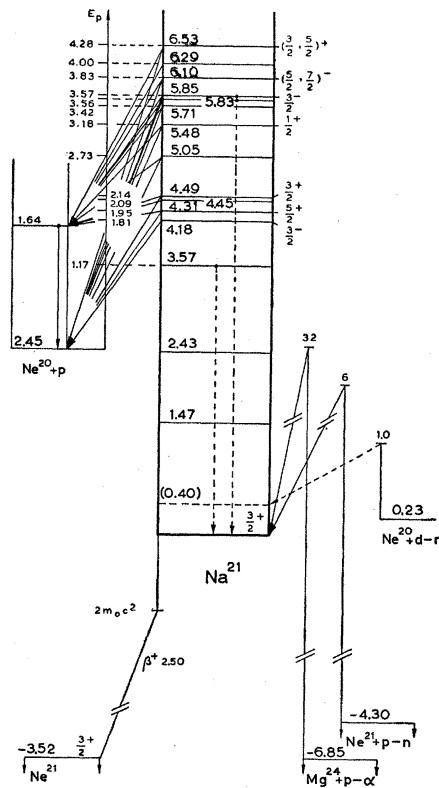


FIG. 1.

II. $\text{Ne}^{20}(\rho, \gamma)\text{Na}^{21}$ $Q_m = 2.45$

Weak resonance at $E_p = 1.165$ Mev found in γ -ray yield for protons in 0.5–1.3-Mev region bombarding a thin isotopic Ne^{20} target, (Br 47). This corresponds to level in Na^{21} at 3.57 Mev. For protons in 1.35–4.4-Mev region, resonances for production of annihilation radiation from Na^{21} decay found at $E_p = 2.15$, (3.45), 3.56, and 3.57 Mev (Co 54b, Va 53).

III. $\text{Ne}^{20}(\rho, \rho)\text{Ne}^{20}$ $E_b = 2.45$
 $\text{Ne}^{20}(\rho, \rho' \gamma)\text{Ne}^{20}$ $E_b = 2.45$ $E_x = 1.63$

Yield of elastically scattered protons measured at six angles from 90° to 167.5° . Energies, widths, spins, and parities as determined by phase-shift analysis in Table I (Ha 53, Ha 55a).

Resonances for inelastic proton scattering leading to 1.63 Mev level of Ne^{20} generally correspond to those for elastic scattering; resonances at $E_p = 2.09$ and 4.00 Mev, found from inelastic scattering only. Cross sections and angular distributions of inelastically scattered protons and 1.63-Mev γ radiation (Ga 53, Co 54b).

IV. $\text{Ne}^{20}(d, n)\text{Na}^{21}$ $Q_m = 0.23$

Slow-neutron thresholds indicate Q values of -1.24 ± 0.02 and -2.201 ± 0.007 Mev, corresponding to levels at 1.47 and 2.43 Mev (Ma 56b). At $E_d = 1.0$ Mev, recoil protons in nuclear emulsions indicate $Q = -0.17 \pm 0.05$ Mev (Sw 52), corresponding to a level at 0.40 Mev.

TABLE I. Resonances in $\text{Ne}^{20} + p$

E_p (Lab) (Mev)	E_z (Mev)	decay \circ	Γ (kev)	J, π
1.165 ^a	3.57	γ^a		
1.81 ^d	4.18	p_0^d	180 ^d	$3/2^-d$
1.953 ^d	4.31	$p_0^d p_1^b$	6 ^d	$5/2^+d$
2.09 ^b	4.45	p_1^b		
2.135 ^d	4.49	$\gamma^o p_0^d p_1^b$	17 ^d	$3/2^+d$
2.73 ^b	5.05	$p_0^d p_1^b$	double ^d	
3.176 ^d	5.48	$p_0^d p_1^b$	110 ^d	$1/2^+d$
3.42 ^d	5.71	$p_0^d p_1^b$	$\approx 20^d$	
3.552 ^d	5.83	$\gamma^o p_0^d p_1^b$	$\approx 2^d$	
3.566 ^d	5.85	$\gamma^o p_0^d p_1^b$	25 ^d	
3.828 ^d	6.10	$p_0^d p_1^b$	6 ^d	$(5/2, 7/2)^{-d}$
4.00 ^b	6.29	p_1^b		
4.28 ^d	6.53	$p_0^d p_1^b$	150 ^d	$(3/2, 5/2)^{+d}$

^a Br 47. ^b Co 54b, ^c Va 53, ^d Ha 55a. ^e Resonances in yield of capture γ rays or in yield of Na^{21} activity indicated by γ , resonances for elastic scattering, by p_0^d , and resonances in yield of 1.63 Mev γ ray from first excited state of Ne^{20} , by p_1^b .

V. $\text{Ne}^{21}(\rho, n)\text{Na}^{21}$ $Q_m = -4.30$

Observed, En 54a.

VI. $\text{Mg}^{24}(\rho, \alpha)\text{Na}^{21}$ $Q_m = -6.85$

Observed, En 54a.

 Na^{22}

(Fig. 2)

I. $\text{Na}^{22}(\beta^+) \text{Ne}^{22}$ $Q_m = 2.840$

Most accurate measurement of half-life yields 2.58 ± 0.03 yr (Me 57). Also En 54a.

Decay proceeds predominantly by β^+ emission followed by a γ ray. Best magnetic spectrometer determinations of the β^+ end point are 542 ± 5 kev (Ma 50a) and 540 ± 5 kev (Wr 53), and of γ -ray energy, 1.277 ± 0.004 Mev (Al 49). Also En 54a.

Ground-state β^+ transition very weak. End point of this high-energy β^+ spectrum is 1.83 ± 0.06 Mev and intensity is (0.062 ± 0.015) percent (Wr 53). Log $ft = 13.1$. Also Mo 49.

Electron capture also occurs. Most accurate measurements yield: $EC/\beta^+ = (11.0 \pm 0.6) \times 10^{-2}$ (Sh 54b), $(12.3 \pm 1.0) \times 10^{-2}$ (Kr 54) and $(12.2 \pm 1.0) \times 10^{-2}$ (Al 55). Also Ho 53b, Ma 54c, Se 54, Ch 55, Di 55. Theory, with screening taking into account, yields 11.1×10^{-2} (Zw 54).

Internal conversion coefficient of 1.28-Mev γ ray measured as $(6.7 \pm 0.7) \times 10^{-6}$, compares with theoretical value for an E2 transition of 6.59×10^{-6} (Le 54). Spin of 1.28-Mev level in Ne^{22} is then 2^+ . Spin of Na^{22} being $J = 3$ (Ma 50), with almost certainly even parity, predominant β^+ branch is allowed in agreement with spectrum shape (Ma 50a, Al 50b, Wo 54). Log $ft = 7.6$. Allowed character confirmed by absence of β - γ angular correlation (St 51a).

Theoretical discussion of Na^{22} ground-state spin, De 53a.

II. $F^{19}(\alpha, n)Na^{22}$ $Q_m = -1.928$

With α particles from an electrostatic generator, thresholds in neutron production observed at $E_\alpha = 2.33$ and 3.04 Mev. At $E_\alpha > 3.04$ Mev a γ ray observed of $E_\gamma = 592 \pm 3$ kev, measured with a scintillation spectrometer. Half-life of corresponding Na^{22} level is < 0.01 sec (He 54b).

Threshold, $E_\alpha = 2.486$ Mev (Bu 56c) but corresponding Q (-2.061 Mev) would be in definite disagreement with Q from masses.

From threshold measurements and from neutron energy measurements with a proton recoil proportional counter, ground-state $Q = -2.0 \pm 0.2$ Mev and Na^{22} levels found at 0.45, 1.15, (1.8), 2.25, and 3.0 Mev, all ± 0.2 Mev (Qu 56).

Resonances, see Na^{23} .

III. $Ne^{20}(d, p)Ne^{21}$ $E_b = 11.274$ $Q_m = 4.532$

Resonances observed corresponding to Na^{22} levels at 12.07 and 12.13 Mev (Go 55).

IV. $Ne^{21}(p, \gamma)Na^{22}$ $Q_m = 6.742$

One resonance in γ -ray yield from a thin enriched Ne^{21} target bombarded with 0.6–1.3-Mev protons observed at $E_p = 765$ kev (Br 47) corresponding to a Na^{22} level at 7.472 Mev.

V. $Ne^{21}(d, n)Na^{22}$ $Q_m = 4.517$

Observed, En 54a.

VI. $Ne^{22}(p, n)Na^{22}$ $Q_m = -3.623$

Not observed.

VII. $Mg^{22}(\beta^+)Na^{22}$. See Mg^{22} VIII. $Na^{23}(\gamma, n)Na^{22}$ $Q_m = -12.416$

Threshold measurements and yield curves, En 54a. Search for isomeric states in Na^{22} with half-lives in 10^{-5} sec– 10^{-1} sec region unsuccessful (Ve 56).

IX. $Mg^{24}(d, \alpha)Na^{22}$ $Q_m = 1.967$

Thin natural magnesium targets bombarded with 5-, 6-, and 7-Mev deuterons. From magnetic analysis ($\theta = 90^\circ$), the ground-state $Q = 1.953 \pm 0.012$ Mev. Excited states at 0.585, 0.893, 1.535, 1.944, 1.990, 2.222, 2.579, 2.977, 3.067, and (3.525) Mev, all ± 0.006 Mev. Upper limit of 3% of ground-state group given for intensity of any group which was not observed at $E_d = 7$ Mev. Observed states should have $T=0$ from isobaric spin selection arguments (Br 55, Br 55a).

Also En 54a.

X. $Mg^{25}(p, \alpha)Na^{22}$ $Q_m = -3.140$

Enriched magnesium targets bombarded with protons from a 8-Mev electrostatic generator. From magnetic

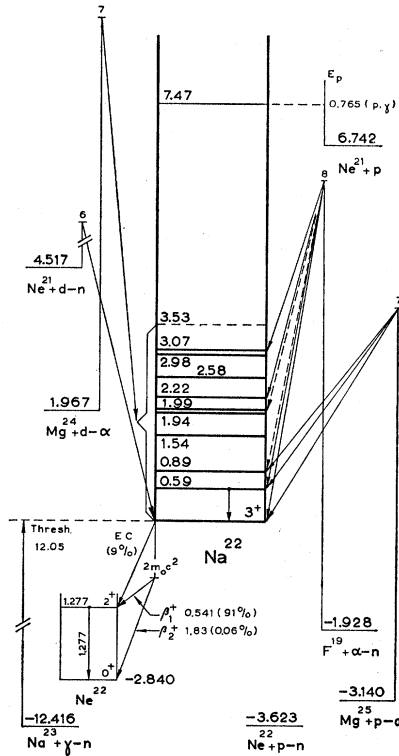


FIG. 2.

analysis ground-state $Q = -3.15$ Mev. Transitions observed to 0.59- and 0.89-Mev levels and some evidence for a level between those two (Br 55a).

Also Ba 54, Co 54a.

GENERAL REMARKS

The 0.59-Mev level probably not the $J=0^+$ $T=1$ level, expected at about 0.6 Mev (St 53b, St 53a, Mo 54, He 54b, Ta 54, Wi 56a), since this level is found from the $Mg^{24}(d, \alpha)Na^{22}$ reaction. The $T=1$ level may have been observed from the $Mg^{25}(p, \alpha)Na^{22}$ reaction.

Theoretical discussion of Na^{22} ground-state spin, Hi 54.

Mg²²

(not illustrated)

A 0.13-sec half-life observed from bombardment of natural magnesium with 23-Mev protons. This might be assigned either to Mg^{22} or to Al^{23} (Ty 54).

Na²³

(Fig. 3)

- I. (a) $F^{19}(\alpha, n)Na^{22}$ $E_b = 10.488$ $Q_m = -1.928$
- (b) $F^{19}(\alpha, n\gamma)Na^{22}$ $E_b = 10.448$ $E_x = 0.592$
- (c) $F^{19}(\alpha, p)Ne^{22}$ $E_b = 10.448$ $Q_m = 1.695$
- (d) $F^{19}(\alpha, p\gamma)Ne^{22}$ $E_b = 10.448$ $E_x = 1.277$
- (e) $F^{19}(\alpha, \alpha)F^{19}$ $E_b = 10.448$
- (f) $F^{19}(\alpha, \alpha\gamma)F^{19}$ $E_b = 10.448$ $E_x = 0.110$ and 0.197

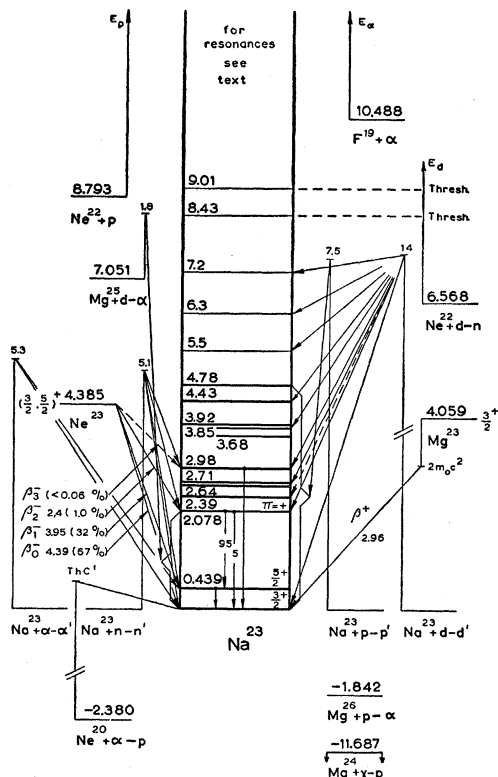


FIG. 3.

Yield of 592-kev radiation from reaction (b), of 1.28-Mev radiation from reaction (d), and of 110- and 197-kev radiation from reaction (f) measured in $E_\alpha=1.0\text{--}3.5\text{-Mev}$ region. Relative yields are given at 18 resonances, all above 1.4 Mev (He 54b). Reactions (d) and (f) explored with better resolution in the $E_\alpha=0.6\text{--}2.8\text{-Mev}$ region, yielding 26 resonances, all above 1.3 Mev (Sh 54e). Yield of reaction (f) at low E_α in agreement with Coulomb excitation theory for E2 excitation (He 54b, Sh 54c, Jo 54). Also, En 54a.

II. $\text{Ne}^{20}(\alpha, p)\text{Na}^{23}$ $Q_m=-2.380$

En 54a. Resonances, Mg^{24} .

- III. (a) $\text{Ne}^{22}(\rho, \gamma)\text{Na}^{23}$ $E_b=8.793$
- (b) $\text{Ne}^{22}(\rho, p)\text{Ne}^{22}$ $E_b=8.793$
- (c) $\text{Ne}^{22}(\rho, p'\gamma)\text{Ne}^{22}$ $E_b=8.793$

Resonances, En 54a.

IV. $\text{Ne}^{22}(d, n)\text{Na}^{23}$ $Q_m=6.568$

Two slow-neutron thresholds observed from deuteron bombardment of natural neon with $Q=-1.866\pm 0.010$ and -2.443 ± 0.015 Mev, corresponding to Na^{23} levels at $E_x=8.434\pm 0.021$ and 9.012 ± 0.024 Mev (Ma 56b). Assignment based on observed intensities.

Also Fr 55.

V. $\text{Ne}^{23}(\beta^-)\text{Na}^{23}$ $Q_m=4.385$

Half-life, 40.2 ± 0.4 sec (Br 50) and 37.6 ± 0.1 sec (Pe 57). Also En 54a, Ha 51a. Decay is complex. End point of ground-state transition ($67\pm 3\%$ intensity) measured by scintillation spectrometer as 4.39 ± 0.05 Mev (Pe 57), in much better agreement with Q_m than a former magnetic spectrometer measurement (En 54a). A $32\pm 3\%$ branch with an end point of 3.95 ± 0.05 Mev is in coincidence with 436 ± 4 -kev γ rays, and a $1.00\pm 0.15\%$ branch with 2.4 ± 0.1 -Mev end point is in coincidence with 1.647 ± 0.016 -Mev γ rays. The two γ rays are also coincident, and have intensities of $100:(3.0\pm 0.3)$. Higher energy γ rays present but have at most an intensity of 0.2% per disintegration. Beta transitions to three lowest Na^{23} states are evidently allowed with $\log ft=5.25, 5.38$, and 5.88 (Pe 57). No superallowed branch occurs in Ne^{23} decay as formerly believed (Ki 55, Fe 55).

Results mentioned in the foregoing confirmed in Ge 55, Ge 56. End point of ground-state beta transition, 3.9 ± 0.3 Mev, lowest-energy γ ray, 440 ± 5 kev. A 3.0-Mev γ ray may be present but intensity relative to 440-kev γ ray is $< 1\%$. Also Go 56.

Allowed character of beta transitions to $3/2^+$ Na^{23} ground state and $5/2^+$ first excited state limit Ne^{23} spin to $3/2^+$ or $5/2^+$. Same possibilities follow from a $\text{Ne}^{22}(d, p)\text{Ne}^{23}$ angular distribution measurement (Bu 56d).

VI. $\text{Na}^{23}(n, n')\text{Na}^{23}$

In $E_n=440\text{--}800$ -kev region, cross section for production of 0.44-Mev γ ray shows resonances at 542, 602, 633, 710, and 780 kev. The γ -ray angular distribution isotropic at 602- and 710-kev resonances, but anisotropic at 633 and 780 kev (Ha 56). At $E_n=2.5$ Mev, γ rays observed of 0.45 ± 0.01 , 1.69 ± 0.03 , and 2.2 ± 0.1 Mev (Wo 56). At $E_n=5.1$ Mev, γ rays reported of 0.439, 0.650, 1.63, 2.07, and 3.01 Mev (Mo 56c). The 0.650-Mev γ ray cannot easily be fitted into the Na^{23} level scheme. Also Cr 56a.

VII. (a) $\text{Na}^{23}(\rho, p')\text{Na}^{23}$

- (b) $\text{Na}^{23}(\rho, p'\gamma)\text{Na}^{23}$

From magnetic analysis at several proton energies in the 7.0–7.5-Mev region and at several different angles, levels in Na^{23} observed at 0.440 ± 0.003 , 2.078 ± 0.004 , 2.393 ± 0.007 , 2.641 ± 0.007 , 2.705 ± 0.007 , 2.983 ± 0.007 , 3.678 ± 0.007 , 3.850 ± 0.008 , 3.915 ± 0.010 , 4.431 ± 0.010 , and 4.778 ± 0.010 Mev (Bu 57). Another value for first level, by magnetic analysis, is 437 ± 5 kev (Sc 56c). Most accurate determination of this level, from electrostatic analysis, is 439 ± 1 kev (Do 53). Also En 54a.

The 0.44-Mev γ -ray transition investigated extensively at $E_p=1.29$ -Mev resonance. Internal conversion coefficient measured as $(4.9\pm 0.6)\times 10^{-5}$ in agreement with theory for M1 or E1 (Be 56a). Using both

$\text{Na}^{23}(p, p'\gamma)$ and $\text{Na}^{23}(\alpha, \alpha'\gamma)$ reactions, half-life of 0.44-Mev level determined with recoil techniques as between 10^{-13} and 10^{-12} sec (Kr 56). Also Sw 56. Gamma-ray angular distribution measurements at 1.29- and 1.46-Mev resonances limit spin of 0.44-Mev level to $5/2^+$ or $3/2^+$ (Re 56b, Be 56a).

Even parity of this level follows also from measurement of ratio of γ -ray yield from $\text{Na}^{23}(p, p'\gamma)$ and $\text{Na}^{23}(\alpha, \alpha'\gamma)$ reactions which is explained by E2 Coulomb excitation. From yield, partial half-life for E2 decay is computed as 3.0×10^{-10} sec (Te 56).

Second level in Na^{23} is fed at the $E_p = 2.89$ -Mev resonance. This level de-excites both to level (1) and to ground state, branching ratio of about 20. Ground-state transition is anisotropic, excluding $J = 1/2$ for level (2) (Go 57b).

Other $\text{Na}^{23} + p$ resonances under Mg^{24} .

VIII. $\text{Na}^{23}(d, d')\text{Na}^{23}$

At $E_d = 14$ Mev, levels in Na^{23} found at 1.9, 2.6, 3.75, 4.45, 5.5, 6.3, and 7.2 Mev (Bo 50). Also Ha 54b, El 56a. At $E_d = 8$ Mev, groups proceeding to levels at 2.08, 2.71, and 3.85 Mev all show angular distributions compatible with $l_d = 2$, which would determine parity of these levels as even (El 56a).

IX. $\text{Na}^{23}(\alpha, \alpha')\text{Na}^{23}$

A 0.44-Mev γ ray observed (Te 54, Te 56, Kr 56). Half-life, quoted under reaction VII, Kr 56. The γ -ray angular distribution measured at $E_\alpha = 2.5$ Mev is only compatible with $J = 5/2^+$ for level (1) (Te 56).

X. $\text{Na}^{23}(\text{N}^{14}, \text{N}^{14'}\gamma)\text{Na}^{23}$

A 435-kev γ ray observed resulting from Coulomb excitation by 15.6-Mev triply charged N^{14} ions (Al 56).

XI. $\text{Mg}^{23}(\beta^+)\text{Na}^{23}$ See Mg^{23}

XII. $\text{Mg}^{24}(\gamma, p)\text{Na}^{23}$ $Q_m = -11.687$

Cross section, Jo 55, Mo 55.

XIII. $\text{Mg}^{25}(d, \alpha)\text{Na}^{23}$ $Q_m = 7.051$

Ground-state Q value, measured by magnetic analysis as 7.019 ± 0.013 Mev, differs from value computed from other links between Na^{23} and Mg^{25} . The Na^{23} levels at 0.44 and 2.08 Mev observed from this reaction (En 52).

XIV. $\text{Mg}^{26}(p, \alpha)\text{Na}^{23}$ $Q_m = -1.842$

Not observed.

Mg²³

(not illustrated)

I. $\text{Mg}^{23}(\beta^+)\text{Na}^{23}$ $Q_m = 4.059$

Half-life, averaged from older determinations (En 54a) and from a more recent one (10.7 ± 0.7 sec; Hu 54), 11.9 ± 0.2 sec.

The β^+ end point = 2.82 Mev with a cloud chamber (Wh 39), 2.99 ± 0.09 Mev (Bo 51), and 2.95 ± 0.07 Mev (Hu 54) with a scintillation spectrometer. No γ rays observed. Decay is superallowed ($\log ft = 3.7$), determining Mg^{23} spin and parity as $3/2^+$.

II. $\text{Ne}^{20}(\alpha, n)\text{Mg}^{23}$ $Q_m = -7.222$

Not observed.

III. $\text{Na}^{23}(p, n)\text{Mg}^{23}$ $Q_m = -4.841$

Revision of generator calibration changed old value for threshold ($E_p = 5.091 \pm 0.010$ Mev; Wi 52) to 5.053 ± 0.010 Mev (Ki 55a).

Resonances under Mg^{24} .

IV. $\text{Mg}^{24}(\gamma, n)\text{Mg}^{23}$ $Q_m = -16.529$

Threshold and yield, En 54a, Ka 54, Na 55, Mo 55, Ye 56.

Al²³

(not illustrated)

Half-life of 0.13 sec observed from bombardment of natural magnesium with 23-Mev protons. This might be assigned to either Al^{23} or Mg^{22} (Ty 54).

Na²⁴

(Fig. 4)

I. (a) $\text{Na}^{24}(\beta^-)\text{Mg}^{24}$ $Q_m = 5.514$

Half-life, averaged from six older determinations (En 54a) and from a more recent measurement (14.90 ± 0.05 hr; To 55c), 15.00 ± 0.02 hr.

Decay scheme of Na^{24} investigated very thoroughly. The β^- decay goes predominantly to 4.12-Mev level of Mg^{24} followed by two γ rays in cascade through 1.37-Mev level. Accurate measurement of the β^- end point: 1.390 ± 0.005 Mev (Si 46). Best magnetic spectrometer determination of γ -ray energies is 2.7535 ± 0.0010 and 1.2680 ± 0.0010 Mev (He 52). Also En 54a. Log ft (for main β^- transition) 6.1.

Experimental material leading to an assignment of spins 0^+ , 2^+ , and 4^+ to Mg^{24} ground state and levels at 1.37 and 4.12 Mev, respectively, and of spin 4^+ to Na^{24} ground state, En 54a.

Ultra-fast delayed $\beta-\gamma$ coincidence measurement of half-life of 1.37-Mev level, yielding $(2.5 \pm 1.7) \times 10^{-11}$ sec, confirmed E2 character of 1.37-Mev transition (Co 55c).

A weak high-energy β^- component, proceeding to 1.37-Mev level, also found, with end point of 4.17 Mev and intensity of 0.003% ($\log ft = 12.7$) (Tu 51). Also Gr 50a.

A 4.12-Mev crossover γ ray not definitely established (En 54a).

From $\text{Na}^{23}(p, \gamma)\text{Mg}^{24}$ measurements, a $J = 3$ level at 5.23 ± 0.04 Mev found in Mg^{24} , de-exciting to 1.37 Mev

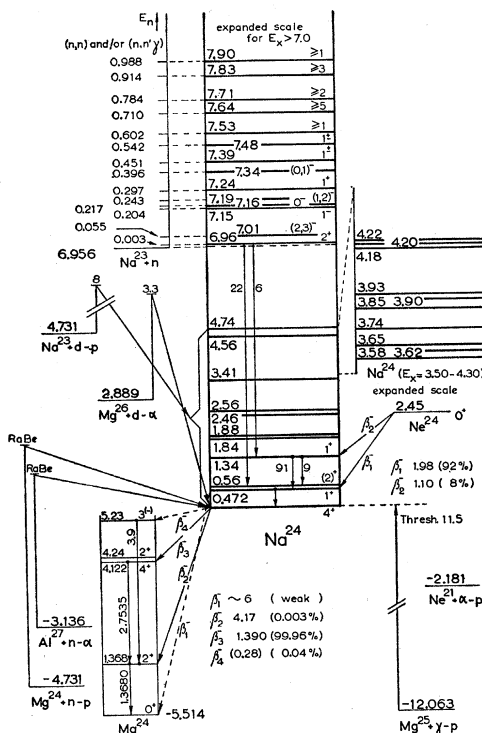


FIG. 4.

level with a 3.86 ± 0.04 Mev γ ray (Ne 54a). This level is probably also fed in $\text{Na}^{24}(\beta^-)\text{Mg}^{24}$ decay. A γ ray of 3.62 ± 0.05 Mev and intensity 0.04% has been reported (Be 51), while others report γ rays of 3.9 and 5.3 Mev (To 55b). Existence of the latter γ seems doubtful as its octupole character would exclude competition with 3.9-Mev dipole transition.

Log $ft = 7.1$ of β^- decay to 5.23-Mev level points to a once-forbidden transition, yielding odd parity for 5.23-Mev level.

Theoretical discussion of Na^{24} spin, De 53a, Hi 54, Sc 54c.

(b) $\text{Na}^{24m}(\beta^-)\text{Mg}^{24}$ See $\text{Ne}^{24}(\beta^-)\text{Na}^{24}$ (reaction VII).

II. $\text{Ne}^{21}(\alpha,p)\text{Na}^{24}$ $Q_m = -2.181$

Not observed.

III. $\text{Ne}^{22}(d,\gamma)\text{Na}^{24}$ $Q_m = 13.424$

Not observed (Al 55b).

IV. $\text{Na}^{23}(n,\gamma)\text{Na}^{24}$ $Q_m = 6.956$

Cross-section measurements, Hu 55c, La 57.

Energies and intensities of thermal neutron capture γ rays determined by magnetic Compton spectrometer (Gr 55a), by magnetic pair spectrometer (Ki 51), with a two-crystal scintillation spectrometer (Br 56e) and with a magnetic lens spectrometer (Mo 56a) in Table II. Also Mi 50a. The 6.96-Mev ground-state transition

not observed; its intensity is smaller than 0.1 per 100 captures (Gr 55a).

The intense γ ray A feeds the 0.56-Mev level, de-excited through the 0.472-Mev level by cascade $Z-Y$. Notable is absence of a 0.56-Mev γ ray. Upper limit for intensity is 3 per 100 captures (Gr 55a).

Few of the γ rays in Table II can be fitted in Na^{24} level scheme with certainty. For γ rays A , Y , and Z see above. Gamma-ray B feeds the 1.34-Mev level, which is de-excited by V to 0.47-Mev level, and probably by W to 0.56-Mev level. The 1.34-Mev level is not de-excited by U to Na^{24} ground state as this would conflict with the spin assignments found from the $\text{Ne}^{24}(\beta^-)\text{Na}^{24}$ decay (reaction VII). The γ rays N and P might feed the 1.34-Mev level from 3.85- and 3.58-Mev levels, respectively (Mo 56a).

IV. $\text{Na}^{23}(n,n)\text{Na}^{23}$ $E_b = 6.956$

Cross sections and resonances, Hu 55c. Sharp resolved resonances at $E_n = 2.9$ kev ($J = 2^+$), 55 kev (3^- or 2^- ; Bl 56, Cr 57), 204 kev (1^-), 217 kev (0^-), 243 kev (1^- or 2^-), 297 kev (1^+), 396 kev (0^- or 1^-), 451 kev (1^+ or 1^-), 542 kev (1^+), 602 kev (≥ 1), 710 kev (≥ 5), 784 kev (≥ 2), 914 kev (≥ 3), and 988 kev (≥ 1). Also Po 54, Pa 55, Jo 55a, To 55a, La 56.

γ rays from inelastic scattering under Na^{23} .

TABLE II. Thermal neutron capture γ rays from sodium (intensities in photons per 100 captures).

γ ray	Gr 55a		Ki 51		Mo 56a	
	Energy (Mev)	Intensity	Energy (Mev)	Intensity	Energy (Mev)	Intensity
A	6.40 ± 0.03	22	6.41 ± 0.03	20		
B	5.61 ± 0.03	6	5.61 ± 0.03	7.5		
B'	(5.30 ± 0.05)	0.3				
C	(5.12 ± 0.05)	0.8	5.13 ± 0.03	1.8		
C'	(4.90 ± 0.05)	1.2				
C''	(4.70 ± 0.05)	0.9				
D	4.50 ± 0.04	2.1				
D'	(4.30 ± 0.05)	0.5				
E	4.18 ± 0.04	2.1				
F	3.98 ± 0.04	17.2	3.96 ± 0.03	20		
G	3.86 ± 0.04	5.9	3.85 ± 0.03	11		
G'	(3.68 ± 0.05)	1.3				
H	3.60 ± 0.03	18	3.60 ± 0.03	10	3.590 ± 0.025	18
I	3.56 ± 0.03		3.56 ± 0.03	20		
J	3.30 ± 0.02	5				
K	3.08 ± 0.02	9.5				
L	2.84 ± 0.02	7				
M	2.68 ± 0.02	8.5				
N	2.52 ± 0.02	21	2.53 ± 0.03	19	2.510 ± 0.020	~ 15
O	2.41 ± 0.03	10.5				
P	2.21 ± 0.03	7.5			2.210 ± 0.015	8
Q	2.02 ± 0.015	11.5	2.02 ± 0.03	12	2.030 ± 0.010	13
R	(1.95 ± 0.03)	4				
S	(1.87 ± 0.03)	5.5			1.900 ± 0.020	~ 3
T	1.66 ± 0.01	7.5	1.66 ± 0.05	5	1.630 ± 0.008	10
U	1.35 ± 0.01	6.5	1.35 ± 0.03	6		
V	0.86 ± 0.01	44	0.86 ± 0.02	34	0.877 ± 0.005	30 ± 10
W	0.79 ± 0.015	4.3				
X	(0.71 ± 0.015)	5				
Y	0.47 ± 0.015	74	0.48 ± 0.02	60	0.473 ± 0.004	50 ± 10
Z					0.090^a	

^a Observed with a scintillation spectrometer (Mo 56a).

V. $\text{Na}^{23}(n,p)\text{Ne}^{23}$ $E_b=6.956$ $Q_m=-3.603$

Cross section from threshold to $E_n=6.0$ Mev; resonances observed corresponding to Na^{24} levels at $E_x=11.93$ and 12.33 Mev (Bo 57a).

VI. $\text{Na}^{23}(d,p)\text{Na}^{24}$ $Q_m=4.731$

Ground-state Q measured by magnetic analysis $=4.731 \pm 0.007$ Mev (Sp 52) and 4.723 ± 0.008 Mev (Mi 52). Eighteen levels in Na^{24} found by high-resolution magnetic analysis at $\theta=90^\circ$ and at deuteron energies between 1.5 and 2.2 Mev (Sp 52) in Table III. Also En 54a, El 56a.

The l_n values found by comparison with stripping theory in Table III. Brackets indicate unresolved groups.

VII. $\text{Ne}^{24}(\beta^-)\text{Na}^{24}$ $Q_m=2.45$

New radioactive nuclide Ne^{24} recently produced (Dr 56) from $\text{Ne}^{22}(t,p)\text{Ne}^{24}$ reaction. Half-life, 3.38 ± 0.02 min.

Two (noncoincident) γ rays observed with a scintillation spectrometer with following energies and relative intensities: γ_1 , 472 ± 5 kev (100); γ_2 , 878 ± 9 kev (8 ± 2). Upper limit of 0.5% given for potential 92- and 564-kev γ rays, and of 1% for a 785-kev γ ray. Two β^- ray branches found with a plastic scintillator with following end points and relative intensities: β_1^- , 1.98 ± 0.05 Mev (92 ± 2), β_2^- , 1.10 ± 0.05 Mev (8 ± 2). The β_1^- branch not in coincidence with γ rays, the β_2^- branch coincident with γ_2 . Both β^- transitions are allowed ($\log ft=4.4$ for both) and have linear Fermi plots. A weak β^- branch with ~ 6 -Mev end point also may be present.

The 472-kev level in Na^{24} is isomeric. From decay of γ_1 , half-life estimated as 20^{+30}_{-15} msec. This explains absence of coincidences of γ_1 with γ_2 or with β^- particles. The weak high-energy β^- branch may be explained as a transition from isomeric state to Mg^{24} ground state.

Observed half-life of 472-kev transition uniquely establishes it as octupole. Spin of 472-kev level must then be $J=1^+$, because of allowed character of β^- transition to this level. Also 1.34-Mev level has $J=1^+$; from allowed character of corresponding β^- transition follows $J=0^+$ or 1^+ , while $\text{Na}^{23}(d,p)\text{Na}^{24}$ angular distribution measurements (see Reaction VI) lead to $J=1^+$ or 2^+ .

That the 0.56-Mev level is not fed in the $\text{Ne}^{24}\beta^-$ decay may be explained by spin assignments of $J=0^+$ or $J \geq 2$. A $0^+ \rightarrow 0^+$ β^- transition would be forbidden by isobaric spin selection rule. Spin 1^+ or 2^+ follows from $\text{Na}^{23}(d,p)\text{Na}^{24}$ angular distribution measurements (see Reaction VI). The 0.56-Mev level then has most likely $J=2^+$, in agreement with fact that no 0.56-Mev γ ray is observed (also Reaction III).

TABLE III. Levels in Na^{24} from $\text{Na}^{23}(d,p)\text{Na}^{24}$ and corresponding neutron orbital momenta l_n .

Reference: Group	Sp 52 Q value (Mev)	Sp 52 Na^{24} level (Mev)	Ta 53 ^a Sh 54 ^b	Br 54c ^c	El 56 ^d
			l_n		
(0)	4.731 ± 0.007	0	2	2	2
(1)	4.259 ± 0.007	0.472 ± 0.008	$\begin{cases} 0 \\ 0 \end{cases}$	$\begin{cases} 0 \\ 0 \end{cases}$	$\begin{cases} 0 \\ 0 \end{cases}$
(2)	4.167 ± 0.007	0.564 ± 0.008			
(3)	3.390 ± 0.006	1.341 ± 0.008	0	0	
(4)	2.887 ± 0.006	1.844 ± 0.008			
(5)	2.847 ± 0.006	1.884 ± 0.008			
(6)	2.267 ± 0.006	2.464 ± 0.008			
(7)	2.170 ± 0.006	2.561 ± 0.008			
(8)	1.322 ± 0.005	3.409 ± 0.008			
(9)	1.149 ± 0.006	3.582 ± 0.009			
(10)	1.108 ± 0.006	3.623 ± 0.009			
(11)	1.083 ± 0.006	3.648 ± 0.009			
(12)	0.993 ± 0.005	3.738 ± 0.008			
(13)	0.881 ± 0.005	3.850 ± 0.008			
(14)	0.832 ± 0.005	3.899 ± 0.008			
(15)	0.802 ± 0.005	3.929 ± 0.008			1
(16)	0.547 ± 0.005	4.184 ± 0.008			
(17)	0.529 ± 0.005	4.202 ± 0.008			1
(18)	0.512 ± 0.005	4.219 ± 0.008			
(19)	0.173 ± 0.005	4.558 ± 0.009			1
(20)		4.74 ± 0.07 ^e			1

^a $E_d=1.15$ Mev; nuclear emulsions.

^b $E_d=3$ Mev; Al absorption.

^c $E_d=10$ Mev; nuclear emulsions.

^d $E_d=8$ Mev; magnetic analysis. Groups (1) and (2) were only partly resolved in this investigation.

^e El 56a.

VIII. $\text{Mg}^{24}(n,p)\text{Na}^{24}$ $Q_m=-4.731$

Cross-section data, En 54a, Co 56, Ve 57.

IX. $\text{Mg}^{25}(\gamma,p)\text{Na}^{24}$ $Q_m=-12.063$

Threshold and cross-section data, En 54a, Ka 54, Mo 55.

X. $\text{Mg}^{26}(d,\alpha)\text{Na}^{24}$ $Q_m=2.889$

Cross section, En 54a.

XI. $\text{Al}^{27}(n,\alpha)\text{Na}^{24}$ $Q_m=-3.136$

Cross section, En 54a.

Mg²⁴

(Fig. 5)

I. $\text{Ne}^{20}(\alpha,p)\text{Na}^{23}$ $E_b=9.307$ $Q_m=-2.380$

Observed at $E_\alpha=3.923$ -Mev resonance (Table IV) (Go 54c).

II. $\text{Ne}^{20}(\alpha,\alpha)\text{Ne}^{20}$ $E_b=9.307$

Thirteen sharp resonances observed in neon elastic cross section at four different scattering angles for $E_\alpha=2-4$ Mev. Eleven assigned to Ne^{20} (Table IV) and two to Ne^{22} . Spins and parities from partial wave analysis (Go 54c). Reaction IV gives comparison with $\text{Na}^{23}+\bar{p}$ resonances.

III. $\text{Ne}^{21}(\alpha,n)\text{Mg}^{24}$ $Q_m=2.550$

Not observed. Reaction chain $\text{Ne}^{20}(\bar{p},\gamma)\text{Na}^{21}(\beta^+)$ $\text{Ne}^{21}(\alpha,n)\text{Mg}^{24}$ believed to be a source of neutrons in a certain stage of stellar development (Ho 56).

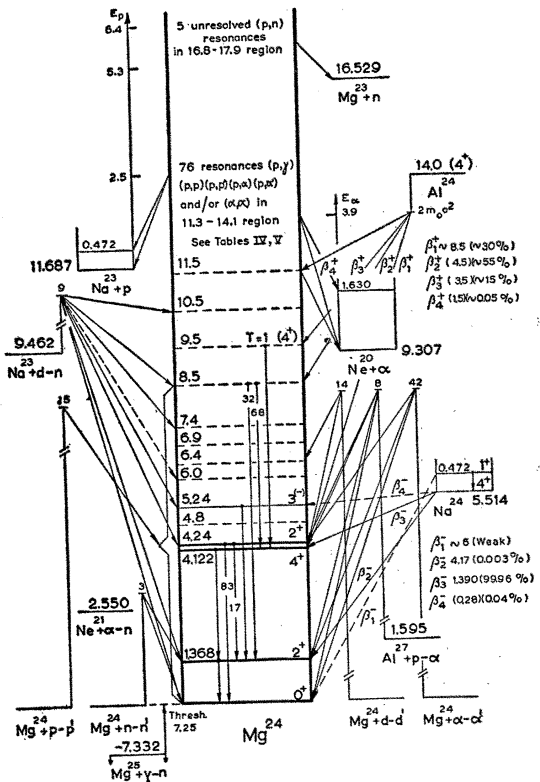


FIG. 5.

- IV. (a) $\text{Na}^{23}(\bar{p},\gamma)\text{Mg}^{24}$ $E_b=11.687$
 (b) $\text{Na}^{23}(\bar{p},n)\text{Mg}^{23}$ $E_b=11.687$ $Q_m=-4.842$
 (c) $\text{Na}^{23}(\bar{p},p)\text{Na}^{23}$ $E_b=11.687$
 (d) $\text{Na}^{23}(\bar{p},p'\gamma)\text{Na}^{23}$ $E_b=11.687$ $E_x=0.439$
 (e) $\text{Na}^{23}(\bar{p},\alpha)\text{Ne}^{20}$ $E_b=11.687$ $Q_m=2.380$
 (f) $\text{Na}^{23}(\bar{p},\alpha\gamma)\text{Ne}^{20}$ $E_b=11.687$ $E_x=1.630$

Large amount of information has become available in recent years on $\text{Na}^{23}+\bar{p}$ resonance reactions (Table V, also En 54a). Most accurate measurements taken for proton resonant energies and total widths given in Table V. Besides references under Table V, also Ny 55 (energies of 5 resonances in 0.5–1.0-Mev region with relative γ -ray yields), Te 54a (energies of 14 resonances

TABLE IV. Resonances in $\text{Ne}^{20}(\alpha,\alpha)\text{Ne}^{20}$ reaction and corresponding Mg^{24} levels (Go 54c).

E_α (lab) (Mev)	E_x (Mg^{24}) (Mev)	Γ (kev)	J, π
2.488	11.380	(0.5)	1 ⁻
2.573	11.451	(1)	0 ⁺
2.652	11.517	(0.5)	2 ⁺
2.903	11.726	10 ± 2	0 ⁺
3.062	11.858	8 ± 2	1 ⁻
3.184	11.960	(0.5)	2 ⁺
3.548	12.263	(1)	3 ⁻
3.780	12.456	7 ± 2	1 ⁻
3.801	12.474	5 ± 1	2 ⁺
3.839	12.506	(1)	4 ⁺
3.923	12.576	6 ± 1	2 ⁺
all ± 0.005			

in 0.85–1.70-Mev region with widths and relative γ -ray yields), and Fa 55. Relative γ -ray yields of 5 resonances in 0.22–0.53-Mev region, Ha 55c. For absolute α_0 yields at the 287-, 338-, and 594-kev resonances, Fl 54.

Spin and parity assignments of 308-, 511-, 594-, and 675-kev resonances based on measurements of γ -ray spectra, angular distributions, $\gamma-\gamma$ angular correlations, and γ -ray widths. The 4.24-Mev Mg^{24} level assigned $J=2^+$. Level at 5.26 Mev observed with $J=3$ and probably negative parity (Gr 55e). Also Ca 53, Tu 53, Ca 54a, Hi 54a, for measurements of γ -ray spectrum at 308-kev resonance.

Spin and parity assignments at 1012-, 1137-, 1166-, and 1288-kev resonances in St 54a based on α_0 angular distribution measurements, those in Ba 56 mainly on p_0 and some on γ angular distribution measurements, and those in Ne 54 mainly on partial widths for different decay processes. Gamma-ray angular distribution and correlation measurements at 1398-kev resonance lead also to assignments of $J=2$ to Mg^{24} 4.24-Mev level (decaying both to ground state and 1.37-Mev level with relative intensity of 1:0.2) and $J=3$ to a 5.23 ± 0.04 -Mev level (decaying through 1.37-Mev level) (Ne 54). The 1⁺ assignment to 1258-kev resonance in Se 53 based on $\alpha_1-\gamma$ angular correlation measurements in planes parallel with and perpendicular to proton beam.

On the average, Mg^{24} excitation energies as found from $\text{Ne}^{20}+\alpha$ are 5 kev higher than those from $\text{Na}^{23}+\bar{p}$. Except for this, there is beautiful agreement between excitation energies, spins and parities of Mg^{24} levels found from $\text{Ne}^{20}+\alpha$ elastic scattering (Table IV) and from $\text{Na}^{23}+\bar{p}$ (Table V). In former reaction, only $T=0$ levels observed with “natural parity” (parity even if J is even, parity odd if J is odd).

The 12.256-Mev level must be a doublet, Gr 55e. A unique 2⁻ assignment follows from $\text{Na}^{23}(\bar{p},\gamma)$, in disagreement with 3⁻ assignment from $\text{Na}^{23}(\bar{p},\bar{p})$ and $\text{Ne}^{20}(\alpha,\alpha)$. Negative parity follows also from a polarization measurement of 10.8-Mev capture radiation, Hu 56.

V. $\text{Na}^{23}(d,n)\text{Mg}^{24}$ $Q_m=9.462$

Angular distributions of neutrons, detected with nuclear emulsions, measured at $E_d=8$ Mev. Transitions to Mg^{24} ground state and 1.37-Mev level very weak; those to 4.12- and 4.24-Mev levels unresolved and weak ($l_p=0+2$); those to 5.1-, 5.5-, and 6.3-Mev levels weak and isotropic. Transitions observed to levels at 7.45, 8.48, and 10.46 Mev, all ± 0.10 Mev, with $l_p=0, 0+2$, and 0, respectively, El 56a.

Essentially same results obtained at $E_d=9$ Mev with a proton recoil triple ionization chamber for neutron detection. Transitions to a 7.5-Mev level assigned $l_p=0+2$, those to a 8.4-Mev level $l_p=0$. No higher levels observed, Ca 55. Also En 54a.

VI. $\text{Na}^{24}(\beta^-)\text{Mg}^{24}$ See Na^{24} .VII. $\text{Mg}^{24}(e, e')\text{Mg}^{24}$

Differential cross section for elastic scattering of 187-Mev electrons and for inelastic scattering leading to level (1) determined, (He 56).

VIII. $\text{Mg}^{24}(n, n')\text{Mg}^{24}$

At $E_n = 2.56$ Mev, only one γ ray ($E_\gamma = 1.368 \pm 0.010$ Mev) from inelastic neutron scattering on natural magnesium can be assigned to Mg^{24} (Da 56c). Also En 54a, Sc 54d, Pa 55, Ra 55, Cr 56a. Elastic neutron scattering, Cu 56.

IX. $\text{Mg}^{24}(p, p')\text{Mg}^{24}$

Most accurate measurement of first Mg^{24} level, done by electrostatic analysis of inelastically scattered protons, 1.371 ± 0.002 Mev (Do 53). Second and third levels measured by magnetic analysis at 4.13 ± 0.02 and 4.24 ± 0.02 Mev (Ha 52). Higher levels reported (all from natural magnesium bombardments) at 4.77, 5.24, 6.00, 6.42, and 6.90 Mev, all ± 0.05 Mev (Gr 56f), at 5.10 Mev (St 52), at 5.1 ± 0.1 , 5.9 ± 0.1 , and 6.3 ± 0.1 Mev (Fi 54), at 5.51 ± 0.3 , 7.32 ± 0.3 , and 8.30 ± 0.4 Mev (Fu 48), and at 6.38 ± 0.08 Mev (Ba 52).

Angular distribution measurements of elastically and inelastically scattered protons, En 54a, Fi 54, Gr 55, Co 55, Gr 56f, Gu 56a, Sh 56.

A $p\gamma$ angular correlation measurement, En 54a.

Resonances, under Al^{25} .

X. $\text{Mg}^{24}(d, d')\text{Mg}^{24}$

Angular distribution measurements of elastically and inelastically scattered deuterons, En 54a, Gr 55, Ha 56c.

XI. $\text{Mg}^{24}(\alpha, \alpha')\text{Mg}^{24}$

Angular distribution measurements of elastically and inelastically scattered α particles, Gu 56, Wa 56a. Groups both to 1.37-Mev level and to doublet at 4.2 Mev agree with direct surface interaction for $0^+ \rightarrow 2^+$ transitions. Thus, the 2^+ 4.24-Mev level is excited but not the 4^+ 4.12-Mev level (Wa 56a).

Resonances, under Si^{28} .

XII. $\text{Al}^{24}(\beta^+)\text{Mg}^{24}$ See Al^{24} .XIII. $\text{Mg}^{25}(\gamma, n)\text{Mg}^{24}$ $Q_m = -7.332$

Threshold and yield, En 54a, Ka 54, Na 55, Ye 56, Mo 55.

XIV. $\text{Al}^{27}(\gamma, t)\text{Mg}^{24}$ $Q_m = -18.217$

Threshold, 18.2 ± 0.2 Mev. Yield from 31-Mev bremsstrahlung in good agreement with statistical theory (Wa 56).

TABLE V. Resonances in $\text{Na}^{23} + p$ reactions.

E_p (lab) (kev)	E_x (Mg^{24}) (Mev)	Decay *	Γ (kev)	J, π
250.8 ± 0.2 a	11.928		γ	0.3 ± 0.2 a
287 ± 1.5 b	11.962	$\alpha\alpha$	γ	0.8 ± 0.3 a
307.8 ± 0.3 a	11.983	$\alpha\alpha$	γ	2^- d
338 ± 1.5 b	12.011	$\alpha\alpha$	γ	2.0 ± 1.0 a
373.5 ± 0.4 a	12.045		γ	0.8 ± 0.3 a
443.8 ± 0.6 a	12.113		γ	0.8 ± 0.3 a
510.9 ± 0.6 a	12.177		γ	0.8 ± 0.3 a
594 °	12.256	p_0	$\alpha\alpha$	2 ± 1 °
675 °	12.334	p_0	γ	< 1 °
725 °	12.382	p_0		7 ± 2 °
740 °	12.396	p_0	γ	< 3 °
744 °	12.400		γ	< 3 °
797 °	12.451	p_0	$\alpha\alpha$	7 ± 2 °
815 °	12.468	p_0	$\alpha\alpha$	5 ± 1 °
849 °	12.501	p_0		$(1)^+$ f
877 °	12.527	p_0	γ	8 ± 2 °
922 °	12.571	p_0	$\alpha\alpha$	6 ± 1 °
989 °	12.635		γ	< 1 °
1011 °,e	12.656	p_1		$\lesssim 0.5$ °
1012 °,e	12.657	p_1	$\alpha\alpha$	0.8 ± 0.1 e
1022 °,e	12.666	p_0	$\alpha\alpha$	6.6 ± 0.5 e
1087 °,e	12.729	p_1	γ	1.1 ± 0.5 e
1094 °,e	12.734	p_1	$\alpha\alpha$	7.9 ± 0.5 e
1137 °,e	12.777	$\alpha\alpha$		30 ± 5 °
1166 °,e	12.804	p_1	$\alpha\alpha$	1.2 ± 0.1 e
1176 °,e	12.814	p_0	$\alpha\alpha$	2.5 ± 0.5 e
1206 °,e	12.844	p_0	$\alpha\alpha$	0.3 ± 0.1 e
1213 °,e	12.849	p_0	$\alpha\alpha$	0.4 ± 0.1 e
1258 °,e	12.893	p_0	$\alpha\alpha$	0.6 ± 0.1 e
1273 °	12.907		γ	
1288 °,e	12.921	p_0	p_1	$\alpha\alpha$
1321 °,e	12.953	p_0	p_1	$\alpha\alpha$
1329 °,e	12.962	p_0	p_1	$\alpha\alpha$
1334 °,e	12.966	p_0	p_1	6.7 ± 0.2 e
1365 °,e	12.996	p_0	p_1	1.2 ± 0.2 e
1398 °,e	13.028	p_0	p_1	$\alpha\alpha$
1419 °,e	13.048	p_1	$\alpha\alpha$	< 0.3 e
1460 °,e	13.087	p_0	p_1	9.8 ± 0.2 e
1511 °,e	13.135	$\alpha\alpha$		< 10 °
1519 °	13.143	\cdots	p_1	$\alpha\alpha$
1558 °	13.170	\cdots	p_1	$\alpha\alpha$
1575 °	13.196	\cdots	$\alpha\alpha$	< 10 °
1638 °	13.257	\cdots	p_1	$\alpha\alpha$
1645 °	13.263	\cdots	p_1	~ 50 °
1653 °	13.271	\cdots	$\alpha\alpha$	~ 8 °
1719 °	13.334	\cdots	p_1	$\alpha\alpha$
1737 °	13.352	\cdots	p_1	2.0 ± 0.5 e
1749 °	13.363	\cdots	p_1	15.2 ± 2 °
1802 °	13.414	\cdots	p_1	$\alpha\alpha$
1805 °	13.417	\cdots	$\alpha\alpha$	4 ± 1 °
1832 °	13.443	\cdots	p_1	6 ± 1 °
1839 °	13.449	\cdots	p_1	< 0.35 e
1870 °	13.479	\cdots	p_1	3.2 ± 0.2 e
1933 °	13.540	\cdots	p_1	$\alpha\alpha$
1976 °	13.581	\cdots	p_1	6.9 ± 0.5 e
1979 °	13.584	\cdots	p_1	23 ± 3 °
2027 °	13.629	\cdots	$\alpha\alpha$	9.5 ± 1 e
2075 °	13.676	\cdots	$\alpha\alpha$	3.3 ± 1 e
2080 °	13.681	\cdots	p_1	8.7 ± 0.5 e
2122 °	13.721	\cdots	p_1	31 ± 2 °
2170 °	13.767	\cdots	p_1	4.8 ± 0.5 e
2200 °	13.795	\cdots	p_1	~ 2 °
2223 °	13.817	\cdots	p_1	3.5 ± 0.5 e
2243 °	13.836	\cdots	p_1	47 ± 5 °
2284 °	13.876	\cdots	p_1	~ 2 °
2297 °	13.888	\cdots	p_1	2.0 ± 0.5 e
2340 °	13.929	\cdots	p_1	~ 28 °
2343 °	13.932	\cdots	p_1	~ 10 °
2354 °	13.943	\cdots	p_1	~ 14 °
2388 °	13.976	\cdots	p_1	~ 4 °
2436 °	14.021	\cdots	p_1	4.9 ± 0.5 e
				6.5 ± 0.5 e

* For observed modes of decay p_0 refers to elastic scattering, p_1 to inelastic protons (observed through the 0.439-Mev Na^{23} γ ray), $\alpha\alpha$ to ground-state α particles, α to short-range α particles (mostly observed through 1.630-Mev Ne^{20} γ rays), and γ to hard γ rays from proton capture.

^a (Ha 55c); ^b (Fl 54); ^c (Ba 56, Pr 56); ^d (Gr 55e); ^e (St 54); ^f (Go 54c); ^g (Ne 54); ^h (St 54a); ⁱ (Se 53); ^j (De 56).

^k No elastic proton scattering measurements available above $E_p = 1.5$ Mev.

^l Hard γ rays very weak or absent above $E_p = 1.5$ Mev.

^m No ground-state α -particle measurements available above $E_p = 2.2$ Mev.

XV. $\text{Al}^{27}(p, \alpha)\text{Mg}^{24}$ $Q_m = 1.595$

Q by electrostatic analysis = 1.594 ± 0.002 Mev (Do 53), and by magnetic analysis = 1.585 ± 0.015 Mev (Fr 50), 1.595 ± 0.007 Mev (Va 52a), 1.61 ± 0.02 Mev (Ru 53a), and 1.596 ± 0.006 Mev (Va 57d).

From electrostatic analysis first level obtained at

1.366 ± 0.004 Mev (Do 53), and from magnetic analysis at 1.366 ± 0.006 Mev (Va 57d).

Transitions to 4.11- and 4.21-Mev levels observed by magnetic analysis at $E_p = 8$ Mev (Re 52).

Resonances, under Si²⁸. Also En 54a, Gr 54a, Pa 54.

Al²⁴

(not illustrated)

I. Al²⁴(β^+)Mg²⁴ $Q_m = 14.0$

Half-life (average of three measurements, En 54a) 2.09 ± 0.04 sec.

Gamma rays observed with a scintillation spectrometer in Table VI. Positrons reported with endpoint of ~ 8.5 Mev. One per several thousand disintegrations proceeds through an excited state in Mg²⁴ which emits α particles of $E_\alpha \sim 2$ Mev (Gl 55).

The β^+ decay seems best explained by assuming a 30% branch to an 8.5-Mev level, probably with spin 3+, de-exciting through the 7.12- and 4.22-Mev γ rays to the 1.37-Mev 2⁺ and 4.12-Mev 4⁺ levels, a 15% branch to a 9.5-Mev level, de-exciting through the 5.35-Mev γ ray to the 4.12-Mev level, and finally a weak transi-

TABLE VI. Gamma rays from the Al²⁴(β^+)Mg²⁴ decay.

Author:	Gl 55 E_γ (Mev)	Rel. int.	Br 54a E_γ (Mev)
	1.39 ± 0.03	0.40	1.38 ± 0.04
	2.73 ± 0.06	0.32	2.70 ± 0.06
	4.22 ± 0.10	0.15	4.21 ± 0.12
	5.35 ± 0.10	0.06	5.37 ± 0.14 (5.66 ± 0.18)
	7.12 ± 0.10	0.07	7.02 ± 0.20

tion to a level at ~ 11 Mev, de-exciting through α emission (Gl 55). The 9.5-Mev level in position expected for $T_z=0$ member of $T=1$ triplet to which also belong $J=4^+$ Na²⁴ ground state and Al²⁴ ground state (presumably also with spin $J=4^+$). The β^+ transition to this level would then be favored (Bo 55, Wi 56a).

II. Mg²⁴(p,n)Al²⁴ $Q_m = -14.8$

Threshold is 15.4 ± 0.3 Mev (Bi 52). Also Ty 54, Co 55b.

Na²⁵

(not illustrated)

I. Na²⁵(β^-)Mg²⁵ $Q_m = 4.0$

Measurements of half-life (En 54a, Iw 55, Na 56), in good agreement, average to 59.5 ± 0.7 sec. The β^- end point, measured with Al absorbers, 3.7 ± 0.3 Mev (Bl 47) and with a scintillation spectrometer, 4.0 ± 0.2 Mev (Ma 55). From analysis of γ spectrum and β^- - γ coincidence spectrum, 65%, 3.5%, 25%, and 6.5% of β^- transitions lead to ground state and to 0.58-, 0.98-, and

1.61-Mev levels of Mg²⁵, respectively (Ma 55). However, intensity ratios in γ spectrum measured with a large NaI crystal show that β^- branching to the 0.58-Mev level is probably less than 1% (Go 56). Branching ratios, log $f\tau$ values, spins, and parities in Table VII. Assignment of 5/2⁺ to Na²⁵ ground state based upon absence of a measurable transition to Mg²⁵ (1) together with allowed character of transitions to Mg²⁵ (0) and (2). Energies and relative intensities of γ rays in Table VIII. Discussion of possibility of favored transitions, Ki 55, Fe 55.

TABLE VII. The β^- decay of Na²⁵ (Go 56).

Mg ²⁵ level (Mev)	0	0.58	0.98	1.16	1.96
Branching ratio (%)	65	<1	30	5	<1
Log $f\tau$	5.2	>6.9	5.2	5.6	>5.9
J and π ; Na ²⁵ (0) = 5/2 ⁺	5/2 ⁺	1/2 ⁺	3/2 ⁺	(7/2) ⁺	5/2 ⁺

II. Ne²²(α,p)Na²⁵ $Q_m = -3.70$

Observed, En 54a.

III. Mg²⁵(n,p)Na²⁵ $Q_m = -3.22$

Cross section, En 54a.

IV. Mg²⁶(γ,p)Na²⁵ $Q_m = -14.21$

Threshold, $E_\gamma = 14.0 \pm 1.0$ Mev. Cross section, En 54a, Ka 54; also Mo 55.

TABLE VIII. Gamma rays following the β^- decay of Na²⁵.^a

	Iw 55	Ma 56	Na 56	Go 56
γ_1	410	384 ± 10 (44±4)	370 ± 10 (108)	400 (95±4)
γ_2	590	576 ± 10 (59±7)	580 ± 10 (135)	580 (89±5)
γ_3	980	978 ± 15 (100±15)	975 (100)	980 (100±3)
γ_4		1603 ± 20 (40±7)		1610 (33±3)

^a Energies in kev; relative intensities normalized to $\gamma_3 = 100$ and placed in brackets.

Mg²⁵

(Fig. 6)

I. Ne²²(α,n)Mg²⁵ $Q_m = -0.483$

Work with Po α -particle sources, En 54a.

II. Mg²⁴(n,γ)Mg²⁵ $Q_m = 7.332$

Thermal neutron capture cross section of natural magnesium is 63 ± 4 mb; those of Mg²⁴, Mg²⁵, and Mg²⁶ are 33 ± 10 , 270 ± 90 , and 60 ± 60 mb, and their abundances 78.6, 10.1, and 11.3%, respectively, indicating approximately 41% of thermal neutron captures in natural magnesium should occur in Mg²⁴ (Hu 55c).

Gamma rays from capture of thermal neutrons in natural magnesium, measured with magnetic pair spectrometer (Ki 51, Ki 53a) and with two-crystal scintillation spectrometer (Br 56e), in Table IX. Intensity of

line J not in agreement with above estimate of contribution of Mg^{24} to capturing cross section of natural magnesium. Possible assignments in Table IX based mainly upon comparison of γ energies with Q values of (d,p) reactions. Great intensity of line J (from capturing state to p level at 3.405 Mev in Mg^{25}) explained by assuming this is most energetic E1 transition. Since this level is de-excited by γ rays K and L to ground state (spin $5/2^+$) and first level (spin $1/2^+$), both these competing transitions must be E1, and spin of 3.405 level is uniquely determined as $3/2^-$ (Ki 54a).

Recalculation of intensities of some lines in photons per 100 captures in Mg^{24} , Ki 54a.

III. $Mg^{24}(n,n)Mg^{24}$ $E_b = 7.332$

Total neutron cross section of natural magnesium, Hu 55c.

TABLE IX. Gamma rays from capture of thermal neutrons in natural magnesium.

γ ray	Energy in Mev	Intensity in photons per 100 captures in natural Mg	Final nucleus and probable transition
A''	11.08 ± 0.025^d		Mg^{26} ($c \rightarrow 0$)
A'	10.08 ± 0.02^d		Mg^{26} ($c \rightarrow 0$)
A	9.26 ± 0.04^a	1 ^a	Mg^{26} ($c \rightarrow 1$)
B''	8.93 ± 0.02^d		Mg^{26} ($c \rightarrow 0$)
B'	8.55 ± 0.02^d		Mg^{26} ($c \rightarrow 0$)
B	8.16 ± 0.03^a	9 ^a	Mg^{26} ($c \rightarrow 2$)
C	7.37 ± 0.08^a	0.5 ^{a,c}	Mg^{25} ($c \rightarrow 0$)
D	7.15 ± 0.04^a	1 ^a	Mg^{26} ($c \rightarrow 3$)
E	6.75 ± 0.04^a	2.5 ^{a,e}	$(Mg^{26}), Mg^{25}$ ($c \rightarrow 1$)
F_1	6.440 ± 0.008^b	1.3 ^{b,e}	Mg^{27} ($c \rightarrow 0$)
F_2	6.358 ± 0.007^b	3.5 ^{b,e}	Mg^{25} ($c \rightarrow 2$)
G	5.73 ± 0.04^a	1 ^a	(Mg^{25}) ($c \rightarrow 3$)
H	5.50 ± 0.04^a	7 ^a	$(Mg^{26}), (Mg^{26})$
I	5.05 ± 0.07^a	9 ^a	(Mg^{25})
J	3.918 ± 0.004^b	70 ^{b,e}	Mg^{25} ($c \rightarrow 8$)
K	3.408 ± 0.018^d	$\sim 10^d$	Mg^{25} ($8 \rightarrow 0$)
L	2.816 ± 0.016^d	$\sim 50^a,c,d$	Mg^{25} ($8 \rightarrow 1$)
M	1.87 ± 0.03^c	22 ^c	Mg^{26} ($1 \rightarrow 0$)
N	1.07 ± 0.05^c	13 ^c	Mg^{26} ($2 \rightarrow 1$)

^a Ki 51. ^b Ki 53a. ^c Br 56e. ^d Ca 56. ^e See also Ki 54a.

Resonance at $E_n = 85$ kev has $J = 3/2^-$ by measurements of total cross section of enriched Mg^{24} (Ta 56) and by measurements of the differential scattering cross section at 90° and 180° (Bl 56). Resonances at $E_n = 275$ and 430 kev also assigned to Mg^{24} ; it is proposed that they have $J = 1/2^-$ and $3/2^-$, respectively (Fi 51).

IV. $Mg^{24}(d,p)Mg^{25}$ $Q_m = 5.107$

Ground-state $Q = 5.097 \pm 0.007$ Mev (En 52b). Ten levels in Mg^{25} (see Table X) found from magnetic analysis with targets of natural magnesium. Assignment of proton groups based on comparison with Mg^{25} levels found from $Al^{27}(d,\alpha)Mg^{25}$ and with proton groups from (d,p) reactions on targets enriched in Mg^{25} and Mg^{26} (En 52a). Also En 54a. Above 4.6 Mev, four incompletely resolved levels found from Al absorption meas-

urements (Ho 53), and several more from low-resolution magnetic analysis (Kr 53a); Table X.

Measurements of γ rays in coincidence with protons which have passed through an Al absorber of variable thickness indicate transitions from the first four excited states of Mg^{25} to ground state and from second and fourth excited states to first one (Mu 56). See Reaction VII for conclusions about spins and parities from γ branching ratios.

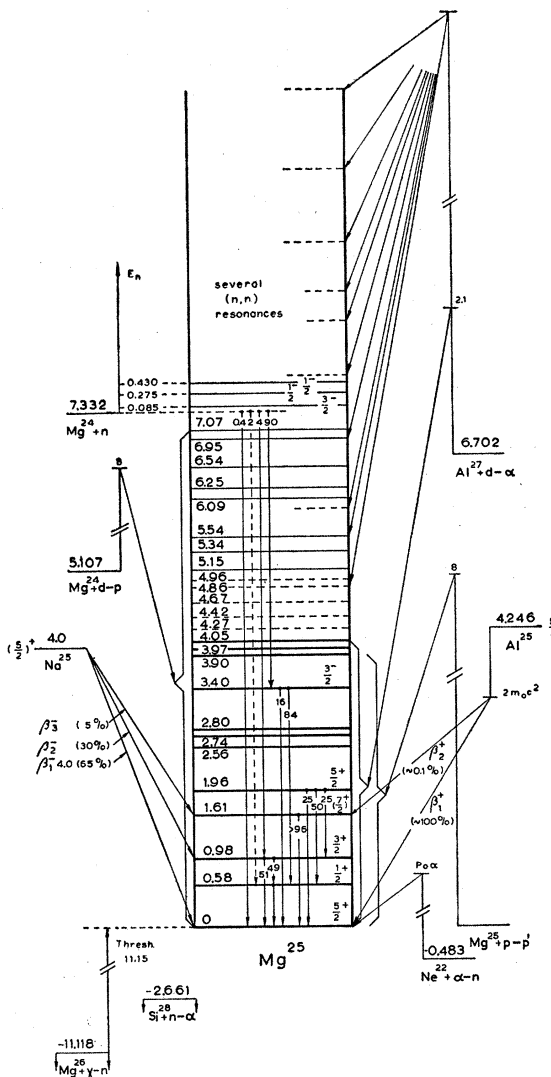


FIG. 6.

Angular distribution measurements yield l_n values in Table X. Angular distribution of protons associated with the 1.61-Mev level is isotropic. Relative intensities of proton groups and neutron capture probabilities, Ho 53.

Angular distribution of protons from (d,p) reaction to 3.40-Mev level and angular correlation between protons and gammas from this level measured at several deuteron energies between 2 and 4 Mev. Results in

accordance with a $3/2^-$ assignment (Wi 55, also Co 56a).

Transition probabilities in $Mg^{24}(d,p)$ and (d,n) reactions, Fu 54.

V. $Na^{25}(\beta^-)Mg^{25}$ See Na^{25}

VI. $Mg^{25}(n,n')Mg^{25}$

A γ ray of 1.616 ± 0.016 Mev results from inelastic scattering of 2.56 Mev neutrons by natural magnesium (Da 56c). Cross section, Da 56c.

With 3.2-Mev neutrons, γ rays of 0.38 ± 0.02 and 0.59 ± 0.02 Mev found together with others which can be ascribed to Mg^{24} or Mg^{26} (Sc 54d). Also Ra 55, Pa 55.

VII. $Mg^{25}(p,p')Mg^{25}$

By magnetic analysis of inelastic scattering of 8-Mev protons by natural magnesium targets, levels found at 0.61, 1.62, 1.98, 2.56, 2.76 (possibly a doublet), 3.41, and 3.91 Mev, all ± 0.02 Mev (Ha 52). These agree well with levels in Mg^{25} found from other reactions. Also Fi 54.

Energy of γ ray from first excited state measured with a scintillation spectrometer, 0.588 ± 0.005 Mev (Ka 55).

Yields of 1.96, 1.61, 0.98, and $(0.40 + 0.58)$ -Mev γ radiation from $Mg^{25}(p,p'\gamma)$ reaction measured as functions of proton energy in range from 1.5 to 3.0 Mev (Go 56).

TABLE X. Energy levels in Mg^{25} from $Mg^{24}(d,p)Mg^{25}$.

Author:	En 52b, En 53a	Ho 53	Kr 53a
E_d (Mev):	1.8	8	4.04
Method:	Magnetic analysis	Al absorption	Magnetic analysis
Q_0 (Mev):	5.097 ± 0.007		
	E_x (Mev)	E_x (Mev) ^a	E_x (Mev)
		l_n	
	0	2	
0.582 \pm 0.006		0	0.50 \pm 0.20
0.976 \pm 0.006		2	1.00 \pm 0.20
1.612 \pm 0.006			1.58 \pm 0.20
1.957 \pm 0.006		2	2.02 \pm 0.20
2.565 \pm 0.006			(2.47 \pm 0.20)
2.742 \pm 0.008			2.70 \pm 0.20
2.806 \pm 0.007			(2.87 \pm 0.20)
3.405 \pm 0.007		1	
3.899 \pm 0.008			3.92 \pm 0.20
3.972 \pm 0.010			(4.03 \pm 0.20)
(4.052 \pm 0.010)			
(4.265 \pm 0.007)			
(4.421 \pm 0.010)			
	4.62 \pm 0.05		4.62 \pm 0.20
			(4.86 \pm 0.20)
5.05 \pm 0.07			(4.96 \pm 0.20)
5.47 \pm 0.07			5.15 \pm 0.20
			5.34 \pm 0.20
6.40 \pm 0.05			5.54 \pm 0.20
			6.09 \pm 0.20
			6.25 \pm 0.20
			6.54 \pm 0.20
			6.95 \pm 0.20
			7.07 \pm 0.20

^a Ground-state $Q = 5.097$ Mev assumed.

TABLE XI. Energy levels in Mg^{25} from $Al^{27}(d,\alpha)Mg^{25}$.

Author:	Sc 50	To 52	En 52b, En 53a
E_d in Mev:	11.1	10.8	2.1
Method:	Al absorption	Nuclear emulsions	Magnetic analysis
Q_0 (Mev):	6.58 ± 0.03	^a	6.694 ± 0.010
Levels in Mg^{25} in Mev	0.57 ± 0.05	0.58 ± 0.02	0.584 ± 0.006
	0.96 ± 0.05	0.93 ± 0.04	0.977 ± 0.010
	1.63 ± 0.04	1.62 ± 0.03	1.610 ± 0.010
	1.97 ± 0.05	2.09 ± 0.05	1.958 ± 0.010
	2.74 ± 0.04	2.74 ± 0.03	2.729 ± 0.010
	3.36 ± 0.04	3.36 ± 0.03	2.791 ± 0.015
	4.01 ± 0.05	4.12 ± 0.04	3.404 ± 0.012
	4.81 ± 0.05	4.87 ± 0.03	3.896 ± 0.015
	5.48 ± 0.05	5.56 ± 0.03	3.960 ± 0.015
	5.95 ± 0.05	5.93 ± 0.03	4.057 ± 0.015
			6.98 ± 0.03
			7.85 ± 0.04
			8.62 ± 0.05
			9.06 ± 0.04
			9.75 ± 0.04
			10.78 ± 0.04
			11.89 ± 0.05

^a Ground-state $Q = 6.694$ Mev assumed.

By comparing γ spectra at different resonances and by measuring $\gamma\gamma$ coincidences, branching ratios of levels at 0.98, 1.61, and 1.96 Mev obtained (Fig. 6) (Go 56, Go 57a). Spins and parities of lower levels agree with these branching ratios, hyperfine-structure measurements (Ra 53), (d,p) angular distributions, $\log ft$ values in decay of Na^{25} and Al^{25} , shell model predictions, and classifications of corresponding levels in the mirror nucleus Al^{25} .

VIII. $Al^{25}(\beta^+)Mg^{25}$ See Al^{25}

IX. $Mg^{26}(\gamma,n)Mg^{25}$ $Q_m = -11.118$

Threshold at 11.15 ± 0.20 (Sh 51a). Cross sections, Ka 54, Na 55, Ye 56; theoretical discussion of observed cross sections, Mo 55.

X. $Al^{27}(d,\alpha)Mg^{25}$ $Q_m = 6.702$

Table XI shows good agreement between level positions found with different bombarding energies and detection methods by different authors and also with level positions deduced from $Mg^{24}(d,p)Mg^{25}$ studies (Table X). Also En 54a, Be 55.

Angular distributions, En 54a.

XI. $Si^{28}(n,\alpha)Mg^{25}$ $Q_m = -2.661$

Not observed.

Al²⁵

(Figs. 7 and 8)

I. $Al^{25}(\beta^+)Mg^{25}$ $Q_m = 4.26$

Half-life is 7.62 ± 0.13 sec (Ch 53, Hu 54b, also Br48). The β^+ end point is 3.24 ± 0.03 Mev, as measured

with a magnetic lens spectrometer (El 55, also Hu 54c). Log $ft = 3.5$.

Decay accompanied by weak 1.58 ± 0.03 -Mev γ ray (Ma 55, also Ch 56), indicating roughly 1% of β^+ transitions go to 1.61-Mev level of Mg^{25} . Log ft value for this transition 5.3. No 1.98-Mev γ ray with intensity >0.5% was detected (St 56).

- II. (a) $Mg^{24}(p,\gamma)Al^{25}$ $E_b = 2.29$
 (b) $Mg^{24}(p,p)Mg^{24}$ $E_b = 2.29$
 (c) $Mg^{24}(p,p'\gamma)Mg^{24}$ $E_b = 2.29$ $E_x = 1.368$

Several authors (Ta 46, Gr 50, Ca 53, Kl 54, Gr 55c, Hu 53, Hu 54b, Hu 55, Cr 56, Ag 56, Li 56a, Va 56b, Va 56c, Ch 56) have observed resonances for the $Mg^{24}(p,\gamma)$ reaction, either by measuring yield of radioactive Al^{25} (Gr 50, Hu 54b, Hu 55), or by measuring yield of capture γ rays (all others). Some resonances found with targets of natural magnesium (Ta 46, Sm 57) ascribed to $Mg^{25}(p,\gamma)Al^{26}$ reaction (Hu 55). Resonances for elastic scattering of protons by Mg^{24}

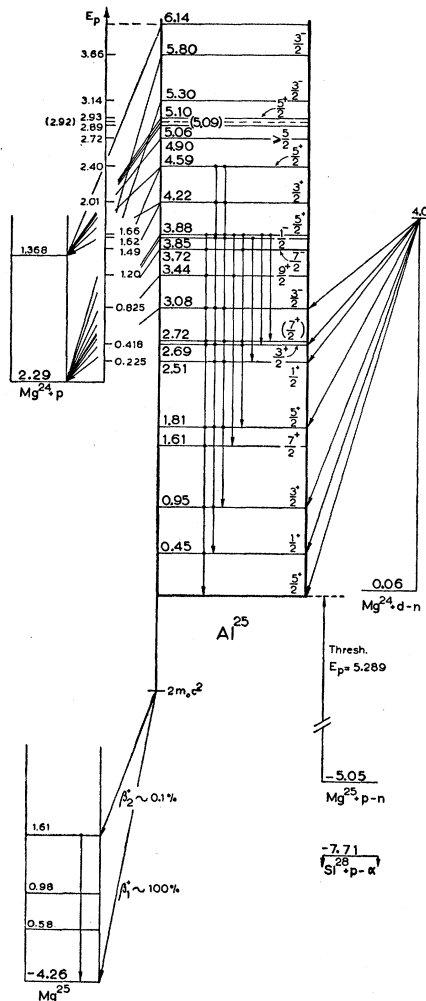


FIG. 7.

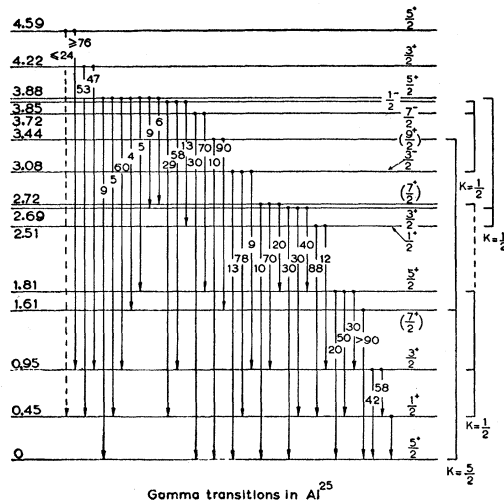


FIG. 8.

observed for proton energies between 0.4 and 3.9 Mev (Mo 51); partial-wave analysis (Ko 52) yields width and classification of eight levels in Al^{25} . For proton energies between 2.0 and 3.0 Mev, eight resonances for inelastic proton scattering observed (Li 56a, Le 56a), three correspond to those found from elastic proton scattering.

The γ decay of first three resonances studied by several authors; references in Table XII, column 3. Coincidences and angular correlations in γ decay of higher resonances studied with two large scintillation crystals; most assignments of spins and parities to levels of Al^{25} result from this work (Li 56a, Li 57). Resonant proton energies, excitation energies, modes of decay, widths, and classifications of $Mg^{24}+p$ resonances in Table XII. Available information on branching ratios, spins and parities in Fig. 8.

TABLE XII. Resonances in $Mg^{24}+p$.

E_p (lab) (kev)	E_x (Al^{25}) (Mev)	Decay ^a	Γ (kev)	J, π
225.5 \pm 0.2 b	2.51	γ c, g, h-j	< 1 m	1/2 ⁺ i
418.4 \pm 0.5 b	2.69	γ c, d, k	< 1 e	3/2 ⁻ e, d, k, l
824.9 \pm 0.4 c	3.08	p_0 e	γ c, d, l	1.5 n
1200 d	3.44		γ d	< 10 d
1490 e	3.72	p_0 e	γ b	(9/2) ⁺ d
1620 e	3.85	p_0 e	γ b	0.3 n
1660 e	3.88	p_0 e	γ d	36 n
2010 e	4.22	p_0 e	p_1 d, f, γ d	0.1 n
2400 e	4.59	p_0 e	p_1 d, f, γ d	0.15 n
2720 d	4.90	p_1 d	< 10 d	3/2 ⁺ d
2890 d	5.06	p_1 d, f	< 10 d	$\geq 5/2$ d
(2920) d	(5.09)	p_1 d		1/2, (3/2 ⁺) f
2930 d	5.10	p_1 d, f	~ 50 d	5/2 ⁺ f
3140 e	5.30	p_0 e	200 n	3/2 ⁻ n
3660 e	5.80	p_0 e	p_1 f	3/2 ⁻ f
	6.14 n	p_1 f		1/2, (3/2 ⁺) f

^a The symbols p_0 , p_1 , and γ refer to elastic proton scattering, inelastic scattering to Mg^{24} (1), and proton capture, respectively.

b Hu 54b. Hu 55. c Ag 56. d Li 56a. e Mo 51. f Le 56a. g Ca 53. h Cr 56. i Va 56b. j Ch 56. k Va 56c. l Gr 55c. m Ta 46. n Ko 52.

TABLE XIII. Levels in Al^{25} from $\text{Mg}^{24}(d,n)\text{Mg}^{25}$ reaction (Go 53).

Q value (Mev)	Excitation energy in Al^{25} (Mev)	J, π
0.07±0.06	0	3/2+, 5/2+
-0.38±0.06	0.45±0.03	1/2+
-0.88±0.05	0.95±0.03	3/2-, 5/2+
-1.74±0.04	1.81±0.04	
-1.87±0.04	(1.94)	
-2.44±0.04	2.51±0.05	
-2.67±0.04	2.70±0.05	
-2.85±0.04	(2.92)	
-3.04±0.03	3.09±0.06	1/2-, 3/2-

III. $\text{Mg}^{24}(d,n)\text{Al}^{25}$ $Q_m=0.06$

Ground state and six excited states of Al^{25} observed with separated Mg^{24} targets at $E_d=4.0$ Mev (Go 53). Neutrons detected at six angles with nuclear emulsions. Q values excitation energies, and classifications based on Butler analysis in Table XIII.

IV. $\text{Mg}^{25}(\bar{p},n)\text{Al}^{25}$ $Q_m=-5.05$

Threshold measured as $E_p=5.1$ Mev (Bl 51), 5.25 ± 0.1 Mev (Sc 54b), and 5.289 ± 0.025 Mev (Ki 55a). Latter value corresponds to $Q=-5.084\pm 0.024$ Mev.

V. $\text{Si}^{28}(\bar{p},\alpha)\text{Al}^{25}$ $Q_m=-7.71$

Not observed.

GENERAL REMARKS

There is a striking correspondence between excitation energies, spins, parities, and γ -branching ratios of the low-lying levels in the mirror nuclei Mg^{25} and Al^{25} . The γ -branching ratios in Al^{25} , about which a large amount of information is available, can be explained on the basis of the collective model if it is assumed that the levels below 4 Mev belong to four rotational bands with $K=5/2, 1/2, 1/2$, and $1/2$ as in Fig. 8. Ground-state M1 transitions from levels of the $K=1/2$ series are attenuated by factors of approximately 20 as compared to M1 transitions between levels in the same bands (Li 56a, Go 56).

Mg²⁸

(Fig. 9)

I. $\text{Ne}^{22}(\alpha,\alpha)\text{Ne}^{22}$ $E_b=10.635$

Thirteen sharp resonances observed in neon elastic cross section for $E_\alpha=2-4$ Mev at four different angles. Two resonances at $E_\alpha=3.245$ Mev ($\Gamma=2.5\pm 0.5$ kev) and $E_\alpha=3.418$ Mev ($\Gamma=3.2\pm 0.5$ kev) assigned to Ne^{22} . For both, $J=3^-$ found from partial wave analysis (Go 54c). They correspond to Mg^{26} levels at 13.380 and 13.526 Mev.

II. $\text{Na}^{23}(\alpha,p)\text{Mg}^{26}$ $Q_m=1.842$

Levels found with α particles from radioactive sources, En 54a.

Yield of 1.83-Mev γ ray de-exciting first Mg^{26} level measured for $E_\alpha=1.9-3.6$ Mev (Te 54; for resonances, Al²⁷). For $p-\gamma$ coincidence measurements at $E_\alpha=7.8$ Mev yielding γ -decay modes of four lowest Mg^{26} levels, En 54a. Also Br 55b.

III. $\text{Mg}^{25}(n,\gamma)\text{Mg}^{26}$ $Q_m=11.118$

Cross section, Hu 55c.

Gamma rays from thermal neutron capture in natural magnesium observed with a pair spectrometer (Ki 51, Ca 56) and with a two-crystal scintillation spectrometer (Br 56e). From neutron binding-energies of Mg^{25} , Mg^{26} , and Mg^{27} , all transitions with $E_\gamma > 7.4$ Mev must be assigned to Mg^{26} . Several other transitions fit well between known levels of Mg^{26} . Energies, intensities, and proposed assignments in Table IX.

IV. $\text{Mg}^{25}(n,n)\text{Mg}^{25}$ $E_b=11.118$

Resonances in total cross section of samples enriched in Mg^{25} observed at $E_n=20$ kev ($\Gamma \sim 1$ kev), 81 kev ($\Gamma \sim 9$ kev), and 101 kev ($\Gamma \sim 10$ kev) (Ta 56).

For Mg^{25} levels observed, under Mg^{25} .

V. $\text{Mg}^{25}(d,p)\text{Mg}^{26}$ $Q_m=8.893$

From magnetic analysis at $E_d=1.8$ Mev (using enriched targets), Q value determined as 8.880 ± 0.012 Mev, while Mg^{26} levels are found at 1.825 ± 0.015 , 2.972 ± 0.010 , 3.969 ± 0.010 , 4.353 ± 0.011 , 4.863 ± 0.011 , 4.924 ± 0.011 , 5.270 ± 0.011 , 5.322 ± 0.011 , 5.502 ± 0.011 ,

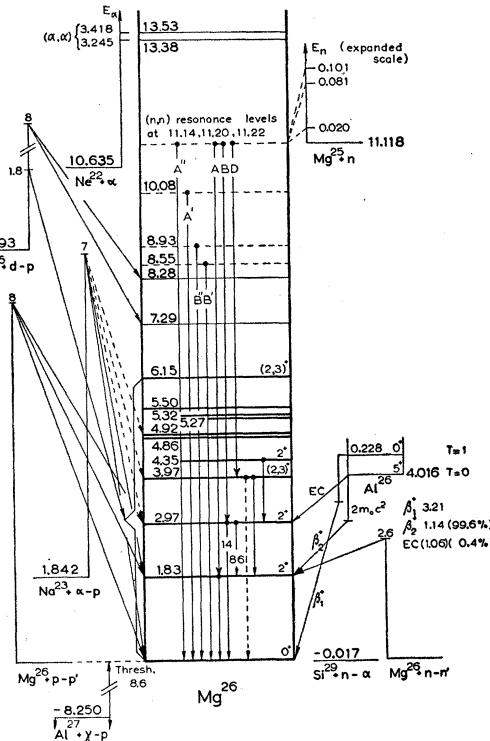


FIG. 9.

and 6.147 ± 0.011 Mev (En 52). Levels from Al absorption or nuclear emulsion methods, En 54a, also Kr 53a.

Angular distribution study at $E_d=8$ Mev indicates neutron orbital angular momentum $l_n=0$ associated with transitions to the 2.97-, 3.97-, 4.35-, and 6.15-Mev levels ($J=2^+$ or 3^+) and both $l_n=0$ and $l_n=2$ with transitions to 1.83-Mev level. Two levels at 7.29 ± 0.06 and 8.28 ± 0.06 Mev found (Ho 53).

Computation of (d,p) reduced widths, Fu 54.

VI. $Mg^{26}(n,n')Mg^{26}$

Inelastic scattering of 2.56-Mev neutrons on natural magnesium gives a 1.820 ± 0.018 -Mev γ ray which must be assigned to Mg^{26} (Da 56c). Also Sc 54d, Ra 55, Pa 55. Resonances, under Mg^{27} .

VII. $Mg^{26}(p,p')Mg^{26}$

Magnetic analysis at $E_p=8$ Mev gives levels at 1.83 ± 0.02 and 2.96 ± 0.02 Mev (Ha 52), also En 54a, Fi 54.

VIII. $Al^{26}(\beta^+)Mg^{26}$ See Al^{26} .

IX. $Al^{27}(\gamma,p)Mg^{26}$ $Q_m = -8.250$

Threshold and cross section, En 54a, also Da 56d, Mo 55.

X. $Si^{29}(n,\alpha)Mg^{26}$ $Q_m = -0.017$

Not observed.

GENERAL REMARKS

For jj -coupling computation of excitation energy of first Mg^{26} level, Th 56.

Angular distribution measurements of protons from $Mg^{25}(d,p)Mg^{26}$ reaction limit spin of the 4.35-Mev level to 2^+ or 3^+ . The 3^+ possibility, however, can be eliminated because this level belongs to the same isobaric spin triplet as the 2^+ 4.55-Mev level in Al^{26} .

Same reasoning can be applied to Mg^{26} first level. The 2^+ assignment found from unique second-forbidden character of $Al^{26}(\beta^+)$ transition to this level (see Al^{26} Reaction Ia) strengthened by 2^+ assignment to analogous level at 2.07 Mev in Al^{26} .

Al^{26}

(Fig. 10)

I. (a) $Al^{26}(\beta^+)Mg^{26}$ $Q_m = 4.016$

Half-life is about 10^6 yr as estimated from $Mg^{25}(d,n)Al^{26}$ yield (Si 54). About 5×10^4 yr would follow from known β^+ end point and an estimated $\log ft = 13$, (En 54c, Ka 55).

Main β^+ branch proceeds to first level in Mg^{26} at 1.83 Mev. The β^+ end point measured by scintillation spectrometer as ~ 1 Mev (Si 54), 1.17 ± 0.05 Mev

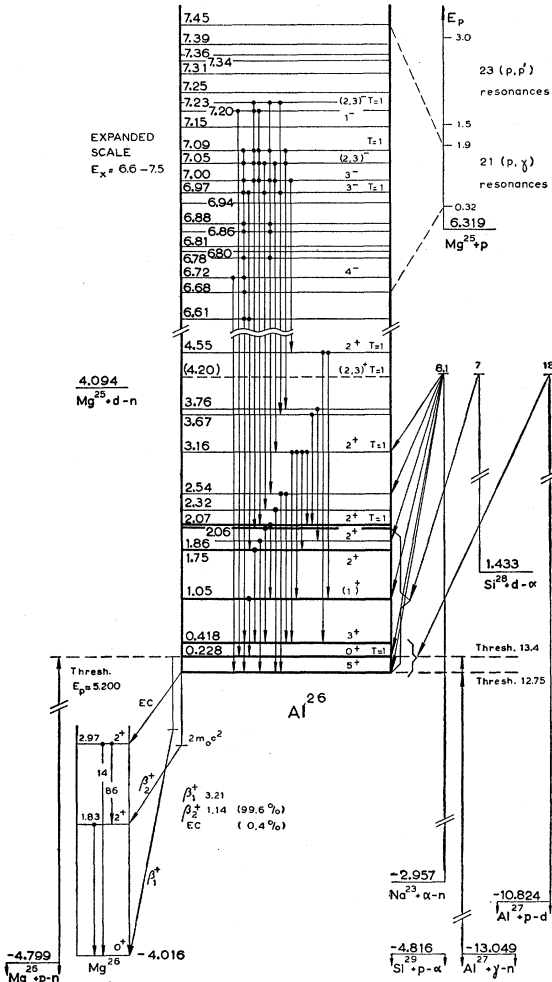


FIG. 10.

(La 55), and 1.14 ± 0.01 Mev (Fe 56), and by Al absorption as 1.30 ± 0.15 Mev (Ha 55b). Shape of β^+ spectrum is unique second forbidden (La 55, Fe 56), which determines spin of first Mg^{26} level (which should be 2^+ or 3^+ from $Mg^{25}(d,p)Mg^{26}$ angular distribution measurements) as 2^+ , and that of Al^{26} ground state [$a (d_{5/2}^{-1}, d_{5/2}^{-1})$ state with $J \leq 5$ and positive parity] as 5^+ . The γ -ray de-exciting first Mg^{26} level measured as 1.9 Mev (Si 54), 1.76 ± 0.1 Mev (La 55), 1.82 Mev (Ha 55b), and 1.84 ± 0.01 Mev (Fe 56). It is in coincidence with β^+ (Ha 55b, Fe 56).

A weak branch proceeds to 2.97-Mev Mg^{26} level, probably by electron capture. A 2.91-Mev γ ray observed with intensity 0.004 relative to that of 1.82-Mev γ ray (Ha 55b). Also a 1.1-Mev γ ray found in coincidence with 1.82-Mev γ ray (Fe 56). A reported 0.717-Mev γ ray (Ha 55b) which cannot be fitted in the Mg^{26} level scheme is probably instrumental (Fe 56).

(b) $Al^{26m}(\beta^+)Mg^{26}$ $Q_m = 4.244$

Half-life averaged from three measurements (6.49 ± 0.10 sec Ka 51, 6.68 ± 0.11 sec Hu 54b, 6.5 ± 0.1 sec

Ha 54a) is 6.55 ± 0.06 sec, in agreement with determinations of 6.47 and 6.40 sec (Gr 54).

The β^+ spectrum is simple and Fermi plot is straight (Ka 55, El 55). End point measured by magnetic spectrometer, 3.20 ± 0.05 Mev (Ka 55), and 3.21 ± 0.03 Mev (El 55), and by Al absorption, 3.2 ± 0.1 Mev (Ha 54a). Older absorption and cloud-chamber determinations, En 54a. No γ rays observed. An upper limit of 0.01% given for potential β^+ branch to 1.83-Mev Mg²⁶ level (Ma 55).

Initial state of β^+ decay is 228 kev first level of Al²⁶, which is $T_z=0$ member of $J=0^+$ $T=1$ isobaric spin triplet (see Reaction X). The ft value of this superallowed $0^+ \rightarrow 0^+$ decay can be used for a determination of the Fermi interaction constant g_F (En 54c, Ka 55).

Discussions of isobaric spin triplets under Mo 54, Wi 56a.

II. Na²³(α, n)Al²⁶ $Q_m = -2.957$

From observation of slow neutron thresholds and from neutron energy determinations with a proton recoil proportional counter, $Q = -2.9 \pm 0.2$ Mev and Al²⁶ levels are found at 0.3, 1.0, 1.4, 1.8, 2.5, and 2.9 Mev, all ± 0.2 Mev. Threshold for positron emission corresponds to $Q = -3.2$ Mev, indicating that 0.228-Mev level is positron emitter (Do 56). Also, En 54a.

III. Mg²⁵(p, γ)Al²⁶ $Q_m = 6.319$

Resonances from enriched target bombardments, observed in γ and/or β^+ yield, in Table XIV. Branching of γ decay to Al²⁶ ground state and first level varies from resonance to resonance with corresponding large

variation of β^+/γ ratio. Absence of β^+ emission at 437- and 958-kev resonances is notable. Proton resonance energies averaged to obtain corresponding Al²⁶ excitation energies. Also in Table XIV are resonance strengths $(2J+1)\Gamma_p\Gamma_\gamma/(\Gamma_p+\Gamma_\gamma)$ as observed from thick target γ -ray yields.

Natural magnesium targets, En 54a, Sm 57.

Spectra of γ rays with relative intensities measured at 317-, 392-, 437-, 496-, 571-, and 597-kev resonances (Kl 54 superseding Kl 54a), and at 686-, 724-, 777-, 816-, 934-, and 959-kev resonances (Gr 56e), while observed γ rays (without relative intensities) also given at 724- and 959-kev resonances (Ka 55). Gamma-gamma coincidence measurements (Ka 55, Gr 56e), and γ -ray angular distribution measurements, (Gr 56e).

Strong direct transitions to Al²⁶ ground state only observed at 437-kev resonance (Kl 54), while first level at 228 kev is fed directly only at 934-kev resonance (Gr 56e). Although positrons are observed at 1191-kev resonance, decay proceeds by at least 99% through Mg²⁵(p, p') reaction to first level in Mg²⁵ (Ka 55). Besides other levels found from the Si²⁸(d, α)Al²⁶ reaction (Reaction X), new levels at 2.09, 2.32, 2.54, 3.16, 3.67, 3.76, and 4.55 Mev are necessary to explain observed single and coincidence γ -ray spectra (Gr 56e). Also a 5.16-Mev level reported (not indicated in Fig. 10) (Br 56i). Some γ -ray energies given with an accuracy surpassing that of the level differences found from Si²⁸(d, α)Al²⁶ reaction. The (2) \rightarrow (0) transition is given as 419 ± 3 kev (En 54c) and 416 ± 4 kev (Ka 55), the (3) \rightarrow (1) transition as 820 ± 4 kev (En 54c) and 833 ± 6 kev (Ka 55), and the (6) \rightarrow (3) transition as 1002 ± 10 kev (En 54c) and 1022 ± 6 kev (Ka 55).

TABLE XIV. Resonances in Mg²⁵(p, γ)Al²⁶.

Observed: Reference:	γ Kl 54	β^+ Ta 54b	γ and β^+ Hu 55	γ and β^+ Ka 55	γ Gr 56e	E_γ (Al ²⁶) (Mev)	$(2J+1)\frac{\Gamma_p\Gamma_\gamma}{\Gamma_p+\Gamma_\gamma}$ (ev) Kl 54 Gr 56e	J, π, T ^a
E_p (lab): (kev)								
	321		316.7 \pm 0.7			6.608	0.3	
	395	388	391.5 \pm 0.5			6.680	0.6	
	441		436.5 \pm 0.4			6.723	0.7	4 $^-$
	501	494	495.6 \pm 0.6			6.780	0.8	
	518	510	513.4 \pm 0.7			6.797	0.8	
			530.4 \pm 0.7			6.813		
	580	563				6.856	1.5	
	607	588				6.877	1.1	
	667	650				6.936	0.3	
	688	683		697	675	6.966	1.6	3 $^-$ ($T=1$)
all ± 15		722		730	720	6.999	2.8	3 $^-$ ($T=0$)
		777			777	7.050	1.9	(2,3) $^-$ ($T=0$)
		812			820	7.088	1.2	$\pi = -$ ($T=1$)
		880		890		7.154		
		928		933	940	7.201	1.5	1 $^-$ ($T=0$)
				958	960	7.225	3.8	(2,3) $^-$ ($T=1$)
		986		990		7.253		
		1043		1046		7.307		
		1081		1086		7.344		
		1098		1105		7.362		
		1132				7.392		
		1197		1185		7.448		
	all $\pm 10-15$							

^a En 54c for assignment at 437-kev resonance, Gr 56e for all others.

Prominent modes of decay of Al^{26} levels up to $E_x = 4.6$ Mev in Fig. 10. Qualitative remarks concerning γ -ray branching percentages, Kl 54, En 54c, Gr 56e. Most spins in Fig. 10 found from γ -ray angular distribution measurements (Gr 56e), some spins and isobaric spins from comparison with Mg^{26} level scheme. Spin assignment to level (3) (probably 1^+) from intensity considerations. Analog of $T=1$, $J=2^+$ or 3^+ level at 3.97 Mev in Mg^{26} not observed. It should have an excitation energy of about 4.20 Mev.

Negative parity resonance levels are each observed to decay predominantly ($\geq 75\%$) either to $T=0$ or to $T=1$ levels. At 686-kev resonance decay proceeds even for 100% to $T=0$ levels. Explained by assuming that resonance levels have T as a fairly good quantum number and that strong transitions from these states are E1 transitions, satisfying the isotopic spin selection rule for self-conjugate nuclei $\Delta T=\pm 1$. Isobaric spins of resonance levels in Table XIV found this way (Gr 56e).

Angular distributions observed at 934-kev $J=1^-$ resonance can only be explained by assuming a large (16 times larger than computed from barrier penetrability alone) f -wave to p -wave ratio (Gr 56e).

IV. $\text{Mg}^{25}(p,n)\text{Al}^{26}$ $E_b = 6.319$ $Q_m = -5.029$

Resonances, En 54a.

Threshold measurements, under Al^{25} .

V. $\text{Mg}^{25}(p,p'\gamma)\text{Mg}^{25}$ $E_b = 6.319$

Yield of 1.96-Mev, 1.61-Mev, 0.98-Mev, and (0.40-Mev + 0.58-Mev) γ rays resulting from inelastic proton scattering measured in $E_p = 1.5$ –3.0-Mev region showing some 23 resonances (not tabulated) (Go 56). Also Ka 55.

VI. $\text{Mg}^{25}(d,n)\text{Al}^{26}$ $Q_m = 4.094$

Thick-target measurements with nuclear emulsions, En 54a.

VII. $\text{Mg}^{26}(p,n)\text{Al}^{26}$ $Q_m = -4.799$ $\text{Mg}^{26}(p,n)\text{Al}^{26m}$ $Q_m = -5.027$

A slow-neutron threshold observed at $E_p = 5.200 \pm 0.010$ Mev corresponding to $Q = -5.006 \pm 0.010$ Mev. No threshold corresponding to Al^{26} ground state found (Ki 55a).

Neutron threshold measured as $E_p = 5.25 \pm 0.1$ Mev (Sc 54b).

VIII. $\text{Al}^{27}(\gamma,n)\text{Al}^{26}$ $Q_m = -13.049$

Threshold for neutron emission measured as 12.75 ± 0.20 Mev (Sh 51a), and threshold for production of Al^{26m} activity as 14.0 ± 0.4 Mev (Mc 49) and 13.4 ± 0.2 Mev (Ha 54a).

Excitation curves, En 54a, Ha 54a, Mo 55.

IX. $\text{Al}^{27}(p,d)\text{Al}^{26}$ $Q_m = -10.824$

At $E_p = 18$ Mev, angular distribution of deuterons proceeding to one or more of the three lowest Al^{26} states corresponds to $l_n = 2$ (Re 56, also Se 56).

X. $\text{Si}^{28}(d,\alpha)\text{Al}^{26}$ $Q_m = 1.433$

At deuteron energies between 5 and 7 Mev and $\theta = 90^\circ$, ground-state Q value measured by magnetic analysis as 1.416 ± 0.008 Mev. Lower energy groups observed with Q values of 0.998 ± 0.008 , 0.364 ± 0.008 , -0.334 ± 0.008 , (-0.430 ± 0.015) , and -0.648 ± 0.008 Mev, corresponding to Al^{26} levels at 0.418, 1.052, 1.750, (1.856), and 2.064 (Mev). It is assumed that all observed states have $T=0$ (Br 54). Transition violating isobaric spin selection rule also found to lowest $T=1$ level, for which $E_x = 228 \pm 5$ kev was measured. Its intensity varies, as a function of E_d and θ , from 2 to 65% of the ground-state transition (Br 56d).

XI. $\text{Si}^{29}(p,\alpha)\text{Al}^{26}$ $Q_m = -4.816$

Not observed.

Si^{26}

(not illustrated)

A 1.7-sec half-life observed from bombardment of aluminum with 23-Mev protons, which might perhaps be attributed to Si^{26} produced through $\text{Al}^{27}(p,2p)$ reaction (Ty 54).

Mg^{27}

(Fig. 11)

I. $\text{Mg}^{27}(\beta^-)\text{Al}^{27}$ $Q_m = 2.594$

Half-life averaged from four determinations (En 54a) is 9.45 ± 0.03 min.

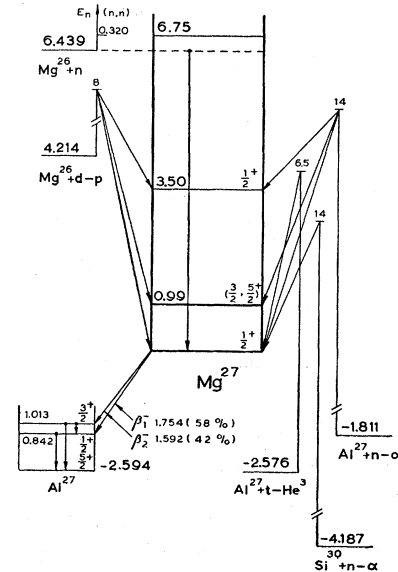


TABLE XV. The $Mg^{27}(\beta^-)Al^{27}$ decay.

Reference:	Da 54a	Ly 56	Transition:
Method:	Lens spectrometer	Scint. spectrom.	
E_{β_1} (Mev)	1.754 ± 0.011 (58%)		$Mg^{27} \rightarrow (1)$
E_{β_2} (Mev)	1.592 ± 0.022 (42%)		$Mg^{27} \rightarrow (2)$
E_{γ_1} (Mev)	0.834 ± 0.008	0.834 (70%)	(1) $\rightarrow (0)$
E_{γ_2} (Mev)	1.015 ± 0.007	1.015 (30%)	(2) $\rightarrow (0)$
E_{γ_3} (Mev)	^a	0.175 ± 0.010 (0.66%)	(2) $\rightarrow (1)$

^a Intensity of internal conversion electrons $<10^{-3}$ per disintegration.

The β^- decay proceeds to two lowest Al^{27} excited states. Both levels are deexcited mainly by direct γ transitions to Al^{27} ground state, although a weak transition $(2) \rightarrow (1)$ has also been observed. Table XV gives recent determinations of β^- and γ energies and intensities, En 54a for older work. The two main γ rays are not coincident (Ma 54a, Ly 56); γ_1 is coincident with β_1^- , and γ_2 with β_2^- (Ma 54a). The two β^- transitions are allowed: $\log ft = 4.75$ and 4.78 for β_1^- and β_2^- , respectively. Computation of matrix elements for these transitions, Fe 55. Also Na 56a.

A reported ground-state transition (Da 53) was later shown to be absent (Da 54a, Ma 54a, Ko 54a).

II. $Mg^{26}(n,\gamma)Mg^{27} Q_m = 6.439$

Cross sections, En 54a and Hu 55c. A recent measurement of thermal neutron activation cross section (25 ± 2 mb; Ly 56) appreciably smaller than older values.

Energies of a number of γ rays from capture of thermal neutrons in natural magnesium determined by pair spectrometer (Ki 51, Ki 53a) (Table IX). Line F_1 ($E_\gamma = 6.440 \pm 0.008$ Mev) results from capture in Mg^{26} and represents ground-state transition.

III. $Mg^{26}(n,n)Mg^{26} E_b = 6.439$

For samples enriched in Mg^{26} , a resonance in total cross section observed at $E_n \sim 320$ kev (Ta 56).

IV. $Mg^{26}(d,p)Mg^{27} Q_m = 4.214$

From magnetic analysis at $E_d = 1.8$ Mev, Q value measured as 4.207 ± 0.006 Mev and a level observed at $E_x = 0.987 \pm 0.006$ Mev (En 52a). Second group with Q value of 0.71 ± 0.05 Mev corresponding to level at $E_x = 3.50$ Mev found by Al absorption at $E_d = 8$ Mev (Ho 53).

Angular distributions measured at $E_d = 8$ Mev yield $l_n = 0$ for transitions to Mg^{27} ground state and to second level, and $l_n = 2$ for transition to first level (Ho 53). Older work, En 54a, also Kr 53a. Computation of reduced widths, Fu 54.

Ratio of stripping to compound nucleus formation measured by comparing yields of Mg^{27} and Na^{24} activities observed from deuteron bombardment of magnesium to those from neutron bombardment of aluminum. Ratio has a maximum of 8–9 for $E_d = 1$ –2 Mev (Ne 56).

V. $Al^{27}(n,p)Mg^{27} Q_m = -1.811$

Proton spectra and angular distributions at $E_n = 14$ Mev (Ha 56a, Ov 56, Al 57a, Co 56b). Transitions observed to known Mg^{27} levels, some indication of transitions to 5.7- and 6.9-Mev levels (Ha 56a). Also En 54a.

VI. $Al^{27}(t,He^3)Mg^{27} Q_m = -2.576$

Observed (En 54a).

VII. $Si^{30}(n,\alpha)Mg^{27} Q_m = -4.187$

Cross section, En 54a.

Al²⁷

(Fig. 12)

I. $Na^{23}(\alpha,n)Al^{26} E_b = 10.092$

Resonances, En 54a. Q value, under Al^{26} .

II. $Na^{23}(\alpha,p\gamma)Mg^{26} E_b = 10.092$

Partially resolved resonances in $E_\alpha = 1.8$ –3.7-Mev region observed in yield of 1.83-Mev γ ray. They correspond to Al^{27} levels at 11.75, 11.91, 12.07, 12.23, 12.27,

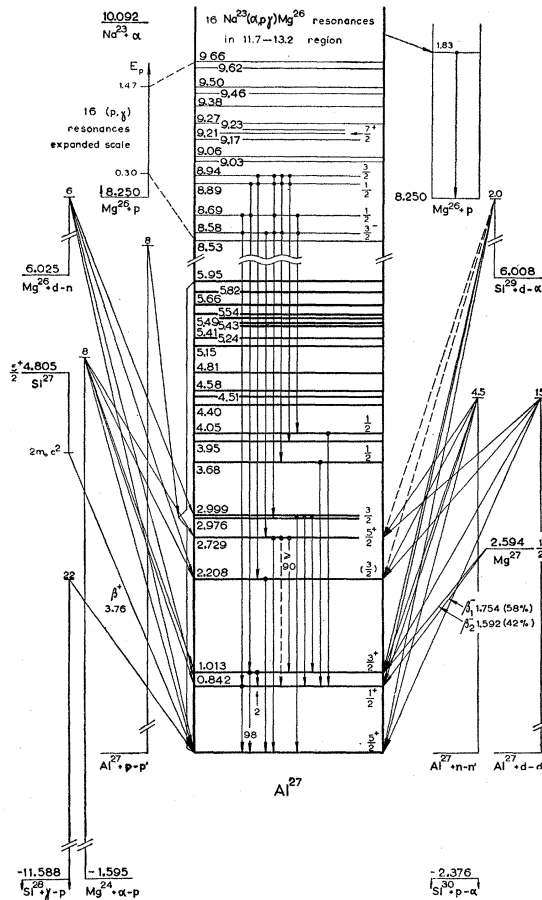


FIG. 12.

TABLE XVI. Resonances in $Mg^{26}(p,\gamma)Al^{27}$.

Reference:	Ta 46	Kl 54	Ru 54a	Hu 55	$E_x (Al^{27})$ (Mev)	$\frac{\Gamma_p \Gamma_\gamma}{\Gamma_p + \Gamma_\gamma}$ (ev)	J, π
E_p (lab) (kev)	290 ± 3	300 ± 15			8.529		
	336 ± 1.5	340 ± 15	343	338.5 ± 0.5	8.575	0.4 ± 0.1 b	$3/2^-$ a, b
	451 ± 2	458 ± 15	450	454.2 ± 0.3	8.687	1.4 ± 0.3 b	$1/2$ b
			662		8.887	0.7 ± 0.2 b	$1/2$ b
			720		8.943	0.21 ± 0.05 b	$3/2$ b
			813		9.033		
			840		9.059		
			954		9.169		
			992		9.205		$7/2^+$ c
			1015		9.227		
			1056		9.267		
			1172		9.379		
			1255		9.459		
			1295		9.497		
			1425		9.622		
			1465		9.661		
			all ± 10 kev				

a Hu 56.
b Va 56d, En 56b.
c Al 57.

12.34, 12.46, 12.68, 12.71, 12.78, 12.84, 12.87, 12.99, 13.07, and 13.14 Mev (Te 54).

III. $Mg^{24}(\alpha, p)Al^{27} Q_m = -1.595$

Resonances under Si²⁸. From comparison of resonances in $Mg^{24}(\alpha, p)Al^{27}$ and $Al^{27}(p, \alpha)Mg^{24}$, $Q = -1.613 \pm 0.010$ Mev (Ka 52).

Direct measurement at $E_\alpha = 8$ Mev with a proportional counter, $Q = -1.63 \pm 0.07$ Mev, and Al^{27} levels at 0.85, 1.06, 2.17, and 2.64 Mev, all ± 0.04 Mev (Gr 56d). Also, Br 55b.

IV. (a) $Mg^{25}(d, n)Al^{26} E_b = 17.143$ (b) $Mg^{25}(d, p)Mg^{26} E_b = 17.143$

Possible resonance, En 54a.

V. $Mg^{26}(p, \gamma)Al^{27} Q_m = 8.250$

Resonances in γ -ray yield from enriched target bombardments (Kl 54, Ru 54a, Hu 55) in Table XVI, in which also those resonances observed by Tangen (Ta 46) from natural magnesium bombardments which can be assigned to Mg^{26} . Corresponding Al^{27} excitation energies computed from weighted average of resonant proton energies. Thirty-five resonances reported in the $E_p = 0.80$ – 2.36 -Mev region (Al 57).

Gamma-ray spectra, γ -ray relative intensities, angular distributions, and γ - γ coincidences measured at 338, 454, 662-, and 720-kev resonances (Va 56d, En 56b), and at some unspecified resonance (Al 57). Resonance spins found from this work in Table XVI.

Parity of 338-kev resonance obtained from polarization measurement of 7.7-Mev γ ray de-exciting the resonance to level (1), which determined character of γ ray as E1 (Hu 56).

Spins of a number of lower levels

0.842 Mev $J = 1/2$, 2.976 and/or 2.999 Mev $J = 3/2$, 2.208 Mev $J = (3/2)$, 3.68 Mev $J = 1/2$, 2.729 Mev $J = 5/2$, 4.05 Mev $J = 1/2$.

Energies of γ rays de-exciting first and second Al^{27} levels: 0.840 ± 0.006 Mev and 1.012 ± 0.008 Mev, Va 56d, En 56b.

Angular distribution measurements (Al 57) yield $J = 3/2$ for 1.013-Mev level, and, very probably, $J = 1/2$ for 0.842-Mev level. The 2.729-Mev level decays for more than 90% to 1.013-Mev level. Angular correlations measured at 986-kev resonance in agreement with $J = 7/2^+$ or $3/2^+$ for the resonance level and $5/2^+$ for 2.729-Mev level. The $7/2^+$ assignment to the resonance is favored because no direct transitions to 0.842- and 1.013-Mev levels observed (intensity at most 3% of ground-state transition).

Also En 54a, Sm 54.

VI. $Mg^{26}(d, n)Al^{27} Q_m = 6.025$

Nuclear emulsion work at $E_d = 1.0$ and 6.0 Mev gives Al^{27} levels at 1.0, 2.3, 2.9, 6.8, 8.2, 9.5, and 10.0 Mev. From angular distribution measurements $l_p = 0$ assigned to transitions proceeding to 6.8-Mev level and $l_p = 1$ to those proceeding to 8.2-Mev level (Tr 56).

Also En 54a.

VII. $Mg^{27}(\beta^-)Al^{27}$ See Mg^{27} .

VIII. $Al^{27}(n, n')Al^{27}$

Numerous authors have published γ -ray energies and intensities from inelastic neutron scattering measured with a scintillation spectrometer, Table XVII. Existence of 1.20-Mev γ ray reported at $E_n = 3.2$ Mev seems doubtful because not found in careful work at $E_n = 2.56$ Mev. The 1.91-Mev γ ray observed at $E_n = 3.7$ Mev also

TABLE XVII. Gamma rays from $\text{Al}^{27}(n,n')\text{Al}^{27}$.

Reference: E_n (Mev): Transition	Da 56c 2.56	σ (mb)	KI 54 2.7	Sc 54d 3.2	Ro 55a 3.7	Gr 55d 4.5
	E_γ (Mev)		E_γ (Mev)	E_γ (Mev)	E_γ (Mev)	E_γ (Mev)
(2)→(1)	0.166±0.003	1.6±0.4		a		
(1)→(0)	0.840±0.008	64±7	0.850±0.025	0.89±0.03	0.835±0.01	0.84±0.02
(2)→(0)	1.017±0.010	142±13	1.025±0.03	1.05±0.03	1.02±0.01	1.02±0.03
(3)→(2)?				1.20±0.05 ^b		
(4)→(2)				1.70±0.08	1.72±0.02	
(4)→(1)?					1.91±0.02	
(3)→(0)	2.21±0.02	87±8	2.23±0.04	2.20±0.18	2.22±0.03	2.27±0.08

^a The 0.05±0.02-Mev γ ray which is also reported might perhaps be identified with 31 kev (1)→(0) transition in Al^{28} following neutron capture.

^b Might be pair peak of 2.21-Mev γ ray.

doubtful because it would correspond to a $5/2^+ \rightarrow 1/2^+$ E2 transition.

Thresholds for 0.84-, 1.01-, and 2.21-Mev γ rays are equal, within experimental limits, to γ -ray energies, proving these are ground-state transitions (KI 54). Also En 54a, Gr 55b, Gr 55d, Pa 55, Ra 55, Ra 55a, Ta 55, Be 56, Cr 56a, Mo 56c, Sm 56, We 56a.

Angular distributions of elastically scattered neutrons, Li 55a, Be 56, Cu 56, Do 56a, Hi 56a.

IX. $\text{Al}^{27}(p,p')\text{Al}^{27}$

Levels found by magnetic or electrostatic analysis in Table XVIII. Excitation energies reported in Re 52 consistently higher by an amount slowly increasing up to 75 kev for the highest levels than the values found from high-resolution work given in Br 54b. Groups corresponding to levels reported in Re 52 at 4.996 and

5.107 Mev are probably from carbon contamination on front and back side of target (Br 54b). Also En 54a, Ma 54b.

Yield of 0.84- and 1.01-Mev γ rays from inelastic proton scattering measured in $E_p=1.40-2.77$ -Mev region (Pa 54, Br 57a). Resonances under Si²⁸. A $P_2(\cos\theta)$ term observed in angular distribution of 1.01-Mev γ ray, showing that spin of 1.01-Mev level is not 1/2. This level is de-excited for 2.2% by a 0.175-Mev cascade transition. Angular correlation of 0.175- and 0.84-Mev γ rays shows no significant deviation from isotropy pointing to a spin $J=1/2$ for 0.84-Mev level (Br 57a). An upper limit of 10^{-10} sec is found for half-life of these γ transitions from recoil techniques (Sw 56).

Angular distributions of protons scattered elastically (En 54a, Da 54, Hi 55, Sh 56, Da 56a, Ge 56a), and inelastically (no groups resolved (Gu 54)).

X. $\text{Al}^{27}(d,d')\text{Al}^{27}$

Low-resolution analysis of inelastically scattered deuterons, En 54a.

Angular distributions for transitions to 2.21- and 2.73-Mev levels at $E_d=15$ Mev (Ha 56c), and for transitions to 2.21 and 2.73 levels and to doublet at 2.99 Mev at $E_d=9$ Mev (Hi 56b). Angular momentum transfer connected with these three transitions determined as $l_d=2$ fixing parity of corresponding levels as positive (Hi 56b).

Elastic scattering angular distribution at $E_d=14$ Mev, Go 50.

XI. $\text{Al}^{27}(\alpha,\alpha')\text{Al}^{27}$

Elastic scattering angular distributions at $E_\alpha=19$ and 40 Mev, Bl 55a, Ig 56, Bl 56a. Inelastic scattering to first two Al^{27} levels (unresolved) also observed (Bl 56a).

XII. $\text{Si}^{27}(\beta^+)\text{Al}^{27}$ See Si^{27}

XIII. $\text{Si}^{28}(\gamma,p)\text{Al}^{27}$ $Q_m=-11.588$

Cross section, Jo 55, Mo 55a.

No activity with a half-life in the μ sec or msec range found from bombardment of natural silicon with 22-Mev bremsstrahlung (Ve 56a).

TABLE XVIII. Levels in Al^{27} from $\text{Al}^{27}(p,p')\text{Al}^{27}$.

Reference: E_p (Mev): Angle: Method:	Sh 51	Re 52	Do 53	Br 54b	Va 57d
	magn. analysis	magn. analysis	electrostat. analysis	magn. analysis	magn. analysis
E_x (Mev)	0.82 1.04 2.23 2.75	0.844 1.016 2.259 2.782	0.843±0.002	0.842 1.013 2.213 2.732	0.842±0.003 1.013±0.003 2.205±0.004 2.727±0.004
	3.046 3.736 4.018 4.115 4.473 4.575 4.647 4.875 4.996 5.107 5.220 5.341 5.501 5.565 5.620 5.736 all ±0.020		3.001 3.677 3.954 4.054 4.403 4.505 4.576 4.807 5.150 5.242 5.410 5.425 5.491 5.544 5.659 5.821 5.951	2.975±0.004 2.998±0.004 3.677 3.954 4.403 4.505 4.576 4.807 5.150 5.242 5.410 5.425 5.491 5.544 5.659 5.821 5.951	
	all ±0.006		all ±0.006		

XIV. $\text{Si}^{29}(d,\alpha)\text{Al}^{27}$ $Q_m = 6.008$

Magnetic analysis of α particles observed at 90° at $E_d = 1.8$ and 2.0 Mev from targets enriched in Si^{29} content yields ground-state Q value of 5.994 ± 0.011 Mev and levels in Al^{27} at 0.837 ± 0.016 and 1.007 ± 0.013 Mev, and possibly at 2.21 ± 0.03 and 2.74 ± 0.02 Mev (Va 52).

XV. $\text{Si}^{30}(p,\alpha)\text{Al}^{27}$ $Q_m = -2.376$

Not observed.

 Si^{27}

(not illustrated)

I. $\text{Si}^{27}(\beta^+)\text{Al}^{27}$ $Q_m = 4.805$

Three measurements of half-life with errors of at most 0.1 sec in rather bad agreement (4.92 ± 0.1 sec El 41; 4.45 ± 0.05 sec Su 53; 4.05 ± 0.10 sec Hu 54). Average value is 4.46 ± 0.18 sec.

The β^+ end point measured by cloud chamber as 3.74 Mev (Mc 40) and 3.54 ± 0.1 Mev (Ba 40), and by scintillation spectrometer as 3.48 ± 0.10 Mev (Bo 51), and 3.76 ± 0.08 Mev (Hu 54). No γ rays reported. Decay is apparently superallowed ($\log ft = 3.6$) determining spin and parity of Si^{27} as $5/2^+$.

II. $\text{Mg}^{24}(\alpha,n)\text{Si}^{27}$ $Q_m = -7.183$

Observed, En 54a.

III. $\text{Al}^{27}(p,n)\text{Si}^{27}$ $Q_m = -5.588$

Recent measurements of threshold are $E_p = 5.792 \pm 0.010$ Mev (Ki 55a, superseding Ki 53) and $E_p = 5.798 \pm 0.008$ Mev (Ma 55a).

Angular distribution measured at $E_p = 23$ Mev (Co 55b).

IV. $\text{Si}^{28}(\gamma,n)\text{Si}^{27}$ $Q_m = -17.176$

Threshold determined as 16.8 ± 0.4 Mev (Mc 49) and 16.9 ± 0.2 Mev (Su 53). Cross section, En 54a, Ka 54, Mo 55a. No activity in the μ sec or msec range observed from bombardment of natural silicon with 22-Mev bremsstrahlung (Ve 56a).

V. $\text{Si}^{28}(p,d)\text{Si}^{27}$ $Q_m = -14.951$

Cross section, Se 56.

 Mg^{28}

(not illustrated)

I. $\text{Mg}^{28}(\beta^-)\text{Al}^{28}$ $Q_m = 1.810$

Mg^{28} has been produced through $\text{Mg}^{26}(\alpha,2p)$, $\text{Si}^{30}(\gamma,2p)$, $\text{Si}^{30}(p,3p)$, and other spallation reactions, and through $\text{Mg}^{26}(t,p)$ reaction.

Half-life, averaged from six measurements (En 54a, Sh 54d), in good mutual agreement, 21.43 ± 0.11 hr.

TABLE XIX. Gamma rays from $\text{Mg}^{28}(\beta^-)\text{Al}^{28}$.

Reference:	Sh 54d		Wa 53		Iw 53
	E_γ (Mev)	Rel. int.	E_γ (Mev)	Rel. int.	E_γ (Mev)
γ_1	0.0319 ± 0.001	0.96	0.0322	(~ 0.70)	
γ_2	0.400 ± 0.01	0.31			0.391 ± 0.005
γ_3	0.949 ± 0.01	0.29			0.95
γ_4	1.346 ± 0.01	0.70			1.35

The β^- spectrum is simple and has allowed shape (Ma 53a, Ol 54). End point 0.40 ± 0.06 Mev (Sh 54d), 0.3 Mev (Jo 53), 0.39 ± 0.05 Mev (Wa 53) (all measured by Al absorption), 0.418 ± 0.010 Mev (Ma 53a), and 0.459 ± 0.002 Mev (Ol 54), latter two measured by magnetic spectrometer. $\log ft = 4.4$.

Four γ rays observed by scintillation spectrometer. Energy and intensity (in photons per disintegration) in Table XIX. Gamma rays γ_2 , γ_3 , and γ_4 coincident with γ_1 , and γ_2 with γ_3 . No measurable delay between γ_1 and γ_4 ($\tau < 2 \times 10^{-9}$ sec) (Sh 54d). Accepting more accurate γ -ray intensities in Sh 54d, conversion coefficient of γ_1 can be computed from intensities as $\alpha_K = 0.032 \pm 0.066$, which determines the character of γ_1 as M1.

From γ -ray energy and coincidence measurements, β^- decay proceeds to 1.37-Mev level in Al^{28} , which decays through 0.97- and 0.03-Mev levels. By the isobaric spin selection rule, excluding $\Delta T = \pm 1$, $0^+ \rightarrow 0^+$, β^- transitions, spin and parity of 1.37 Mev level determined as 1^+ . Assuming $J = 3^+$ for Al^{28} ground state and $J = 2^+$ for 0.03-Mev level then leaves possibilities $J = 0^+$ or 2^+ for 0.97-Mev level to explain absence of β^- -decay to this level and observed γ -ray branching from 1.37-Mev level.

 Al^{28}

(Fig. 13)

I. $\text{Al}^{28}(\beta^-)\text{Si}^{28}$ $Q_m = 4.648$

Half-life, averaged from three most accurate measurements (En 54a, Co 56), in good mutual agreement, is 2.28 ± 0.02 min.

The β^- spectrum is simple with allowed shape. Two most accurate magnetic spectrometer determinations of end point are 2.865 ± 0.010 Mev (Mo 52) and 2.878 ± 0.014 Mev (Ol 54). $\log ft = 4.9$.

Each β^- particle followed by one γ quantum. Best determinations of γ -ray energy are 1.782 ± 0.010 Mev (magn. spectrometer, Mo 52), and 1.769 ± 0.010 Mev (scint. spectrometer, Sh 54d). Also En 54a, Ma 54a, Na 54a, Na 56a.

II. $\text{Mg}^{25}(\alpha,p)\text{Al}^{28}$ $Q_m = -1.204$

From enriched-target measurement at $E_\alpha = 8$ Mev, with proportional counter for proton detection, Q value is -1.29 Mev. Levels in Al^{28} reported at 1.00 , 1.57 , 2.18 , 2.54 , and 2.96 Mev, all ± 0.04 Mev (Gr 56d). Also En 54a.

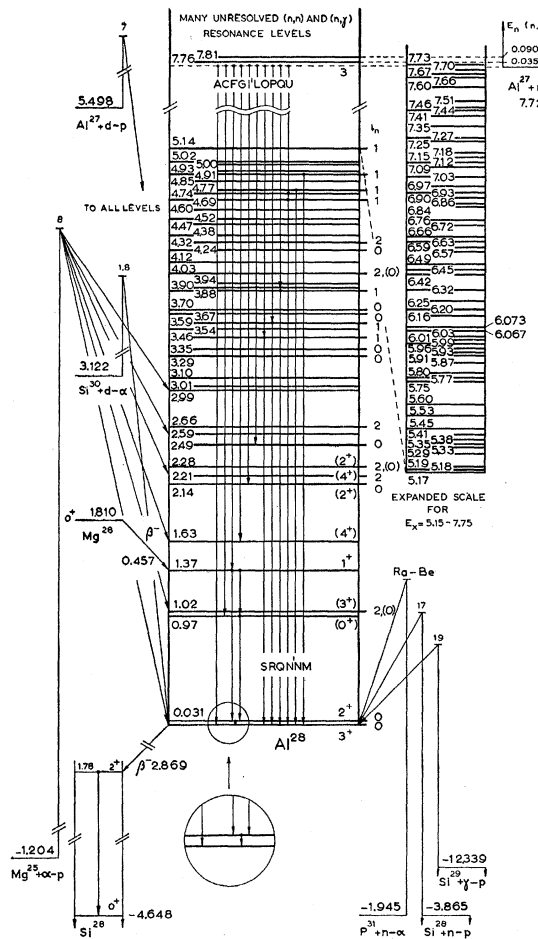


FIG. 13.

III. $\text{Al}^{27}(n,\gamma)\text{Al}^{28}$ $Q_m = 7.723$

Cross section, Hu 55c.

Twenty-nine γ rays resulting from capture of thermal neutrons in aluminum found by pair spectrometer (Ki 51, Ki 53d), Table XX. Strong γ -ray *A* represents ground-state transition. Its great intensity is a notable exception to rule that only E1 ground-state transitions are intense (Ki 52b). Impossible to fit other γ rays uniquely into the complicated Al^{28} level scheme. Lines *C*, *F*, *G*, *I'*, *J*, *L*, and all lower energy lines could be transitions from capturing state to known Al^{28} levels. Lines *B*, *B'*, *D*, *E*, *F'*, *G'*, *H*, *K*, and *L* cannot be explained this way but have to be transitions from level to ground or from level to level.

From $\text{Al}^{27}(d,p)\text{Al}^{28}$ reaction (see Table XXI) the parity of levels (17), (19), (22), (33), (35), (37), and (41) is negative. It is possible to explain many strong γ rays (e.g., *M*, *N*, *N'*, *O*, *P*, *Q*, *R*, *S*, *U*, *V*) of Table XX as E1 transitions to and from these levels (En 56d).

With two-crystal scintillation spectrometer, γ rays from thermal neutron capture observed with the following energies and relative intensities (in photons per 100 captures): $E_\gamma = 0.97 \pm 0.03$ Mev (10), 2.26 ± 0.03 Mev

(14), ~ 2.5 Mev (11), ~ 2.8 Mev (14), and ~ 3.1 Mev (17). Last three γ rays not resolved (Br 56e).

Also En 54a.

IV. $\text{Al}^{27}(n,n)\text{Al}^{27}$ $E_b = 7.723$

Cross section, Hu 55c. Resonances at $E_n = 35 \pm 2$ kev ($\Gamma = 1.2 \pm 0.5$ kev), and 90 ± 4 kev ($\Gamma = 7 \pm 2$ kev) have both $J = 3^+$ (Hu 55c, To 55a, Bl 56). In Cr 57, however, $J = 2^+$ is assigned to 35-kev resonance.

Angular distributions, Hu 55c, Hi 56a, Na 57.

V. $\text{Al}^{27}(d,p)\text{Al}^{28}$ $Q_m = 5.498$

Fifty proton groups corresponding to Al^{28} levels up to $E_x = 6.3$ found by high-resolution magnetic analysis ($\theta = 90^\circ$) at deuteron energies up to 2.1 Mev (En 51, En 52a, En 53a). Later work with still better resolution, at $E_d = 6$ and 7 Mev and at several angles of observation, 100 groups found in a region of excitation in Al^{28} up to neutron threshold (Bu 56). Ground-state Q value is 5.494 ± 0.008 Mev (En 52a, En 53a), and 5.502 ± 0.010 Mev (Bu 56).

Excitation energies of Al^{28} levels reported in Bu 56 in Table XXI. Corresponding Q values all have errors of 10 kev. Excitation energies might have errors ranging from 5 kev for lower to 10 kev for highest levels. Groups corresponding to levels above threshold for neutron emission of low intensity and not tabulated. Their positions correspond approximately to apparently unresolved resonances in Al^{27} total neutron cross section (Hu 55c).

Angular distributions covering the region from 5° to 60° measured at $E_d = 6$ Mev for transitions leading to levels (0) through (41) (En 56a, En 56). About half have stripping character, while the others are fairly isotropic. The l_n values of stripping distributions and corresponding reduced widths in relative measure (times $(2J+1)$) in Table XXI. For transitions to level (3), where $l_n = 2$ and $l_n = 0$ contributions are mixed, the $l_n = 0$ contribution is 12%. For levels (8) and (25) it

TABLE XX. Gamma rays from thermal neutron capture in aluminum (Ki 51, Ki 53d).

γ ray	Energy (Mev)	Intensity in photons per 100 captures γ ray	Energy (Mev)	Intensity in photons per 100 captures
<i>A</i>	7.724 ± 0.006	35	<i>L</i>	5.21 ± 0.02
<i>B</i>	7.34 ± 0.04	0.7	<i>M</i>	4.94 ± 0.05
<i>B'</i>	6.98 ± 0.04	0.7	<i>N</i>	4.79 ± 0.02
<i>C</i>	6.77 ± 0.02	1.4	<i>N'</i>	4.66 ± 0.05
<i>D</i>	6.61 ± 0.03	0.4	<i>N''</i>	4.45 ± 0.02
<i>E</i>	6.50 ± 0.03	0.4	<i>O</i>	4.29 ± 0.02
<i>F</i>	6.33 ± 0.02	2	<i>P</i>	4.16 ± 0.02
<i>F'</i>	6.22 ± 0.03	0.7	<i>P'</i>	4.06 ± 0.04
<i>G</i>	6.13 ± 0.02	2	<i>Q</i>	3.88 ± 0.02
<i>G'</i>	6.01 ± 0.05	0.7	<i>R</i>	3.62 ± 0.02
<i>H</i>	5.89 ± 0.04	1.0	<i>S</i>	3.46 ± 0.02
<i>I</i>	5.78 ± 0.03	1.4	<i>T</i>	3.29 ± 0.02
<i>I'</i>	5.60 ± 0.02	3	<i>U</i>	3.02 ± 0.05
<i>J</i>	5.41 ± 0.03	3	<i>V</i>	2.84 ± 0.03
<i>K</i>	5.32 ± 0.03	1.0		

is very small. Possible $l_n=3$ admixtures to $l_n=1$ distributions undetected because of limited angular region of observation.

From angular distribution measurements it is reasonably certain that ground-state doublet has the ($d_{5/2}, s_{1/2}$) configuration predicted by shell model. For a 3^+ ground state and a 2^+ first level the intensity ratio of transitions to these states should be 1.4 (assuming equal reduced widths) while experiment (at 6.0 Mev) yields 1.95 (see Table XXI) (En 53a, En 54, En 56).

TABLE XXI. Levels in Al^{28} from $\text{Al}^{27}(d,p)\text{Al}^{28}$ (Bu 56, En 56a, En 56).^a

Level number	E_x (Mev)	l_n	\times reduced width ^b	(2J+1)	Level number	E_x (Mev)
(0)	0	0	700	(50)	5.445	
(1)	0.0312 ± 0.0005 c	0	360	(51)	5.525	
(2)	0.973	(52)	5.596	
(3)	1.017	2, (0)	600	(53)	5.746	
(4)	1.372	(54)	5.766	
(5)	1.633	(55)	5.802	
(6)	2.143	0	220	(56)	5.867	
(7)	2.207	2	160	(57)	5.909	
(8)	2.279	2, (0)	400	(58)	5.931	
(9)	2.490	0	40	(59)	5.960	
(10)	2.589	(60)	5.989	
(11)	2.663	2	400	(61)	6.012	
(12)	2.988	(62)	6.027	
(13)	3.011	(63)	6.067	
(14)	3.102	(64)	6.073	
(15)	3.294	0	20	(65)	6.163	
(16)	3.347	0	25	(66)	6.201	
(17)	3.461	1	320	(67)	6.247	
(18)	3.537	(68)	6.322	
(19)	3.591	1	410	(69)	6.424	
(20)	3.669	0	12	(70)	6.446	
(21)	3.704	0	35	(71)	6.485	
(22)	3.878	1	120	(72)	6.569	
(23)	3.900	(73)	6.591	
(24)	3.935	(74)	6.626	
(25)	4.030	2, (0)	300	(75)	6.657	
(26)	4.115	(76)	6.719	
(27)	4.243	0	20	(77)	6.760	
(28)	4.315	2	110	(78)	6.835	
(29)	4.383	(79)	6.856	
(30)	4.466	(80)	6.896	
(31)	4.518	(81)	6.934	
(32)	4.595	(82)	6.970	
(33)	4.685	1	650	(83)	7.025	
(34)	4.741	(84)	7.090	
(35)	4.767	1	500	(85)	7.121	
(36)	4.845	(86)	7.149	
(37)	4.906	1	330	(87)	7.180	
(38)	4.928	(88)	7.247	
(39)	4.999	(89)	7.274	
(40)	5.019	(90)	7.345	
(41)	5.138	1	340	(91)	7.408	
(42)	5.168	(92)	7.444	
(43)	5.179	(93)	7.460	
(44)	5.191	(94)	7.505	
(45)	5.289	(95)	7.596	
(46)	5.331	(96)	7.655	
(47)	5.346	(97)	7.669	
(48)	5.377	(98)	7.700	
(49)	5.405	(99)	7.731	

^a Note added in proof.—Improved and extended angular distribution data in H. A. Enge, M.I.T., Laboratory for Nuclear Science Progress Report, November 30, 1956.

^b Reduced width given in relative measure.

^c Other errors, see text.

TABLE XXII. Rotational bands in Al^{28} (Sh 56a).

E_x (Mev)	0	0.031	0.97	1.02	1.37	1.63	2.14	2.21	2.28
J, π	3 ⁺	2 ⁺	0 ⁺	3 ⁺	1 ⁺	4 ⁺	2 ⁺	2 ⁺	4 ⁺
	3	2	0	2	1	3	1	0	2

A 31.4 ± 1.0 -kev γ ray observed following $\text{Al}^{27}(d,p)\text{Al}^{28}$ reaction at $E_d=0.7$ Mev both by proportional counter and by scintillation spectrometer (Sm 51a). Half-life of first level measured with a recoil method, yielding $(2.1 \pm 0.4) \times 10^{-9}$ sec (Se 56a).

Also En 54a, Kr 54b, Fu 54, Be 55.

VI. $\text{Mg}^{28}(\beta^-)\text{Al}^{28}$ See Mg^{28}

VII. $\text{Si}^{28}(n,p)\text{Al}^{28}$ $Q_m=-3.865$

Cross section, En 54a, Co 56, Ma 56.

VIII. $\text{Si}^{28}(\gamma,p)\text{Al}^{28}$ $Q_m=-12.339$

Cross section, Ka 54.

IX. $\text{Si}^{30}(d,\alpha)\text{Al}^{28}$ $Q_m=3.122$

Ground-state $Q=3.120 \pm 0.010$ Mev measured with enriched targets and magnetic analysis at $E_d=1.8$ Mev (St 51). An α -particle group leading to 31-kev level in Al^{28} observed at several deuteron energies up to $E_d=2.0$ Mev, but with insufficient resolution to determine corresponding excitation energy (En 53a).

X. $\text{P}^{31}(n,\alpha)\text{Al}^{28}$ $Q_m=-1.945$

Cross section, En 54a.

GENERAL REMARKS

Arguments for a rotational character of nine lowest states in Al^{28} , Sh 56a. There are four bands (Table XXII); those with $K=2$ and $K=3$ have ($d_{5/2}, s_{1/2}$) configuration, while those with $K=0$ and $K=1$ belong to ($s_{1/2}, s_{1/2}$). The 4^+ spin assigned in Sh 56a to 2.28-Mev level conflicts with 2^+ or 3^+ assignment from $\text{Al}^{27}(d,p)\text{Al}^{28}$ angular distribution measurements. It would be better to assign 4^+ ($K=2$) to 2.21-Mev level and 2^+ ($K=0$) to 2.28-Mev level.

Si²⁸

(Fig. 14)

I. $\text{Mg}^{24}(\alpha,p)\text{Al}^{27}$ $E_b=9.990$ $Q_m=-1.595$

In experiments with thin separated Mg^{24}F_2 targets and magnetic analysis of protons, resonances observed at $E_\alpha=3.214$, 3.420, 3.448, 3.502, 3.660, 3.737, and 3.827 Mev corresponding to levels in Si^{28} at 12.745, 12.921, 12.945, 12.992, 13.127, 13.193, and 13.270 Mev. Same levels found in inverse reaction $\text{Al}^{27}(\rho,\alpha)\text{Mg}^{24}$, when a Q value of 1.613 ± 0.010 Mev is assumed. Intensities of corresponding peaks in good agreement, as

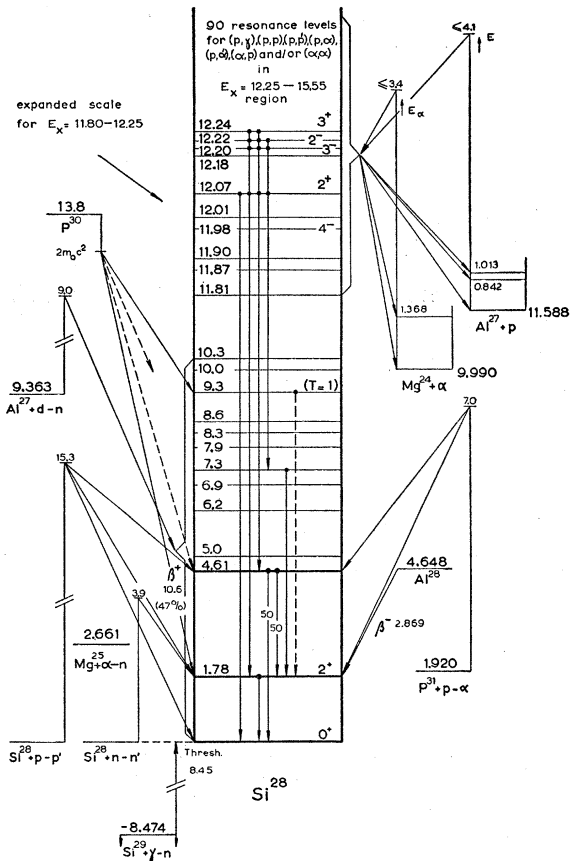


FIG. 14.

suggested by principle of detailed balancing. A weak resonance found at $E_\alpha = 2.84$ Mev without corresponding resonance in (p,α) reaction (Ka 52). Also Al^{27} , for Q -value measurements.

II. $\text{Mg}^{24}(\alpha,\alpha)\text{Mg}^{24} \quad E_b = 9.990$

Resonances in yield of elastically scattered α particles observed, again in good agreement with many resonances in the $\text{Al}^{27}(\rho,\alpha)\text{Mg}^{24}$ and $\text{Al}^{27}(\rho,\rho)\text{Al}^{27}$ reactions, (Ka 52). Partial-wave analysis yields following spins and parities for compound nucleus: $J=0^+$ for resonances at $E_\alpha = 2.84$ and 3.00 Mev, and $J=2^+$ for resonance at $E_\alpha = 2.93$ Mev. S -wave α -scattering resonance at $E_\alpha = 3.07$ Mev corresponds to S -wave proton scattering resonance at $E_p = 1.45$ Mev. No single J value of compound nucleus can explain this behavior. No (α,ρ) nor (ρ,α) transitions observed at $E_\alpha = 3.07$ Mev. Anomaly near $E_\alpha = 3.25$ Mev probably is caused by two overlapping levels in Si^{28} (Ka 52).

III. $\text{Mg}^{25}(\alpha,n)\text{Si}^{28} \quad Q_m = 2.661$

En 54a.

IV. $\text{Al}^{27}(\rho,\gamma)\text{Si}^{28} \quad Q_m = 11.588$

Resonances up to $E_p = 1.38$ Mev in Table XXIII. Energies of six lowest resonances in good agreement

with those in Ta 46. Thirty-one γ -ray resonances in $E_p = 0.46$ –2.6-Mev region in Pl 40. Fourteen are below $E_p = 1.4$ Mev, their energies in fair agreement with energies in Br 47a. Resonances at 504-, 630-, and 728-kev decay also by α emission (Ru 53).

Spin and parity assignments (Ru 54) result from measurements of γ -ray spectra, γ -ray angular distributions, and α -particle yield. The 1.78-Mev level in Si^{28} has $J=2^+$. At most resonances, transitions observed to 7.1- and 4.6-Mev levels, which both de-excite by cascades through 1.78-Mev level (Ru 54). The 4.6-Mev level, however, also deexcites to the Si^{28} ground state with intensity about equal to that of cascade (Go 57).† Parity of 652-kev resonance has been determined from a γ -ray polarization measurement (Hu 56).

Precision measurements of energy of prominent 991-kev resonance yield 993.1 ± 1 kev (He 49) and 990.8 ± 0.2 kev (Bu 56b). Width is 100 ev (Be 49) and 50 ± 30 ev (Bu 56b). From Doppler-shift measurements of 1.78-Mev γ ray, half-life of 1.78-Mev level follows as either

TABLE XXIII. Resonances in $\text{Al}^{27}(\rho,\gamma)\text{Si}^{28}$ below $E_p = 1.38$ Mev.

E_p (kev)	E_x (Si^{28}) (Mev)	Relative intensity ^{a,c}	J, π
226.3 ± 1.5 ^a	11.806	0.005	
294.1 ± 0.5 ^a	11.871	0.015	
325.6 ± 0.4 ^a	11.902	0.080	
404.7 ± 0.4 ^a	11.978	0.30	4^- ^b
438.5 ± 0.5 ^a	12.011	0.050	
504.0 ± 0.6 ^a	12.074	2.0	$2^+ b$
609°	12.175	0.4	
630°	12.195	8.2	$3^- b$
652°	12.217	3.3	$2^- b, f$
677°	12.241	1.3	$3^+ b$
728°	12.290	3.0	
733°	12.295	4.2	
738°	12.300	0.7	
757°	12.318	3.8	
764°	12.325	4.5	
771°	12.331	11.5	
880°	12.436	0.5	
918°	12.473	4.1	
932°	12.487	3.9	
991 ^{e,g,h}	12.544	47.0	
994°	12.547	2.0	
1018°	12.570	7.2	
1083°	12.632	1.5	
1091°	12.640	0.8	
1112°	12.660	13.5	
1165°	12.711	2.4	
1176°	12.722	6.5	
1192°	12.737	...	
1205°	12.750	11.0	
1255°	12.798	13.0	
1268°	12.811	1.0	$0^+ e$
1309°	12.850	14.0	
1320°	12.861	10.5	
1355°	12.895	15.0	
1372°	12.911	105.0	
1379°	12.918	105.0	

^a Hu 53. ^b Ru 54. ^c Br 47a (errors in proton energies are 0.2%, widths of all resonances observed are ≤ 1 kev). ^d Ta 46. ^e Ka 52 (from $\text{Mg}^{24}(\alpha,\alpha)\text{Mg}^{24}$ partial wave analysis). ^f Hu 56. ^g He 49. ^h Bu 56b.

† Note added in proof.—Recent measurements, however, show that no such crossover exists in decay of 4.6-Mev level (Go 57b).

$<3 \times 10^{-14}$ sec or $>9 \times 10^{-13}$ sec (De 56a). For γ -ray spectrum at this resonance, Ha 55.

Resonances above $E_p=1.4$ Mev in Pl 40, Sh 51, Go 54, Pa 54. Yields of hard and weak γ rays, of elastically and inelastically scattered protons, and of α particles leading to ground state and first excited state in Mg²⁴ in Sh 51 for region $E_p=0.6$ –4.1 Mev. From published yield curves, resonance energies for 64 resonances in 1.4–4.1-Mev region computed in Al 50, quoted in En 54a. No hard γ rays from capture observed above $E_p=1.8$ Mev. Comparison of resonance strengths (Go 53a) makes it probable that resonances at $E_p=1355$, 1372, and 1379 kev from Br 47a correspond to resonances at 1370, 1385, and 1393 kev in Sh 51, Al 50. Not possible at present to decide which energy scale is better. Angular distributions of γ -ray transitions leading to level (1) measured at 17 resonances in $E_p=0.65$ –2.20-Mev region, and of ground-state transition at 771-kev resonance (Go 57b).

Twenty-three resonances, yielding 0.84-Mev and/or 1.01-Mev γ rays from inelastic scattering observed in the $E_p=1.40$ –2.77 Mev region (Br 57a).

V. Al²⁷(p,n)Si²⁷ $E_b=11.588$ $Q_m=-5.610$

Broad resonances in Si²⁷ yield observed at $E_p=6.17$ and 6.37 Mev (Bl 51). See Si²⁷ for threshold measurements.

VI. (a) Al²⁷(p,p)Al²⁷ $E_b=11.588$

(b) Al²⁷(p,α)Mg²⁴ $E_b=11.588$ $Q_m=1.595$

Resonances, Sh 51, Pa 54, quoted under Reaction IV.

VII. Al²⁷(d,n)Si²⁸ $Q_m=9.363$

Determinations of excitation energies of levels in Si²⁸, and angular distribution measurements, Table XXIV. Relative intensities of neutron groups, Ca 55. Comparison of Al²⁷(d,p) and Al²⁷(d,n) angular distributions makes it probable that 9.16-Mev level in Si²⁸ is lowest $T=1$ state (Ca 55).

With a magnetic pair spectrometer, γ rays resulting from deuteron bombardment ($E_d=4.6$ Mev) of an aluminum target have these energies: $E_\gamma=6.9 \pm 0.1$, 7.41 ± 0.05 , 7.58 ± 0.05 , 7.94 ± 0.03 , 8.31 ± 0.03 , 8.78 ± 0.03 , 9.11 ± 0.03 , 9.49 ± 0.07 , 9.91 ± 0.07 , and 10.8 ± 0.2 Mev. Most of these probably follow Al²⁷(d,n)Si²⁸ reaction, as levels in Al²⁸ above 7.72 Mev and levels in Mg²⁵ above 7.33 Mev, which might be reached by (d,p) or (d,α) reaction, are unstable for neutron emission (Be 55).

VIII. Al²⁸(β^-)Si²⁸ See Al²⁸

IX. Si²⁸(e,e')Si²⁸

Differential cross section for elastic scattering of 187-Mev electrons and for inelastic scattering leading to level (1), (He 56).

TABLE XXIV. Neutron groups from the reaction Al²⁷(d,n)Si²⁸.

Reference:	Pe 49	Ru 56	Ca 55
Method of detection:	nucl. emuls.	nucl. emuls.	triple ion. chamber
E_d (Mev):	3.68	2.17	9.02
Q_0 (Mev)	9.08 ± 0.20	...	$l_n=2$
E_x (Si ²⁸): in Mev	1.78 ± 0.13 4.47 ± 0.10 (4.91 ± 0.21) 6.11 ± 0.10 6.65 ± 0.14 (7.10 ± 0.12) (7.55 ± 0.12) 8.18 ± 0.10 9.16 ± 0.17	1.78 ± 0.10 4.54 ± 0.2 4.95 ± 0.2 6.24 ± 0.06 6.88 ± 0.06 7.39 ± 0.06 7.89 ± 0.06 8.31 ± 0.10 8.57 ± 0.08 9.37 ± 0.04 10.00 ± 0.10 10.25 ± 0.06	$l_n=0$... $l_n=0$ $l_n=0$ $l_n=0$ $l_n=0$ $l_n=0$

X. Si²⁸($n,n'\gamma$)Si²⁸

Gamma rays of 1.29, 1.78 ± 0.02 , and 2.19 Mev observed from inelastic neutron scattering ($E_n=0.35$ –3.9 Mev) on natural silicon (Da 56). They have to be assigned to deexcitation of first levels in Si²⁹, Si²⁸, and Si³⁰, respectively. A 1.78 ± 0.02 -Mev γ ray, Ro 55a.

XI. Si²⁸(p,p')Si²⁸

From magnetic analysis at $E_p=5.6$ and 8.4 Mev, first Si²⁸ level observed at 1.777 ± 0.010 Mev (Br 54b). At $E_p=15.3$ Mev, a level at 4.6 ± 0.3 Mev found by low-resolution magnetic deflection, Fu 48.

At $E_p=12$ Mev, angular distribution of proton group leading to level (1), Co 55.

Resonances in yield of 1.78 Mev γ ray, P²⁹.

XII. P²⁸(β^+)Si²⁸ See P²⁸

XIII. Si²⁹(γ,n)Si³⁰ $Q_m=-8.474$

Threshold is 8.45 ± 0.20 Mev (Sh 51a). Cross section, Ka 54.

XIV. P³¹(p,α)Si²⁸ $Q_m=1.920$

Ground-state Q by magnetic analysis = 1.85 ± 0.02 Mev (Fr 51), 1.909 ± 0.010 Mev (Va 52a), 1.911 ± 0.005 Mev (Va 56), and 1.909 ± 0.010 Mev (En 57b). Levels in Si²⁸ observed at 1.771 ± 0.010 and 4.617 ± 0.010 Mev (En 57b). Resonances, S³².

P²⁸

(not illustrated)

I. P²⁸(β^+)Si²⁸ $Q_m=13.8$

Half-life, averaged from two measurements (Gl 55, Br 54a) in good mutual agreement, is 0.285 ± 0.007 sec.

The β^+ decay quite complicated. Highest energy branch proceeds to 1.78-Mev Si²⁸ level with end point of 10.6 ± 0.4 Mev, intensity $47 \pm 15\%$. Observed gamma

TABLE XXV. Gamma rays in decay of P^{28} .

Reference:	E_γ (Mev)	Gl 55	Rel. int.	Br 54a
				E_γ (Mev)
	1.79±0.02 (2.6 ±0.2)		0.75	1.78±0.04 2.67±0.08 (3.01±0.07) (4.26±0.12)
	4.44±0.05 (4.93±0.08)		0.10	4.63±0.10 4.89±0.09 (5.16±0.12) (5.46±0.10)
	6.14±0.10 6.70±0.12 7.04±0.08 7.59±0.15		0.10 0.10 0.10 0.05	6.65±0.11 7.10±0.12 (7.44±0.14) (7.73±0.14) (8.12±0.21)

rays in Table XXV. No delayed α particles observed (Gl 55).

Most of observed high-energy γ rays cannot be fitted uniquely into Si^{28} level scheme. A natural explanation of the 7.59-Mev γ ray, Gl 55, assumes part of the β^+ decay proceeds to 9.3-Mev level which is de-excited through 1.78-Mev level. Superallowed character of such a β^+ transition ($\log ft=3.4-3.7$) would be in accordance with assignment of $T=1$ to 9.3-Mev level (Bo 55, Wi 56a).

$\log ft=4.9$ for main β^+ transition to 1.78-Mev level, equal to that of Al^{28} β^- decay to same level. This is another proof of charge symmetry of nuclear forces (Gl 55).

II. $Si^{28}(p,n)P^{28}$ $Q_m=-14.6$

Threshold for P^{28} yield measured as $E_p=15.6\pm 0.3$ Mev (Gl 55) and 15.4 ± 0.5 Mev (Br 54a).

Al²⁹

(not illustrated)

I. $Al^{29}(\beta^-)Si^{29}$ $Q_m=3.98$

Measurements of half-life yield an average of 6.52 ± 0.05 min (En 54a).

The β^- decay proceeds to first and third excited states of Si^{29} (at $E_x=1.28$ and 2.43 Mev) which are de-excited by γ transitions to ground state. No 2.03-Mev γ ray of intensity $\geq 4\%$ observed; no evidence found for cascade de-excitation of 2.43-Mev level through that at 1.28 Mev (Ro 55, Br 56). Energies and relative intensities of β^- and γ rays Table XXVI. Also Br 57.

TABLE XXVI. The $Al^{29}(\beta^-)Si^{29}$ decay.

Author	Method	E_{β_1} (Mev)	E_{β_2} (Mev)	E_{γ_1} (Mev)	E_{γ_2} (Mev)
Me 37	Al abs	2.75			
Be 39	cl. ch.	2.5			
Se 49	Al abs	2.5 (70%)	1.4 (30%)	1.25±0.02	2.35±0.5
Na 54b	scint. sp		1.55±0.1	1.31±0.05	2.42±0.05
Ro 55	scint. sp			1.28 (85%)	2.43 (15%)
Br 56	scint. sp			1.28 (94%)	2.43 (6%)

Log ft values for transitions to 1.28-, 2.03-, and 2.43-Mev levels are <5.2 , >6.5 , and 5.2, respectively (Br 57).

Also Na 54a.

II. $Mg^{26}(\alpha,p)Al^{29}$ $Q_m=-3.19$

With 8-Mev cyclotron α particles and detection of protons with a proportional counter, ground-state Q value is -2.90 Mev; a probable level at 1.69 ± 0.04 Mev (Gr 56d). Also En 54a, Br 56b.

III. $Al^{27}(t,p)Al^{29}$ $Q_m=8.38$

Observed (En 54a).

IV. $Si^{29}(n,p)Al^{29}$ $Q_m=-3.20$

Cross section, En 54a.

V. $Si^{30}(\gamma,p)Al^{29}$ $Q_m=-13.81$

Cross section, Ka 54, En 54a.

Si²⁹

(Fig. 15)

I. $Mg^{26}(\alpha,n)Si^{29}$ $Q_m=0.017$

En 54a, Na 53a, Br 55b.

II. $Mg^{25}(\alpha,p)Al^{28}$ $E_b=11.135$ $Q_m=-1.204$

En 54a, Na 53a.

III. $Si^{28}(n,\gamma)Si^{29}$ $Q_m=8.474$

Thermal-neutron capture cross section of natural silicon is 130 ± 30 mb; isotopic cross sections of Si^{28} , Si^{29} , and Si^{30} are 80 ± 30 , 270 ± 90 , and 400 ± 400 mb, and their abundances 92.27, 4.68, and 3.05%, respectively, so approximately 73% of the thermal-neutron captures in natural silicon should occur in Si^{28} (Hu 55c).

Energies and intensities of γ rays from capture of thermal neutrons in natural silicon in Table XXVII. Assignment of most γ transitions based on comparison of γ energy with binding energies and excitation energies in Si^{29} , Si^{30} , and Si^{31} as measured by magnetic analysis of (d,p) reactions. The γ spectrum of the $Si^{28}(n,\gamma)Si^{29}$ reaction dominated by two cascades via levels at 4.93 and 6.38 Mev; see General Remarks.

IV. $Si^{28}(n,n)Si^{28}$ $E_b=8.474$

$Si^{28}(n,n')Si^{28}$ $E_b=8.474$

Total neutron cross section of natural silicon, Hu 55c. Resonances at $E_n=195$ and 570 kev are assigned to Si^{28} and have $J=1/2^+$ and $3/2^-$, respectively (Fi 51, Hu 55c). See Da 56 for inelastic-scattering resonances.

V. $Si^{28}(d,p)Si^{29}$ $Q_m=6.249$

Thirteen proton groups found by magnetic analysis at $\theta=90^\circ$ and E_p up to 2.1 Mev (En 51a, Va 52). Q

TABLE XXVII. Gamma rays from thermal neutron capture in natural silicon.

Reference: Method: Line	K1 51, K1 53c Pair spectrometer		Ad 56a Compton el. spectr.		Br 56e Scint. spectr.		Final nucleus and probable transition
	E _γ (Mev)	Intensity ^a	E _γ (Mev)	Intensity ^a	E _γ (Mev)	Intensity ^a	
A	10.599±0.011	(0.4)	10.59 ±0.03	(0.2)			Si ³⁰ (c)→(0)
B	8.467±0.008	(2 ^b)	8.482±0.015	(1.6)			Si ²⁹ (c)→(0)
C	7.79 ±0.05	(1)					
D	7.36 ±0.08	(2)	(7.38 ±0.03)	(0.5)			(Si ³⁰)
E	7.18 ±0.03	(8 ^b)	7.22 ±0.03	(6.1)			Si ²⁹ (c)→(1)
E'	6.88 ±0.03	(0.7)					
F	6.76 ±0.04	(4)	6.758±0.020	(1.4)			(Si ³⁰)
G	6.40 ±0.03	(11 ^b)	6.354±0.015	(9.2)			Si ²⁹ (12)→(0)
H	6.11 ±0.05	(4)	6.04 ±0.05	(1)			(Si ²⁹)
I'	5.70 ±0.04	(2)					
I	5.52 ±0.05	(2)					
I''			5.24 ±0.03	(0.8)			
J	5.11 ±0.04	(8 ^b)	5.118±0.015	(2.3)			(Si ²⁹)
K	4.933±0.005	(75 ^b)	4.930±0.010	(37.4)			Si ²⁹ (9)→(0)
K'	4.60 ±0.08	(4)					
L	4.20 ±0.03	(19)	(4.30 ±0.05)	(2)			
L'			3.976±0.020	(4.2)			(Si ²⁹)
L''			3.8	(3)			(Si ³⁰)
L'''			3.667±0.020	(3.2)			
M	3.540±0.006	(60 ^b)	3.547±0.010	(36.5)	3.6 ±0.06	(49)	Si ²⁹ (c)→(9)
N	2.69 ±0.05	(65)			2.65±0.03	(11)	
O			2.10 ±0.01	(12.8)	2.13±0.03	(19)	Si ²⁹ (c)→(12)
P			1.95 ±0.02	(3.4)			
Q			1.7	(3)			(Si ²⁹)
R			1.5	(3)			(Si ²⁹)
S			1.28 ±0.01	(16)	1.26±0.03	(14)	Si ²⁹ (1)→(0)

^a Intensity in photons per 100 captures in natural silicon.^b Intensity in photons per 100 captures in Si²⁸; see K1 54a.

values and excitation energies in Table XXVIII agree with values obtained by absorption measurements at $E_d=3.7$ Mev (Mo 50). Excellent agreement between levels found here and from P³¹(d, α)Si²⁹ (Table XXIX).

Angular distributions of most prominent proton groups measured at $E_d=8.2$ Mev; angular momenta of capture neutrons, from stripping theory, in Table XXVIII; these l_n values and neutron capture probabilities discussed on basis of shell model (Ho 53a, Ho 53d). Assignment of $l_n=0$ to ground state was confirmed by measurements at $E_d=9$ Mev (Ca 56a). Polarization of protons leading to p states at 4.93 and 6.38 Mev measured (Ju 56).

TABLE XXVIII. Energy levels in Si²⁹ from Si²⁸(d, p)Si²⁹.

Author: E_d (Mev):	Va 52 1.8-2.1	Ho 53d 8.2
Method: Q_0 (Mev):	magnetic analysis 6.246±0.010 E_x (Mev)	Al absorption l_n
	0	0
	1.278±0.007	2
	2.027±0.007	2
	2.426±0.007	isotropic
	3.070±0.007	2
	3.623±0.007	3
	4.078±0.008	
	4.840±0.008	
	4.897±0.008	
	4.934±0.008	1
	5.946±0.009	
	6.105±0.009	
	6.380±0.009	1

Measurements and discussion of reduced widths for Si²⁸(d, p)Si²⁹ and Si²⁸(d, n)P²⁹ ground-state transitions, Fu 54, Ca 56a.

Levels at 1.28, 2.03, 2.43, 3.07, 4.93, and 6.38 Mev all decay by γ transitions directly to ground state (Al 49b, Th 54, Ro 55).

Angular correlation of protons and gammas corresponding to 1.28-Mev level differs from that predicted by simple stripping theory (Al 56a).

VI. Al²⁹(β^-)Si²⁹ See Al²⁹VII. Si²⁹(n,n'γ)Si²⁹

The 1.28-Mev level is excited by inelastic scattering of neutrons with energies up to 3.9 Mev (Da 56).

VIII. Si²⁹(p,p'γ)Si²⁹

Angular distributions of 2.03-Mev γ ray measured at $E_p=2.798$ and 2.934 Mev. Presence of P_4 terms indi-

TABLE XXIX. P³¹(d, α)Si²⁹ reaction (En 51a, Va 52a).

Group	Q value (Mev)	Si ²⁹ level (Mev)
A	8.158±0.011	0
B	6.885±0.020	1.274±0.010
C	6.126±0.020	2.032±0.014
D	5.727±0.020	2.431±0.015
E	5.086±0.020	3.072±0.016
F	4.539±0.020	3.619±0.017
G	4.080±0.020	4.078±0.018
H	3.221±0.020	4.937±0.020

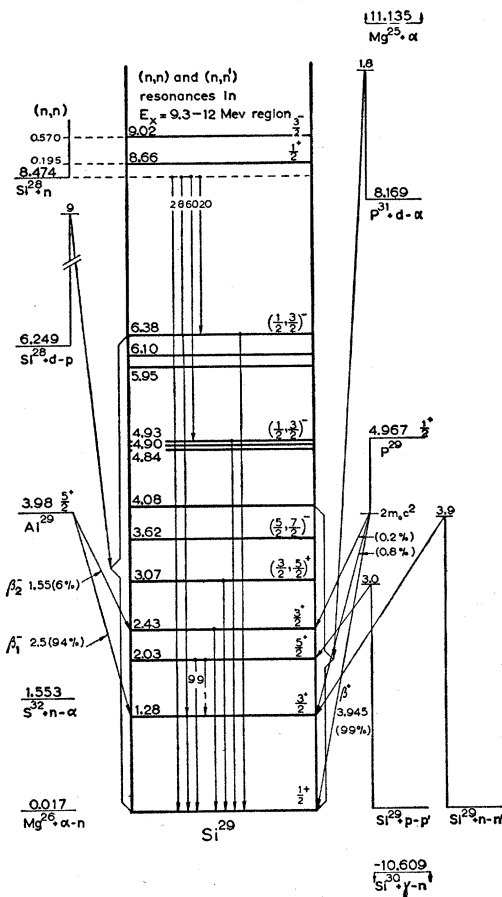


FIG. 15.

cates that 2.03-Mev level has $J=5/2^+$. From coincidence measurements, this level decays for about 0.5% via a cascade through 1.28-Mev level. Angular distributions of 1.28-Mev γ ray at $E_p=2.798$ and 2.922 Mev are consistent with assignment of $3/2^+$ to 1.28-Mev level (Br 56, Br 57).

IX. $\text{P}^{29}(\beta^+) \text{Si}^{29}$ See P^{29}

X. $\text{Si}^{30}(\gamma, n) \text{Si}^{29}$ $Q_m = -10.609$

Cross sections, Ka 54.

XI. $\text{P}^{31}(d, \alpha) \text{Si}^{29}$ $Q_m = 8.169$

Eight α -particle groups (Table XXIX) found by high-resolution magnetic analysis at $\theta=90^\circ$ and $E_d=1.8$ Mev (En 51a). Ground-state Q value given as 8.170 ± 0.020 Mev later remeasured as 8.158 ± 0.011 Mev (Va 52a). Excitation energies of Si^{29} levels in Table XXIX corrected accordingly. Also Be 55.

XII. $\text{S}^{32}(n, \alpha) \text{Si}^{29}$ $Q_m = 1.553$

En 54a, Hu 55a.

GENERAL REMARKS

The p states at 4.93 and 6.38 Mev are strongly excited, both in $\text{Si}^{28}(d, p) \text{Si}^{29}$ and in $\text{Si}^{28}(n, \gamma) \text{Si}^{29}$ reactions; these may be single-particle $p_{3/2}$ and $p_{1/2}$ states predicted by shell model. Ground state and 1.28- and 3.62-Mev levels may be regarded as $s_{1/2}$, $d_{3/2}$, and $f_{7/2}$ states (Ho 53d, Ki 54a).

Spin of ground state of Si^{29} is $1/2^+$ (Ra 53, Wh 53, Wi 54, Og 54). Assignment of $3/2^+$, $5/2^+$, and $3/2^+$ to the levels at 1.28, 2.03, and 2.43 Mev, respectively, of $1/2^+$ to P^{29} (0) and $5/2^+$ to Al^{29} (0) in agreement with observed log ft values, (d, p) and $(p, p' \gamma)$ angular distributions, and γ branching ratios.

Application of strong-coupling collective model to low levels of Si^{29} , Br 57c.

P^{29}

(Fig. 16)

I. $\text{P}^{29}(\beta^+) \text{Si}^{29}$ $Q_m = 4.967$

Half-life is 4.6 ± 0.2 sec (Wh 41) and 4.45 ± 0.05 sec (Ro 55).

The β^+ end point by magnetic spectrometer is 3.945 ± 0.005 Mev, yielding $\log ft = 3.723 \pm 0.007$ (Ro 55). Gamma rays of 1.28 and 2.43 Mev in coincidence with positrons observed; branching ratios, log ft values, and proposed classifications in Table XXX. Spins and parities of Si^{29} levels, see Si^{29} , general remarks. Theo-

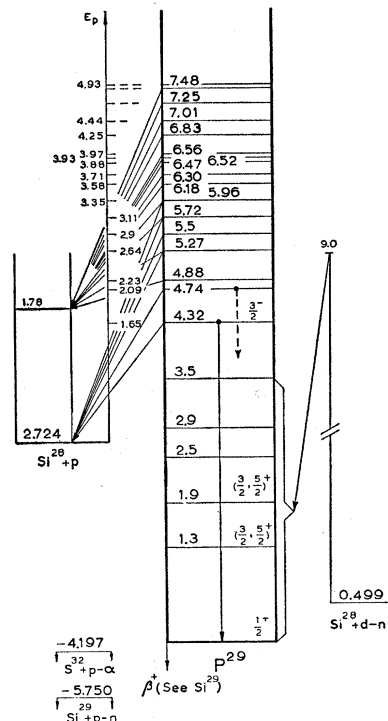


FIG. 16.

TABLE XXX. The $P^{29}(\beta^+)Si^{29}$ decay (Ro 55).

Si ²⁹ level (Mev)	Branching ratio %	Log ft
2.43	0.24 ± 0.26	4.5
2.03	≤ 0.15	≥ 5.2
1.28	0.80 ± 0.20	5.0
0	98.8 ± 0.4	3.72

TABLE XXXI. Resonances in $Si^{28} + p$.

E_p (lab) (Mev)	E_x (P^{29}) (Mev)	Decay ^a	Γ (kev)
(0.703) ^b	(3.40)	γ^a	
(0.944) ^b	(3.64)	γ^a	
(0.989) ^b	(3.68)	γ^a	
1.65 ^e	4.30	p_0^e	50.5 ^f
2.09 ^e	4.74	p_0^e	12 ^f
2.27 ^f	4.92	p_1^f	<4 ^f
2.64 ^d	5.27	p_1^d	
2.9 ^e	5.5	p_0^e	broad ^e
3.11 ^e	5.72	$p_0^e p_1^e$	12 ^e
3.35 ^e	5.96	$p_0^e p_1^e$	11 ^e
3.58 ^e	6.18	p_1^e	70 ^e
3.71 ^e	6.30	p_1^e	40 ^e
3.88 ^d	6.47	p_1^d	
3.93 ^d	6.52	p_1^d	
3.97 ^d	6.56	p_1^d	
4.25 ^e	6.83	p_1^e	22 ^e
4.44 ^e	7.01	p_1^e	$\sim 100^e$ (double?)
	7.25 ^e	p_1^e	
	7.44 ^e	p_1^e	
4.93 ^d	7.48	p_1^d	

^a Symbols p_0 , p_1 , γ , and γ_0 refer to elastic proton scattering, inelastic scattering leading to Si^{28} (1), proton capture, and proton capture with a strong ground-state transition, respectively.
^b Se 55. ^c Co 55a. ^d Wi 56. ^e Vo 57. ^f Ne 57.

retical discussion of β^+ - and γ -transition probabilities, Go 56b.

II. (a) $Si^{28}(p,\gamma)P^{29}$ $E_b=2.724$

(b) $Si^{28}(p,p'\gamma)Si^{28}$ $E_b=2.724$ $E_x=1.78$

With natural silicon, resonances in yield of γ rays observed for proton energies below 1.2 Mev (Se 55); most of these can be assigned to Si^{29} or Si^{30} ; assignment of resonances at 703, 944, and 989 kev uncertain. Resonances at $E_p=1.63$ and 2.08 Mev assigned to $Si^{28}(p,\gamma)P^{29}$. First of these has $\Gamma=50.5$ kev, $\Gamma_\gamma=1.73$ ev, $J=3/2^-$, and the main γ transition goes directly to ground state. Reduced width indicates this is $p_{3/2}$ single particle state (Ne 57).

Yield of 1.78-Mev γ rays from $Si^{28}(p,p'\gamma)Si^{28}$ reaction shows several resonances, Table XXXI. Resonance at $E_p=4.44$ Mev is possibly a doublet (Co 55a).

III. $Si^{28}(d,n)P^{29}$ $Q_m=0.499$

Ground-state Q values: -0.80 ± 0.10 Mev (Pe 48), 0.29 ± 0.04 Mev (Ma 52), and 0.6 ± 0.1 Mev (Ca 57).

Angular distribution measurements at $E_d=9$ Mev yield a $l_p=0$ assignment for ground-state transitions. Levels in P^{29} at 1.30 Mev ($l_p=2$), 1.92 Mev ($l_p=2$), and 3.5 Mev (Ca 57), while additional levels at $E_d=2.5$ and 2.9 Mev in Gr 55f. Also Ca 56a.

IV. $Si^{29}(p,n)P^{29}$ $Q_m=-5.750$

Observed (En 54a, Ty 54).

V. $S^{32}(p,\alpha)P^{29}$ $Q_m=-4.197$

Not observed.

Si³⁰

(Fig. 17)

I. $Mg^{26}(\alpha,p)Al^{29}$ $E_b=10.626$ $Q_m=-3.18$

Resonances, En 54a.

II. $Al^{27}(\alpha,p)Si^{30}$ $Q_m=2.376$

Investigations with α particles from radioactive sources, En 54a.

Nuclear emulsion work at $E_\alpha=8$ Mev yields $Q=2.38 \pm 0.03$ Mev, and levels in Si^{30} at $E_x=2.23 \pm 0.02$, 3.52 ± 0.02 , 3.80 ± 0.04 , 4.83 ± 0.02 , 5.28 ± 0.02 , 5.52 ± 0.03 , 5.94 ± 0.04 , 6.52 ± 0.03 , 7.10 ± 0.03 , and 7.38 ± 0.05 Mev. No levels at 5.07 and 5.62 Mev (Ha 56e). Angular distributions at $E_\alpha=8$ Mev (Vo 56). At $E_\alpha=22$ Mev, levels found from Al absorption at 5.61, 7.35, 8.37, 9.43, 10.04, and 11.03 Mev (Br 49).

Energies of γ rays in coincidence with selected proton groups measured by scintillation spectrometer at $E_\alpha=7.8$ Mev. A 2.32 ± 0.05 -Mev γ ray, de-exciting first excited state, and a 3.63 ± 0.15 -Mev γ ray, representing unresolved ground-state transitions from second and third excited states. The 5.07-Mev level is de-excited through third level with γ rays of 1.28 ± 0.06 and 3.66 ± 0.15 Mev, and for less than 15% through first level (Al 55). Also La 51, Be 48, Br 55b.

III. $Si^{29}(n,\gamma)Si^{30}$ $Q_m=10.609$

Cross section, Hu 55c.

Energy of γ ray corresponding to ground-state transi-

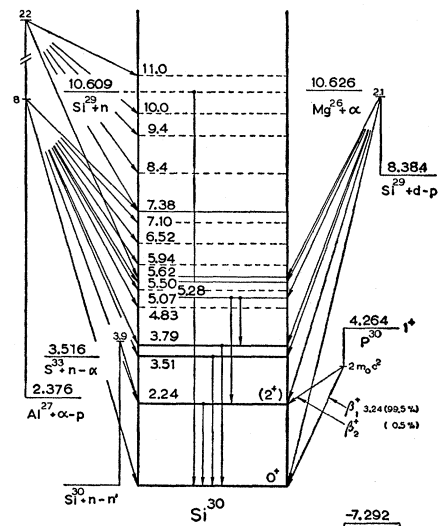


FIG. 17.

TABLE XXXII. The $\text{Si}^{29}(d,p)\text{Si}^{30}$ reaction.

Q value (Va 52) in Mev	Si^{30} level (Va 52) in Mev	Si^{30} level (Mo 50) in Mev
8.388 \pm 0.013	0	0
6.149 \pm 0.015	2.239 \pm 0.020	(2.4 \pm 0.2)
4.873 \pm 0.009	3.515 \pm 0.016	
4.602 \pm 0.015	3.786 \pm 0.020	3.91 \pm 0.15
	(5.075 \pm 0.015)	5.00 \pm 0.15
	(5.497 \pm 0.015)	
	(5.622 \pm 0.015)	5.7 \pm 0.2

tion after capture of thermal neutrons in Si^{29} by pair spectrometer is 10.599 ± 0.011 Mev (Table XXVII). Transition energy obtained by adding 2 kev, nuclear recoil energy, to γ energy (Ki 53c). Same γ ray reported in Ad 56a (Table XXVII). It is uncertain which of the other γ rays given in Ad 56a should be assigned to $\text{Si}^{29}(n,\gamma)$ reaction.

IV. $\text{Si}^{29}(d,p)\text{Si}^{30} Q_m = 8.384$

Several proton groups from enriched Si^{29} targets found by high-resolution magnetic analysis ($\theta = 90^\circ$) at deuteron energies up to 2.1 Mev (Va 52). Q values and corresponding Si^{30} levels in Table XXXII together with Si^{30} levels obtained by Al absorption at $E_d = 3.7$ Mev from enriched targets (Mo 50).

V. $\text{Si}^{30}(n,n'\gamma)\text{Si}^{30}$

Yield of 2.19-Mev γ ray from natural Si targets measured up to $E_n = 3.9$ Mev (Da 56).

VI. $\text{P}^{30}(\beta^+,\text{Si}^{30})$ See P^{30}

VII. $\text{P}^{31}(\gamma,p)\text{Si}^{30} Q_m = -7.292$

Not observed.

VIII. $\text{S}^{33}(n,\alpha)\text{Si}^{30} Q_m = 3.516$

Not observed.

P^{30}

(Fig. 18)

I. $\text{P}^{30}(\beta^+,\text{Si}^{30}) Q_m = 4.264$

Most accurate half-life measurement yields 2.55 ± 0.02 min (Ko 54a). Other recent determinations (Ba 52a, St 53b, Gr 56) with larger errors are in good agreement with this value, while older measurements (En 54a) scatter appreciably.

Best determination of β^+ end point by magnetic spectrometer is 3.24 ± 0.04 Mev (Gr 56), in good agreement with values of 3.31 ± 0.07 Mev obtained by scintillation spectrometer (Hu 54a), and of 3.23 ± 0.07 Mev by Al absorption (Ko 54a). Older less accurate measurements, En 54a. Log $f_t = 4.84$.

Although absence of γ rays in P^{30} decay is reported in St 53b, Ko 54a, and Gr 56, a 2.24-Mev γ ray recently observed with 0.5% intensity (Mo 56d). Log $f_t = 4.9$.

This uniquely fixes P^{30} ground-state spin as 1^+ , if spin of Si^{30} first level is 2^+ .

II. $\text{Al}^{27}(\alpha,n)\text{P}^{30} Q_m = -2.671$

Threshold reported as $E_\alpha = 3.409$ Mev corresponding to a Q value of -2.969 Mev (Bu 56c). This leads to a P^{30} mass about 300 kev higher than value from other reactions. Also En 54a.

III. $\text{Si}^{28}(\text{He}^3,p)\text{P}^{30} Q_m = 6.318$

Observed, En 54a.

IV. $\text{Si}^{29}(\beta,\gamma)\text{P}^{30} Q_m = 5.562$

Resonance energies and corresponding P^{30} excitation energies, resonance strengths, and assignments of spins, parities, and isobaric spins in Table XXXIII. The γ -ray energies measured at four lowest resonances lead to Q value of 5.57 ± 0.03 Mev (Va 57). From relative γ -ray intensities reported in Br 56h, Va 57, branching ratios can be computed for resonance levels and several lower P^{30} levels, Fig. 18. Excitation energy of first P^{30} level, which is strongly excited at the 414-kev resonance, is measured by scintillation spectrometer as 688 ± 7 kev (En 54b), and as 690 ± 10 kev (Br 56a). The $T=1$ analog of Si^{30} ground state is expected at about this position (Mo 54, Wi 56a). Isotropy of 690-kev γ ray, together with anisotropy of γ -ray feeding level (1) at 414-kev resonance, presents a strong argument for a

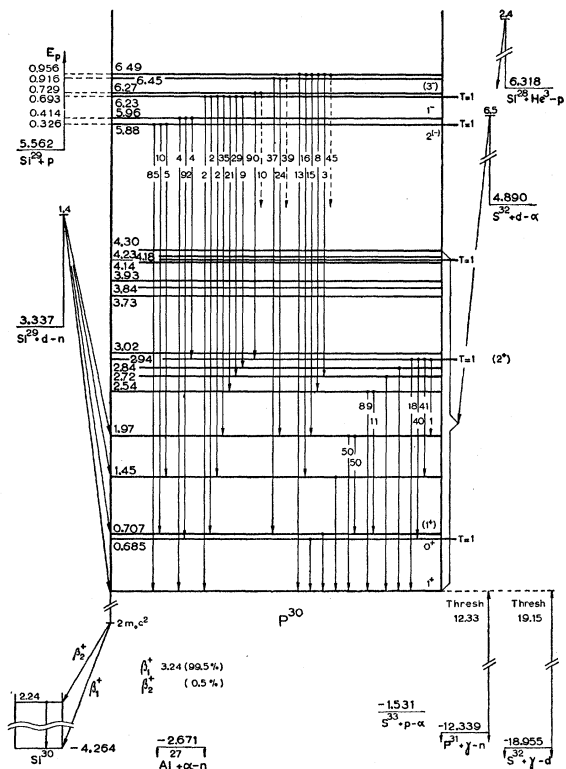


FIG. 18.

TABLE XXXIII. Resonances in $\text{Si}^{29}(\rho, \gamma)\text{P}^{30}$.

E_ρ in kev	E_π (P^{30}) in Mev	$(2J+1)\Gamma_\rho\Gamma\gamma/(\Gamma_\rho+\Gamma\gamma)$ in ev	J, π, T ^g
326 a, b, c	5.877	0.05 ^f	$J=2^-, T=1$
414 a, b, c, d	5.962	0.23 ^e	$J=1^-, T=0$
693 b, c, d	6.232	0.11 ^e	(π negative), $T=1$
729 b, c, d	6.267	0.11 ^e	$J=(3^-), T=0$
916 c, d	6.447		
956 c, d	6.486		

^a Ta 46. ^b KI 55a. ^c Mi 55. ^d Br 56i. ^e Br 56h. ^f Va 57. ^g All J, π , and T assignments, partly from intensity considerations (Br 56h), and partly from angular distribution measurements (Br 56a, Va 57) are preliminary.

$J=0^+$ assignment to level (1) (Br 56a). Recently observed that level (1) is a close doublet. At 414- and 723-kev resonances, lowest energy γ ray is measured as 686 ± 4 and 686 ± 6 kev, respectively. At 326- and 696-kev resonances, however, the γ -ray energy is distinctly higher, 703 ± 6 and 705 ± 5 kev. Angular distribution of this γ ray, measured at 326-kev resonance, is anisotropic (Va 57). Both levels also observed from $\text{S}^{32}(d, \alpha)\text{P}^{30}$ reaction (Reaction XI). A preliminary spin assignment to 0.71-Mev $T=0$ level is $J=1^+$ (Va 57).

At least the four lowest resonances seem to decay almost exclusively to either $T=0$ to $T=1$ levels, pointing to negative parity of the resonance levels and operation of E1 isobaric spin selection rule. Remarkable is also strong E2 transition between the lowest two $T=1$ levels.

V. $\text{Si}^{29}(\rho, \rho'\gamma)\text{Si}^{29}$ $E_b=5.562$

In $E_\rho=2.5$ –3.0-Mev region, resonances in yield of a 1.28-Mev γ ray observed at $E_\rho=2.614, 2.678, 2.700, 2.720, 2.760, 2.798, 2.843, 2.876, 2.922, 2.934, 2.958, 2.982$, and 2.995 Mev. A 2.03-Mev γ ray also observed at 2.678-, 2.700-, 2.798-, 2.876-, 2.934-, and 2.958-Mev resonances. A 2.43-Mev γ ray only appears weakly at 2.982-Mev resonance (Br 57). For γ -ray angular distributions, Si^{29} .

VI. $\text{Si}^{29}(d, n)\text{P}^{30}$ $Q_m=3.337$

By nuclear emulsion technique, ground-state $Q=3.27 \pm 0.04$ Mev, and levels found at $0.75 \pm 0.06, 1.46 \pm 0.06$, and 2.00 ± 0.06 Mev by bombarding enriched silicon targets at $E_d=1.4$ Mev (Ma 52). A ground-state Q value of 3.38 ± 0.17 Mev and a level at 1.27 ± 0.48 Mev by bombarding natural silicon targets at $E_d=3.7$ Mev (Pe 58).

VII. $\text{Si}^{30}(\rho, n)\text{P}^{30}$ $Q_m=-5.047$

Observed, En 54a.

VIII. $\text{P}^{31}(\gamma, n)\text{P}^{30}$ $Q_m=-12.339$

Threshold is 12.35 ± 0.2 Mev (Mo 49), 12.4 ± 0.2 Mev (Ka 51a), 12.05 ± 0.20 Mev (Sh 51a), and 12.33 ± 0.05 Mev (Sc 55a). Cross section, En 54a, Na 54. Sharp bends in P^{30} yield curve, not corresponding to known levels in P^{30} , observed at $12.58 \pm 0.07, 12.75$

$\pm 0.08, 12.90 \pm 0.08, 13.18 \pm 0.10$, and 13.38 ± 0.10 Mev (Ba 55).

IX. $\text{S}^{32}(\gamma, d)\text{P}^{30}$ $Q_m=-18.955$

Threshold reported at 19.15 ± 0.20 Mev (Ka 51a). Yield measurements, En 54a, Ri 55.

X. $\text{S}^{32}(n, t)\text{P}^{30}$ $Q_m=-12.697$

Observed, En 54a.

XI. $\text{S}^{32}(d, \alpha)\text{P}^{30}$ $Q_m=4.890$

Magnetic analysis at $E_d=6.0$ and 6.5 Mev and at angles of 90° and 130° , ground-state Q value $= 4.887 \pm 0.010$ Mev, while levels in P^{30} observed at $0.680 \pm 0.010, 0.708 \pm 0.008, 1.451, 1.972, 2.538, 2.723, 2.839, 2.937, 3.018, 3.734, 3.836, 3.926, 4.141, 4.181, 4.230, 4.296, 4.342, 4.421, 4.501, 4.625, 4.734, 4.929, 5.024, 5.200, (5.233), 5.412, 5.504, 5.598, 5.700$, and 5.790 , all ± 0.010 Mev. Levels above 4.30 Mev not indicated in Fig. 18. States at $0.680, 2.937, 4.181$, and 4.501 Mev regarded as $T=1$ levels because of low intensity of corresponding groups. They are analogs of Si^{30} ground state and Si^{30} levels at $2.24, 3.51$, and 3.79 Mev (Pa 57). A ground-state Q value of 4.831 ± 0.013 Mev, in bad agreement with the value quoted, also reported, in addition to α -particle groups corresponding to levels at $0.693, 1.440$, and 1.97 Mev (Le 56b).

XII. $\text{S}^{33}(\rho, \alpha)\text{P}^{30}$ $Q_m=-1.531$

Not observed.

Si³¹

(Fig. 19)

I. $\text{Si}^{31}(\beta^-)\text{P}^{31}$ $Q_m=1.481$

Half-life, averaged from five determinations (En 54a) in good mutual agreement, 157.2 ± 0.4 min.

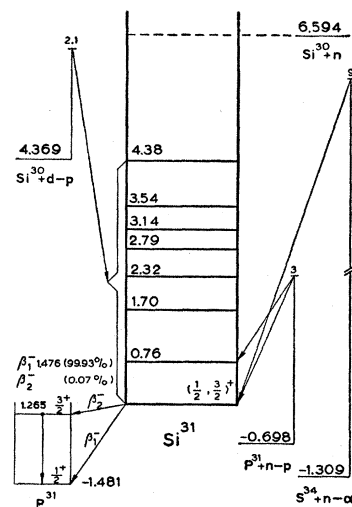


FIG. 19.

The β^- spectrum is simple and has allowed shape. End point measured by lens spectrometer as 1.471 ± 0.008 Mev (Mo 52a) and 1.486 ± 0.012 Mev (Wa 52, Wa 53a). Log $ft = 5.5$. A 1.26-Mev γ ray of intensity 0.07% detected by scintillation spectrometer. Corresponding β^- transition is allowed (log $ft = 5.6$) (Ly 54).

Theoretical remarks concerning Si³¹ decay, Go 56b.

II. Si³⁰(n, γ)Si³¹ $Q_m = 6.594$

Cross section, Hu 55c.

III. Si³⁰(d,p)Si³¹ Q_m=4.369

By magnetic analysis at deuteron energies up to 2.1 Mev, ground-state Q value = 4.364 ± 0.007 Mev, and levels in Si^{31} found at 0.757 ± 0.007 , 1.699 ± 0.007 , 2.319 ± 0.008 , 2.791 ± 0.008 , 3.140 ± 0.008 , 3.539 ± 0.008 , and 4.384 ± 0.008 Mev (Va 52). Also En 54a.

IV. $P^{31}(n,p)Si^{31}$ $Q_m = -0.698$

By measuring pulse height from a P_2O_3 gas-filled ionization chamber bombarded by $D(d,n)$ neutrons, ground-state Q value = -0.97 ± 0.13 Mev and a level in Si^{31} at 0.7 Mev (Me 48). Cross section, En 54a. Resonances under P^{32} .

V. $S^{34}(n,\alpha)Si^{31}$ $Q_m = -1.309$

Cross section, En 54a.

P³¹

(Figs. 20 and 21)

- $$\text{I. (a) } \text{Al}^{27}(\alpha, n) \text{P}^{30} \quad E_b = 9.668 \quad Q_m = -2.722 \\ \text{(b) } \text{Al}^{27}(\alpha, p) \text{Si}^{30} \quad E_b = 9.668 \quad Q_m = 2.376$$

Thick target resonances observed with radioactive α -particle sources, En 54a.

II. $\text{Si}^{28}(\alpha, p)\text{P}^{31}$ $Q_m = -1.920$

From bombardment of natural silicon with Th($B+C$) α particles, three proton groups are observed corresponding to ground-state Q value of -2.23 Mev and levels in P^{31} at 1.05 and 1.69 Mev (Ha 35, Li 37). From 7-Mev

TABLE XXXIV. Resonances in the $\text{Si}^{30}(p,\gamma)\text{P}^{31}$ reaction.

E_p (kev)	E_x (P ⁸⁰) (Mev)	$(2J+1)\Gamma\gamma$ (ev)	J, π
500 ^a	7.776	0.20 ^a	0.06 ^b
625 ^a	7.897	1.92 ^a	1.8 ^b
675 ^a	7.945	0.087 ^a	0.06 ^b
760 ^a	8.028	0.17 ^a	0.08 ^b
775 ^a	8.042	0.93 ^a	1.0 ^b
840 ^a	8.105	0.192 ^a	$3/2^+ a, b$ $(3/2, 5/2)^+ a$
955 ^a	8.216		
980 ^a	8.241		
995 ^a	8.255		
1000 ^a	8.260		

^a Br 56i.

" BI 501.
b Ho 57,

cyclotron α particles on natural silicon, a γ ray is found of 2.3 ± 0.3 Mev as measured by absorption (Al 48).

III. Si³⁰(p, γ)P³¹ $Q_m = 7.292$

Resonances observed, corresponding P^{31} excitation energies, resonance strengths, and resonance spins and parities deduced from γ -ray angular distribution measurements (Br 56i) in Table XXXIV. Proton energies at five lower resonances in fair agreement with Kl 55a. Also Se 55. A resonance reported at $E_p = 367$ kev (Ta 46) not observed in later work (Kl 55a). Twenty-five resonances reported in the 1.7-2.3-Mev region. Those at $E_p = 1.73$ and 1.82 Mev have $J = 3/2^+$ (Pa 56).

Gamma-ray intensities at five lower resonances in En 56b, Ho 57. Corresponding branching percentages in Fig. 21. Branching percentages indicated for 3.414-, 4.188-, 4.430-, 5.012-, 6.22-, 6.43-, and 6.55-Mev levels and for resonances at $E_p = 840, 980$, and 1000 kev from Br 56i.

Gamma-ray angular distributions (Br 56i, En 56b), and γ - γ angular correlation measurements (Pa 56, Li 57) in agreement with a $J=1/2^+$ assignment to P^{31}

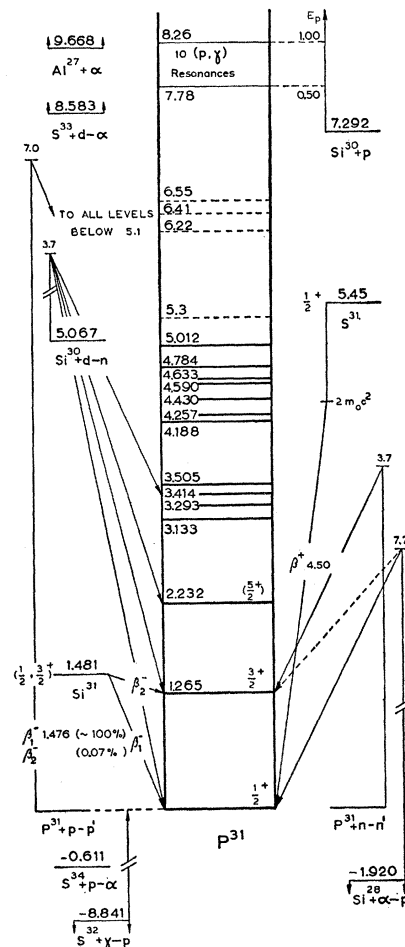


FIG. 20.

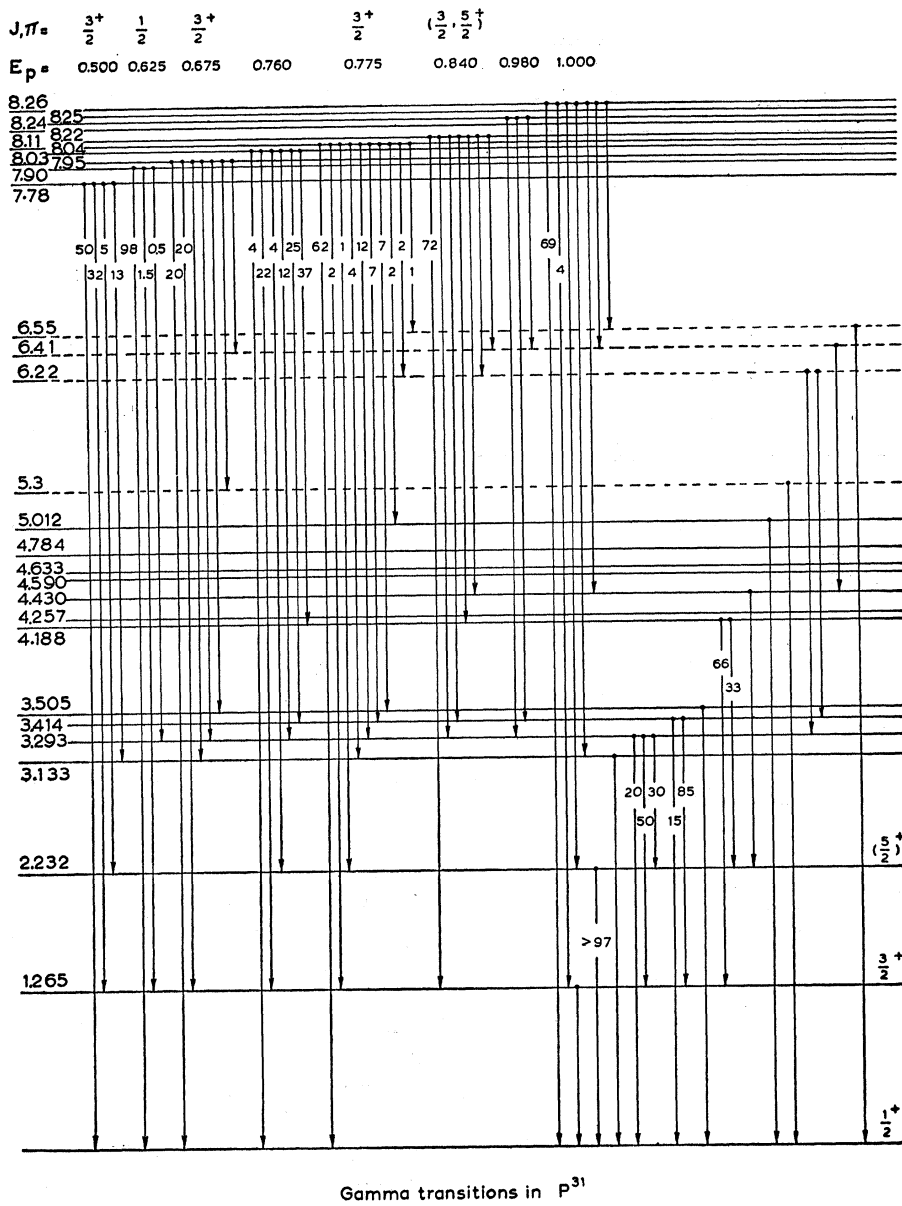


FIG. 21.

ground state, and indicate $J=3/2^+$ for level (1) and very probably $J=5/2^+$ for level (2). The latter level decays for at least 97% by an E2 transition to ground state (Li 57), in remarkable analogy with Si²⁹. Collective motion might be responsible for these anomalies.

Positive parities assigned to resonance levels in Table XXXIV found from γ -ray angular distribution measurements which can only be explained through mixing of M1 and E2 radiation.

IV. $Si^{30}(d,n)P^{31}$ $Q_m = 5.067$

From natural silicon bombardments at $E_d = 3.7$ Mev and with nuclear emulsion technique for neutron detection, Q values are found of 4.56 ± 0.14 , 4.12 ± 0.16 ,

3.57 ± 0.15 , and 2.78 ± 0.16 Mev (Pe 48). With enriched Si³⁰ targets and nuclear emulsions, at $E_d = 1.4$ Mev Q values have been measured of 4.92, 4.59, 3.73, 2.70, and 1.51 Mev, all ± 0.04 Mev (Ma 52). Averaging these results (and assuming that in the earlier data ground-state transition has been missed) following excitation energies in P^{31} are obtained: 0.4, (0.9), 1.4, 2.3, and 3.4 Mev.

V. $Si^{31}(\beta^-)P^{31}$ See Si^{31}

VI. $P^{31}(n,n'\gamma)P^{31}$

No γ rays observed at $E_n = 1.2$ Mev (Va 56a). At $E_n = 2.45$ Mev, a γ ray of 1.25 ± 0.03 Mev is reported

TABLE XXXV. Levels in P^{31} found from $P^{31}(p,p')P^{31}$.

Reference:	En 57a	Va 56, Va 57c, Va 57a
Incident proton energy (Mev):	7.04	3.72 and 4.66
Angle:	90° and 130°	90°
Level in P^{31} (Mev):	1.267	1.264±0.004
	2.234	2.230±0.005
	3.133	3.134±0.006
	3.293	3.292±0.005
	3.414	
	3.505	
	4.188	
	4.257	
	4.430	
	4.590	
	4.633	
	4.784	
	5.012	
	all ±0.005	

(Cr 56a). At $E_n=3.5$ Mev, an intense γ ray is found of 1.24 ± 0.05 Mev, and weak γ rays of 1.0 ± 0.05 , 1.60 ± 0.07 , 1.75 ± 0.08 , and 2.05 ± 0.18 Mev (Sc 54d).

VII. $P^{31}(p,p')P^{31}$

Levels found from this reaction by magnetic analysis at $E_p=7.04$ Mev (En 57a), and at 4.65 Mev (Va 56, Va 57a, Va 57c) in Table XXXV.

In region $E_p=2.3$ – 3.36 Mev, twenty-one resonances observed yielding a 1.26 ± 0.015 -Mev γ ray (Ol 55).

VIII. $S^{31}(\beta^+)P^{31}$ See S^{31}

IX. $S^{32}(\gamma,p)P^{31} Q_m=-8.841$

Cross section, Jo 55, Ri 55, Mo 55a.

X. $S^{33}(d,\alpha)P^{31} Q_m=8.583$

Not observed.

XI. $S^{34}(p,\alpha)P^{31} Q_m=-0.611$

Not observed.

GENERAL REMARKS

Theoretical remarks concerning P^{31} ground-state configuration, Hu 55b, Go 56b.

S^{31}

(Fig. 22)

I. $S^{31}(\beta^+)P^{31} Q_m=5.45$

Half-life averaged from two accurate post-war determinations (Ha 52a, Hu 54) is 2.62 ± 0.09 sec. The β^+ end point determined with cloud chambers as 3.85 ± 0.07 Mev (Wh 41) and 3.87 ± 0.15 Mev (El 41), and with a scintillation spectrometer as 4.50 ± 0.10 Mev (Hu 54). Log $ft=3.7$, indicating a superallowed transition. Hence, S^{31} has $J=1/2^+$.

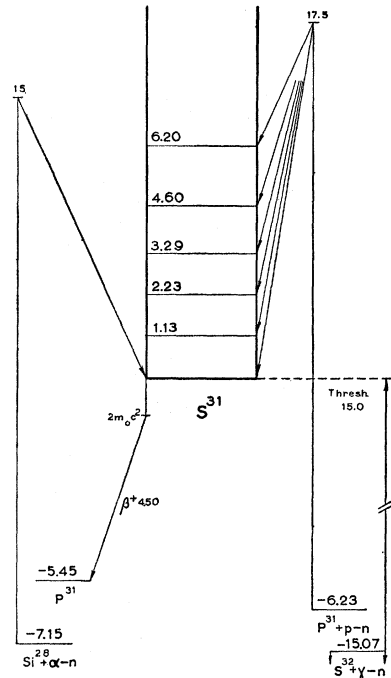


FIG. 22.

II. $Si^{28}(\alpha,n)S^{31} Q_m=-7.15$

Observed (En 54a).

III. $P^{31}(p,n)S^{31} Q_m=-6.23$

With nuclear emulsions at $E_p=17.5$ Mev, the Q value = -6.03 ± 0.2 Mev and levels in S^{31} observed at 1.13 ± 0.2 , 2.23 ± 0.15 , 3.29 ± 0.15 , 4.60 ± 0.15 , and 6.20 ± 0.2 Mev (Ru 55). Agreement with level scheme of P^{31} mirror nucleus is as good as can be expected taking into account relatively low resolution of neutron energy measurement.

IV. $S^{32}(\gamma,n)S^{31} Q_m=-15.07$

Threshold measured as 15.0 ± 0.3 Mev (Be 47a), 14.8 ± 0.4 Mev (Mc 49), and 15.0 ± 0.1 Mev (Ha 52a). Cross section, En 54a, Mo 55a.

Si^{32}

(not illustrated)

I. $Si^{32}(\beta^-)P^{32} Q_m=0.10$

Radioactive Si^{32} produced from reaction $Cl^{37}(p,\alpha 2p)Si^{32}$ at $E_p=340$ Mev. From measured activity and estimated reaction cross section, a half-life is calculated between 100 and 710 years. The β^- spectrum end point is ~ 100 kev. There are no γ rays (Li 53a). Also Li 53. Also produced from neutron capture in Si^{31} in a high-flux reactor. From yield, half-life (in years) computed as 600 times the cross section (in barns) (Tu 54).

P³²
(Fig. 23)

I. P³²(β^-)S³² $Q_m = 1.704$

Six determinations (En 54a) of half-life yield average value of 14.32 ± 0.03 days.

Determinations of β^- end point by magnetic spectrometer in Table XXXVI. Average is 1.7080 ± 0.0026 Mev. Spectrum has allowed shape. Coefficient $r < 0.03$ mc² in a possible Fierz correction $(1+r/W)^{1/2}$ to Kurie plot (Po 56). No discrete γ rays observed (La 54, Go 54b). Log $ft = 7.9$, very large for an allowed transition but this can be explained by l forbiddenness.

Many authors investigated continuous γ radiation (internal bremsstrahlung) (En 54a, Go 54b, Mi 54a, Li 55, Fo 56), internal pair formation (Mc 54, We 54, Mi 56, Gr 56b, Hu 56a), and other small effects involving atomic electron cloud (Ch 54, Ch 55a, Re 55).

II. Si²⁹(α, p)P³² $Q_m = -2.474$

Observed, En 54a.

III. Si³⁰(He³, p)P³² $Q_m = 7.494$

Observed, En 54a.

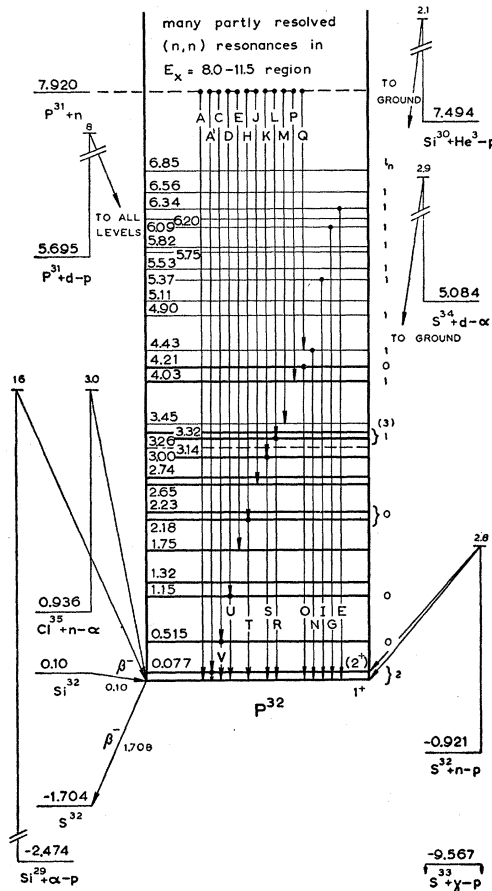


FIG. 23.

TABLE XXXVI. Magnetic-spectrometer determinations of the P³²(β^-)S³² end point.

Reference	End point (Mev)	Reference	End point (Mev)
Ly 37	1.69 \pm 0.03	Sh 51	1.695 \pm 0.005
La 39a	1.72 \pm 0.01	Je 52	1.704 \pm 0.008
Wi 41	1.75 \pm 0.02	Mo 52a	1.697 \pm 0.010
Si 46	1.712 \pm 0.008	Wo 54	1.714 \pm 0.008
La 49a	1.689 \pm 0.010	An 54a	1.712 \pm 0.008
Ag 50	1.718 \pm 0.010	Da 54a	1.711 \pm 0.006
Wa 50	1.708 \pm 0.008	Po 56	1.712 \pm 0.004

IV. P³¹(n, γ)P³² $Q_m = 7.920$

Cross section, Hu 55c.

Twenty γ rays found by high-resolution pair spectrometry from capture of thermal neutrons in phosphorus (Ki 52), and three more found with a two-crystal scintillation spectrometer (Br 56e). Table XXXVII. All γ rays, except B , can be regarded as transitions from capturing state to known levels in P³², or as transitions from known levels to ground. However, intensities of γ rays feeding and de-exciting a level may differ appreciably, indicating that decay scheme may be considerably more complicated.

V. P³¹(n, n)P³¹ $E_b = 7.920$

Cross section and resonances, Hu 55c, Pa 55b, Pa 55.

VI. P³¹(n, p)Si³¹ $E_b = 7.920$ $Q_m = -0.698$

Resonances, En 54a.

Q -value measurements, Si³¹.

VII. P³¹(d, p)P³² $Q_m = 5.695$

Levels in P³² found by magnetic analysis, and l_n values deduced from angular distributions of corre-

TABLE XXXVII. Gamma rays from thermal neutron capture in phosphorus.

γ ray ^a	Energy in Mev	Intensity in photons per 100 captures
A	7.94 \pm 0.03	0.5
A'	7.85 \pm 0.05	1.5
B	7.62 \pm 0.03	2
C	7.42 \pm 0.03	7
D	6.76 \pm 0.03	24
E	6.33 \pm 0.03	0.7
F	6.14 \pm 0.03	1.5
G	6.02 \pm 0.04	1.5
H	5.71 \pm 0.03	6
I	5.41 \pm 0.03	2
J	5.27 \pm 0.03	8
K	4.92 \pm 0.03	4
L	4.68 \pm 0.03	26
M	4.49 \pm 0.03	4
N	4.38 \pm 0.03	11
O	4.20 \pm 0.03	7
P	3.92 \pm 0.03	25
Q	3.55 \pm 0.03	22
R	3.28 \pm 0.04	9
S	3.04 \pm 0.04	7
T	2.19 \pm 0.03	41
U	1.13 \pm 0.03	14
V	0.51 \pm 0.02	28

^a References: Ki 52 for γ rays A through S, Br 56e for γ rays T through V.

TABLE XXXVIII. Levels in P^{32} from the reaction $P^{31}(d,p)P^{32}$.

Reference:	Va 52b	Da 57	l_n
E_d (Mev):	1.8 and 2.0	8	
E_x (P^{32}) (Mev)	E_x (P^{32}) (Mev)		
	0	0	
	0.077 ± 0.002		{ 2
	0.515 ± 0.005		0
	1.154 ± 0.007		0
	1.316 ± 0.008		... ^a
	1.750 ± 0.009		... ^a
	2.177 ± 0.009		... ^a
	2.227 ± 0.009		} 0 or 1
	2.650 ± 0.008		... ^a
	2.742 ± 0.008		... ^a
	2.999 ± 0.010		... ^a
	(3.141 ± 0.012)		... ^a
	3.259 ± 0.009		... ^a
	3.318 ± 0.009		} 1
		3.45 ± 0.1	(3)
	4.032 ± 0.009		1
	4.207 ± 0.010		0
		4.43 ± 0.1	1
		4.66 ± 0.1	weak
		4.90 ± 0.07	1
		5.11 ± 0.1	(isotropic)
		5.37 ± 0.07	1
		5.53 ± 0.07	1
		5.75 ± 0.1	weak
		5.82 ± 0.07	1
		6.09 ± 0.07	1
		6.20 ± 0.1	weak
		6.34 ± 0.1	1
		6.56 ± 0.07	1 or 2
		6.69 ± 0.1	weak
		6.85 ± 0.1	weak

^a Not observed or weak.

sponding proton groups in Table XXXVIII. Ground-state Q value is 5.704 ± 0.008 Mev (Va 52b). The $l_n = 2$ assignment to ground-state doublet also found at $E_d = 7.2$ Mev (Pa 52) and at $E_d = 14.3$ Mev (Bl 53). The $l_n = 0$ admixture to this group is less than 5% (Pa 52).

Experimental yield ratio (excited-state protons over ground-state protons) at $\theta = 90^\circ$ is 1.7 at $E_d = 1.8$ Mev and 1.2 at $E_d = 2.0$ Mev (Va 52b). This agrees reasonably with predicted ratio of 1.67 for ground-state spin $J = 1^+$ and excited-state spin $J = 2^+$ (En 53a, En 54).

See S^{32} , reaction V, for γ rays from $P^{31} + d$ reactions.

VIII. $S^{32}(n,p)P^{32} Q_m = -0.921$

Ionization chamber measurement with pulse-height analysis yields -0.93 ± 0.1 Mev for ground-state Q value (Hu 41). At $E_n = 2.56$ Mev, a 77 ± 2 -kev γ ray observed with a scintillation spectrometer (Da 56c).

Cross section, En 54a, Hu 55a.

Resonances, S^{32} .

IX. $S^{32}(\gamma,p)P^{32} Q_m = -9.567$

Not observed.

X. $S^{34}(d,\alpha)P^{32} Q_m = 5.084$

By magnetic analysis at $E_d = 1.6\text{--}2.9$ Mev and $\theta = 63^\circ$ and 90° , with enriched S^{34} targets, ground-state $Q = 5.04$

± 0.02 Mev (Le 56b). This might be too small since also the value obtained by these authors for $S^{32}(d,\alpha)P^{30}$ ground-state Q value is too small by 60 kev.

XI. $Cl^{35}(n,\alpha)P^{32} Q_m = 0.936$

From ionization chamber pulse-height analysis, ground-state Q values of 1.07 ± 0.15 Mev (Fo 52) and 0.97 ± 0.16 Mev (Ad 53).

Cross section, En 54a.

GENERAL REMARKS

Theoretical discussion of P^{32} spin, Hi 54. Discussion regarding doublet levels in P^{32} , In 53.

S^{32}

(Fig. 24)

I. $Si^{29}(\alpha,n)S^{32} Q_m = -1.553$

Not observed.

II. (a) $P^{31}(p,\gamma)S^{32} Q_m = 8.841$

(b) $P^{31}(p,p'\gamma)P^{31} E_b = 8.841$

(c) $P^{31}(p,\alpha)Si^{28} E_b = 8.841, Q_m = 1.923$

Resonances in these reactions in Table XXXIX. Proton energies listed are weighted averages of values given by different observers. In Pa 55a, only resonances

TABLE XXXIX. Resonances in the $P^{31} + p$ reactions.

E_p (kev)	E_x (S^{32}) (Mev)	Γ (kev)	Decay γ	$(2J+1)\Gamma\gamma^*$ (ev)	J, π^*
355 ^a	9.185		γ		
440 ^{a,b,c}	9.267		γ		
540 ^{a,b,e}	9.364		γ		
648 ^{b,c,d}	9.469		$\gamma \alpha_0$		
816 ^{b,c,e}	9.631		γ_1	1.8	
825 ^e	9.640		γ_0	0.36	1
892 ^{b,c,d}	9.705		$\gamma \alpha_0$		
1050 ^{b,c,d,f}	9.858		$\gamma \alpha_0$		
1084 ^{b,c}	9.891		γ		
1117 ^{b,c,e}	9.923		γ_0	1.9	1
1146 ^{b,c,e}	9.951		γ_1	2.2	
1248 ^{b,c,e}	10.050		$\gamma_0 \gamma_1$	0.24, 3.7 ^h	2
1408 ^{b,c}	10.205		γ		
1443 ^{b,c}	10.239		γ		
1482 ^{b,c}	10.283		γ		
1520 ^f	10.314	9.0 ^f	α_0		
1549 ^{b,c,e}	10.342		γ_1		
1571 ^{b,c}	10.363		γ		
1598 ^{b,c}	10.389		γ		
1640 ^f	10.430	~ 5 ^f	α_0		
1892 ^{c,e,f}	10.674	24 ^{e,f}	$\gamma_0 \alpha_0$	37	1 ⁻
1916 ^e	10.697		γ		
1980 ^e	10.759		α_0		
1985 ^{e,e}	10.764	10 ^e	γ_0	13	1
1990 ^e	10.767		α_0		
2027 ^{e,f}	10.805	24 ^{e,f}	$\gamma_0 \alpha_0$	26	1 ⁻
2120 ^e	10.895	5 ^e	$\gamma_0 \alpha_0$	4.0	1 ⁻
2320 ^e	11.092	8 ^e	γ_0	20	1
2340 ^e	11.111	8 ^e	γ_0	64	1

^a Ta 46, ^b Gr 51, ^c Ke 56a, ^d Fr 51, ^e Pa 55a, ^f Cl 55.^g The symbols have the following meaning: γ gamma radiation observed without specification as to energy; γ_0 transition to S^{32} ground state, γ_1 transition to S^{32} first excited state, α_0 ground-state transition of $P^{31}(p,\alpha)Si^{28}$ reaction, ^h Two values listed relate to γ_0 and γ_1 , respectively.

are listed which decay either to S^{32} ground state or to first excited state. List of resonances decaying through the $P^{31}(p,\alpha)Si^{28}$ ground-state transition is not complete. Altogether, there are 16 resonances in $E_p=1.0\text{--}2.5$ Mev region, decaying in this way, most of which do not decay by γ -ray emission (Cl 55).

There are 21 resonances in $E_p=2.3\text{--}3.36$ Mev region showing a 1.26 ± 0.015 Mev γ ray from $P^{31}(p,p'\gamma)P^{31}$ reaction. For $E_p > 2.47$ Mev, also a 1.8-Mev γ ray observed from $P^{31}(p,\alpha)Si^{28}$ leading to first level in Si^{28} (Ol 55).

Spin and parity assignments in Table XXXIX from γ -ray angular distribution measurements. Spin of first level in S^{32} probably 2^+ (Pa 55a). For γ -ray energies measured at several resonances, Ke 56a. Also Sm 54, Va 56. See P^{31} and Si^{28} for levels observed in these nuclei from reactions b and c.

III. $P^{31}(d,n)S^{32}$ $Q_m=6.616$

With nuclear emulsions, ground-state $Q=6.63\pm 0.08$ Mev measured at $E_d=8$ Mev. Transitions observed to known lower levels in S^{32} and to new levels at 6.29, 7.28, and 8.33 Mev, all ± 0.10 Mev. Angular distribution measurements yield $l_p=0$ for transitions to ground and to 3.78-Mev level, and $l_p=2$ for transitions to 2.24-Mev level (El 55a). This in agreement with results in Ca 55, obtained at $E_d=9$ Mev with a triple ionization chamber for neutron detection. However, transition to 3.78-Mev level not resolved from those to 4.29- and 4.47-Mev levels. Group leading to 5.76-Mev level has an $l_p=2$ angular distribution. Also En 54a.

Gamma rays, following bombardment of phosphorus with 4.6-Mev deuterons, observed with a magnetic pair spectrometer with following energies: 4.43 ± 0.03 , 4.73 ± 0.03 , 4.95 ± 0.03 , 5.31 ± 0.03 , 5.81 ± 0.03 , 6.13 ± 0.03 , 6.86 ± 0.03 , 7.49 ± 0.07 , 8.19 ± 0.03 , and 8.56 ± 0.03 Mev. Neutron binding energies in S^{32} , P^{32} , and Si^{29} are 15.08, 7.92, and 8.47 Mev, respectively, showing that only last two γ rays can be assigned to this reaction with certainty. However, several other γ rays could also be regarded as transitions in S^{32} from level to ground (Be 55).

Theoretical discussion of lowest three S^{32} states, Hu 55b.

IV. $P^{32}(\beta^-)S^{32}$ See P^{32}

V. $S^{32}(e,e')S^{32}$

Differential cross section measured for elastic scattering of 187-Mev electrons, and for inelastic scattering to 2.24-, 3.78-, 5.76-Mev levels and to a new level at 6.6 Mev. From comparison with $\sigma(\theta)$ for the excitation of 2^+ levels in other even-even nuclei it is highly probable that 2.24-Mev level in S^{32} has also $J=2^+$ (He 56).

VI. $S^{32}(n,n')S^{32}$

Inelastic scattering of neutrons studied with scintillation spectrometers. At $E_n=2.56$ Mev, a γ ray of

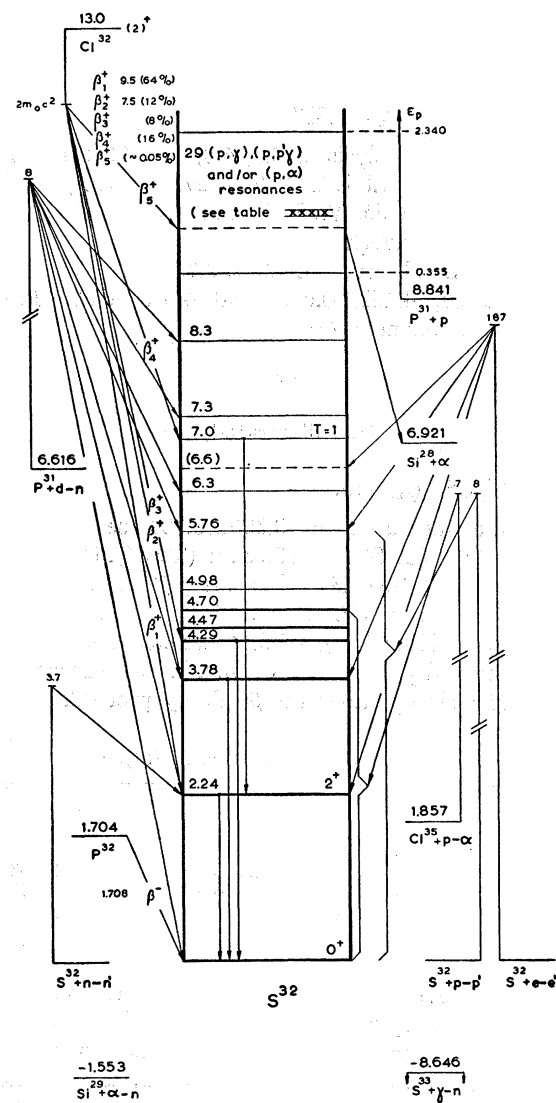


FIG. 24.

2.23 ± 0.02 Mev found (Da 56c). At $E_n=3.7$ Mev, energy of this γ ray measured as 2.25 ± 0.03 Mev; no others observed (Ro 55a).

Also En 54a, Mo 56c.

Elastic scattering angular distributions and inelastic scattering cross section, En 54a, Li 55a, El 56.

VII. $S^{32}(p,p')S^{32}$

By magnetic analysis, at $E_p=8$ Mev, levels in S^{32} found at 2.25, 3.81, 4.32, 4.50, 4.74, 5.04, and 5.83 Mev, all ± 0.02 Mev (Ar 52). By comparison with the results obtained by these authors in Al^{27} , excitation energies are probably too high by an amount slowly increasing up to 70 kev for highest levels.

See Cl^{32} for resonances in yield of a 2.2-Mev γ ray.

VIII. $Cl^{32}(\beta^+)S^{32}$ See Cl^{32}

IX. $S^{33}(\gamma, n)S^{32}$ $Q_m = -8.646$

Not observed.

X. $Cl^{35}(p, \alpha)S^{32}$ $Q_m = 1.857$

By magnetic analysis at 2.5, 4.0, and 7.0 Mev, the ground-state $Q = 1.865 \pm 0.015$ Mev (Al 55a), 1.860 ± 0.005 Mev (Va 56, Va 57d), and 1.863 ± 0.008 Mev (En 56c), respectively.

Levels in S^{32} observed at 2.237, 3.780, 4.287 Mev, all ± 0.008 Mev, 4.465 ± 0.010 , and 4.698 ± 0.010 Mev (En 56c). Resonances, A³⁶.

 Cl^{32}

(not illustrated)

I. $Cl^{32}(\beta^+)S^{32}$ $Q_m = 13.0$

Half-life measured as 0.306 ± 0.004 sec (Gl 55), 0.32 ± 0.01 sec (Br 54a) and 0.28 sec (Ty 54). Maximum β^+ energy is 9.5 ± 0.4 Mev, indicating β^+ transitions to 2.24-Mev level in S^{32} . This branch has intensity of $48 \pm 15\%$, yielding $\log ft = 4.6$. A weaker branch with ~ 7.5 -Mev end point also observed. In one per several thousand disintegrations the β^+ decay proceeds to an

TABLE XL. Gamma rays from $Cl^{32}(\beta^+)S^{32}$.

Reference:	Gl 55	Br 54a
E_γ in Mev	2.21 ± 0.03 2.77 or 3.79 ± 0.08 4.27 ± 0.08 4.77 ± 0.04	(0.70) (0.10) (0.07) (0.14)
		2.25 ± 0.04 (3.79 ± 0.08) 4.33 ± 0.09 4.82 ± 0.08

α -unstable level in S^{32} with $E_\alpha = 2-3$ Mev (Gl 55). Gamma-ray energies and intensities in Table XL.

Three lowest-energy γ rays well explained as ground-state transitions of corresponding S^{32} levels. The 4.8-Mev γ ray might be transition from $T=1$ analog of the P^{32} and Cl^{32} ground states at 7.0 Mev, to first level. The β^+ transition to $T=1$ level is superallowed ($\log ft = 3.8$) (Bo 55, Wi 56a). From γ -ray intensities branchings of 64, 12, 8, and 16% computed for β^+ transitions to the 2.24-, 3.78-, 4.29-, and 7.0-Mev levels.

II. $S^{32}(p, n)Cl^{32}$ $Q_m = -13.8$

Threshold is measured as 14.3 ± 0.5 Mev (Gl 55), and 14.5 ± 0.6 Mev (Br 54a).

At $E_p = 17.5$ Mev, neutron groups leading to Cl^{32} levels at 1.0, 1.4, and 2.0 Mev observed with nuclear emulsions (Aj 55).

 P^{33}

(not illustrated)

I. $P^{33}(\beta^-)S^{33}$ $Q_m = 0.249$

Average value of 24.5 ± 0.2 days for half-life from four determinations (En 54a, Ni 54).

The β^- end point determined by magnetic spectrometer as 0.27 ± 0.02 Mev (Sh 51c), 0.26 ± 0.02 Mev (Je 52), 0.251 ± 0.005 Mev (El 54), and 0.249 ± 0.002 Mev (Ni 54), and as 0.246 ± 0.005 Mev by Al absorption (We 52). The β^- transition is allowed ($\log ft = 5.1$) but l forbidden. No γ rays found (We 52, also La 54).

II. $Si^{30}(\alpha, p)P^{33}$ $Q_m = -2.982$

Not observed.

III. $S^{33}(n, p)P^{33}$ $Q_m = 0.534$

Cross section, En 54a, Ni 54.

IV. $S^{34}(\gamma, p)P^{33}$ $Q_m = -10.885$

Observed, En 54a.

V. $S^{36}(\rho, \alpha)P^{33}$ $Q_m = 0.5$

Not observed.

VI. $Cl^{37}(\gamma, \alpha)P^{33}$ $Q_m = -7.864$

Observed, En 54a.

 S^{33}

(Fig. 25)

I. $Si^{30}(\alpha, n)S^{33}$ $Q_m = -3.516$

Not observed.

II. $S^{32}(n, \gamma)S^{33}$ $Q_m = 8.646$

Cross sections and abundances of sulfur isotopes (Hu 55c) indicate that probably most of thermal-neutron captures in natural sulfur occur in S^{32} .

Gamma rays from thermal neutron capture in natural sulfur in Table XLI. Remarkable are strong E1 transitions to and from p states in S^{33} at 3.22 and 5.71 Mev. Of all proton groups observed from $S^{32}(d, p)S^{33}$ reaction at $E_d = 6.55$ Mev, both at 90° and at 130° , groups leading to these levels have also largest intensity (see Reaction V). Several of weaker γ rays of Table XLI might also be explained as transitions to or from known levels in S^{33} , but their assignment is less certain.

III. $S^{32}(n, n)S^{32}$ $E_b = 8.646$

Cross section and resonances, Hu 55c, Mo 55b, Pa 55, Mo 56b, La 56a. Fifteen resolved resonances observed below $E_n = 1.1$ Mev. Characteristics of seven lowest-energy resonance in Table XLII. Recently, $J \geq 5/2$, $l_n \geq 2$ reported for 585-kev resonance, La 56a.

IV. (a) $S^{32}(n, p)P^{32}$ $E_b = 8.646$ $Q_m = -0.921$ (b) $S^{32}(n, \alpha)Si^{29}$ $E_b = 8.646$ $Q_m = 1.553$

Cross section, En 54a, Hu 55a.

Also P^{32} and Si^{29} for reactions (a) and (b), respectively.

TABLE XLI. Gamma rays from thermal neutron capture in sulfur.

Reference: Method: Gamma ray	Gr 55a		Ki 52, Ki 54a		Probable transition in S ³³ b
	Magnetic Compton spectrometer	Intensity in photons per 100 captures	Magnetic pair spectrometer	Intensity in photons per 100 captures a	
	Energy in Mev		Energy in Mev		
A	8.63 ± 0.04	1.8	8.64 ± 0.02	1.2	(c) → (0)
B	7.80 ± 0.04	2.6	7.78 ± 0.03	1.6	(c) → (1)
C	7.42 ± 0.05	0.6	7.42 ± 0.03	0.3	
D	7.20 ± 0.05	0.5	7.19 ± 0.03	0.2	
E	6.62 ± 0.05	0.5	6.64 ± 0.03	0.25	(c) → (2)
F	5.88 ± 0.05	0.4	5.97 ± 0.06	0.6	
G	5.44 ± 0.02	48.0	5.43 ± 0.02	60	(c) → (7)
H	5.07 ± 0.03	3.5	5.03 ± 0.06	3.5	
I	4.87 ± 0.02	12.0	4.84 ± 0.06	11	(32) → (1)
J	4.58 ± 0.03	1.2	4.60 ± 0.03	3.5	
K	4.40 ± 0.02	6.0	4.38 ± 0.03	7	
L	3.66 ± 0.05	2.0	3.69 ± 0.05	4	
M	3.41 ± 0.01	7.1	3.36 ± 0.05	7	(32) → (3)
N	3.27 ± 0.01	19.0	3.21 ± 0.03	20	(7) → (0)
N'	3.10 ± 0.03	2.0			
O	2.975 ± 0.01	13.0	2.94 ± 0.05	20	(c) → (32)
P	2.82 ± 0.02	4.0			
Q	2.70 ± 0.05	2	Br 56e. Two-crystal scintillation spectrometer		
R	2.550 ± 0.02	4.4	2.34 ± 0.03	37	
S	2.415 ± 0.01	30			(7) → (1)
T	2.29 ± 0.03	5			(3) → (0)
U	2.00 ± 0.02	3			(2) → (0)
V			1.52 ± 0.05	1	(3) → (1)
W	0.84 ± 0.01	47	0.84 ± 0.02	56	(1) → (0)

a Where possible, intensities are taken from Ki 54a. For γ rays C, D, F, H, and J, from Ki 52, multiplied by correction factor varying from 0.4 to 0.7.

b Numbering of levels from Table XLII. The capturing state is denoted by (c). All transitions are assumed to result from $S^{32}(n,\gamma)S^{33}$ reaction.

V. $S^{32}(d,p)S^{33} Q_m = 6.421$

By magnetic analysis at $E_d = 1.8, 2.9$, and 6.5 Mev, the ground-state Q value = 6.422 ± 0.011 Mev (St 51), 6.408 ± 0.020 Mev (Le 56b), and 6.413 ± 0.006 Mev (Pa 57), respectively. Sixty-seven levels in S^{33} found recently by high-resolution magnetic analysis, Pa 57, Table XLIII, together with l_n values from angular distribution measurements (Ho 53a, Ho 53d). Levels in the $E_x = 6.54\text{--}7.2$ -Mev region not indicated in Fig. 25. Also, En 54a.

VI. $P^{33}(\beta^-)S^{33}$ See P^{33}

VII. $Cl^{33}(\beta^+)S^{33}$ See Cl^{33}

VIII. $S^{34}(\gamma,n)S^{33} Q_m = -11.419$

Threshold measured as 10.85 ± 0.20 Mev (Sh 51a). Cross section, En 54a.

IX. $Cl^{35}(d,\alpha)S^{33} Q_m = 8.278$

From magnetic analysis, at $\theta = 90^\circ$, ground-state $Q = 8.277 \pm 0.010$ Mev, and levels in S^{33} are observed at

TABLE XLII. Resonances in the sulfur total neutron cross section (Pe 50, Hu 55c).

E_n (kev)	E_x (S^{33}) (Mev)	J, π	l_n	Γ_n (kev)
111 ± 2	8.754	1/2 ⁺	0	18 ± 3
203 ± 2	8.843		≥ 1	< 2
274 ± 2	8.912		≥ 1	< 3
290 ± 2	8.927		≥ 1	< 3
375 ± 3	9.010	1/2 ⁺	0	12 ± 2
585 ± 3	9.213	3/2 ⁻	1	1.4 ± 0.5
700 ± 4	9.325	1/2 ⁺	0	14 ± 3

TABLE XLIII. Levels in S^{33} from $S^{32}(d,p)S^{33}$.

Level	E_x (S^{33}) in Mev a	l_n b	Level	E_x (S^{33}) in Mev a
(0)	...	2	(34)	5.888
(1)	0.839	0	(35)	5.915
(2)	1.965		(36)	5.982
(3)	2.314		(37)	6.067
(4)	2.869		(38)	(6.079)
(5)	2.936		(39)	6.101
(6)	2.971		(40)	6.131
(7)	3.222	1	(41)	6.234
(8)	3.832		(42)	6.261
(9)	3.935		(43)	6.310
(10)	4.049		(44)	6.326
(11)	4.095		(45)	6.360
(12)	4.145		(46)	6.372
(13)	4.211	1	(47)	6.416
(14)	4.377		(48)	6.427
(15)	4.425		(49)	6.487
(16)	4.732		(50)	6.513
(17)	4.747		(51)	6.526
(18)	4.869		(52)	6.559
(19)	4.919		(53)	6.616
(20)	4.941		(54)	6.675
(21)	5.177		(55)	6.689
(22)	5.210		(56)	6.710
(23)	5.272		(57)	6.720
(24)	5.287		(58)	6.788
(25)	5.340		(59)	6.892
(26)	5.351		(60)	6.903
(27)	5.399		(61)	6.965
(28)	5.479		(62)	6.999
(29)	5.597		(63)	7.017
(30)	5.613		(64)	7.037
(31)	5.622		(65)	7.133
(32)	5.711	1	(66)	7.164
(33)	5.864		(67)	7.183

a (Pa 57). Preliminary results obtained at $E_d = 6.0$ and 6.5 Mev, $\theta = 90^\circ$ and 130° . Errors of 6 kev are assigned to all excitation energies, except to that of level (1) which has a 5-kev error. The proton groups leading to levels (5), (7), (32), (34), (48), (54), (55), and (67) are exceptionally intense.

b (Ho 53a, Ho 53d). Angular distribution measurements at $E_d = 8.0$ Mev, using Al absorption for separation of proton groups.

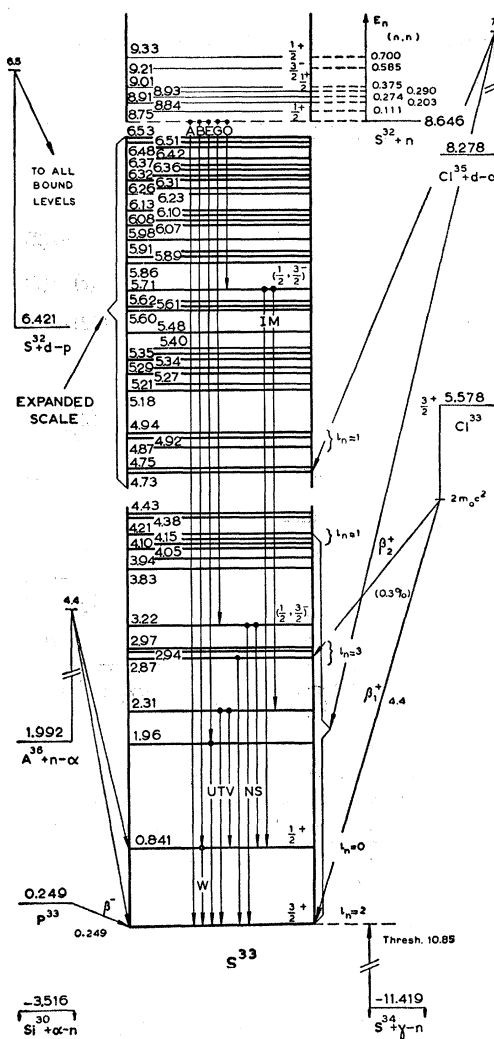


FIG. 25.

0.844 ± 0.006 , 1.966 ± 0.007 , 2.312 , 2.869 , 2.938 , 2.969 , 3.227 , all ± 0.008 , 3.840 , 3.947 , 4.060 , 4.105 , 4.159 , 4.224 , all ± 0.009 , and 4.749 ± 0.010 Mev. Barium-chloride targets containing natural Cl were bombarded with deuterons of several energies between 3.0 and 7.5 Mev (Pa 55c). A recent re-evaluation has shown that reported 3.365 Mev level does not exist. Alpha-particle groups leading to 4.38- and 4.43-Mev levels, observed from $S^{32}(d,p)S^{33}$ reaction, may have been present, but were weak or obscured by contaminant groups (Pa 57).

X. $A^{36}(n,\alpha)S^{33} Q_m = 1.922$

Ionization-chamber measurements with pulse-height analysis at $E_n = 2.15$ – 4.40 Mev yield 2.0 ± 0.1 Mev for ground-state Q value. A level at 1.1 ± 0.1 Mev also observed (To 53). Also, En 54a.

Cl³³

(Fig. 26)

I. $Cl^{33}(\beta^+)S^{33} Q_m = 5.578$

Half-life measurements yield 2.8 sec (Ho 40) and 2.8 sec (Sc 48). Other determinations, 2.4 ± 0.2 sec (Wh 41) and 1.8 ± 0.1 sec (Bo 51), in doubt as possibly a mixture of Cl^{33} and Cl^{34} has been studied (St 53).

Possible confusion with short-lived Cl^{34} also sheds doubt on measurements of beta-spectrum end point: 4.13 ± 0.07 Mev with a cloud chamber (Wh 41), and 4.43 ± 0.13 Mev (Bo 51) and 4.2 ± 0.2 Mev (Na 53) with a scintillation spectrometer. Log $ft = 3.7$, approximately.

A γ ray of 2.85 Mev with an intensity of 0.3% per disintegration observed (Me 54).

II. $S^{32}(p,\gamma)Cl^{33} Q_m = 2.285$

In $E_p = 200$ – 800 kev region, one resonance found at $E_p = 594 \pm 5$ kev. Three γ rays with following energies and relative intensities observed:

$$\begin{aligned}\gamma_1 & 2.862 \pm 0.015 \text{ Mev (0.51)}, \\ \gamma_2 & 2.053 \pm 0.015 \text{ Mev (0.49)}, \\ \gamma_3 & 0.806 \pm 0.004 \text{ Mev (0.50)}.\end{aligned}$$

Last γ ray is coincident with γ_2 but not with γ_1 . Gamma-ray angular distribution measurements are only consistent with a $J = 3/2^+$ assignment to the resonance and confirm assignments of $3/2^+$ to the ground state and $1/2^+$ to the 0.806 Mev level. Both γ_1 and γ_2 are of mixed $M1+E2$ character with mixing ratios of $x^2 = 0.10 \pm 0.01$ and 0.005 ± 0.003 , respectively (Va 56f).

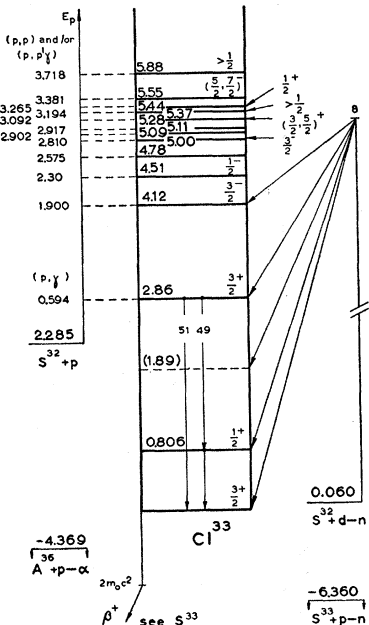


TABLE XLIV. Resonances for elastic proton scattering on S^{32} , and corresponding Cl^{33} levels (Ol 56).

E_p (Mev)	E_x (Cl^{33}) (Mev)	Γ (kev)	J, π
1.900	4.122	8.5	$3/2^-$
2.30	4.51	52	$1/2^-$
2.575	4.775	≤ 5	
2.810	5.002	~ 6	$3/2^-$
2.902	5.092	≤ 5	
2.917	5.107	≤ 5	
3.092	5.275	≤ 2	$(3/2, 5/2)^+$
3.194	5.373	≤ 2	$> 1/2$
3.265	5.442	32	$1/2^+$
3.381	5.554	≤ 2	$(5/2, 7/2)^-$
3.718	5.880	≤ 2	$> 1/2$

III. (a) $S^{32}(p,p)S^{32}$ $E_b=2.285$ (b) $S^{32}(p,p'\gamma)S^{32}$ $E_b=2.285$ $E_\gamma=2.24$

Resonances observed in elastic scattering cross section at five different angles in Table XLIV. Essentially same results for $E_p=1.90$ - and 2.30-Mev resonances also given, Fe 53. Two more very broad ($\Gamma \sim 300$ kev) resonances probably present at about $E_p=3.5$ Mev (Ol 56). States at $E_p=2.81, 2.90, 2.92, 3.09, 3.19, 3.38$, and 3.72 Mev also resonant for 2.24-Mev γ rays from inelastic scattering, Le 56.

IV. $S^{32}(d,n)Cl^{33}$ $Q_m=0.060$

Several neutron groups observed with nuclear emulsions at $E_d=8$ Mev. Ground-state Q value is 0.25 Mev, and levels found at $E_x=0.76 \pm 0.07$, (1.89), 2.84 ± 0.06 , and 4.22 ± 0.08 Mev. Several more closely spaced levels found above 4.22 Mev. From angular distribution measurements and Butler analysis, Cl^{33} ground state can be characterized as $J=(3/2, 5/2)^+$ ($l_p=2$), level at 0.76 Mev as $J=1/2^+$ ($l_p=0$), while levels at 2.84 and 4.22 Mev check best with $J=(1/2, 3/2)^-$ ($l_p=1$) (Mi 53).

V. $S^{33}(p,n)Cl^{33}$ $Q_m=-6.360$

Observed, En 54a.

VI. $A^{36}(p,\alpha)Cl^{33}$ $Q_m=-4.369$

Not observed.

P³⁴

(not illustrated)

I. $P^{34}(\beta^-)S^{34}$ $Q_m=5.2$

Best measurement of half-life yields 12.40 ± 0.12 sec (Bl 46, also Co 40, Hu 45).

The β^- decay proceeds predominantly to ground state and first excited state of S^{34} (Bl 46); in addition, the γ spectrum reveals weak branching to a 4.0-Mev level (Mo 56d). End point of high-energy β^- branch is 5.1 ± 0.2 Mev, that of second branch, 3.2 ± 0.2 Mev, as measured by Al absorption (Bl 46). Branching ratios and $\log ft$ in Table XLV.

TABLE XLV. The $P^{34}(\beta^-)S^{34}$ decay.

E_x (S^{34}) (Mev)	0	2.10	3.22	4.0 b
E_{β^-} (Mev)	5.1 ± 0.2 a	3.2 ± 0.2 a	...	0.2 b
Branching ratio (%)	75 a	25 a	...	
$\log ft$	5.1 a	4.7 a	> 5.6 b	4.9 b

a Bl 46, b Mo 56d.

Spin and parity of P^{34} very probably 1^+ (see S^{34} , general remarks).

Discussion of β^- transition probabilities, De 53b.II. $P^{33}(n,\gamma)P^{34}$ $Q_m=6.5$

Perhaps observed, En 54a.

III. $S^{34}(n,p)P^{34}$ $Q_m=-4.4$

Cross section, En 54a.

IV. $S^{36}(d,\alpha)P^{34}$ $Q_m=4.8$

Not observed.

V. $Cl^{37}(n,\alpha)P^{34}$ $Q_m=-1.4$

Cross section, En 54a.

S³⁴

(Fig. 27)

I. $P^{31}(\alpha,p\gamma)S^{34}$ $Q_m=0.611$

Investigated with 8.1-Mev cyclotron α particles and with scintillation counters for energy and coincidence

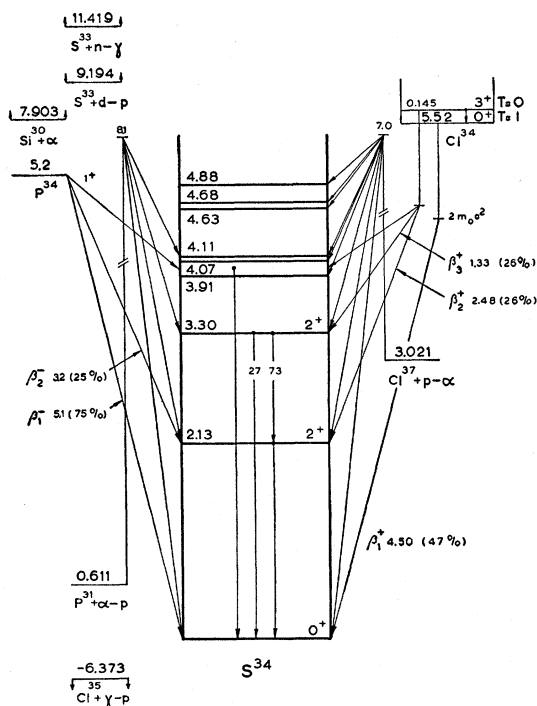


FIG. 27.

measurements of protons and γ quanta. Ground-state Q value = 0.7 ± 0.1 Mev; levels found at 2.13 ± 0.02 , 3.33 ± 0.05 , 4.32 ± 0.08 , and 4.8 ± 0.1 Mev. Branching of γ decay of 3.30-Mev level is $(73 \pm 4)\%$ to 2.13-Mev level and $(27 \pm 4)\%$ to ground state (St 56b).

II. $S^{33}(n,\gamma)S^{34}$ $Q_m = 11.419$

Not observed.

III. $S^{33}(d,p)S^{34}$ $Q_m = 9.194$

Reaction reported (En 54a). Not confirmed (Pa 57).

IV. $P^{34}(\beta^-)S^{34}$ See P^{34}

V. $Cl^{34}(\beta^+)S^{34}$ See Cl^{34}

VI. $Cl^{35}(\gamma,p)S^{34}$ $Q_m = -6.373$

Not observed.

VII. $Cl^{37}(\rho,\alpha)S^{34}$ $Q_m = 3.021$

Ground-state Q value measured by magnetic analysis as 3.015 ± 0.015 (Al 55a), 3.028 ± 0.006 (Va 56, Va 57d), and 3.026 ± 0.008 Mev (En 56c).

Also by magnetic analysis, at E_p between 1.8 and 4.0 Mev, a level was found at 2.129 ± 0.014 Mev (Va 56), while at $E_p = 7.0$ Mev, levels found at 2.127, 3.302, 3.915, 4.073, 4.114, 4.621, 4.685, and 4.876, all ± 0.008 Mev (En 56c).

GENERAL REMARKS

From allowed character of P^{34} decay to S^{34} ground state and to 2.13-Mev level, and of Cl^{34m} ($J=3^+$) decay to 2.13-Mev level follow assignment of $J=1^+$ to P^{34} and 2^+ to S^{34} (2.13). From $\gamma-\gamma$ angular correlations, spin of 3.30-Mev level is 2^+ (Ha 56d). If 4.0-Mev γ rays observed in decay of P^{34} and Cl^{34} (Mo 56d) come from same state, this should also have 2^+ . More accurate energy measurements necessary to establish this assignment.

Theoretical discussion of position of lowest 2^+ states in even-even nuclei, Th 56.

Cl³⁴

(Fig. 28)

I. $Cl^{34}(\beta^+)S^{34}$ $Q_m = 5.52$

Half-life measured as 1.58 ± 0.05 (St 53b), and 1.53 ± 0.02 sec (Kl 54b). Best measurement of half-life of isomeric state yields 32.40 ± 0.04 min (Gr 56), in agreement with less accurate determinations (En 54a).

Measurements of positron energies and intensities in Table XLVI.

The 4.5-Mev β^+ branch is emitted by ground state (Ar 53, also Ma 54a); the ft value is 3160 ± 120 sec (Gr 56), indicating that Cl^{34} ground state is the $T=1$,

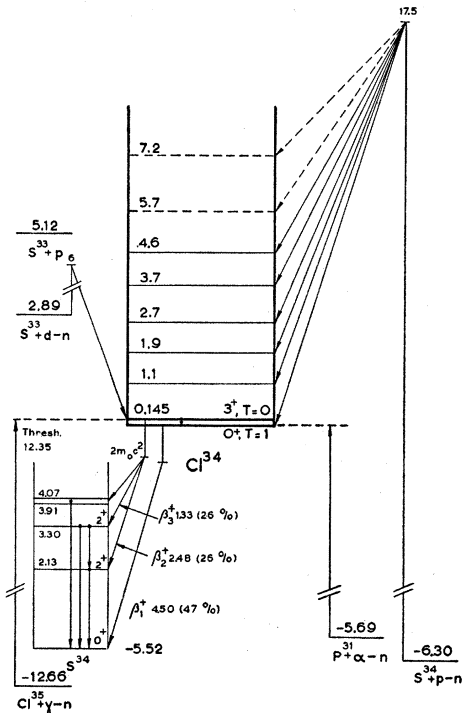


FIG. 28.

$J=0^+$ analog of S^{34} ground state (also Qu 56). Log ft for transitions from Cl^{34m} to S^{34} (2.13) and (3.30) are 6.1 and 4.9, respectively.

Energies of γ rays in decay of Cl^{34m} in Table XLVII. From conversion coefficient of 145-kev γ ray, which is $(14 \pm 4)\%$ (St 53), it follows that this is a M3 transition. Hence, isomeric state has $J=3^+$. Intensity of 4.0-Mev γ ray indicates log ft = about 5.4 for corresponding β^+ transition (Mo 56d). Angular correlation of 1.17- and 2.13-Mev γ rays indicates that both 2.13- and 3.30-Mev level have $J=2^+$. The 1.17-Mev γ ray has a 1.7% E2 admixture (Ha 56d). Discussion of spins and parities of S^{34} levels, under S^{34} , general remarks.

II. $P^{31}(\alpha, n)Cl^{34}$ $Q_m = -5.69$

Ground-state Q value, as derived from threshold measurements, is -5.7 ± 0.2 Mev. This corresponds to threshold for slow neutron production as well as for production of 1.58-sec ground-state activity (Qu 56).

TABLE XLVI. The β^+ decay of Cl^{34} and Cl^{34m} .

Reference:	Ru 51 Magnetic spectrometer	Hu 54a Scintillation spectrometer	Gr 56 Magnetic spectrometer
End point β_1^+ (Mev)	4.45 ± 0.11 (46%)	4.45 ± 0.10	4.50 ± 0.03 (47%)
End point β_2^+ (Mev)	2.58 ± 0.26 (28%)		2.48 ± 0.07 (26%)
End point β_3^+ (Mev)	1.3 ± 0.2 (26%)		1.33 ± 0.10 (26%)

TABLE XLVII. Gamma rays in the decay of Cl^{34m}.

Reference:	Ru 51	Ti 51	Mo 56d
Method:	Magnetic spectrometer	Scintillation spectrometer	Scintillation spectrometer
E_{γ_1} (Mev)	0.145 ± 0.003		
E_{γ_2} (Mev)		1.16 ± 0.03	
E_{γ_3} (Mev)	2.13 ± 0.12	2.10 ± 0.03	
E_{γ_4} (Mev)	3.30 ± 0.14	3.22 ± 0.03	
E_{γ_5} (Mev)			4.0 (0.2%)

III. S³³(p, γ)Cl³⁴ $Q_m = 5.12$

Not observed.

IV. S³³(d,n)Cl³⁴ $Q_m = 2.89$

Observed, En 54a.

V. S³⁴(p,n)Cl³⁴ $Q_m = -6.30$

Studied with 17.5-Mev protons and detection of neutrons by nuclear emulsions. Highest Q value observed was -6.1 Mev; if this corresponds to Cl³⁴ ground state, there are levels at 1.1, 1.9, 2.7, 3.7, 4.6, (5.7), and (7.2) Mev (Aj 55).

VI. Cl³⁵(γ ,n)Cl³⁴ $Q_m = -12.66$

The Q value for transition to 32-min metastable state at 0.145 Mev is -12.35 ± 0.35 Mev (De 55). Cross section, En 54a, Go 54a.

GENERAL REMARKS

Positions of the lowest $T=0$ and $T=1$ states in Cl³⁴ and other self-conjugated odd-odd nuclei, St 53b, St 53a, Pe 53, Mo 54, Wi 56a. Discussion of Cl³⁴ ground-state configuration, Ku 53, De 53a. See Cl³⁶, General remarks, for discussion of relation between excitation energies in Cl³⁴ and Cl³⁶.

S³⁵
(Fig. 29)

I. S³⁵(β^-)Cl³⁵ $Q_m = 0.168$

Half-life averaged from four determinations (En 54a) is 87.3 ± 1.1 days. Five magnetic or electrostatic spectrometer determinations (En 54a, Fe 54a) of β^- spectrum end point yield an average value of 168.1 ± 0.5 kev. Spectrum has allowed shape, at least down to 2 kev (En 54a, Mo 54a, Di 55). Log $f_t = 5.0$. A spin $J = 3/2$ for S³⁵ found from microwave experiments (We 51). Computation of β^- matrix element based on jj coupling, Gr 56.

II. S³⁴(n, γ)S³⁵ $Q_m = 6.988$

Cross section, En 54a, Hu 55c.

III. S³⁴(d,p)S³⁵ $Q_m = 4.763$

From bombardment of natural sulfur targets at $E_d = 6.5$ Mev and $\theta = 90^\circ$, weak proton groups observed by magnetic analysis corresponding to transitions to

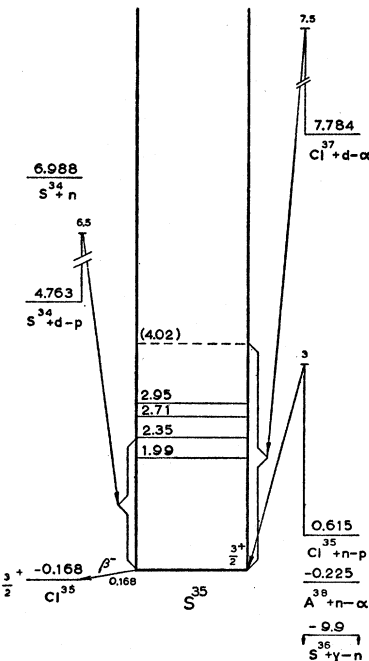


FIG. 29.

S³⁵ ground state ($Q = 4.76$ Mev) and to levels at 1.99 and 2.35 Mev (Pa 57).

IV. Cl³⁵(n,p)S³⁵ $Q_m = 0.615$

Cross section, En 54a, Hu 55c, Be 55c. Q value determined from ionization-chamber pulse-height analysis both with thermal and with $D(d,n)$ neutrons as 0.52 ± 0.04 Mev (Gi 44).

V. S³⁶(γ ,n)S³⁵ $Q_m = -9.9$

Not observed.

VI. Cl³⁷(d,α)S³⁵ $Q_m = 7.784$

From bombardment of BaCl₂ targets containing natural chlorine, at several deuteron energies between 3.0 and 7.5 Mev, Q value determined by magnetic analysis at $\theta = 90^\circ$ as 7.783 ± 0.012 Mev. Levels in S³⁵ observed at (1.922), (2.348), 2.714, and (4.025) Mev, all ± 0.010 Mev (Pa 55c). A recent re-evaluation shows that an additional α -particle group which had been assigned to Cl³⁵(d,α) reaction actually has to be ascribed to Cl³⁷(d,α) leading to a S³⁵ level at 2.955 ± 0.010 Mev (Pa 57).

VII. A³⁸(n,α)S³⁵ $Q_m = -0.225$

Not observed.

Cl³⁵

(Fig. 30)

I. S³²(α,p)Cl³⁵ $Q_m = -1.857$

Work with α particles from natural radioactive sources, En 54a.

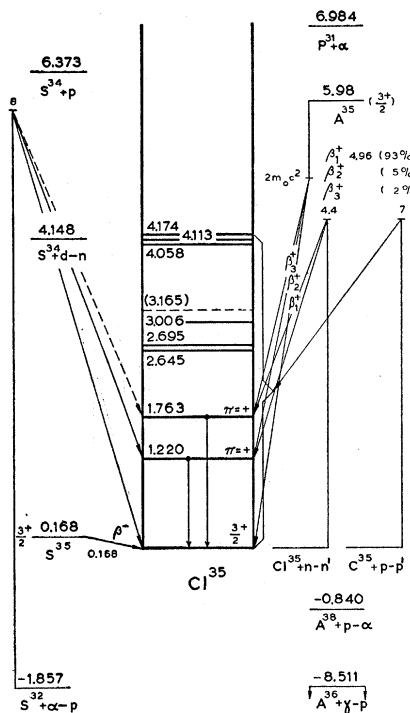


FIG. 30.

With 8-Mev cyclotron α particles and proton detection with a scintillation spectrometer, Q value determined as -2.3 Mev and levels in Cl^{35} observed at (0.7), 1.1, and (1.7) Mev (Pi 55).

II. $\text{S}^{34}(\rho, \gamma)\text{Cl}^{35} Q_m = 6.373$

With 1% energy resolution, resonances found in bombardment of sulfur with protons of 0.9 Mev $< E_p < 1.9$ Mev at $E_p = 1.37, 1.61, 1.69, 1.8$, and 1.86 Mev. As target shows no radioactivity these resonances are attributed to S^{34} , but, in view of short half-life of Cl^{35} , capture in S^{32} should not be excluded (Ha 51).

III. $\text{S}^{34}(d, n)\text{Cl}^{35} Q_m = 4.148$

Not observed.

TABLE XLVIII. Levels in Cl^{35} found from $\text{Cl}^{35}(\rho, \rho')\text{Cl}^{35}$ by magnetic analysis.

Reference:	Va 56	Sc 56e	En 56c
E_p (Mev):	3.6-3.8	4.6-5.6	7.0
Angle of observation:	90°	90° and 130°	
Target:	natural Cl	enriched Cl	natural Cl
E_x (Cl^{35}) in Mev	1.219 ± 0.005 1.760 ± 0.004	1.220 ± 0.005 1.766 ± 0.006	1.221 1.763 2.645 2.695 3.006 (3.165) 4.058 4.113 4.174 all ± 0.005

IV. $\text{S}^{35}(\beta^-)\text{Cl}^{35}$ See S^{35}

V. $\text{Cl}^{35}(n, n'\gamma)\text{Cl}^{35}$

At $E_n = 4.4$ Mev, γ rays of 1.23 ± 0.01 , and 1.77 ± 0.01 Mev observed with a scintillation spectrometer, (Si 56).

VI. $\text{Cl}^{35}(\rho, \rho')\text{Cl}^{35}$

Levels in Cl^{35} given in Table XLVIII.

VII. $\text{A}^{35}(\beta^+)\text{Cl}^{35}$ See A^{35}

VIII. $\text{A}^{36}(\gamma, p)\text{Cl}^{35} Q_m = -8.511$

Not observed.

IX. $\text{A}^{38}(\rho, \alpha)\text{Cl}^{35} Q_m = -0.840$

Not observed.

A^{35}

(not illustrated)

I. $\text{A}^{35}(\beta^+)\text{Cl}^{35} Q_m = 5.98$

Determinations of half-life yield 2.2 ± 0.2 sec (Wh 41), 1.88 ± 0.04 sec (El 41), 1.84 sec (Sc 48), and 1.83 ± 0.03 sec (Ki 56), giving average value of 1.85 ± 0.03 sec.

The β^+ end point determined by magnetic spectrometer as 4.96 ± 0.04 Mev. Weak γ rays of 1.19 ± 0.04 and 1.73 ± 0.04 Mev with intensities of 5 ± 2 and $2 \pm 1\%$, respectively, observed by scintillation spectrometer. The β^+ transitions to Cl^{35} ground state, the first, and the second level have $\log ft = 3.8, 4.7$, and 4.5, respectively (Ki 56).

II. $\text{S}^{32}(\alpha, n)\text{A}^{35} Q_m = -8.62$

Observed, En 54a.

III. $\text{Cl}^{35}(\rho, n)\text{A}^{35} Q_m = -6.76$

Observed, En 54a, Ki 56.

IV. $\text{A}^{36}(\gamma, n)\text{A}^{35} Q_m = -15.27$

Not observed.

S^{36}

(not illustrated)

I. $\text{Cl}^{36}(EC)\text{S}^{36}$ See Cl^{36}

II. $\text{Cl}^{37}(\gamma, p)\text{S}^{36} Q_m = -8.4$

Not observed.

III. $\text{A}^{40}(\gamma, \alpha)\text{S}^{36} Q_m = -6.8$

Alpha particles perhaps observed as background of large pulses from an argon-filled ionization chamber bombarded by 17.6-Mev γ rays (Wi 51).

Cl³⁶

(Fig. 31)

- I. (a) $\text{Cl}^{36}(\beta^-)\text{A}^{36}$ $Q_m=0.714$
 (b) $\text{Cl}^{36}(EC)\text{S}^{36}$ $Q_m=1.2$

Half-life measured by absolute β^- counting, using samples of known Cl^{36} content, as $(4.4 \pm 0.5) \times 10^5$ yr (Wu 49) and $(3.08 \pm 0.03) \times 10^5$ yr (Ba 55a).

End point of β^- spectrum is 0.714 ± 0.005 Mev (Fe 52, Wu 49). Shape of beta spectrum, investigated extensively with thin sources, is consistent with a $\Delta J=2$, no, transition (Wu 50, Fu 51, Fe 52, Jo 56). Log $ft=13.4$. Number of positrons is less than 10^{-4} times number of electrons (Wu 49, Jo 49), and no γ rays present with energy $E_\gamma > 20$ kev and intensity of more than 5% (Wu 49).

Observation of K quanta in a proportional counter shows that Cl^{36} also decays by K capture to S^{36} with $K/\beta^-=(1.7 \pm 0.1)\%$ (Dr 55).

A spin $J=2$ obtained for Cl^{36} by microwave experiments (To 49, Jo 51, Gi 52a, Aa 55).

Theoretical discussions of Cl^{36} ground-state configuration, Ku 53, De 53a, Hi 54, Sc 54c. Discussion of log ft value, Fo 54, Jo 56.

- II. $\text{S}^{33}(\alpha, p)\text{Cl}^{36}$ $Q_m=-1.923$

Not observed.

- III. $\text{Cl}^{35}(n, \gamma)\text{Cl}^{36}$ $Q_m=8.580$

From thermal-neutron activation cross sections and abundances of Cl^{36} and Cl^{37} , it follows that probably less than 1% of thermal-neutron captures in natural chlorine occur in Cl^{37} (Hu 55e).

Gamma rays observed from capture of thermal neutrons in natural chlorine in Table XLIX. Apparently, many simple two-step cascades occur from capturing state through one Cl^{36} excited state to ground state. Cascades involving 0.790-, 1.16-, and 1.60-Mev levels confirmed by coincidence measurements with two scintillation spectrometers. A 735-kev γ ray (not in Table XLIX) observed in coincidence with line B can only be explained as transition to unknown 7.84-Mev level (Re 54).

- IV. $\text{Cl}^{35}(n, n)\text{Cl}^{35}$ $E_b=8.580$

Cross section and resonances, Hu 55c, Br 56c. With enriched material, resonance observed at $E_n=26.5$ kev with $\Gamma=0.34$ kev (To 55).

- V. $\text{Cl}^{35}(d, p)\text{Cl}^{36}$ $Q_m=6.355$

By magnetic analysis of (d, p) reactions with natural chlorine targets, at $\theta=90^\circ$ and E_d between 3.0 and 7.5 Mev, ground-state $Q=6.354 \pm 0.008$ Mev (Pa 55c). Levels observed in Cl^{36} in Table L. From low-resolution

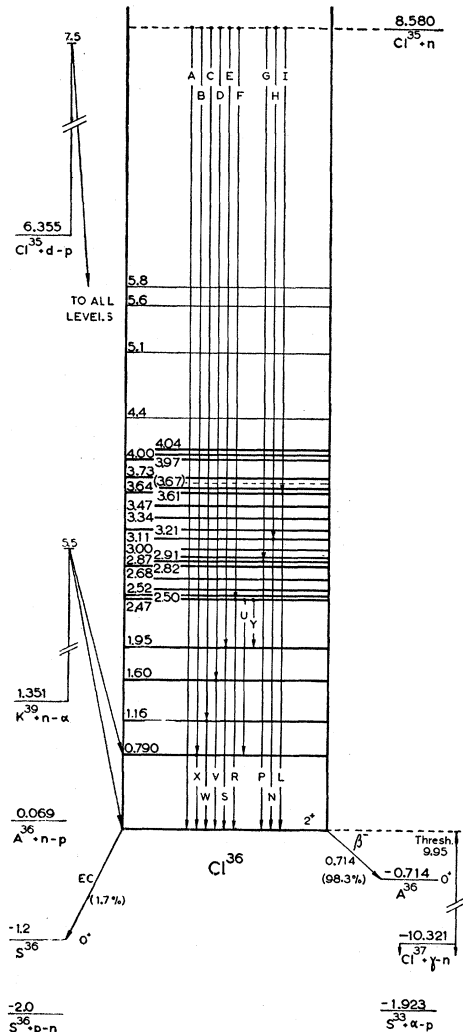


TABLE XLIX. Gamma rays from thermal neutron capture in chlorine.

Reference:	KI 52		Gr 55a		Ha 52b		Re 53		Probable transition in Cl ³⁶ b
Method:	Pair spectrometer		Compton spectrometer		Scintillation spectrometer		Two-crystal scintillation spectrometer		
Line	Energy (Mev)	Intensity a	Energy (Mev)	Intensity a	Energy (Mev)	Intensity a	Energy (Mev)	Intensity a	
A	8.56±0.03	3	8.55 ±0.04	2.8					(c)→(0)
B	7.77±0.03	10	7.78 ±0.03	7.8	7.7 ±0.2				(c)→(1)
C	7.42±0.03	8	7.41 ±0.03	14					(c)→(2)
D	6.98±0.03	1	6.96 ±0.04	1.9					(c)→(3)
E	6.62±0.06	4	6.64 ±0.04	14.4					(c)→(4)
F	6.12±0.03	6	6.12 ±0.03	21.4	6.2 ±0.2				(c)→(5)
G	5.72±0.03	2	5.72 ±0.03	5.6					(c)→(10)
H	5.51±0.03	1	5.49 ±0.04	2					(c)→(13)
H'			(5.28 ±0.05)	1.6					
I	5.01±0.03	4	5.01 ±0.04	6			4.67±0.10		(c)→(17)
I'			(4.79 ±0.05)	1.9					
I''			(4.64 ±0.05)	2.3					
J	4.46±0.04	2	(4.50 ±0.05)	2.2					
J'			(4.15 ±0.05)	2.3					
K	4.06±0.04	3	(4.05 ±0.05)	2.1			3.71±0.10	23	
K'			(3.90 ±0.05)	1.8					
L	3.62±0.05	2	(3.63 ±0.05)	2.9					(17)→(0)
M			3.40 ±0.05	3.6					
N	Br 56e		3.09 ±0.02						
O	Two crystal scintillation spectrometer		3.02 ±0.03	8.0					(13)→(0)
P	2.84±0.03	6	2.87 ±0.02	9.5			2.68±0.10	10	(10)→(0)
Q			2.68 ±0.02	2.0					
R	2.42±0.05	1	2.51 ±0.03	1.0			2.03±0.10		(5)→(0)
S	1.96±0.03	34	1.97 ±0.01	29	2.00 ±0.025		1.77±0.10	19	(4)→(0)
T			1.72 ±0.02	1					
U			1.67 ±0.02	1.0					(5)→(1)
V			1.60 ±0.01	2.4	1.59 ±0.013				(3)→(0)
W	1.14±0.03	8	1.165±0.01	36	1.15 ±0.01		1.12±0.10	29	(2)→(0)
X	0.75±0.03	10	0.77 ±0.01	23	0.784±0.01		0.70±0.10	35	(1)→(0)
Y	0.48±0.03	10	0.485±0.01	26					(5)→(4)

^a All intensities are given in photons per 100 captures.^b The numbering of Cl³⁶ levels is taken from Table L; (c) stands for the capturing state.

the Cl³⁷ isotope, as calculated threshold of Cl³⁵(γ, n)Cl³⁴ is considerably higher (12.7 Mev). Also Go 54a.

IX. K³⁹(n, α)Cl³⁶ $Q_m=1.351$

By irradiation of KI crystals with D(d,n) neutrons and pulse-height analysis of scintillation spectrum, ground-state $Q=1.25\pm 0.2$ Mev. Transition to a Cl³⁶ level at 0.87±0.1 Mev also observed (Sc 56a).

GENERAL REMARKS

Pure jj coupling predicts a linear relation between excitation energies of ($d_{3/2}$, $d_{3/2}^{-1}$) levels in Cl³⁶ and

TABLE L. Levels in Cl³⁶ from Cl³⁵(d,p)Cl³⁶ (Pa 55c).

Level	E_x (Cl ³⁶) (Mev)	Level	E_x (Cl ³⁶) (Mev)
(1)	0.790±0.005	(13)	3.110±0.008
(2)	1.163±0.006	(14)	3.214±0.008
(3)	1.600±0.007	(15)	3.341±0.008
(4)	1.952±0.007	(16)	3.474±0.008
(5)	2.473±0.007	(17)	3.606±0.008
(6)	2.498±0.007	(18)	3.644±0.008
(7)	2.523±0.007	(19)	(3.673±0.008)
(8)	2.684±0.007	(20)	3.732±0.008
(9)	2.820±0.007	(21)	3.970±0.008
(10)	2.872±0.007	(22)	4.003±0.008
(11)	2.905±0.007	(23)	4.043±0.008
(12)	3.004±0.007		

those of ($d_{3/2}$, $d_{3/2}^{-1}$) levels in Cl³⁴ (Pa 56a). Most natural way to obtain in Cl³⁴ a 0⁺ ground state, a 3⁺ 142-kev level, and a 2⁺ level at about 2.13 Mev (as in S³⁴), would be to assign 2⁺, 3⁺, 1⁺, and 0⁺ to Cl³⁶ ground state and to levels at 0.790, 1.60, and 3.34 Mev, respectively. This entails 1⁺ and 2⁺ levels in Cl³⁴ at 0.51 and 1.80 Mev, respectively.

A³⁶

(Fig. 32)

I. S³³(α, n)A³⁶ $Q_m=-1.922$

Not observed.

II. Cl³⁵(p, γ)A³⁶ $Q_m=8.511$

Eighty-six resonances in γ -ray yield from targets containing natural chlorine found at proton energies between 500 and 2150 kev. From targets enriched in Cl³⁵, resonances observed at 858, 888, 1102, 1258, 1484, and 1510 kev (Br 51).

Gamma-ray spectra measured at the 858-, 1484-, and 1510-kev resonances, and at an additional resonance at $E_p=1580$ kev which also has to be assigned to Cl³⁵.

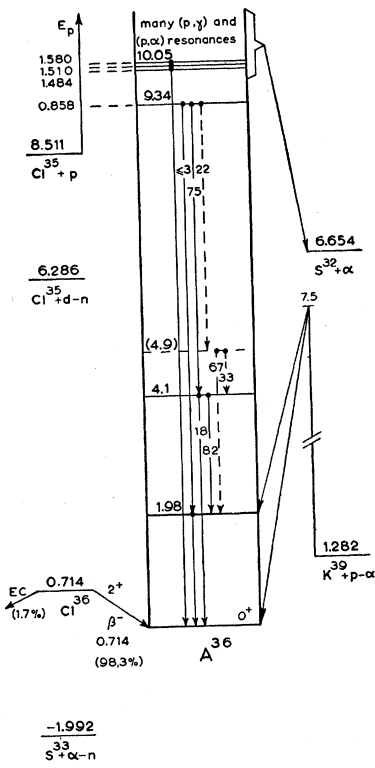


FIG. 32.

These have $(2J+1)\Gamma_\gamma = 9.6, 8.0, 32$, and 22 ev, respectively. The 858-kev resonance decays through levels at 1.95, 4.1, and (4.9) Mev. Branching ratios in Fig. 32. Coincidence measurements confirmed 5.1—4.1- and 5.1—2.15—1.95-Mev cascades. Other three resonances decay directly to A^{36} ground state. Measured γ -ray energies lead to $Q = 8.4 \pm 0.15$ Mev (To 57).

III. $Cl^{35}(p,\alpha)S^{32}$ $E_b = 8.511$ $Q_m = 1.857$

Eighteen resonances observed in $E_p = 1.30$ – 2.51 -Mev region (Al 55a). For Q values, see S^{32} .

IV. $Cl^{35}(d,n)A^{36}$ $Q_m = 6.286$

Not observed.

V. $Cl^{36}(\beta^-)A^{36}$ See Cl^{36}

VI. $K^{39}(p,\alpha)A^{36}$ $Q_m = 1.282$

Magnetic analysis at $E_p = 1.9$ Mev, ground state $Q = 1.267 \pm 0.020$ Mev (Al 55a), while at E_p between 6.0 and 7.5 Mev, $Q = 1.286 \pm 0.010$ Mev and a level in A^{36} at 1.977 ± 0.008 Mev have been observed (Sp 55, Sp 55b).

GENERAL REMARKS

Lowest $T=1$ level in A^{36} expected at 6.06 ± 0.06 Mev (Wi 56a).

S^{37}

(not illustrated)

I. $S^{37}(\beta^-)Cl^{37}$ $Q_m = 4.7$

Half-life, 5.04 ± 0.02 min. The β^- spectrum, measured by Al absorption, consists of two components with the following end points and relative intensities: 4.3 ± 0.3 Mev (10%) and 1.6 ± 0.1 Mev (90%). Second component in coincidence with a 2.7 ± 0.2 -Mev γ ray (Bl 46). Essentially same results obtained by scintillation spectrometer: $E_{\beta_1} \sim 4.7$ Mev (10%), $E_{\beta_2} = 1.6$ Mev (90%), $E_\gamma = 3.1$ Mev. No other γ ray with more than 1% intensity observed (Mo 56). Energy of γ ray more accurately determined as 3.09 ± 0.03 Mev, also by scintillation spectrometer (St 56a).

The β^- ground-state transition is evidently forbidden [$\log ft = 7.2$ and $\log (W^2 - 1) ft = 9.2$] while transition to 3.1-Mev level in Cl^{37} is allowed ($\log ft = 4.2$).

II. $S^{36}(n,\gamma)S^{37}$ $Q_m = 4.4$

Cross section, Hu 55c.

III. $S^{36}(d,p)S^{37}$ $Q_m = 2.2$

Not observed.

IV. $Cl^{37}(n,p)S^{37}$ $Q_m = -3.9$

Cross section, En 54a, Co 56.

V. $A^{40}(n,\alpha)S^{37}$ $Q_m = -2.3$

From ionization-chamber pulse-height analysis, at $E_n = 14$ Mev, $Q = -2.5 \pm 0.1$ Mev. Four more α -particle groups are observed leading to S^{37} levels at 1.3 ± 0.05 , 2.2 ± 0.1 , 2.7 ± 0.1 , and 3.5 ± 0.2 Mev (Be 55a).

Cl^{37}

(Fig. 33)

I. $Cl^{36}(n,\gamma)Cl^{37}$ $Q_m = 10.321$

Cross section, Bo 55a.

II. $S^{37}(\beta^-)Cl^{37}$ See S^{37}

III. $Cl^{37}(p,p')Cl^{37}$

From bombardment of natural chlorine targets with 7.0-Mev protons and magnetic analysis at $\theta = 90^\circ$ and 130° , levels in Cl^{37} observed at 0.838, 1.728, 3.087, and 3.105 Mev, all ± 0.005 Mev (En 56c). With enriched Cl^{37} targets, magnetic analysis at E_p between 4.6 and 5.6 Mev yields only one level below $E_x = 2$ Mev, at $E_x = 1.713 \pm 0.010$ Mev (Sc 56c).

IV. $A^{37}(EC)Cl^{37}$ See A^{37}

No other reactions leading to Cl^{37} have been observed. It can be reached in principle by $S^{34}(\alpha,p)Cl^{37}$

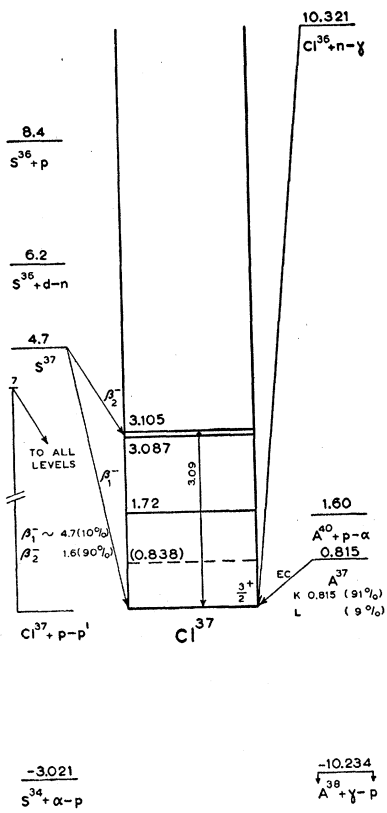


FIG. 33.

$(Q_m = -3.021)$, S³⁶(p, γ)Cl³⁷ ($Q_m = 8.4$), S³⁶(d, n)Cl³⁷ ($Q_m = 6.2$), A³⁸(γ, p)Cl³⁷ ($Q_m = -10.234$), and A⁴⁰(p, α)Cl³⁷ ($Q_m = 1.60$).

A 37

(Fig. 34)

I. $A^{37}(EC)Cl^{37}$ $Q_m = 0.815$

Half-life averaged from two measurements (En 54a),
 34.4 ± 0.4 days. Log $ft = 5.0$.

Shape and intensity of internal bremsstrahlung spectrum investigated by several authors (An 53, Em 54, Li 55b, Sa 56). Results are in agreement with theory

taking account of capture from P states (Gl 56). End point is in agreement with decay energy computed from threshold for $\text{Cl}^{37}(p,n)\text{A}^{37}$ reaction (Reaction III). Decay energy also obtained from recoil measurements as 827 ± 16 kev (Sn 55) and 812 ± 8 kev (Ko 54, Wi 55a, Ru 55b). The L - to K -capture ratio measured with proportional counters as 0.08 to 0.09 (Po 49a), and 0.092 ± 0.010 (La 55a, La 56b). For other small effects (e.g., the production of double holes in K shell), Mi 54, Wo 54a, Wi 56b.

Theoretical discussion of matrix element, Go 56b, Gr 56c.

Upper limit of $9 \times 10^{-46} \text{ cm}^2$ given for the cross section of inverse reaction $\text{Cl}^{37}(\bar{\nu}, e^-)\text{A}^{37}$ (Da 55, Da 56b).

III. $S^{34}(\alpha, n)A^{37}$ $Q_m = -4.619$

Observed, En 54a.

III. $A^{36}(n,\gamma)A^{37}$ $Q_m = 8.792$

Cross section, Hu 55c.

IV. $A^{36}(d,p)A^{37}$ $O_m = 6,567$

Q values and A^{37} levels obtained from deuteron bombardment of argon gas enriched in A^{36} content and proton-energy determination by Al absorption, in Table LI.

$$\text{V. } \text{Cl}^{37}(p,n)\text{A}^{37} \quad Q_m = -1.598$$

Threshold measured as $E_p = 1.60$ Mev (Bl 51), 1640 ± 4 kev (Ri 50), and 1641 ± 2 kev (Sc 52a). By nuclear emulsion technique, neutron groups found with $Q = -1.58$ and -2.99 Mev corresponding to a A^{37} level at 1.41 ± 0.05 Mev (St 52a). By the same method,

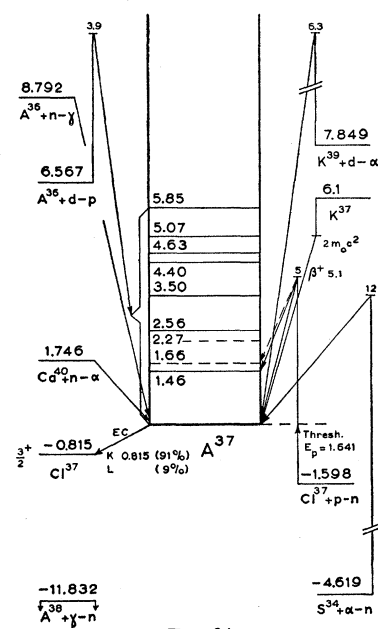


FIG. 34.

A^{37} levels found at 1.40 and 1.65 Mev (Gr 50b). See A^{38} for resonances.

VI. $A^{38}(\gamma, n)A^{37}$ $Q_m = -11.832$

Not observed.

VII. $K^{39}(d, \alpha)A^{37}$ $Q_m = 7.849$

Observed, En 54a.

VIII. $Ca^{40}(n, \alpha)A^{37}$ $Q_m = 1.746$

Observed, En 54a.

Ke³⁷

(not illustrated)

I. $K^{37}(\beta^+)A^{37}$ $Q_m = 6.1$

Half-life = 1.3 ± 0.1 sec (La 48), 1.2 ± 0.2 sec (Bo 51), and 1.2 sec (Su 56). The β^+ end point measured by scintillation spectrometer as 4.57 ± 0.13 Mev (Bo 51), and 5.06 ± 0.11 Mev (Ki 54b), and by magnetic spectrometer as 5.1 Mev (Su 56). Log $ft = 3.6$.

II. $A^{36}(\phi, \gamma)K^{37}$ $Q_m = 1.9$

No resonances found in bombardments with protons of $0.5 < E_p < 1.8$ Mev of targets containing separated A^{36} (Br 48a).

III. $A^{36}(d, n)K^{37}$ $Q_m = -0.3$

Not observed.

IV. $Ca^{40}(\phi, \alpha)K^{37}$ $Q_m = -5.2$

Observed, Su 56.

Cl³⁸

(Fig. 35)

I. $Cl^{38}(\beta^-)A^{38}$ $Q_m = 4.910$

Best measurement of half-life yields 37.29 ± 0.04 min (Co 50a), in good agreement with other less accurate measurements (En 54a, Ma 55b).

The β^- spectrum is complex and can be analyzed into three branches. Two γ rays observed. Energies and relative intensities determined by magnetic spectrom-

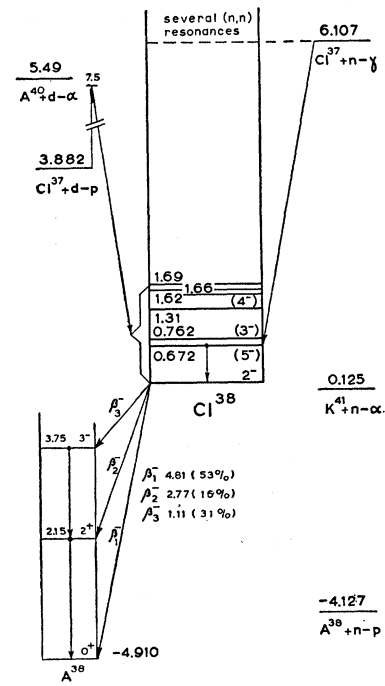


FIG. 35.

eter in Table LII. Intensity of a potential 3.75-Mev cross-over γ ray is less than 0.03% per β^- particle (My 49). Shape of the high-energy β^- spectrum and its ft value [$\log ft = 7.5$ and $\log (W_{\beta^2} - 1) ft = 9.5$] characteristic for once-forbidden transitions ($J = 2$, yes) (La 50, Wu 50). The β^- transitions to 2.15-Mev level also forbidden ($\log ft = 6.9$) while those to 3.75-Mev level allowed ($\log ft = 4.9$). From data given above and from measured $\gamma-\gamma$ angular correlation (Wa 41, Ki 42, St 50, Kr 54a), spins and parities can be assigned as shown in A^{38} level diagram.

II. $Cl^{37}(n, \gamma)Cl^{38}$ $Q_m = 6.107$

Cross section, Hu 55c.

From thermal neutron capture in concentrated Cl^{37} , an isomeric state found emitting γ rays of $E_\gamma = 660 \pm 20$ kev with half-life of 1.0 ± 0.2 sec (Sc 54).

III. $Cl^{37}(n, n)Cl^{37}$ $E_b = 6.107$

Resonances in total neutron cross section observed with enriched material (neutron energies in kev, widths between brackets in kev): 8.8 (0.09), 26.5 (0.33), 47.4 (0.20), 55.5 (0.18), 65.0 (0.18), and 94.2 (0.80) (To 55).

IV. $Cl^{37}(d, p)Cl^{38}$ $Q_m = 3.882$

Targets containing natural Cl bombarded with deuterons of several energies between 3.0 and 7.5 Mev. By magnetic analysis at $\theta = 90^\circ$, ground-state $Q = 3.881 \pm 0.008$ Mev, and levels in Cl^{38} observed at 0.672 ± 0.005 , 0.762 ± 0.005 , 1.312 ± 0.006 , 1.620 ± 0.007 , 1.658 ± 0.007 , and 1.693 ± 0.007 Mev. Intensity ratio of proton groups leading to ground state and first excited

TABLE LII. Beta decay of Cl³⁸.

Reference:	Wa 39	Cu 40	It 41	Ho 46	La 50
E_{β_1} (Mev)	4.99 ± 0.06			5.2	4.81 ± 0.05
				(53%)	(53.4%)
E_{β_2} (Mev)				2.70	2.77 ± 0.05
				(11%)	(15.8%)
E_{β_3} (Mev)	1.08 ± 0.06			1.19	1.11 ± 0.01
				(36%)	(30.8%)
E_{γ_1} (Mev)		2.15	2.19 ± 0.03	2.15	
		(57%)	(53%)	(57%)	
E_{γ_2} (Mev)		1.65	1.64 ± 0.02	1.60	
		(43%)	(47%)	(43%)	

state is 0.43 ± 0.04 , as measured at $E_d = 5.6$ Mev, in agreement with spins of 2^- and 5^- respectively (Pa 55c). Also, En 54a.

V. $A^{38}(n,p)Cl^{38}$ $Q_m = -4.127$

Not observed.

VI. $A^{40}(d,\alpha)Cl^{38}$ $Q_m = 5.49$

Perhaps observed, En 54a.

VII. $K^{41}(n,\alpha)Cl^{38}$ $Q_m = -0.125$

Cross section, En 54a.

GENERAL REMARKS

For pure jj coupling, a linear relation can be derived between excitation energies of $(d_{3/2}, f_{7/2})$ states in Cl^{38} and those of $(d_{3/2}^{-1}, f_{7/2})$ states in K^{40} . From known excitation energies and spins in K^{40} one predicts a 2^- ground state in Cl^{38} and levels at 0.702 (5^-), 0.751 (3^-), and 1.328 Mev (4^-) (Go 56a, Pa 56a), in very good agreement with experiment. Also, Pa 57a.

Theoretical discussions of the Cl^{38} ground-state configuration, Ku 53, De 53a, Hi 54.

A^{38}

(Fig. 36)

I. $Cl^{35}(\alpha,p)A^{38}$ $Q_m = 0.840$

From bombardment of enriched Cl^{35} targets with 7.5-Mev cyclotron α particles, and proton energy determination by Al absorption, $Q = 0.81 \pm 0.08$ Mev, and levels in A^{38} observed at 2.13 ± 0.04 and 3.73 ± 0.04 Mev (Kr 53).

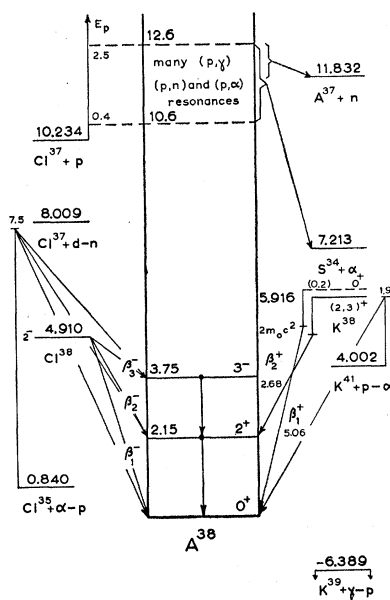


FIG. 36.

Energies of γ rays measured by pair formation in a β spectrometer as $E_\gamma = 1.7 \pm 0.2$, 2.7 ± 0.3 , and 3.9 ± 0.4 Mev (Ma 37, Ma 41). Also, En 54a.

II. (a) $Cl^{37}(p,\gamma)A^{38}$ $E_b = 10.234$

(b) $Cl^{37}(p,n)A^{37}$ $E_b = 10.234$ $Q_m = -1.598$

(c) $Cl^{37}(p,\alpha)S^{34}$ $E_b = 10.234$ $Q_m = 3.021$

Many resonances observed in these reactions, En 54a, Al 55a, To 57.

Gamma-ray spectra measured at $E_p = 1070$, 1135-, 1533-, and 1725-kev resonances. First three have $(2J+1)\Gamma_\gamma = 9, 14$, and 28 ev, respectively. Decay at 1070- and 1135-kev resonances proceeds mainly to 2.15- and 3.75-Mev levels in A^{38} , and to a new level at about 5 Mev, decaying to ground state and 2.15-Mev level. The 1533-kev resonance decays to 2.15- and 5-Mev levels, while 1725-kev resonance decays mainly to a new 6.7-Mev level, which is de-excited to 3.75-Mev level. The $Q = 10.15 \pm 0.15$ Mev from γ -ray energies (To 57).

III. $Cl^{37}(d,n)A^{38}$ $Q_m = 8.009$

Not observed.

IV. $Cl^{38}(\beta^-)A^{38}$ See Cl^{38}

V. $K^{38}(\beta^+)A^{38}$ See K^{38}

VI. $K^{39}(\gamma,p)A^{38}$ $Q_m = -6.389$

Not observed.

VII. $K^{41}(\rho,\alpha)A^{38}$ $Q_m = 4.002$

Magnetic analysis at $E_p = 1.9$ Mev and $\theta = 90^\circ$, gives $Q = 4.002 \pm 0.015$ Mev (Al 55a).

GENERAL REMARKS

Theoretical discussions on low-lying excited states in A^{38} , Ta 54, Th 56.

K^{38}

(not illustrated)

I. (a) $K^{38}(\beta^+)A^{38}$ $Q_m = 5.916$

Weighted average of all half-life measurements for which errors have been given (En 54a, Gr 56), 7.62 ± 0.06 min.

The β^+ end point measured with lens spectrometer is 2.68 ± 0.03 Mev. Spectrum has allowed shape. Log $f\tau = 5.0$. Intensity of possible higher energy β^+ transitions smaller than 0.6% of main transition. No conversion lines observed (Gr 56).

The β^+ decay is followed by a γ ray with energy $E_\gamma = 2.16 \pm 0.03$ Mev as measured by scintillation spectrometer (Ti 51).

Results given above limit K^{38} spin to $(2,3)^+$.

For jj -coupling calculation of β^+ matrix element, Gr 56c.

Also En 54a.

(b) $K^{38m}(\beta^+)A^{38}$

Half-life, 0.95 ± 0.03 sec (St 53b) and 0.935 ± 0.025 sec (Kl 54b).

The β^+ end point measured with scintillation spectrometer as 5.06 ± 0.11 Mev (Hu 54a). Possible confusion with K^{37} .

Measured end point would place isomeric state about 0.2 Mev above K^{38} ground state. The β^+ transition is superallowed ($\log ft = 3.5$), corresponding to a $J=0^+$, $T=1$, assignment to isomeric state. Occurrence of isomerism requires a spin difference with the ground state of at least 3, which determines K^{38} ground state as 3^+ . Theoretical discussions concerning the isobaric spin of levels in K^{38} , see Mo 54, Ta 54, Wi 56a.

II. $Cl^{35}(\alpha, n)K^{38} Q_m = -5.859$

Observed, En 54a.

III. $A^{38}(\rho, n)K^{38} Q_m = -6.699$

Not observed.

IV. $K^{39}(\gamma, n)K^{38} Q_m = -13.088$

Threshold for production of 7.6-min activity, 13.2 ± 0.2 Mev (Mc 49), and 13.00 Mev (De 55). Cross section, En 54a.

V. $Ca^{40}(d, \alpha)K^{38} Q_m = 4.651$

Q value of transition to lowest $T=0$ state = 4.650 ± 0.010 Mev by magnetic analysis at $\theta = 90^\circ$ and at several deuteron energies up to 7 Mev. Level observed with $Q = 4.20 \pm 0.01$ Mev (Br 56f). Observed excited state has also very probably $T=0$.

Cl³⁹

(not illustrated)

I. $Cl^{39}(\beta^-)A^{39} Q_m = 3.44$

Half-life, 55.5 ± 0.2 min (Ha 50a) and 56.5 min (Ru 52).

Beta decay is complex. By magnetic spectrometer, three branches observed with following end points and relative intensities: 3.45 ± 0.02 Mev ($7 \pm 2\%$), 2.18 Mev ($8 \pm 4\%$), and 1.91 ± 0.02 Mev ($85 \pm 6\%$). Shape of high-energy branch characteristic of unique, once-forbidden transition ($\Delta J = 2$, yes). By scintillation spectrometer, three γ rays observed with following energies and relative intensities: $E_{\gamma_1} = 0.246 \pm 0.003$ Mev (0.9 ± 0.1), $E_{\gamma_2} = 1.266 \pm 0.010$ Mev (1), $E_{\gamma_3} = 1.520 \pm 0.010$ Mev (0.85 ± 0.05). Upper limits of 2.1×10^{-3} , 1.6×10^{-3} , and 3.2×10^{-3} for conversion coefficients of γ_1 , γ_2 , and γ_3 , respectively. Coincidences observed of γ_1 with γ_2 , while γ_3 is not coincident with γ_1 , nor with γ_2 . The β^- spectrum, coincident with γ_1 , γ_2 , and γ_3 has an end point at 1.90 ± 0.05 Mev.

The $\beta-\gamma$ coincidences delayed; half-life, $(9.5 \pm 0.5) \times 10^{-10}$ sec.

$\log ft$ for β^- transitions to A^{39} (0), (1.27), and (1.52) = 8.3, 6.8, and 5.6, respectively.

All data in agreement with assignments of $3/2^+$ to Cl^{39} ground state, and of $7/2^-$, $(3/2, 5/2)^-$, and $3/2^+$ to A^{39} ground state and to levels at 1.27 and 1.52 Mev, respectively (Pe 56).

For $j-j$ -coupling computation of the β^- matrix element, Gr 56c.

Also, En 54a.

II. $S^{36}(\alpha, p)Cl^{39} Q_m = -5.7$

Observed, En 54a.

III. $A^{40}(\gamma, p)Cl^{39} Q_m = -12.50$

Threshold, 14.2 ± 0.2 Mev (Ha 50a). This value probably too high because no correction applied for penetration of proton through Coulomb barrier. Q value also measured at $E_\gamma = 17.6$ Mev from proportional counter pulse-height analysis as -10.8 ± 0.1 Mev. A second proton group may be present leading to a Cl^{39} level at about 1 Mev (Wi 51).

Cross sections, Mc 54a, Sp 55a.

A³⁹

(Fig. 37)

I. $A^{39}(\beta^-)K^{39} Q_m = 0.565$

Half-life, 265 ± 30 yr (Ze 52).

The β^- spectrum end point is determined by lens spectrometer as 565 ± 5 kev. Shape of spectrum is unique first forbidden ($\Delta J = 2$, yes) which agrees with the high ft value ($\log ft = 9.9$ and $\log(W_0^2 - 1) ft = 10.4$) (Br 50). No γ rays observed (Br 50, An 52).

II. $A^{38}(n, \gamma)A^{39} Q_m = 6.607$

Cross section, Hu 55c.

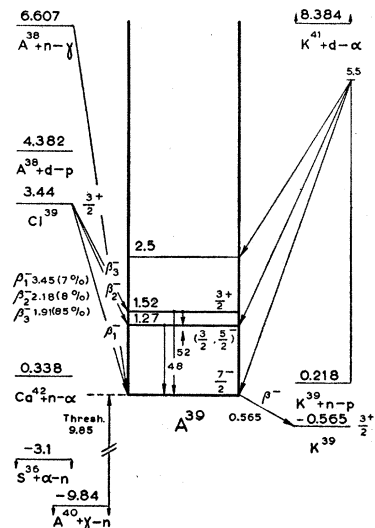


FIG. 37.

III. $\text{Cl}^{39}(\beta^-)\text{A}^{39}$ See Cl^{39} IV. $\text{K}^{39}(n,p)\text{A}^{39}$ $Q_m = 0.218$

A KI scintillation crystal bombarded with 2.0–5.5 Mev neutrons; from pulse-height analysis, proton groups observed leading to A^{39} levels at 1.24 ± 0.05 and 2.46 ± 0.1 Mev, if ground-state $Q=0.20$ Mev is assumed (Sc 56a).

V. $\text{A}^{40}(\gamma,n)\text{A}^{39}$ $Q_m = -9.84$

Threshold, 9.85 ± 0.15 Mev (Ha 54). Cross section, Fe 54, Mc 54a.

VI. The following reactions leading to A^{39} have not been observed: $\text{S}^{36}(\alpha,n)\text{A}^{39}$ ($Q_m = -3.1$), $\text{A}^{38}(d,p)\text{A}^{39}$ ($Q_m = 4.382$), $\text{K}^{41}(d,\alpha)\text{A}^{39}$ ($Q_m = 8.384$), $\text{Ca}^{42}(n,\alpha)\text{A}^{39}$ ($Q_m = 0.338$).

K³⁹
(Fig. 38)

I. $\text{A}^{36}(\alpha,p)\text{K}^{39}$ $Q_m = -1.282$

At $E_\alpha = 7.4$ Mev, with enriched targets and proton detection with nuclear emulsions, $Q = -1.28 \pm 0.03$, -3.78 ± 0.06 , and -4.15 ± 0.04 Mev, corresponding to transitions to K^{39} ground state and to levels at 2.50 and 2.87 Mev (Sc 56b).

II. (a) $\text{A}^{38}(p,\gamma)\text{K}^{39}$ $Q_m = 6.389$
(b) $\text{A}^{38}(d,n)\text{K}^{39}$ $Q_m = 4.164$

Not observed.

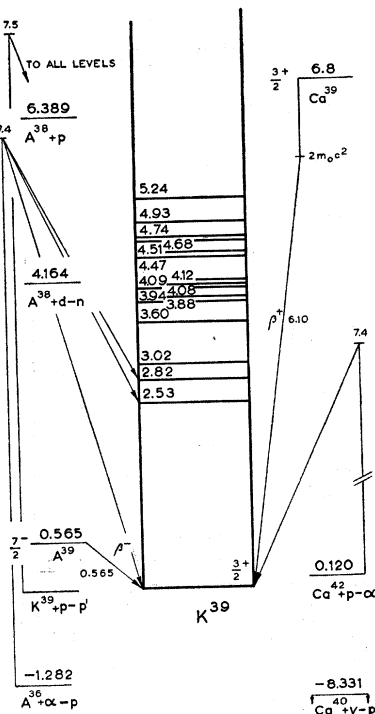


FIG. 38.

III. $\text{A}^{39}(\beta^-)\text{K}^{39}$ See A^{39} IV. $\text{K}^{39}(p,p')\text{K}^{39}$

By magnetic analysis at several angles of observation and at several proton energies up to 7.5 Mev, K^{39} levels observed at 2.526, 2.819, 3.018, 3.600, 3.880, 3.936, 4.080, 4.091, 4.121, 4.472, 4.512, 4.679, 4.735, 4.928, and 5.238 Mev, all ± 0.010 Mev (Sp 55, Sp 55b). Absence of levels below $E_x = 2$ Mev has been confirmed (Sc 56c).

V. $\text{Ca}^{39}(\beta^+)\text{K}^{39}$ See Ca^{39} VI. $\text{Ca}^{40}(\gamma, p)\text{K}^{39}$ $Q_m = -8.331$

Cross section, Jo 55, Mo 55a.

VII. $\text{Ca}^{42}(p,\alpha)\text{K}^{39}$ $Q_m = 0.120$

By magnetic analysis at $\theta = 90^\circ$ and $E_p = 6.5$ and 7.4 Mev, the ground-state $Q = 0.118 \pm 0.005$ Mev (Br 56f).

Ca³⁹

(not illustrated)

I. $\text{Ca}^{39}(\beta^+)\text{K}^{39}$ $Q_m = 6.8$

Half-life averaged from four measurements, (En 54a, Kl 54b) 0.93 ± 0.03 sec.

The β^+ end point, determined by scintillation spectrometer, $= 6.10 \pm 0.15$ Mev (Hu 54) and by Al absorption $= 6.7 \pm 0.5$ Mev (Br 53).

Log $f t = 3.7$.

II. $\text{A}^{36}(\alpha,n)\text{Ca}^{39}$ $Q_m = -8.9$

Not observed.

III. $\text{K}^{39}(p,n)\text{Ca}^{39}$ $Q_m = -7.6$

Not observed.

IV. $\text{Ca}^{40}(\gamma,n)\text{Ca}^{39}$ $Q_m = -15.9$

Threshold, 15.8 ± 0.1 Mev (Su 53), 15.9 ± 0.4 Mev (Mc 49), and 16.0 ± 0.3 Mev (Be 47).

Cross section, En 54a, Go 54a, Mo 55a.

Cl⁴⁰

(not illustrated)

I. $\text{Cl}^{40}(\beta^-)\text{A}^{40}$ $Q_m = 7.5$

Half-life, 1.4 min. The β^- spectrum investigated with a scintillation spectrometer; end point, 7.5 Mev. Strong β^- transition with end point between 3.0 and 3.5 Mev also present. Gamma rays of 1.46, 2.75, and 6.0 Mev observed; first two have about equal intensities. Data suggest decay scheme as in Fig. 39. Compatible with assignment of 2^- to Cl^{40} and 0^+ , 2^+ , and 1^- to ground

state and levels at 1.46 and 6.0 Mev of A^{40} , respectively (Mo 56b).

II. $A^{40}(n,p)Cl^{40}$ $Q_m = -6.7$

Observed, Mo 56b.

A^{40}

(Fig. 39)

I. $A^{40}(e,e')A^{40}$

Magnetic analysis of scattering of 187-Mev electrons shows levels at 1.46 and 2.4 Mev; angular distributions also measured (He 56).

II. $A^{40}(p,p')A^{40}$

Inelastic scattering of protons by A^{40} investigated with 9.5-Mev cyclotron protons and nuclear emulsions for detection of scattered protons. Levels found at 1.48 ± 0.02 Mev (Fr 54), and at 1.48 ± 0.02 , 2.22 ± 0.04 , (2.66), 3.12 ± 0.03 , 3.80 ± 0.03 , (4.40), 4.50 ± 0.05 , and 4.98 ± 0.05 Mev (Va 56e). Angular distributions of elastically and inelastically scattered protons, (He 47, Fr 54, Hi 55, Bu 56a, Hi 56, Va 56e).

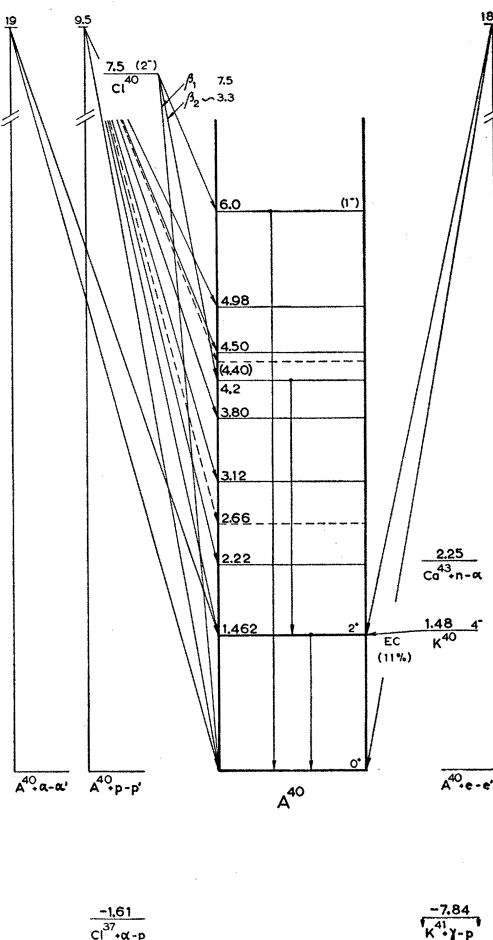


FIG. 39.

III. $A^{40}(\alpha,\alpha')A^{40}$

Scattering of 19-Mev α particles by argon and angular distributions of groups leading to ground state and to 1.46-Mev level, (Bl 56a).

IV. $K^{40}(EC)A^{40}$ See K^{40}

V. Following reactions leading to A^{40} not observed: $Cl^{37}(\alpha,p)A^{40}$ ($Q_m = -1.61$), $K^{41}(\gamma,p)A^{40}$ ($Q_m = -7.84$), and $Ca^{43}(n,\alpha)A^{40}$ ($Q_m = 2.25$).

K^{40}

(Fig. 40)

I. $K^{40}(EC)A^{40}$ $Q_m = 1.48$ $K^{40}(\beta^-)Ca^{40}$ $Q_m = 1.319$

Most accurate measurement of number of β^- particles emitted per sec per g of potassium yields 27.50 ± 0.25 (Mc 56), in excellent agreement with weighted average, 27.4 ± 0.6 , of other, less accurate, measurements (En 54a, He 54a, Su 55, Ko 55).

Measurements of β^- end point (En 54a, Ko 55) yield weighted average of 1.328 ± 0.010 Mev; $\log ft = 18.1$,

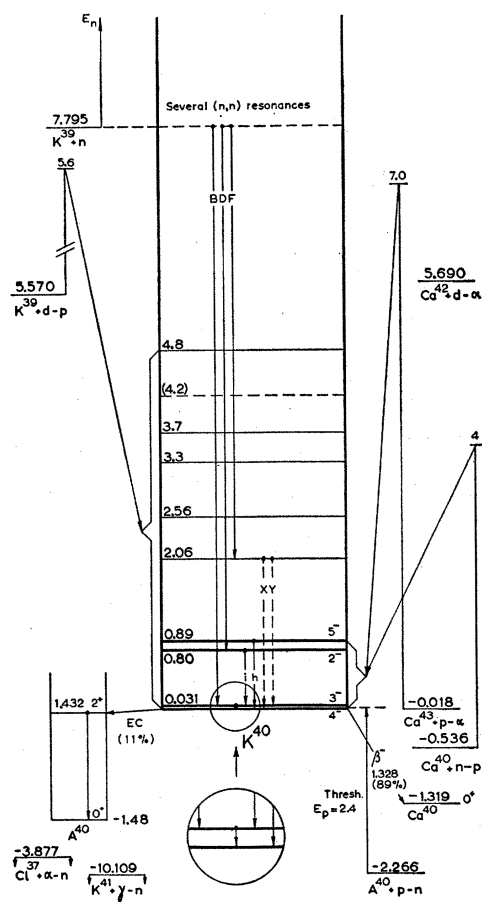


FIG. 40.

and shape of spectrum is unique third forbidden (En 54a, Ko 55), in agreement with assignment of $J=4^-$ to K^{40} (see Ra 53) and $J=0^+$ to Ca^{40} .

Measurement with lowest stated error of number of γ quanta emitted per sec per g of potassium yields 2.96 ± 0.04 (Su 55), while weighted average of six less accurate results (Gl 47, Ah 48, Fa 50, Ho 50, Bu 53, Ba 55b) is 3.42 ± 0.06 . This discrepancy discussed below.

Measurements of γ energy (En 54a, Me 56) yield a weighted average of 1.462 ± 0.005 Mev. The $K^{40}-Ca^{40}$ and $K^{40}-A^{40}$ mass differences determined mass-spectroscopically as 1.30 ± 0.07 and 1.49 ± 0.07 Mev, respectively (Jo 52a), indicating that γ ray must follow electron capture. This confirmed by independent experiments (see under A^{40} and Ca^{40}) which show that A^{40} has excited state at 1.48 ± 0.02 Mev, and that first excited state of Ca^{40} is at 3.35 Mev. Coincidences between γ quanta and Auger electrons also confirm assignment of γ ray to A^{40} (Pa 52, Pa 52a).

Most accurate direct measurements of ratio of number of γ quanta to number of electrons yield 0.124 ± 0.002 and 0.121 ± 0.004 (Mc 56); less accurate measurements (En 54a) were lower. Adopting 0.123 ± 0.002 , and combining this with adopted value of 27.5 ± 0.2 for number of β^- particles emitted per sec per g of potassium, gives emission rate of 3.38 ± 0.07 γ quanta per sec per g of potassium, in good agreement with all except one of direct determinations of this number (see above). Errors involved in the thick-source method, devised especially for routine measurements, amount to five to ten % (Su 55), so the discrepancy between quoted result of 2.96 ± 0.04 and value of 3.38 ± 0.05 which we adopt is not as serious as would appear from the stated errors.

Ratio of number of electron captures over number of β^- emissions given as 0.135 ± 0.040 (Sa 50a, also En 54a); not clear, however, whether L capture could have been detected with same efficiency as K capture in this experiment, in which Auger electrons were detected with a G-M counter. Number of K captures per sec per g of potassium measured with a proportional counter as 1.42 ± 0.23 (He 54), indicating a ratio of L captures over K captures of approximately 1.4.

Upper limits for rate of positron emission determined by comparison of intensity of annihilation radiation with that of 1.46-Mev γ radiation or β^- radiation (En 54a). Appears well established that less than 0.05% of the K^{40} decay goes by positron emission to A^{40} ground state. Since approximately 1.48 Mev is available for positron decay, ratio of K captures to ground state over positron emissions is expected to be about 200 (Mo 51a). It is not excluded, therefore, that an appreciable fraction of decay to A^{40} goes by electron capture directly to ground state. Results on total yield of K Auger electrons (see above), as well as geochemical measurements (see below), show that this fraction cannot be very large, however. This conclusion supported

by theoretical arguments: the ft for β^+ and β^- transitions to ground states of A^{40} and Ca^{40} expected to be same, hence, intensity ratio of β^+ and β^- transitions expected to be of order of $1:10^4$ (Mo 51a).

Measurements of amount of argon in minerals of known age which contain potassium, and mass spectrometer studies of relative amounts of A^{40} , K^{40} , and Ca^{40} in such minerals (En 54a, Sh 54a, Wa 55c, We 56) yield values for electron capture to β^- emission branching ratio which generally come out lower than value deduced from counting experiments (however, In 50). Recent review of geochemical experiments (We 56), however, shows several older determinations need upward revision and that geological evidence gives a branching ratio of 0.117 ± 0.015 , in good agreement with value, 0.123 ± 0.002 , deduced from counting experiments on assuming every electron capture is followed by a 1.46-Mev γ transition.

Foregoing discussions may be summarized as follows: it is definitely established that K^{40} decays by 1.33-Mev β^- transition to ground state of Ca^{40} and by electron capture to first excited state of A^{40} , which in in turn decays to ground state by a 1.46-Mev γ transition. Ratio of β^- emissions to γ emissions is 89.0 to 11.0. It is not excluded that a few % of the decays go by electron capture directly to ground state of A^{40} ; γ -emission rate of 11% of total decay rate, therefore, sets only a lower limit for rate of decay to A^{40} .

Abundance of K^{40} in natural potassium is $(1.178 \pm 0.004) \times 10^{-4}$ (Ni 50, Re 52a, Re 56c), from which follow the decay constants $\lambda_{\beta^-} = (4.78 \pm 0.04) \times 10^{-10}$ yr^{-1} and $\lambda_{EC} \geq (5.88 \pm 0.09) \times 10^{-11} yr^{-1}$, partial half-lives $\tau_{\beta^-} = (1.449 \pm 0.013) \times 10^9 yr$ and $\tau_{EC} \leq (1.18 \pm 0.02) \times 10^{10} yr$, and total half-life $\tau \leq (1.291 \pm 0.013) \times 10^9 yr$.

Other reviews of K^{40} decay, We 56, Sh 57.

II. $Cl^{87}(\alpha, n)K^{40} Q_m = -3.877$

Work with α particles from radioactive sources, En 54a.

III. $K^{39}(n, \gamma)K^{40} Q_m = 7.795$

Thermal neutron absorption cross section of natural potassium is 1.97 ± 0.06 b; the isotopic cross section of K^{39} , K^{40} , and K^{41} are 1.87 ± 0.15 , 70 ± 20 , and 1.19 ± 0.10 b, and their abundances 93.1, 0.012, and 6.9%, respectively, so that approximately 95% of the thermal neutron captures in natural potassium should occur in K^{39} (Hu 55c).

Energies and intensities of γ rays resulting from the capture of thermal neutrons in natural potassium in Table LIII. Assignments of γ rays A'' and A' to K^{41} based upon experiments with potassium enriched in K^{40} . Energy of C corresponds with neutron binding energy of K^{42} . Lines B and D go to ground state and second excited state of K^{40} , while h and i fit between low-lying levels of K^{40} ; several others must be assigned

TABLE LIII. Gamma rays from thermal neutron capture in potassium.

Reference: Method:	Ki 52, Ba 53		Ad 56		
	Pair spectrometer	Intensity ^a	Compton spectrometer	Intensity ^a	Final nucleus
Line	E _γ (Mev)		E _γ (Mev)	Intensity ^a	
A''	9.39 ± 0.06	(0.02)			K ⁴¹
A'	8.45 ± 0.02	(0.1)			K ⁴¹
B	7.757 ± 0.008	(3.5)	7.763 ± 0.010	(4.4)	K ⁴⁰
C	7.34 ± 0.02	(0.1)	7.32 ± 0.03	(0.2)	K ⁴²
D	6.994 ± 0.007	(1.3)	7.000 ± 0.015	(1.6)	K ⁴⁰
E	6.31 ± 0.06	(0.3)			
F	5.740 ± 0.012	(6)	5.725 ± 0.015	(11)	K ⁴⁰
F'	5.66 ± 0.02	(4)	(5.65 ± 0.03)	(3)	
F''	5.50 ± 0.02	(2.5)			
G	5.38 ± 0.03	(6)	5.40 ± 0.02	(6.4)	
G'	5.18 ± 0.02	(2)	5.25 ± 0.05	(2.5)	
H	5.06 ± 0.02	(3)	5.02 ± 0.03	(4.5)	
H'			4.81 ± 0.04	(1.5)	
H''			4.70 ± 0.03	(1)	
H'''			4.50 ± 0.04	(1)	
I	4.39 ± 0.03	(4)	4.39 ± 0.02	(5)	
J	4.18 ± 0.05	(6)	4.11 ± 0.03	(4)	
K	3.92 ± 0.05	(5)	3.97 ± 0.03	(5)	
K'			3.81 ± 0.05	(2)	
L	3.67 ± 0.05	(8)	3.70 ± 0.03	(4)	
Br 56e					
M	Two-crystal scint.		3.60 ± 0.03	(4)	
N	spectrometer		3.55 ± 0.05	(2)	
O	3.45 ± 0.05	(8)	3.40 ± 0.05	(4)	
P			(3.15 ± 0.05)	(1.5)	
Q			3.05 ± 0.03	(3)	
R	2.80 ± 0.03	(6)	2.75 ± 0.04	(4)	
S			(2.60 ± 0.04)	(4)	
T			(2.55 ± 0.03)	(4)	
U			(2.42 ± 0.03)	(4)	
V			(2.37 ± 0.03)	(2)	
W			(2.30 ± 0.03)	(3)	
X			2.06 ± 0.01	(9)	K ⁴⁰
Y	2.03 ± 0.03	(13)	2.02 ± 0.02	(7)	K ⁴⁰
Z			1.95 ± 0.02	(4)	
a			1.85 ± 0.02	(3)	
b			1.75 ± 0.02	(3)	
c	1.61 ± 0.03	(5)	1.61 ± 0.01	(13)	K ⁴⁰
d			1.51 ± 0.01	(5)	
e			1.40 ± 0.02	(2)	
f			1.27 ± 0.02	(2)	
g	1.19 ± 0.03	(8)	1.18 ± 0.02	(7)	K ⁴⁰
h			0.90 ± 0.02	(2)	K ⁴⁰
i	0.77 ± 0.03	(24)	0.77 ± 0.01	(26)	K ⁴⁰
j			0.625 ± 0.010	(3)	

^a In photons per 100 captures in natural potassium.

to K⁴⁰ because of intensities. Further experiments on K³⁹(d,p)K⁴⁰ reaction are necessary for determination of energy levels of K⁴⁰, without which it is impossible to make unambiguous assignments of other γ rays. Proposed level scheme which accounts for several of observed γ transitions, Ad 56.

IV. K³⁹(n,n)K³⁹ E_b = 7.795

Cross sections, Hu 55c, Jo 55a, To 55; nine resonances found at neutron energies below 110 kev (To 55), several more above 110 kev (Hu 55c).

V. K³⁹(d,p)K⁴⁰ Q_m = 5.570

Ground-state Q value = 5.506 ± 0.010 Mev by magnetic analysis at E_d from 4.8 to 5.7 Mev; excited states found at 0.032 ± 0.002, 0.800 ± 0.010, and 0.893 ± 0.010

Mev (Bu 53a). With range measurements at E_d = 3.9 Mev, partly resolved levels found at 2.01 ± 0.03, 2.56 ± 0.05, and 3.3, 3.7, (4.2), and 4.8, all ± 0.1 Mev (Sa 50).

VI. A⁴⁰(p,n)K⁴⁰ Q_m = -2.266

Threshold of E_p = 2.4 Mev, (Ri 48).

VII. Ca⁴⁰(n,pγ)K⁴⁰ Q_m = -0.536

Gamma rays of 0.030 ± 0.002, 0.767 ± 0.007, and 0.877 ± 0.017 Mev found from bombardment of calcium with 4-Mev neutrons. They represent transitions in K⁴⁰ from (1) to (0), from (2) to (1), and from (3) to (0) or (1), respectively (Da 56c).

VIII. K⁴¹(γ,n)K⁴⁰ Q_m = -10.109

Not observed.

IX. Ca⁴²(d,α)K⁴⁰ Q_m = 5.690

Not observed.

X. Ca⁴³(p,α)K⁴⁰ Q_m = -0.018

Ground-state Q value = -0.014 ± 0.008 Mev by magnetic analysis at E_p = 6.5 and 7.0 Mev. Groups of α particles leading to first three excited states of K⁴⁰ observed (Br 56f).

GENERAL REMARKS

Ground state of K⁴⁰ has J = 4 (Ra 53). Together with first three excited states, it forms a multiplet with spins 4⁻, 3⁻, 2⁻, and 5⁻, resulting from coupling of a f_{7/2} neutron with a d_{5/2} proton hole (En 54a). See under Cl³⁸, general remarks, for discussion of a relation between excitation energies in Cl³⁸ and K⁴⁰ based on jj coupling. Theoretical discussions of K⁴⁰ ground state configuration, Ku 53, De 53a, Hi 54, Ma 54, Sc 54c, Ta 54a, Pa 56a, Pa 57a.

Ca⁴⁰

(Fig. 41)

I. K³⁹(d,n)Ca⁴⁰ Q_m = 6.106

Not observed.

II. K³⁹(p,γ)Ca⁴⁰ Q_m = 8.331

Yield curve measured in region 0.5–1.15 Mev, showing resonances at E_p = 0.883, 0.925, 0.980, and 1.150 Mev, all ± 10 kev (De 57), and in region 0.8–1.8 Mev, showing resonances at 1.120, 1.300, 1.338, and 1.566 Mev, all ± 5 kev (To 57). First four resonances decay mainly to ground state; at 1.150-Mev resonance, a direct ground-state transition and cascades through the 3.35- and 3.73-Mev levels are found. Angular distribution of 9.29-Mev γ ray indicates this is an E1 transition. High-energy γ rays at 1.150-Mev resonance measured

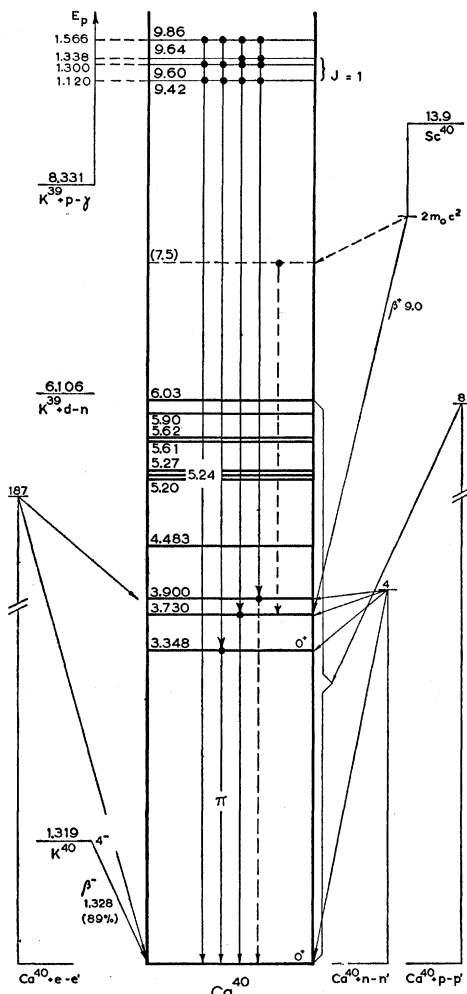


FIG. 41.

with a three-crystal pair spectrometer, indicating $Q=8.17\pm 0.03$ Mev, (De 57).

The 1120-, 1300-, and 1566-kev resonances decay with strong ground-state transitions, weak transitions to lowest three levels [those to (2) and (3) unresolved], and perhaps transitions to level (4). The 1338-kev resonance decays to level (2) and (3). Angular distribution measurements yield $J=1$ to the 1120- and 1300-kev resonances, (To 57).

III. $K^{40}(\beta^-)Ca^{40}$ See K^{40}

IV. $Ca^{40}(e,e')Ca^{40}$

Magnetic analysis of scattering of 183-Mev electrons by calcium shows unresolved group leading to levels at 3.73 and 3.90 Mev, also elastically scattered electrons. Angular distributions giving charge distribution, (Ha 56b). Inelastic group leads to 3.73-Mev level, which probably has $J=3^-$ (He 56).

TABLE LIV. Excited states of Ca^{40} (energy in Mev) from $Ca^{40}(p,p')Ca^{40}$ (Br 56b).

3.348 ± 0.004	5.202 ± 0.008	5.621 ± 0.008
3.730 ± 0.004	5.241 ± 0.006	5.901 ± 0.008
3.900 ± 0.004	5.272 ± 0.006	6.029 ± 0.008
4.483 ± 0.005	5.606 ± 0.008	

V. $Ca^{40}(n,n')Ca^{40}$

Gamma rays of 3.74 ± 0.04 and 3.9 ± 0.1 Mev, in addition to annihilation radiation, result from inelastic scattering of 4-Mev neutrons by calcium. Threshold for production of positrons is $E_n = 3.36 \pm 0.05$ Mev (c.m.), showing that first excited state decays by pair emission (Da 56c). Half-life of this state measured with a pulsed neutron source; preliminary value of 1.4×10^{-9} sec obtained, (Kl 57). Elastic neutron scattering, We 56a, Cu 56.

VI. $Ca^{40}(p,p')Ca^{40}$

Magnetic analysis of inelastic scattering of 6- to 8-Mev protons by Ca^{40} shows excited states in Table LIV (Br 56b). With a magnetic spectrometer, 3.35-Mev level found to decay by pair emission; no γ ray found. Hence, its spin and parity must be 0^+ (Be 55b).

Angular distribution of an unresolved proton group to levels at 3.73 and 3.90 Mev, taken at $E_p = 7.7$ Mev, nearly isotropic (Ha 52c).

VII. $Sc^{40}(\beta^-)Ca^{40} Q_m = 13.9$

Half-life is 0.22 ± 0.3 sec. Maximum positron energy, measured with a scintillation spectrometer, is 9.0 ± 0.4 Mev, which, assuming a branching of 100%, gives $\log ft = 4.1$. A γ ray of 3.75 ± 0.04 Mev, as measured with a scintillation spectrometer, accompanies the decay (Gl 55). Possibility that a 5-Mev super-allowed β^+ branch leads to lowest $T=1$ state, expected at 7.5 Mev, not excluded by experimental data (Bo 55). No delayed α particles observed (Gl 55). Theoretical discussion of position of $T=1$ states in self-conjugated nuclei, Wi 56a.

A^{41}

(Fig. 42)

I. $A^{41}(\beta^-)K^{41} Q_m = 2.524$

Half-life averaged from four measurements (En 54a, Ha 51d) is 109.6 ± 0.4 min. Also An 54.

The β^- decay proceeds by two branches. End point of ground-state transition measured by magnetic spectrometer as 2.48 ± 0.04 Mev (intensity 0.88%) which yields $\log ft = 8.5$ and $\log(W_f^2 - 1) ft = 10.0$. Shape of spectrum is unique once-forbidden ($\Delta J = 2$, yes) (Sc 56). End point of main branch measured by magnetic spectrometer as 1.199 ± 0.008 Mev (Sc 56), and 1.245 ± 0.005 Mev (Br 50c). Spectrum has allowed shape. Log $ft = 5.1$.

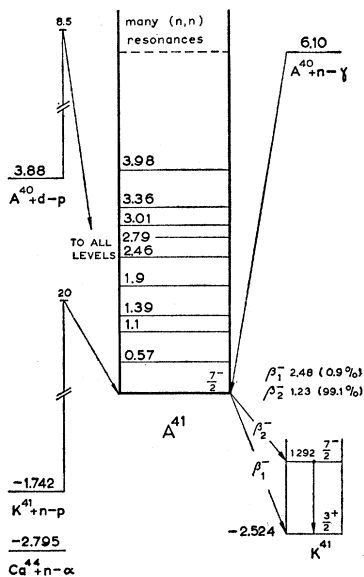


FIG. 42.

Energy of γ ray following main β^- branch measured by scintillation spectrometer as 1.298 ± 0.010 Mev (Kl 55), and 1.290 ± 0.005 Mev (Sc 56).

By $\beta-\gamma$ delayed coincidence measurements half-life of 1.3-Mev level in K^{41} is established as $(6.7 \pm 0.5) \times 10^{-9}$ sec (El 52a) and 6.6×10^{-9} sec (En 53) which agrees with theoretical value for M2 transitions.

Also En 54a.

For jj -coupling computation of β^- matrix element, Gr 56c.

II. (a) $A^{40}(n,\gamma)A^{41} E_b = 6.10$

(b) $A^{40}(n,n)A^{40} E_b = 6.10$

Cross section, Hu 55c.

III. $A^{40}(d,p)A^{41} Q_m = 3.88$

Results of Q -value and angular distribution measurements in Table LV. At $E_d = 3.9$ Mev, by Al absorption,

TABLE LV. The $A^{40}(d,p)A^{41}$ reaction.

Reference:	Da 49	Gi 52	Bu 56d
E_d (Mev):	3.4	7.8	8.5
Method:	Al abs.	Nucl. emuls.	Magn. anal.
Q_0 (Mev):	3.84 ± 0.03	3.90 ± 0.08	\dots^b
E_x (Mev)	E_x (Mev)	E_x (Mev)	E_x (Mev)
0	3	0	3
0.66 ± 0.05^a	0.50 ± 0.08^a	0.57 ± 0.05	1
1.21 ± 0.04^a		1.11 ± 0.1	
1.34 ± 0.04^a	1.34 ± 0.08^a	0, (1)	1
1.94 ± 0.04^a		1.93 ± 0.1	
2.27 ± 0.05^a		2.46 ± 0.05	1
2.80 ± 0.05^a		2.79 ± 0.05	1
3.29 ± 0.03^a		3.01 ± 0.05	1
3.69 ± 0.05^a		3.36 ± 0.05	1
4.01 ± 0.05^a		3.98 ± 0.05	1

^a In original paper errors were only assigned to Q values. Same errors have been used here for the corresponding excitation energies.

^b A ground-state Q value of 3.90 Mev is assumed.

ground-state Q value $= 3.80 \pm 0.06$ Mev (Sa 49). Theoretical analysis of A^{41} levels, Ra 56a.

Also Fu 54, Fr 55, En 54a.

IV. $K^{41}(n,p)A^{41} Q_m = -1.742$

Cross section, En 54a.

V. $Ca^{44}(n,\alpha)A^{41} Q_m = -2.795$

Not observed.

K^{41}

(Fig. 43)

I. $A^{40}(p,\gamma)K^{41} Q_m = 7.84$

Thin targets enriched in A^{40} content bombarded with protons from 0.5 to 1.8 Mev. Resonances in γ -ray yield found (Br 48a) at

E_p	900	1050	1080	1100	1235	kev
Rel. int.	0.2	0.4	0.5	1.0	0.5	

II. $A^{40}(d,n)K^{41} Q_m = 5.62$

Neutron detection with a double proportional counter, at $E_d = 3.2$ Mev, gives ground-state Q value $= 5.97 \pm 0.25$ Mev and levels at 1.34 ± 0.15 , 3.10 , and 4.0 Mev (Wo 50).

III. $K^{40}(n,\gamma)K^{41} Q_m = 10.109$

Cross section, Hu 55c.

Two γ rays A'' and A' of Table LIII produced by neutron capture in potassium assigned to K^{41} on account of their energies and from experiments with targets enriched in K^{40} . If originating from the capturing state, they would proceed to K^{41} levels at 0.72 and 1.66 Mev (Ba 53, Ki 52).

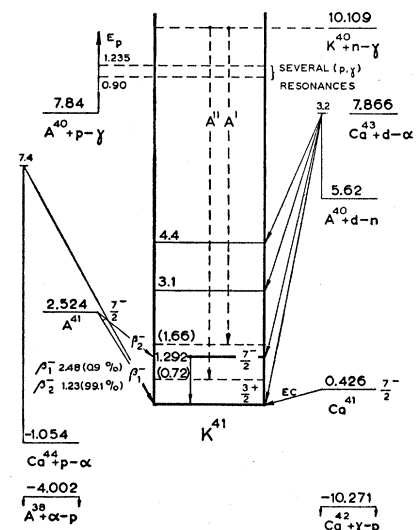


FIG. 43.

IV. $A^{41}(\beta^-)K^{41}$ See A^{41}

V. $Ca^{41}(EC)K^{41}$ See Ca^{41}

VI. $Ca^{44}(p,\alpha)K^{41}$ $Q_m = -1.054$

By magnetic analysis at $\theta=90^\circ$, $E_p=6.5$ and 7.4 Mev, ground-state Q value $= -1.057 \pm 0.010$ Mev (Br 56f).

VII. Following reactions leading to K^{41} have not been observed: $A^{38}(\alpha,p)K^{41}$ ($Q_m = -4.002$), $Ca^{42}(\gamma,p)K^{41}$ ($Q_m = -10.271$), $Ca^{43}(d,\alpha)K^{41}$ ($Q_m = 7.866$).

Ca^{41}

(Fig. 44)

I. $Ca^{41}(EC)K^{41}$ $Q_m = 0.426$

Half-life is $(1.1 \pm 0.3) \times 10^5$ yr, assuming a Ca^{40} thermal neutron capture cross section of 0.22 b (Br 51a, Br 53a).

II. $A^{38}(\alpha,n)Ca^{41}$ $Q_m = -5.211$

Not observed.

III. $Ca^{40}(n,\gamma)Ca^{41}$ $Q_m = 8.364$

Thermal-neutron absorption cross section of natural calcium is 0.43 ± 0.02 b; main contributions from Ca^{40} and Ca^{42} , with cross sections of 0.22 ± 0.04 and 40 ± 3 b, and abundances of 97% and 0.64%, respectively, indicating that these isotopes should contribute about equally to cross section of natural calcium (Hu 55c).

Energies and intensities of γ rays in Table LVI. By using enriched material it has been made probable that lines F and F' result from capture in Ca^{42} (Ad 56). Strong E1 transitions occur between the capturing state and levels (1), (3), and (21). Of all proton groups observed in $Ca^{40}(d,p)Ca^{41}$ reaction, transitions to these p states have also largest intensity (see Reaction V). Many weaker lines could also be fitted into Ca^{41} level scheme but great level density prevents unique assignment.

Comparison between spectra from natural calcium and Ca^{40} suggests 90% of the integrated intensity of spectrum from natural calcium must be ascribed to Ca^{40} (Ad 56), in disagreement with cross-section measurements (see the foregoing).

IV. $Ca^{40}(n,n)Ca^{40}$ $E_b = 8.364$

Cross section, Hu 55c, Pa 55, We 56b, Cr 55.

V. $Ca^{40}(d,p)Ca^{41}$ $Q_m = 6.139$

By magnetic analysis at $\theta=90^\circ$ and at several bombarding energies between 2.5 and 7.0 Mev, ground-state Q value $= 6.140 \pm 0.009$ Mev (Br 56f, Br 56g). Levels in Ca^{41} in Table LVII. Angular distributions also measured with a high-resolution magnetic analyzer at $E_d = 7.0$ Mev (Bo 56, Bo 56a); l_n assignments in Table LVII. Transitions to Ca^{41} ground state and to levels (1), (3), and (21) very intense. Level density above $E_x = 4.2$ Mev increases very fast. Two groups leading to levels at 4.76 and 5.72 Mev, both with $l_n = 2$, observed in older low-resolution work (Ho 53c).

Also En 54a.

Discussion of reduced widths, Fu 54, Ra 56.

TABLE LVI. Gamma rays from thermal neutron capture in natural calcium.

Reference: Method: Line	Ad 56		Ki 52		Probable transition in Ca^{41} ^b
	Magn. Compton spectrometer Energy (Mev)	Intensity ^a	Magn. pair spectrometer Energy (Mev)	Intensity ^a	
<i>A</i>			7.83 ± 0.05	1	
<i>B</i>			7.43 ± 0.05	1.4	
<i>C</i>	6.406 ± 0.015	22	6.42 ± 0.03	83 (80) ^c	$(c) \rightarrow (1)$
<i>D</i>	5.904 ± 0.030	3.8	5.89 ± 0.03	11 (12) ^c	$(c) \rightarrow (3)$
<i>E</i>	5.696 ± 0.030	1.2	5.66 ± 0.06	3	
<i>F</i>	5.50 ± 0.035	1.2	5.49 ± 0.05	4	$Ca^{42}(n,\gamma)Ca^{43}$
<i>F'</i>	5.15 ± 0.035	0.9			$Ca^{42}(n,\gamma)Ca^{43}$
<i>H</i>	4.944 ± 0.030	2.3	4.95 ± 0.03	8	
<i>I</i>	4.764 ± 0.030	2.5	4.76 ± 0.03	6	
<i>J</i>	4.418 ± 0.015	12.3	4.45 ± 0.05	30	$(c) \rightarrow (21)$
<i>J'</i>	3.762 ± 0.020	1.8			
<i>L</i>	3.60 ± 0.010	6.4	3.62 ± 0.05	16	
<i>M</i>	2.810 ± 0.035	≥ 3.6			
<i>N</i>	2.660 ± 0.050	≥ 2.0	^{Br 56e} Two-crystal scint. spectrometer		$(21) \rightarrow (1), (2) \rightarrow (0)$
<i>O</i>	2.004 ± 0.010	12.7			
<i>P</i>	1.944 ± 0.008	39	1.93 ± 0.03	45	$(1) \rightarrow (0)$
<i>Q</i>	1.844 ± 0.015	6.4			
<i>R</i>	1.790 ± 0.015	≥ 3.6			
<i>S</i>	~ 1.48	≥ 3.2			$(21) \rightarrow (3)$
<i>T</i>	~ 1.2	≥ 4.8			
<i>U</i>	0.532 ± 0.010	≥ 5			$(3) \rightarrow (1)$
<i>V</i>	0.463 ± 0.010	≥ 9	0.48 ± 0.05	15	$(3) \rightarrow (2)$

^a Intensities given as number of photons per 100 captures in natural calcium.

^b For numbering of Ca^{41} levels, see Table LVII. Capturing state is denoted by (c).

^c Intensities in brackets are numbers of photons per 100 captures in Ca^{40} , recalculated with assumption that 50% of the captures in natural calcium occur in Ca^{40} (Ki 54a).

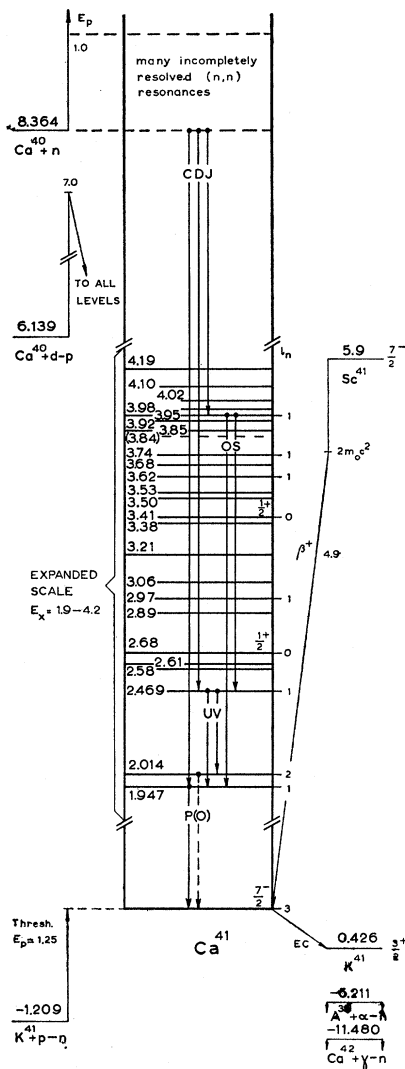


FIG. 44.

VI. $K^{41}(p,n)Ca^{41}$ $Q_m = -1.209$

Threshold for neutron emission, $E_p = 1.25 \pm 0.02$ Mev (Ri 50). Resonances, En 54a.

TABLE LVII. Levels in Ca^{41} from $Ca^{40}(d,p)Ca^{41}$ reaction.

Reference:	Br 56f, Br 56g E_x (Mev)	Bo 56f, l_n	Br 56f, Br 56g E_x (Mev)	Bo 56a, l_n
(0)	0	3	(13)	3.500 ± 0.007
(1)	1.947 ± 0.004	1	(14)	3.531 ± 0.007
(2)	2.014 ± 0.005	2	(15)	3.619 ± 0.007
(3)	2.469 ± 0.005	1	(16)	3.682 ± 0.007
(4)	2.584 ± 0.006	(17)	3.736 ± 0.007	1
(5)	2.612 ± 0.006	(18)	(3.836 ± 0.007)	
(6)	2.677 ± 0.006	0	(19)	3.854 ± 0.007
(7)	2.890 ± 0.006	(20)	3.921 ± 0.007	
(8)	2.967 ± 0.006	1	(21)	3.950 ± 0.007
(9)	3.056 ± 0.006	(22)	3.982 ± 0.007	
(10)	3.206 ± 0.006	(23)	4.023 ± 0.007	
(11)	3.375 ± 0.007	(24)	4.101 ± 0.007	
(12)	3.405 ± 0.007	0	(25)	4.194 ± 0.007

VII. $Sc^{41}(\beta^+)Ca^{41}$ $Q_m = 5.9$

Half-life, 0.87 ± 0.03 sec (El 41), and 0.873 sec (Ma 52a). The β^+ end point by cloud chamber is 4.94 ± 0.07 Mev (El 41). Log $f t = 3.4$, indicating super-allowed transition.

VIII. $Ca^{42}(\gamma,n)Ca^{41}$ $Q_m = -11.480$

Not observed.

 A^{42}

(not illustrated)

This nucleus has been produced by successive capture of two neutrons in A^{40} in a nuclear reactor. Presence detected by observation of 12.5-hr K^{42} daughter activity in milkings from irradiated argon gas. From the fact that the milkings over a period of 400 days did not show a decrease in activity of more than 20%, half-life of $A^{42} > 3.5$ yr and thermal neutron activation cross section of $A^{41} > 0.06$ b (Ka 52a).

 K^{42}

(Fig. 45)

I. $K^{42}(\beta^-)Ca^{42}$ $Q_m = 3.528$

Best measurement of half-life, 12.516 ± 0.007 hr (Bu 53), in good agreement with other less accurate measurements (En 54a).

The β^- spectrum is complex; β^- and γ energies and intensities in Table LVIII. Older measurements, En 54a.

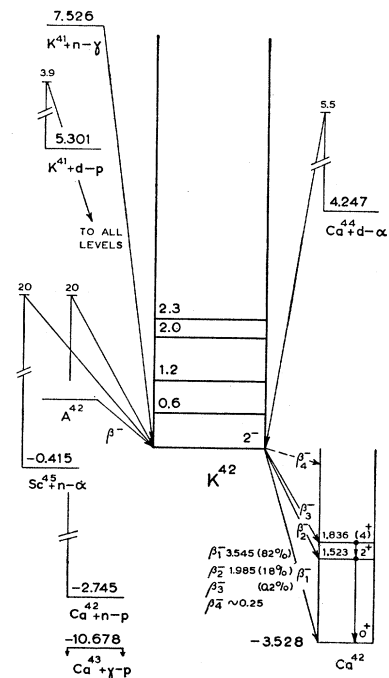


FIG. 45.

TABLE LVIII. The $K^{42}(\beta^-)Ca^{42}$ decay.

Reference	Method	E_{β_1} (Mev)	E_{β_2} (Mev)	E_{γ_1} (Mev)	E_{γ_2} (Mev)
Si 47	magn. spectrom.	3.58 ± 0.07 (75%)	2.04 (25%)	1.51	
Si 47a	β - γ coinc. spectrom.		1.92 (16%)		
Ko 54	magn. spectrom.	3.56 (81.8%)			
	β - γ coinc. spectrom.		1.97 (18.2%)		
La 54	scint. spectrom.			1.52 (100%)	0.309 (1.5%)
Em 55	abs. β and γ counting		(10.8 ± 0.6)%		
Po 56	magn. spectrom.	3.545 ± 0.010	1.985 ± 0.010^a	1.53 ± 0.01 (100%)	0.320 ± 0.005 (0.8%)

^a A third β^- branch with ~ 0.25 -Mev end point may be present.

Shape of high-energy β^- spectrum and ft value ($\log ft = 7.9$ and $\log(W_0^2 - 1) ft = 9.7$) in agreement with a $\Delta J = 2$, yes, assignment which characterizes K^{42} as $J = 2^-$ (Si 47, Sh 49, Ko 54, Po 56). Direct measurement by magnetic resonance in atomic beam yields also $J = 2^-$ (Be 53). Assignment of $J = 2^+$ to 1.523-Mev level in Ca^{42} in agreement with ft value of low-energy β^- branch (Sh 49) ($\log ft = 7.4$) and with measured β - γ angular correlation (Be 50, St 51b).

No polarization found of γ rays emitted at 90° to β rays, although some polarization is predicted from measured β - γ angular correlation (Ha 53a).

Measurement of angular correlation of the 0.31- and 1.52-Mev γ rays suggests assignments of $J=0, 2$, and 4 to Ca⁴² ground state and levels at 1.523 and 1.836 Mev, respectively (Ca 54). However, intensity ratio observed disagrees with that from more direct measurements (Table LVII).

Theoretical discussion of the K⁴² spin, De 53a, Sc 54c.

$$\text{II. (a) } K^{41}(n,\gamma)K^{42} \quad E_b = 7.526 \\ \text{(b) } K^{41}(n,n)K^{41} \quad E_b = 7.526$$

Cross section, Hu 55c, To 55.

None of γ rays observed from thermal neutron capture in natural potassium can be assigned to K^{41} with confidence.

III. $K^{41}(d,p)K^{42}$ $Q_m = 5.301$

At $E_d=3.9$ Mev, from enriched target bombardment and range analysis, ground-state $Q=5.12\pm 0.10$ Mev, and levels in K^{42} observed at 0.62 ± 0.07 , 1.18 ± 0.07 , 1.97 ± 0.15 , and 2.29 ± 0.07 Mev (Sa 50).

IV. $\text{Ca}^{42}(n,p)\text{K}^{42}$ $Q_m = -2.745$

Cross section, En 54a.

$$\text{V. } \text{Ca}^{43}(\gamma, p) \text{K}^{42} \quad Q_m = -10.678$$

Not observed.

VI. $\text{Ca}^{44}(d,\alpha)\text{K}^{42}$ $Q_m = 4.247$

Observed, En 54a.

$$\text{VII. } \text{Sc}^{45}(n,\alpha)\text{K}^{42} \quad O_m = -0.415$$

Observed, En 54a.

Ca⁴²

(Fig. 46)

I. $K^{39}(\alpha, p)Ca^{42}$ $Q_m = -0.120$

At $E_\alpha = 8.2$ Mev, from enriched target bombardments and range analysis, ground-state $Q = -0.19 \pm 0.07$ Mev, and levels in Ca⁴² observed at 1.51 ± 0.05 , 1.95 ± 0.07 , 2.29 ± 0.05 , 2.59 ± 0.07 , 3.02 ± 0.05 , (3.30 ± 0.10) , 3.75 ± 0.07 , and (4.09 ± 0.10) Mev. Proton groups leading to additional levels above 3 Mev present but not resolved (Sc 55). Also, En 54a.

II. K⁴¹(*p,n*)Ca⁴¹ E_b=10.271 Q_m=-1.209

Resonances (incompletely resolved), En 54a.

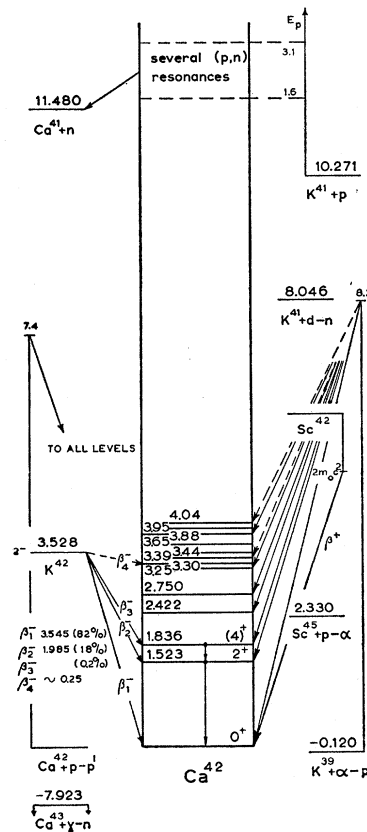


FIG. 46.

III. $K^{42}(\beta^-)Ca^{42}$ See K^{42} IV. $Ca^{42}(p,p')Ca^{42}$

Magnetic analysis, at 90° and 120° and at several bombarding energies between 6.5 and 7.0 Mev, gives levels in Ca^{42} at 1.523 ± 0.004 , 1.836 ± 0.004 , 2.422 ± 0.005 , 2.750 ± 0.005 , 3.250 ± 0.006 , 3.297 ± 0.006 , 3.389 ± 0.006 , 3.442 ± 0.006 , 3.651 ± 0.006 , 3.883 ± 0.007 , 3.949 ± 0.007 , and 4.043 ± 0.007 Mev (Br 56f).

V. $Sc^{42}(\beta^+)Ca^{42}$

A 0.62 ± 0.05 sec β^+ activity observed from bombardment of natural potassium with 18-Mev α particles. About same half-life estimated for a superallowed $0^+ \rightarrow 0^+$ transition between $T=1$ states (Mo 55c). Also, Mo 54.

VI. Following reactions leading to Ca^{42} have not been observed: $K^{41}(p,\gamma)Ca^{42}$ ($Q_m = 10.271$), $K^{41}(d,n)Ca^{42}$ ($Q_m = 8.046$), $Ca^{43}(\gamma,n)Ca^{42}$ ($Q_m = -7.923$), and $Sc^{45}(p,\alpha)Ca^{42}$ ($Q_m = 2.330$).

GENERAL REMARKS

Computation of excitation energy of first level in Ca^{42} , Sc 54a, Th 56.

 K^{43}

(Fig. 47)

I. $K^{43}(\beta^-)Ca^{43}$ $Q_m = 1.84$

Half-life = 22.4 hr (Ov 49), 21.5 hr (Ru 52a) and 22.0 hr (Li 54a).

The β^- decay is complex; β^- and γ -ray energies and intensities in Table LIX.

Shape of β_1 spectrum is unique once-forbidden ($J=2$, yes) with $\log ft = 8.7$ and $\log(W_0^2 - 1) ft = 10.0$ (Li 54a). All γ rays reported in Be 57 can be explained as transitions between Ca^{43} states at 0, 371, 591, 985, and 1373 kev. The β_5^- branch given in Li 54a must then be

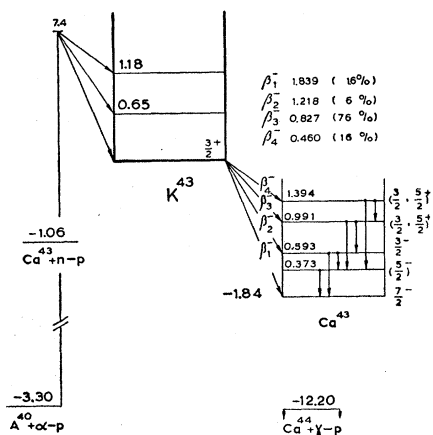


FIG. 47.

TABLE LIX. $K^{43}(\beta^-)Ca^{43}$ decay.

Reference:	Li 54a		Be 57	
	Method:	magn. spectrom. E_β, E_γ (kev) rel. int.	magn. spectrom. E_γ (kev) rel. int.	scint. spectrom. E_γ (kev) rel. int.
β_1^-	1839 ± 30	1.6%		
β_2^-	1218 ± 25	5.4%		
β_3^-	827 ± 20	83.1%		
β_4^-	460 ± 20	5.4%		
β_5^-	243 ± 30	4.5%		
γ_1	219 ± 4 a	1		
γ_2	369 ± 3 a	67	371 ± 2 a,d 388 ± 2 a,d	100 14
γ_3			394 ± 2 a	16
γ_4	393 ± 4 a	6	591 ± 2 a,d	23
γ_5			614 ± 4 a	91
γ_6	627 ± 6 a,b	100		615 ± 5
γ_7	1000 ± 20 a,c	4		1005 ± 10 91 3.5

a Measured from external conversion spectrum.

b Also internal conversion line observed with $\alpha_K \sim 2 \times 10^{-4}$.

c Also observed by scintillation spectrometer (Li 54a).

d From $\beta-\gamma$ and $\gamma-\gamma$ coincidence measurements these transitions lead to Ca^{43} ground state (Be 57).

regarded as nonexistent. This interpretation entails branching ratios of 6, 76, and 16% for β^- transitions to 593-, 991-, and 1394-kev levels respectively, corresponding to $\log ft = 7.4$, 5.6, and 5.3.

Conclusions regarding spins and parities in Fig. 48.

II. $A^{40}(\alpha,p)K^{43}$ $Q_m = -3.30$

From nuclear emulsion measurements, at $E_\alpha = 7.4$ Mev and $\theta = 90^\circ$, ground-state Q value = -3.36 ± 0.03 Mev, and levels in K^{43} at 0.65 ± 0.04 , and 1.18 ± 0.07 Mev (Sc 56b).

III. $Ca^{43}(n,p)K^{43}$ $Q_m = -1.06$

Not observed.

IV. $Ca^{44}(\gamma,p)K^{43}$ $Q_m = -12.20$

Not observed.

 Ca^{43}

(Fig. 48)

I. $A^{40}(\alpha,n)Ca^{43}$ $Q_m = -2.25$

Cross section, Sc 56b.

Resonances, Ca^{44} .

II. $Ca^{42}(n,\gamma)Ca^{43}$ $Q_m = 7.923$

Cross section, Hu 55c.

The γ rays F and F' (Table LVI) from thermal-neutron capture in natural calcium assigned to $Ca^{42}(n,\gamma)Ca^{43}$ reaction (Ad 56).

III. $Ca^{42}(d,p)Ca^{43}$ $Q_m = 5.708$

Many Ca^{43} levels observed from $Ca^{43}(p,p')Ca^{43}$ also found by magnetic analysis of this reaction (Table LX). Ground-state Q value = 5.711 ± 0.010 Mev (Br 56f, Br 57b). Results from angular distribution measurements obtained by magnetic analysis at $E_d = 7.0$ Mev in Table LX (Bo 55b, Bo 57). Theoretical interpretation of measured angular distributions, Fr 55, Ra 56.

TABLE LX. Levels in Ca^{43} , and corresponding $\text{Ca}^{42}(d,p)\text{Ca}^{43}$ relative intensities and l_n values (Br 56f, Br 57b, Bo 55b, Bo 57).

Level	E_x (Ca^{43}) (Mev) ^d	Relative yield at maximum at $E_d = 7.0$ Mev	l_n
(0)	0	100	3
(1)	0.373 ± 0.003 a, b	<7	
(2)	0.593 ± 0.003 a, b	36	1
(3)	0.991 ± 0.003 a, b	14	2
(4)	1.394 ± 0.004 a, b	<4	
(5)	1.678 ± 0.004 a, b	10	
(6)	1.904 ± 0.004 a, b	<7	
(7)	1.932 ± 0.004 a, b	<7	
(8)	1.957 ± 0.004 a, b	100 (at 10°)	0
(9)	1.985 ± 0.005 a	<23	
(10)	2.048 ± 0.005 a, b	750	1
(11)	2.069 ± 0.005 b	<270	
(12)	2.095 ± 0.005 b	<29	
(13)	(2.107 ± 0.005) b	<23	
(14)	2.225 ± 0.005 a, b	<23	
(15)	2.250 ± 0.005 a, b	<23	
(16)	2.273 ± 0.005 b	<14	
(17)	2.409 ± 0.005 a, b	<11	
(17')	(2.53) ^e	13	1
(18)	2.607 ± 0.005 a, b	84	1
(19)	2.673 ± 0.005 b	<14	
(20)	2.696 ± 0.005 b	<14	
(21)	2.753 ± 0.005 b	<17	
(22)	2.844 ± 0.005 a, b	<17	
(23)	2.880 ± 0.005 a, b	61	1
(24)	2.947 ± 0.005 a, b	61	1
(25)	3.027 ± 0.006 b	<11	
(26)	3.047 ± 0.006 a, b	<11	
(27)	3.074 ± 0.006 b	<11	
(28)	3.094 ± 0.006 a, b	<7	
(29)	3.194 ± 0.006 b	<27	
(30)	3.279 ± 0.006 b	<22	
(31)	3.293 ± 0.006 b	53	
(32)	3.369 ± 0.006 b	<14	
(33)	3.398 ± 0.006 b	<31	
(34)	3.419 ± 0.006 a, b	<31	
(35)	3.584 ^e	64	1

^a Observed from $\text{Ca}^{42}(d,p)\text{Ca}^{43}$ reaction at several deuteron energies between 2.9 and 7.0 Mev and at $\theta = 90^\circ$ (Br 56f, Br 57b).

^b Observed from $\text{Ca}^{42}(p,p')\text{Ca}^{43}$ reaction at $E_p = 6.5$ Mev and $\theta = 90^\circ$, and at $E_p = 7.0$ Mev and $\theta = 130^\circ$ (Br 56f, Br 57b).

^c Additional level observed from $\text{Ca}^{42}(d,p)\text{Ca}^{43}$ reaction (Bo 57).

^d Listed energies are weighted averages (where possible) of results obtained from $\text{Ca}^{42}(d,p)\text{Ca}^{43}$ and $\text{Ca}^{42}(p,p')\text{Ca}^{43}$ reactions.

IV. $\text{K}^{43}(\beta^-)\text{Ca}^{43}$ See K^{43}

V. $\text{Ca}^{43}(p,p')\text{Ca}^{43}$

Levels observed by magnetic analysis at $E_d = 6.5$ and 7.0 Mev, and at $\theta = 90^\circ$ and 130° in Table LX (Br 56f, Br 57b).

TABLE LXI. Positron decay of Sc^{43} .

Reference	Method	E_{β^+} (Mev)	E_{β^+} (Mev)	E_γ (Mev)
Ha 52d	magn. spectrom.	1.18 ± 0.02 (72%)	0.77 ± 0.04 (28%)	0.375 ± 0.002
Nu 53	scint. spectrom.			0.375 ± 0.004 (25 ± 2%)
Li 54b	magn. spectrom.	1.20 ± 0.01 (82%)	0.82 ± 0.02 ^a (18%)	0.369 ± 0.005 (16%)

^a Also reported in Li 54 are a β^+ branch of 0.39 ± 0.03 Mev endpoint (4%), and γ rays of 0.25 ± 0.01 Mev (1%), 0.627 ± 0.005 Mev (4%), and 0.84 ± 0.02 Mev (weak). Existence of last two γ rays not substantiated in later work (Va 57b).

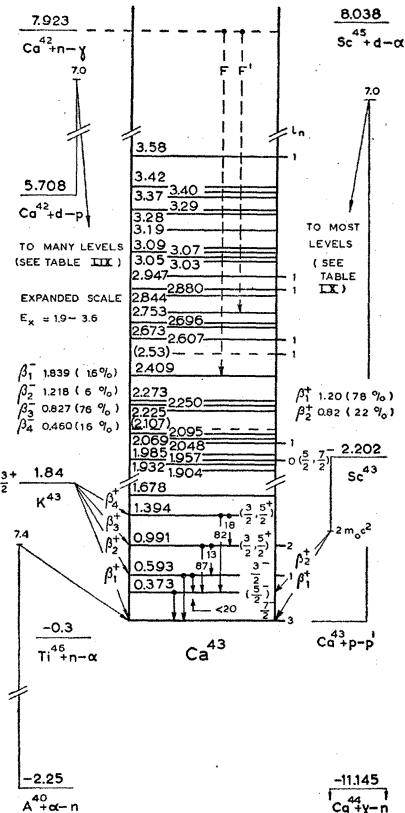


FIG. 48.

VI. $\text{Sc}^{43}(\beta^+)\text{Ca}^{43} Q_m = 2.202$

Most accurate measurement of half-life, 3.92 ± 0.02 hr (Hi 45), in reasonable agreement with other measurements (En 54a, Li 54).

The β^+ decay is complex; β^+ spectrum end points, relative intensities, and energies of γ rays in Table LXI. Both β^+ transitions are allowed: $\log ft = 5.1$ for the 1.20 Mev branch and $\log ft = 4.7$ for the 0.82-Mev branch.

Spin of Ca^{43} measured as $J = 7/2$ by magnetic resonance (Je 53) and from hyperfine spectra (Ke 54). For jj -coupling computation of β^+ matrix elements, Gr 56c.

VII. $\text{Ca}^{44}(\gamma,n)\text{Ca}^{43} Q_m = -11.145$

Cross section, En 54a.

VIII. $\text{Sc}^{45}(d,\alpha)\text{Ca}^{43} Q_m = 8.038$

Not observed.

IX. $\text{Ti}^{46}(n,\alpha)\text{Ca}^{43} Q_m = -0.3$

Not observed.

GENERAL REMARKS

Detailed theoretical predictions of properties of Ca^{43} levels, as computed from known Ca^{41} and Ca^{42} level schemes, Le 55.

K⁴⁴

(not illustrated)

I. K⁴⁴(β^-)Ca⁴⁴ $Q_m = 6.1$

Half-life, 18 ± 1 min (Wa 37), 20 min (An 54), and 22.0 ± 0.5 min (Co 54).

The β^- decay is complex. By scintillation spectrometer, β^- branches observed with end points of 4.9 and 1.5 Mev, and γ rays of 1.13, 2.07, 2.48, and (3.6) Mev, together with some unresolved γ rays of $E_\gamma < 0.5$ Mev (Co 54). Log ft of two β^- branches would be at least 7.0 and 4.7, respectively. Probable that 4.9-Mev β^- branch proceeds to first excited state in Ca⁴⁴.

II. Ca⁴⁴(n,p)K⁴⁴ $Q_m = -5.3$

Observed, En 54a, Co 54.

III. Ca⁴⁶(d, α)K⁴⁴

Not observed.

Ca⁴⁴

(Fig. 49)

I. A⁴⁰(α ,n)Ca⁴³ $E_b = 8.90$ $Q_m = -2.25$

Resonances observed with Th C' α particles, En 54a.

II. K⁴¹(α ,p)Ca⁴⁴ $Q_m = 1.054$

Bombardment of enriched targets with 7.8-Mev α particles and range analysis, gives ground-state Q value $= 0.98 \pm 0.10$ Mev, and levels in Ca⁴⁴ at 1.13, 1.92, 2.28, 2.58, 2.97, and 3.17 Mev, all ± 0.05 Mev (Sc 55).

III. Ca⁴³(d,p)Ca⁴⁴ $Q_m = 8.920$

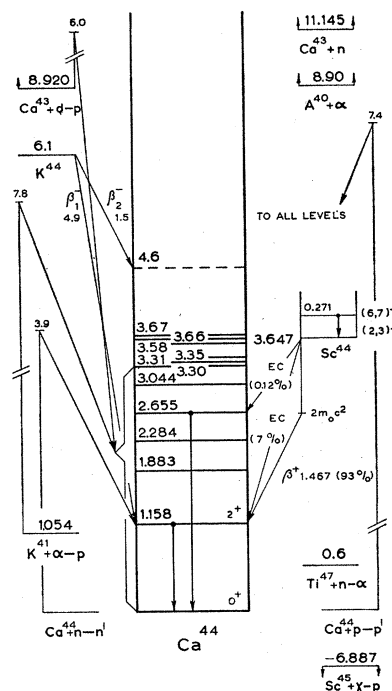
At $E_d = 4.2$ Mev, using enriched targets and range analysis, ground-state $Q = 9.07 \pm 0.07$ Mev, with Ca⁴³ levels at 1.15 and 2.28 Mev (Sc 55). Magnetic analysis at $E_d = 6.0$ Mev and $\theta = 90^\circ$, proton groups observed leading to seven lowest states in Ca⁴⁴ from which ground-state $Q = 8.913 \pm 0.014$ Mev (Br 56f).

IV. K⁴⁴(β^-)Ca⁴⁴ See K⁴⁴**V. Ca⁴⁴(n,n' γ)Ca⁴⁴**

From inelastic scattering of 3.9-Mev neutrons on natural calcium, a 1.152 ± 0.020 -Mev γ ray observed with a scintillation spectrometer (Da 56c).

VI. Ca⁴⁴(p,p')Ca⁴⁴

Magnetic analysis at $E_p = 6.5$ Mev and $\theta = 90^\circ$, $E_p = 7.0$ Mev and $\theta = 120^\circ$, and $E_p = 7.4$ Mev and $\theta = 90^\circ$, levels in Ca⁴⁴ observed at 1.156 ± 0.004 , 1.883 ± 0.004 , 2.284 ± 0.005 , 2.655 ± 0.005 , 3.044 ± 0.005 , 3.297 ± 0.006 , 3.305 ± 0.006 , 3.354 ± 0.006 , 3.581 ± 0.006 , 3.656 ± 0.006 , and 3.671 ± 0.006 Mev (Br 56f).



K⁴⁵

(not illustrated)

A 34 min $A=45$ activity obtained by electromagnetic separation of a vanadium target bombarded by 187-Mev protons. Tentatively assigned to K⁴⁵ (An 54).

Ca⁴⁵

(Fig. 50)

I. Ca⁴⁵(β^-)Sc⁴⁵ $Q_m = 0.256$

Most accurate measurement of half-life, 163.5 ± 4 days (De 53). Also En 54a.

The β^- spectrum is simple, no γ rays observed. Three magnetic spectrometer measurements of end point in good mutual agreement, average value, 256 ± 2 kev (En 54a). Kurie plot is straight and $\log ft = 5.7$.

II. Ca⁴⁴(n, γ)Ca⁴⁵ $Q_m = 7.413$

Cross section, Hu 55c.

III. Ca⁴⁴(d,p)Ca⁴⁵ $Q_m = 5.188$

By magnetic analysis, at several deuteron energies between 2.9 and 7.0 Mev and $\theta = 90^\circ$, ground-state Q value $= 5.188 \pm 0.010$ Mev (Br 56f). Levels in Ca⁴⁵ (Br 56f), and angular distribution measurements at $E_d = 7.0$ Mev, also by magnetic analysis (Co 57), in Table LXII.

Large intensity of ground-state transition makes it probable that Ca⁴⁵ ground state is a $f_{7/2}$ single-neutron state.

Theoretical remarks on the angular distributions, Fr 55, Ra 56.

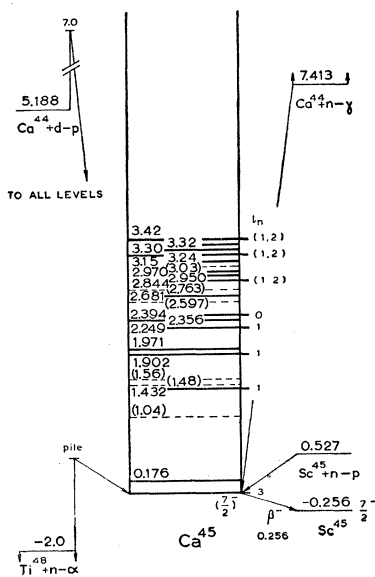


FIG. 50.

TABLE LXII. Levels in Ca⁴⁵ from Ca⁴⁴(d,p)Ca⁴⁵.

Level	E_α (Ca ⁴⁵) (Mev) ^a	Angle of maximum yield ^b	Relative yield at maximum ^b	l_n ^b
(0)	0	40°	100	3
(1)	0.176 ± 0.003	50°	3.0	...
(2)	(1.036 ± 0.010)		<11	...
(3)	1.432 ± 0.004	20°	200	1
(4)	(1.475 ± 0.006)		<7	
(5)	(1.557 ± 0.010)		<6	
(6)	1.902 ± 0.004	20°	115	1
(7)	1.971 ± 0.004	50°	3.1	...
(8)	2.249 ± 0.005	15°	190	1
(9)	2.356 ± 0.005	30°	1.7	...
(10)	2.394 ± 0.005	<7½°	190 (at 7½°)	0
(11)	(2.597 ± 0.005)		<4	
(12)	2.681 ± 0.005	20°	3.9	...
(13)	(2.763 ± 0.005)		<8	
(14)	2.844 ± 0.005	20°	212	(1,2)
(15)	2.950 ± 0.005		<5	
(16)	2.970 ± 0.005	10°	19.5	...
(17)	(3.032 ± 0.006)			
(18)	3.148 ± 0.006		<5	
(19)	3.244 ± 0.006	20°	104	(1,2)
(20)	3.296 ± 0.006		<4	
(21)	3.319 ± 0.006	40°	18.9	...
(22)	3.419 ± 0.006	15°	430	(1,2)

^a From Br 56f.^b From Co 57.**IV. Sc⁴⁵(n,p)Ca⁴⁵ $Q_m = 0.527$**

Observed, En 54a.

V. Ca⁴⁶(γ ,n)Ca⁴⁵

Not observed.

VI. Ti⁴⁸(n, α)Ca⁴⁵ $Q_m = -2.0$

Cross section, En 54a.

Ca⁴⁶

(not illustrated)

No reactions leading to Ca⁴⁶ have been observed. Possibilities would be Ca⁴⁴(t,p)Ca⁴⁶ or Ti⁴⁹(n, α)Ca⁴⁶. Nor has Ca⁴⁶ been concentrated sufficiently to make a study of inelastic scattering feasible.

Ca⁴⁷

(not illustrated)

I. Ca⁴⁷(β^-)Sc⁴⁷ $Q_m = 2.0$

Half-life average from several measurements (En 54a, Ly 55, Li 56, see also Wa 55) 4.7 ± 0.2 days.

The β^- decay is complex (Table LXIII; also En 54a). Log ft values for β_1 and β_2 are 8.5 and 6.0 respectively. The first is unexpectedly large for a presumably allowed transition (also Gr 56c).

II. Ca⁴⁶(n, γ)Ca⁴⁷

Observed, En 54a.

TABLE LXIII. $\text{Ca}^{47}(\beta^-)\text{Sc}^{47}$.

Reference:	Co 53 ^a Method: magn. spectrom.	Ma 53 magn. spectrom.	Ly 55 Al abs. +scint. spectrom.	Li 56 magn. spectrom. +scint. spectrom.
E_{β_1} (Mev)	1.4 ± 0.1 (40%)	2.060 ± 0.020 ^b (19%)	1.93 ± 0.02 (24 ± 6)%	1.940 ± 0.020 ^b (17%)
E_{β_2} (Mev)	0.46 ± 0.02 (60%)	0.685 ± 0.006 (81%)	0.70 ± 0.02 (76 ± 6)%	0.660 ± 0.010 ^b (83%)
E_{γ_1} (Mev)	1.303 ± 0.040		1.29 (14.2 ± 1.2)	1.31 ± 0.02 ^c (13 ± 2)
E_{γ_2} (Mev)	0.800 ± 0.025		0.812 (1 ± 0.1)	0.83 ± 0.02 ^c (1 ± 0.1)
E_{γ_3} (Mev)	0.495 ± 0.015		0.500 (1)	0.48 ± 0.02 ^c (1)

^a Additional γ rays of 234.0 and 149.5 kev reported in Co 53, not observed by others.

^b Kuri plot is straight.

^c Coincidences observed between γ_2 and γ_3 ; neither γ_2 nor γ_3 coincident with γ_1 .

III. Following reactions leading to Ca^{47} have not been reported: $\text{Ca}^{46}(d,p)\text{Ca}^{47}$, $\text{Ca}^{48}(\gamma,n)\text{Ca}^{47}$ ($Q_m = -11.0$), $\text{Ti}^{50}(n,\alpha)\text{Ca}^{47}$ ($Q_m = -3.5$).

Ca^{48}

(not illustrated)

I. $\text{Ca}^{48}(\beta^-)\text{Sc}^{48}$ $Q_m = 0.2$

Half-life $> 2 \times 10^{16}$ yr (Jo 52). Also, En 54a.

II. $\text{Ca}^{48}(\beta^-\beta^-)\text{Ti}^{48}$ $Q_m = 4.2$

Double β^- decay of Ca^{48} with half-life of $(1.6 \pm 0.7) \times 10^{17}$ yr and total kinetic energy of two electrons of 4.1 ± 0.3 Mev reported (Mc 55). However, lower limit for half-life given as 2×10^{18} yr (Aw 56).

III. $\text{Ca}^{48}(p,p')\text{Ca}^{48}$

From magnetic analysis at $E_p = 6.5, 7.0$, and 7.4 Mev and at several angles of observation, levels in Ca^{48} observed at 3.825 ± 0.006 and 4.499 ± 0.007 Mev (Br 56f). Search for de-excitation of the first level by internal pair formation unsuccessful (Kr 57).

Ca^{49}

(Fig. 51)

I. $\text{Ca}^{49}(\beta^-)\text{Sc}^{49}$ $Q_m = 5.1$

Half-life averaged from two measurements (Ke 56, Ma 56a) is 8.83 ± 0.14 min.

The β^- decay is complex (Table LXIV). Beta transitions with $\log ft$ values of 4.9, 4.6, and 4.5 occur to Sc^{49} levels at 3.09, 4.05, and 4.68 Mev respectively, which are de-excited by γ -ray transitions directly to Sc^{49} ground state.

II. $\text{Ca}^{48}(n,\gamma)\text{Ca}^{49}$ $Q_m = 5.1$

Cross section, En 54a.

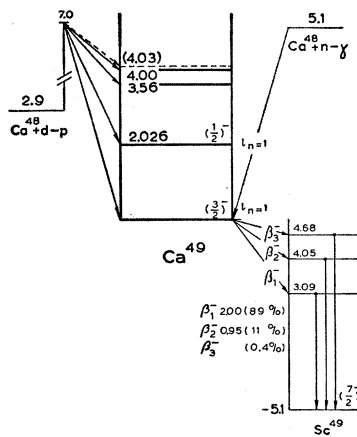


FIG. 51.

III. $\text{Ca}^{48}(d,p)\text{Ca}^{49}$ $Q_m = 2.9$

From magnetic analysis at $E_d = 6.5$ and 7.0 Mev and $\theta = 90^\circ$, ground-state Q value $= 2.916 \pm 0.006$ Mev, and levels in Ca^{49} found at 2.026 ± 0.005 , 3.589 ± 0.006 , 4.004 ± 0.007 , and (4.026 ± 0.010) Mev (Br 56f). By Al absorption, $Q = 2.80 \pm 0.30$ Mev (Wa 54).

Angular distribution measurements at $E_d = 6.5$ Mev, also by magnetic analysis, show that both ground state and first level are p states ($l_n = 1$) (Bu 54).

Atomic Mass Excesses

Atomic mass excesses used for computation of Q_m values given in the present compilation in Table LXV.

Masses of most nuclides with $A > 32$ are from En 57. They were computed from Q -value chains connecting them to S^{32} , for which nuclide the accurate mass-spectroscopic value was used (Qu 56a). Masses of nuclides in the $16 < A < 32$ region are obtained from those computed by Wapstra (Wa 55a) from Q -value measurements. However, Wapstra finds a S^{32} mass which is smaller by 41.7 kev than the mass-spectroscopic value. To obtain a smooth fit to the $A > 32$ region an appropriate correction was applied to the $A < 32$ masses given by Wapstra. Of course, this correction is small for nuclides near O^{16} , and relatively large for nuclides near S^{32} . In principle the correction can be obtained from a lengthy and tedious least-squares analysis. This was avoided by the use of a resistor net-

TABLE LXIV. $\text{Ca}^{49}(\beta^-)\text{Sc}^{49}$.

Reference:	Ke 56 ^a Method: scint. spectrom.	Ma 56a ^b scint. spectrom.
E_{β_1} (Mev)	1.95 ± 0.05 (88%)	2.12 ± 0.10
E_{β_2} (Mev)	0.95 ± 0.15 (12%)	~1.0
E_{γ_1} (Mev)	3.10 ± 0.03 (90 ± 2%)	3.07 ± 0.05 (89%)
E_{γ_2} (Mev)	4.05 ± 0.05 (10 ± 2%)	4.04 ± 0.06 (10%)
E_{γ_3} (Mev)	4.68 ± 0.05 (0.38 ± 0.1%)	4.7 ± 0.1 (0.8%)

^a Intensity of a possible 0.95-Mev γ ray is <2%. No γ - γ coincidences are observed.

^b Intensity of ground-state β^- transition is <1%. Intensity of a possible 0.97 Mev γ ray is <3%.

TABLE LXV. Table of atomic mass excesses.

Nuclide	<i>M-A</i> (Mev)	Nuclide	<i>M-A</i> (Mev)
n^1	8.3675 ± 0.0014 ^a	Cl^{34}	-14.35 ± 0.03 ⁿ
H^1	7.5845 ± 0.0014 ^a	S^{35}	-18.489 ± 0.008 ^d
H^2	13.7256 ± 0.0026 ^a	Cl^{35}	-18.657 ± 0.008 ^d
H^3	15.835 ± 0.005 ^a	A^{35}	-12.68 ± 0.04 ⁿ
He^3	15.817 ± 0.005 ^a	S^{36}	-20.04 ± 0.06 ^o
He^4	3.6073 ± 0.0024 ^a	Cl^{36}	-18.870 ± 0.018 ^d
		A^{36}	-19.584 ± 0.018 ^d
F^{19}	4.147 ± 0.006 ^b	S^{37}	-16.1 ± 0.1 ^p
Ne^{20}	-1.137 ± 0.007 ^b	Cl^{37}	-20.824 ± 0.014 ^d
Na^{20}	14.2 ± 0.5 ^b	A^{37}	-20.009 ± 0.015 ^d
Ne^{21}	0.473 ± 0.008 ^b	K^{37}	-13.9 ± 0.1 ⁿ
Na^{21}	3.99 ± 0.03 ^b	Cl^{38}	-18.564 ± 0.017 ^d
Ne^{22}	-1.525 ± 0.013 ^b	A^{38}	-23.474 ± 0.032 ^d
Na^{22}	1.315 ± 0.014 ^b	K^{38}	-17.558 ± 0.026 ^d
Ne^{23}	1.651 ± 0.015 ^b	Cl^{39}	-18.274 ± 0.026 ⁿ
Na^{23}	-2.734 ± 0.007 ^b	A^{39}	-21.714 ± 0.021 ^d
Mg^{23}	1.325 ± 0.012 ^f	K^{39}	-22.279 ± 0.020 ^d
Ne^{24}	1.13 ± 0.04 ^g	Ca^{39}	-15.5 ± 0.2 ^q
Na^{24}	-1.323 ± 0.008 ^b	Cl^{40}	-15.7 ± 1.0 ⁿ
Mg^{24}	-6.837 ± 0.008 ^b	A^{40}	-23.19 ± 0.03 ^r
Al^{24}	7.2 ± 0.3 ^b	K^{40}	-21.707 ± 0.021 ^d
Na^{25}	-1.80 ± 0.20 ^h	Ca^{40}	-23.026 ± 0.024 ^d
Mg^{25}	-5.802 ± 0.009 ^b	Sc^{40}	-9.1 ± 0.4 ^s
Al^{25}	-1.54 ± 0.02 ⁱ	A^{41}	-20.925 ± 0.035 ^d
Mg^{26}	-8.553 ± 0.010 ^b	K^{41}	-23.449 ± 0.028 ^d
Al^{26}	-4.537 ± 0.018 ^j	Ca^{41}	-23.023 ± 0.026 ^d
Mg^{27}	-6.625 ± 0.010 ^b	Sc^{41}	-17.1 ± 0.1 ^t
Al^{27}	-9.219 ± 0.007 ^b	K^{42}	-22.608 ± 0.033 ^d
Si^{27}	-4.414 ± 0.009 ^k	Ca^{42}	-26.136 ± 0.021 ^d
Mg^{28}	-6.765 ± 0.022 ^b	K^{43}	-23.86 ± 0.03 ⁿ
Al^{28}	-8.575 ± 0.009 ^b	Ca^{43}	-25.702 ± 0.023 ^d
Si^{28}	-13.223 ± 0.009 ^b	Sc^{43}	-23.500 ± 0.030 ^d
P^{28}	0.6 ± 0.3 ^b	K^{44}	-22.4 ± 0.3 ⁿ
Al^{29}	-9.35 ± 0.10 ^b	Ca^{44}	-28.480 ± 0.026 ^d
Si^{29}	-13.330 ± 0.009 ^b	Sc^{44}	-24.833 ± 0.027 ^u
P^{29}	-8.363 ± 0.009 ^b	Ca^{45}	-27.527 ± 0.028 ^d
Si^{30}	-15.572 ± 0.010 ^b	Sc^{45}	-27.783 ± 0.028 ^d
P^{30}	-11.308 ± 0.012 ^l	Sc^{46}	-28.41 ± 0.08 ^e
Si^{31}	-13.799 ± 0.009 ^b	Ti^{46}	-30.77 ± 0.08 ^e
P^{31}	-15.280 ± 0.008 ^b	Ca^{47}	-28.64 ± 0.08 ^v
Si^{31}	-9.83 ± 0.07 ^b	Sc^{47}	-30.59 ± 0.08 ^w
Si^{32}	-14.73 ± 0.05 ^b	Ti^{47}	-31.19 ± 0.08 ^e
P^{32}	-14.833 ± 0.004 ^b	Ca^{48}	-30.26 ± 0.12 ^x
Si^{32}	-16.5373 ± 0.0008 ^c	Sc^{48}	-30.35 ± 0.09 ^e
Cl^{32}	-3.5 ± 0.4 ^b	Ti^{48}	-34.34 ± 0.08 ^e
P^{33}	-16.567 ± 0.010 ⁿ	Ca^{49}	-27.04 ± 0.12 ^y
Si^{33}	-16.816 ± 0.008 ^d	Sc^{49}	-32.09 ± 0.10 ^e
Cl^{33}	-11.238 ± 0.012 ^m	Ti^{49}	-34.09 ± 0.08 ^e
P^{34}	-14.67 ± 0.14 ⁿ	Ti^{50}	-36.71 ± 0.08 ^e
Si^{34}	-19.868 ± 0.016 ^d		

^a Wa 55a.^b Wa 55a plus correction as described in text.^c Qu 56a. Note added in proof.—A recent remeasurement [Quisenberry, Giesen, and Benson, Bull. Am. Phys. Soc. Ser. II, 2, 223 (1957)] gives -16.5396 ± 0.0010 Mev for the S^{32} mass excess.^d En 57.^e Wa 55b.^f Connected to Na^{23} through a new value for the $Na^{23}(\beta, n)Mg^{23}$ threshold (Ki 55a).^g Connected to Na^{24} through the $Ne^{24}(\beta^-)Na^{24}$ decay (Dr 56).^h Connected to Mg^{25} through the $Na^{25}(\beta^-)Mg^{25}$ decay (Ma 55).ⁱ Computed from the $Al^{25}(\beta^+)Mg^{25}$ decay (El 55), and from $Mg^{24}(\beta, \gamma)Al^{25}$ (Hu 55, Ag 56, Cr 56, Va 56b), which reactions yield Al^{25} masses in good mutual agreement.^j Values for Al^{24} mass excess computed from $Si^{28}(d, \alpha)Al^{24}$ (Br 54) and $Mg^{24}(\beta, n)Al^{24m}$ (Ki 55a). Q values are -4.521 ± 0.012 and -4.558 ± 0.014 Mev respectively, in rather serious disagreement. A weighted average has been taken, which agrees well with measured $Al^{20m}(\beta^+)Mg^{26}$ decay energy (Ka 55, El 55).^k Connected to Al^{27} through recent measurements of $Al^{27}(\beta, n)Si^{27}$ threshold (Ki 55a, Ma 55a).^l Connected to S^{32} through $S^{32}(d, \alpha)P^{30}$ reaction (Pa 57). P^{30} mass thus obtained is in good agreement with less accurate values computed from $P^{30}(\beta^+)S^{30}$ decay (Gr 56), and from $Si^{29}(\beta, \gamma)P^{30}$ (Va 57), $Si^{29}(d, n)P^{30}$ (Ma 52), and $P^{31}(\gamma, n)P^{30}$ (Sc 55a) reactions. Serious disagreement with Q values reported in Bu 56c for $Al^{27}(\alpha, n)P^{30}$, and in Le 56b for $S^{32}(d, \alpha)P^{30}$ reaction.^m Connected to S^{32} through the $S^{32}(\beta, \gamma)Cl^{32}$ reaction (Va 56f).ⁿ Connected through beta decay to nuclides listed in En 57.^o From microwave measurements yielding $(S^{36} - S^{32})/(S^{36} - S^{34}) = 1.998320 \pm 30$ (Ge 56c).

work, to be described elsewhere. Each resistor represents a Q -value measurement. Its resistance is taken proportional to the square of the experimental error of the corresponding measurement. Resistors are soldered to jacks representing nuclides. If an external potential difference of 41.7 v is applied between the S^{32} and O^{16} jacks, the potential difference (in v) between any arbitrary jack and O^{16} gives the corresponding mass correction (in kev). The error to be assigned to any mass value is obtained by measuring the resistance between the corresponding jack and O^{16} .

REFERENCES

- Aa 55 L. C. Aamodt and P. C. Fletcher, Phys. Rev. **98**, 1317 (1955).
 Ad 53 Adler, Huber, and Hälg, Helv. Phys. Acta **26**, 349 (1953).
 Ad 56 Adyasevich, Groshev, Demidov, and Lysenko, Atomnaja Energ. **2**, 28 (1956).
 Ad 56a Adyasevich, Groshev, and Demidov, Atomnaja Energ. **2**, 40 (1956), and J. Nuclear Energy **3**, 258 (1956).
 Ag 50 H. M. Agnew, Phys. Rev. **77**, 655 (1950).
 Ag 56 Ager-Hanssen, Lönsjö, and Nordhagen, Phys. Rev. **101**, 1779 (1956).
 Ah 48 L. H. Ahrens and R. D. Evans, Phys. Rev. **74**, 279 (1948).
 Aj 52 F. Ajzenberg and T. Lauritsen, Revs. Modern Phys. **24**, 321 (1952).
 Aj 55 Ajzenberg, Rubin, and Likely, Phys. Rev. **99**, 654(A) (1955) plus verbal report to Nuclear Data Group.
 Al 48 D. E. Alburger, Phys. Rev. **73**, 1014 (1948).
 Al 49 D. E. Alburger, Phys. Rev. **76**, 435(L) (1949).
 Al 49a D. E. Alburger, Phys. Rev. **75**, 51 (1949).
 Al 50 D. E. Alburger and E. M. Hafner, Revs. Modern Phys. **22**, 373 (1950).
 Al 50a L. W. Alvarez, Phys. Rev. **80**, 519 (1950).
 Al 50b Alburger, Hughes, and Eggler, Phys. Rev. **78**, 318(A) (1950).
 Al 51 Allen, May, and Rall, Phys. Rev. **84**, 1203 (1951).
 Al 55 Allen, Burcham, Chackett, Munday, and Reasbeck, Proc. Phys. Soc. (London) **A68**, 681 (1955).
 Al 55a Almqvist, Clarke, and Paul, Phys. Rev. **100**, 1265(A) (1955).
 Al 55b H. R. Allan and N. Sarma, Proc. Phys. Soc. (London) **A68**, 535 (1955).
 Al 56 Alkhazov, Andreyev, Greenberg, and Lemberg, Physica **22**, 1129(A) (1956).
 Al 56a Allen, Collinge, Hird, Maglić, and Orman, Proc. Phys. Soc. (London) **A69**, 705 (1956).
 Al 57 Almqvist, Bromley, Ferguson, Gove, Litherland, and Paul (private communication).
 Al 57a D. L. Allan, Proc. Phys. Soc. (London) **A70**, 195 (1957).
 An 52 Anderson, Wheeler, and Watson, Phys. Rev. **87**, 897(L) (1952).
 An 53 Anderson, Wheeler, and Watson, Phys. Rev. **90**, 606 (1953).

^{*} From $S^{37}(\beta^-)Cl^{37}$ (Bl 46, Mo 56, St 56a) and $A^{40}(\bar{n}, \alpha)S^{37}$ (Be 55a) Q values in good mutual agreement.[†] Average of masses computed from $Ca^{39}(\beta^+)K^{39}$ (Hu 54) and $Ca^{40}(\gamma, n)Ca^{39}$ (Su 53) Q values.[‡] Mass adopted for A^{40} makes the energy available for $K^{40}(EC)A^{40}$ decay leading to first A^{40} level equal to only 20 kev which is necessary to explain the long observed half-life (also Wa 55). This mass is in fair agreement with that computed from $A^{40}(d, p)A^{41}$ Q value (Da 49, Gi 52). Note added in proof.—The adopted A^{40} mass excess is in excellent agreement with a recent precision measurement by mass spectrometer [L. G. Smith, Bull. Am. Phys. Soc. Ser. II, 2, 223 (1957)] yielding -23.1893 ± 0.0004 Mev.^{*} Average of masses computed from $Sc^{40}(\beta^+)Ca^{40}$ and $Ca^{40}(\bar{n}, \alpha)Sc^{40}$ Q values (Gi 55).[†] Average of masses computed from $Sc^{41}(\beta^+)Ca^{41}$ (El 41) and $Ca^{40}(d, n)Sc^{41}$ (Pi 55) Q values.[‡] Value given here slightly different from that in En 57, where $Sc^{40}(\beta^+)Ca^{40}$ decay energy reported in Bl 55 had been overlooked.[§] Connected to Sc^{47} through $Ca^{47}(\beta^-)Sc^{47}$ decay (Co 53, Ma 53, Ly 55a, Li 56).^{**} Connected to Ti^{47} through $Sc^{47}(\beta^-)Ti^{47}$ decay (Ch 53a, Ni 55, Gr 56a).^{††} Connected to Ca^{49} through $Ca^{49}(\beta^+)Ca^{49}$ Q value (Br 56f).^{†††} Connected to Sc^{49} through $Ca^{49}(\beta^-)Sc^{49}$ decay (Ke 56, Ma 56a).^{‡‡} Lowest $T=0$ state.

- An 54 G. Andersson, Phil. Mag. **45**, 621 (1954).
 An 45a Anton'eva, Bashilov, Dzhelepov, and Orlov, Izvest. Akad. Nauk. Ser. Fiz. SSSR **18**, 93 (1954).
 Ar 52 Arthur, Allen, Bender, Hausman, and McDole, Phys. Rev. **88**, 1291 (1952).
 Ar 53 W. Arber and P. Stähelin, Helv. Phys. Acta **26**, 584(A) (1953).
 Aw 56 M. Awschalom, Phys. Rev. **101**, 1041 (1956).
 Ba 40 Barkas, Creutz, Delsasso, Sutton, and White, Phys. Rev. **58**, 383(L) (1940).
 Ba 51 Batzel, Miller, and Seaborg, Phys. Rev. **84**, 671 (1951).
 Ba 52 Baker, Dodd, and Simmons, Phys. Rev. **85**, 1051(L) (1952).
 Ba 52a K. Baskova and A. Kudriavtseva, Zhur. Eksptl. i Teoret. Fiz. **23**, 483 (1952).
 Ba 53 G. A. Bartholomew and B. B. Kinsey, Can. J. Phys. **31**, 927 (1953).
 Ba 54 R. E. Batzel and G. H. Coleman, Phys. Rev. **93**, 280 (1954).
 Ba 55 R. Basile and C. Schuhl, Compt. rend. **240**, 2399 (1955).
 Ba 55a Bartholomew, Boyd, Brown, Hawkings, Lounsbury, and Merritt, Can. J. Phys. **33**, 43 (1955).
 Ba 55b G. Backenstoss and K. Goebel, Z. Naturforsch. **10a**, 920 (1955).
 Ba 56 Baumann, Prosser, Read, and Krone, Phys. Rev. **104**, 376 (1956).
 Be 39 H. A. Bethe and W. J. Henderson, Phys. Rev. **56**, 1060(L) (1939).
 Be 47 Becker, Hanson, and Diven, Phys. Rev. **71**, 466(A) (1947).
 Be 48 B. B. Benson, Phys. Rev. **73**, 7 (1948).
 Be 49 Bender, Shoemaker, Kaufmann, and Bouricius, Phys. Rev. **76**, 273 (1949).
 Be 50 J. R. Beyster and M. L. Wiedenbeck, Phys. Rev. **79**, 728(L) (1950).
 Be 51 Beghian, Bishop, and Halban, Phys. Rev. **83**, 186(L) (1951).
 Be 53 E. H. Bellamy and K. F. Smith, Phil. Mag. **44**, 33 (1953).
 Be 55 Bent, Bonner, McCrary, and Ranken, Phys. Rev. **100**, 774 (1955).
 Be 55a E. H. Bellamy and F. C. Flack, Phil. Mag. **46**, 341 (1955).
 Be 55b Bent, Bonner, and McCrary, Phys. Rev. **98**, 1325 (1955).
 Be 55c H. Berthet and J. Rossel, Helv. Phys. Acta **28**, 265 (1955).
 Be 56 Beyster, Walt, and Salmi, Phys. Rev. **104**, 1319 (1956).
 Be 56a Berenbaum, Towle, and Matthews, Proc. Phys. Soc. (London) **A69**, 858(L) (1956).
 Be 57 Benczer-Koller, Schwartschild, and Wu, Bull. Am. Phys. Soc. Ser. II, **2**, 23 (1957).
 Bi 52 A. C. Birge, Phys. Rev. **85**, 753(A) (1952).
 Bl 46 E. Bleuler and W. Zünti, Helv. Phys. Acta **19**, 137 (1946).
 Bl 47 E. Bleuler and W. Zünti, Helv. Phys. Acta **20**, 195 (1947).
 Bl 51 Blaser, Boehm, Marmier, and Scherrer, Helv. Phys. Acta **24**, 465 (1951).
 Bl 55 J. W. Blue and E. Bleuler, Phys. Rev. **100**, 1324 (1955).
 Bl 55a E. Bleuler and D. J. Tendam, Phys. Rev. **99**, 1652(A) (1955).
 Bl 56 R. C. Block and H. W. Newson, Bull. Am. Phys. Soc. Ser. II, **1**, 55 (1956).
 Bl 56a Bleuler, Gailar, Seidlitz, and Tendam, Physica **22**, 1127(A) (1956).
 Bo 50 K. Boyer, M.I.T., Laboratory for Nuclear Science and Engineering Progress Report, July 1, 1950.
 Bo 51 F. J. Boley and D. J. Zaffarano, Phys. Rev. **84**, 1059(L) (1951).
 Bo 53 F. J. Boley, Iowa State Coll. J. Sci. **27**, 129 (1953).
 Bo 55 M. Bolsterli and E. Feenberg, Phys. Rev. **97**, 736 (1955).
 Bo 55a Boyd, Brown, and Lounsbury, Can. J. Phys. **33**, 35 (1955).
 Bo 55b Bockelman, Braams, Buechner, and Guthe, Phys. Rev. **99**, 655(Å) (1955).
 Bo 55c Bockelman, Cobb, and Guthe, M.I.T., Laboratory for Nuclear Science Progress Report, May 31 (1955).
 Bo 56 C. K. Bockelman, Bull. Am. Phys. Soc. Ser. II, **1**, 223 (1956).
 Bo 56a C. K. Bockelman, M.I.T., Laboratory for Nuclear Science Progress Report, May 31 (1956).
 Bo 57 Bockelman, Braams, Browne, Buechner, Sharp, and Sperduto, Phys. Rev. **107**, 176 (1957).
 Bo 57a Bostrom, Moore, and Morgan, Bull. Am. Phys. Soc. Ser. II, **2**, 104 (1957).
 Br 47 Broström, Huus, and Koch, Nature **160**, 498(L) (1947).
 Br 47a Broström, Huus, and Tangen, Phys. Rev. **71**, 661 (1947).
 Br 48 H. Bradner and J. D. Gow, Phys. Rev. **74**, 1559(A) (1948).
 Br 48a Broström, Huus, and Koch, Nature **162**, 695(L) (1948).
 Br 49 Brolley, Sampson, and Mitchell, Phys. Rev. **76**, 624 (1949).
 Br 50 Brosi, Zeldes, and Ketelle, Phys. Rev. **79**, 902(L) (1950).
 Br 50a H. Brown and V. Perez-Mendez, Phys. Rev. **78**, 649 (1950).
 Br 50b J. A. Bruner and L. M. Langer, Phys. Rev. **79**, 606 (1950).
 Br 51 Broström, Madsen, and Madsen, Phys. Rev. **83**, 1265(L) (1951).
 Br 51a Brown, Hanna, and Yaffe, Phys. Rev. **84**, 1243(L) (1951).
 Br 53 R. Braams and C. L. Smith, Phys. Rev. **90**, 995(L) (1953).
 Br 53a Brown, Yaffe, and Hanna, Proc. Roy. Soc. (London) **220A**, 203 (1953).
 Br 54 C. P. Browne, Phys. Rev. **95**, 860(L) (1954).
 Br 54a Breckon, Henrikson, Martin, and Foster, Can. J. Phys. **32**, 223 (1954).
 Br 54b Browne, Zimmerman, and Buechner, Phys. Rev. **96**, 725 (1954).
 Br 54c Bretscher, Alderman, Elwyn, and Shull, Phys. Rev. **96**, 103 (1954).
 Br 55 C. P. Browne and W. C. Cobb, Phys. Rev. **99**, 644(A) (1955).
 Br 55a C. P. Browne, M.I.T., Laboratory for Nuclear Science Progress Report, May 31 (1955).
 Br 55b R. J. Breen and M. R. Hertz, Phys. Rev. **98**, 599 (1955).
 Br 56 Bromley, Gove, Litherland, Paul, and Almqvist, Bull. Am. Phys. Soc. Ser. II, **1**, 30 (1956).
 Br 56a Broude, Green, Singh, and Willmott, Phys. Rev. **101**, 1052 (1956).
 Br 56b C. M. Braams, Phys. Rev. **101**, 1764 (1956).
 Br 56c Brugger, Evans, Joki, and Shankland, Phys. Rev. **104**, 1054 (1956).
 Br 56d C. P. Browne, Bull. Am. Phys. Soc. Ser. II, **1**, 212 (1956) and M.I.T., Laboratory for Nuclear Science Progress Report, May 31 (1956).
 Br 56e T. H. Braid, Phys. Rev. **102**, 1109 (1956).
 Br 56f C. M. Braams, thesis Utrecht (1956).
 Br 56g C. M. Braams, Phys. Rev. **103**, 1310 (1956).
 Br 56h Broude, Green, Singh, and Willmott (private communication to Nuclear Data Group).
 Br 56i Broude, Green, Willmott, and Singh, Physica **22**, 1139(A) (1956), and private communication.
 Br 57 Bromley, Gove, Paul, Litherland, and Almqvist, Can. J. Phys. **35**, 1042 (1957).
 Br 57a Bromley, Gove, Litherland, and Almqvist (private communication).
 Br 57b C. M. Braams, Phys. Rev. **105**, 1023 (1957).
 Br 57c Bromley, Gove, and Litherland, Can. J. Phys. **35**, 1057 (1957).
 Bu 53 P. R. J. Burch, Nature **172**, 361(L) (1953).
 Bu 53a Buechner, Sperduto, Browne, and Bockelman, Phys. Rev. **91**, 1502 (1953).
 Bu 54 W. W. Buechner, Proceedings of the Glasgow Conference, Pergamon Press, London (1954).
 Bu 56 Buechner, Mazari, and Sperduto, Phys. Rev. **101**, 188 (1956).
 Bu 56a Burge, Fujimoto, and Hossain, Phil. Mag. **1**, 19 (1956).
 Bu 56b Bumiller, Müller, and Staub, Helv. Phys. Acta. **29**, 234(A) (1956), and **29**, 83 (1956).
 Bu 56c B. S. Burton and R. M. Williamson, Bull. Am. Soc. Ser. II, **1**, 264 (1956).
 Bu 56d Burrows, Green, Hinds, and Middleton, Proc. Phys. Soc. (London) **A69**, 310 (1956).

- Bu 57 W. W. Buechner and A. Sperduto, Phys. Rev. **106**, 1008 (1957).
 Ca 53 H. Casson, Phys. Rev. **89**, 809 (1953).
 Ca 54 U. Cappeller and R. Klingelhöfer, Z. Naturforsch. **9A**, 1052(L) (1954).
 Ca 54a Carlson, Geer, and Nelson, Phys. Rev. **94**, 1311 (1954).
 Ca 55 Calvert, Yaffe, Litherland, and Maslin, Proc. Phys. Soc. (London) **A68**, 1008 (1955).
 Ca 56 P. J. Campion and G. A. Bartholomew, Bull. Am. Phys. Soc. Ser. II, **1**, 28 (1956) plus verbal report to Nuclear Data Group.
 Ca 56a Calvert, Yaffe, and Maslin, Phys. Rev. **101**, 501(L) (1956).
 Ca 57 Calvert, Yaffe, and Maslin, Proc. Phys. Soc. (London) **A70**, 78 (1957).
 Ch 53 Churchill, Jones, and Hunt, Nature **172**, 460(L) (1953).
 Ch 53a L. S. Cheng and M. L. Pool, Phys. Rev. **90**, 886 (1953).
 Ch 54 G. Charpak and F. Suzor, J. phys. radium **15**, 378 (1954).
 Ch 55 G. Charpak, J. phys. radium **16**, 62 (1955).
 Ch 55a G. Charpak, J. phys. radium **16**, 567 (1955).
 Ch 56 Chick, Evans, Hancock, Hunt, and Pope, Proc. Phys. Soc. (London) **A69**, 624 (1956).
 Cl 55 Clarke, Almqvist, and Paul, Phys. Rev. **99**, 654(A) (1955).
 Co 40 J. M. Cork and W. Middleton, Phys. Rev. **58**, 474(L) (1940).
 Co 50 F. C. W. Colmer and D. J. Littler, Proc. Phys. Soc. (London) **A63**, 1175 (1950).
 Co 50a J. W. Cobble and R. W. Atteberry, Phys. Rev. **80**, 917(L) (1950).
 Co 53 Cork, LeBlanc, Brice, and Nester, Phys. Rev. **92**, 367 (1953).
 Co 54 B. L. Cohen, Phys. Rev. **94**, 117 (1954).
 Co 54a Cohen, Reynolds, and Zucker, Phys. Rev. **96**, 1617 (1954).
 Co 54b Cox, Van Loef, and Lind, Phys. Rev. **93**, 925(A) (1954).
 Co 55 H. E. Conzett, Phys. Rev. **100**, 1794(A) (1955).
 Co 55a Cohn, Bair, Kington, and Willard, Phys. Rev. **99**, 644(A) (1955) plus verbal report to Nuclear Data Group.
 Co 55b B. L. Cohen, Phys. Rev. **98**, 49 (1955).
 Co 55c C. F. Coleman, Phil. Mag. **46**, 1135(L) (1955).
 Co 56 A. V. Cohen and P. H. White, Nuclear Physics **1**, 73 (1956).
 Co 56a S. A. Cox and R. M. Williamson, Bull. Am. Phys. Soc. Ser. II, **1**, 196 (1956).
 Co 56b L. Colli and U. Facchini, Physica **22**, 1158(A) (1956).
 Co 57 W. R. Cobb and D. B. Guthe, Phys. Rev. **107**, 181 (1957).
 Cr 40 Creutz, Fox, and Sutton, Phys. Rev. **57**, 567(A) (1940).
 Cr 55 W. G. Cross and R. G. Jarvis, Phys. Rev. **99**, 621(A) (1955).
 Cr 56 D. S. Craig, Phys. Rev. **101**, 1479 (1956).
 Cr 56a L. Cranberg and J. S. Levin, Phys. Rev. **103**, 343 (1956).
 Cr 57 Crutchfield, Haeberli, and Newson, Bull. Am. Phys. Soc. Ser. II, **2**, 33 (1957).
 Cu 40 Curran, Dee, and Strothers, Proc. Roy. Soc. (London) **A174**, 546 (1940).
 Cu 56 Culler, Fernbach, and Sherman, Phys. Rev. **101**, 1047 (1956).
 Da 49 Davison, Buchanan, and Pollard, Phys. Rev. **76**, 890 (1949).
 Da 53 Daniel, Koester, and Mayer-Kuckuk, Z. Naturforsch. **8a**, 447(L) (1953).
 Da 54 I. E. Dayton, Phys. Rev. **95**, 754 (1954).
 Da 54a H. Daniel and W. Bothe, Z. Naturforsch. **9a**, 402 (1954).
 Da 55 R. Davis, Phys. Rev. **97**, 766 (1955).
 Da 56 Day, Johnsrud, and Lind, Bull. Am. Phys. Soc. Ser. II, **1**, 56 (1956) plus verbal report to Nuclear Data Group.
 Da 56a I. E. Dayton and G. Schrank, Phys. Rev. **101**, 1358 (1956).
 Da 56b R. Davis, Bull. Am. Phys. Soc. Ser. II, **1**, 219 (1956).
 Da 56c R. B. Day, Phys. Rev. **102**, 767 (1956).
 Da 56d W. K. Dawson, Can. J. Phys. **34**, 1480 (1956).
 Da 57 Dalton, Hinds, and Parry, Proc. Phys. Soc. (London) **A70**, 586 (1957).
 De 53 C. F. G. Delaney and J. H. J. Poole, Phys. Rev. **89**, 529(L) (1953).
 De 53a A. De-Shalit, Phys. Rev. **91**, 1479 (1953).
 De 53b A. De-Shalit and M. Goldhaber, Phys. Rev. **92**, 1211 (1953).
 De 55 M. de Souza Santos *et al.*, Geneva Conference Report 8/P/897 (1955).
 De 56 G. Dearnaley, Phil. Mag. **1**, 821 (1956).
 De 56a Devons, Manning, and Towle, Proc. Phys. Soc. (London) **A69**, 173 (1956).
 De 57 J. de Veiga Simao and J. P. F. Sellschap (to be published).
 Di 55 Dixon, McNair, and Curran, J. phys. radium **16**, 538 (1955).
 Do 53 Donahue, Jones, McEllistrem and Richards, Phys. Rev. **89**, 824 (1953).
 Do 56 W. T. Doyle and A. B. Robbins, Phys. Rev. **101**, 1056 (1956).
 Do 56a Dolan, Fincher, Kenny, Berko, and Whitehead, Bull. Am. Phys. Soc. Ser. II, **1**, 339 (1956).
 Dr 55 R. W. P. Drever and A. Moljk, Phil. Mag. **46**, 1337 (1955).
 Dr 56 B. J. Dropesky and A. W. Schardt, Phys. Rev. **102**, 426 (1956).
 El 41 D. R. Elliot and L. D. P. King, Phys. Rev. **60**, 489 (1941).
 El 52 L. G. Elliot, Phys. Rev. **85**, 942(L) (1952).
 El 54 Elbek, Nielsen, and Nielsen, Phys. Rev. **95**, 96 (1954).
 El 55 Elbek, Madsen, and Nathan, Phil. Mag. **46**, 663 (1955).
 El 55a F. A. El Bedewi and M. A. El Wahab, Proc. Phys. Soc. (London) **A68**, 754 (1955).
 El 56 J. O. Elliot, Phys. Rev. **101**, 684 (1956).
 El 56a M. El-Wahab, thesis, Alexandria (1956).
 Em 54 Emmerich, Singer, and Kurbatov, Phys. Rev. **94**, 113 (1954).
 Em 55 E. W. Emery and N. Veall, Proc. Phys. Soc. (London) **A68**, 346(L) (1955).
 En 51 Enge, Buechner, Sperduto, and Van Patter, Phys. Rev. **83**, 31 (1951).
 En 51a Endt, Van Patter, Buechner, and Sperduto, Phys. Rev. **83**, 491 (1951).
 En 51b W. W. Ennis, Phys. Rev. **82**, 204(A) (1951).
 En 52 Endt, Haffner, and Van Patter, Phys. Rev. **86**, 518 (1952).
 En 52a Enge, Buechner, and Sperduto, Phys. Rev. **88**, 963 (1952).
 En 52b Endt, Enge, Haffner, and Buechner, Phys. Rev. **87**, 27 (1952).
 En 53 T. C. Engelder, Phys. Rev. **90**, 259 (1953).
 En 53a H. A. Enge, Universitetet i Bergen Årbok (1953).
 En 54 A. A. Enge, Phys. Rev. **94**, 730(L) (1954).
 En 54a P. M. Endt and J. C. Kluyver, Revs. Modern Phys. **26**, 95 (1954).
 En 54b Endt, Kluyver, and van der Leun, Phys. Rev. **95**, 580(L) (1954).
 En 54c Endt, Kluyver, and van der Leun, Physica **20**, 1299 (1954).
 En 56 Enge, Anglemann, and Jarrell, M.I.T., Laboratory for Nuclear Science Progress Report, May 31 (1956).
 En 56a Enge, Buechner, Sperduto, and Mazari, Bull. Am. Phys. Soc. Ser. II, **1**, 212 (1956).
 En 56b P. M. Endt, Physica **22**, 1062 (1956).
 En 56c Endt, Paris, Sperduto, and Buechner, Phys. Rev. **103**, 961 (1956).
 En 57 Endt, Buechner, Braams, Paris, and Sperduto, Phys. Rev. **105**, 1002 (1957).
 En 57a P. M. Endt and C. H. Paris, Phys. Rev. **106**, 764 (1957).
 Fa 50 W. R. Faust, Phys. Rev. **78**, 624(L) (1950).
 Fa 55 Farney, Givin, Kern, and Hahn, Phys. Rev. **97**, 720 (1955).
 Fe 52 L. Feldman and C. S. Wu, Phys. Rev. **87**, 1091 (1952).
 Fe 53 A. J. Ferguson and H. E. Gove, Phys. Rev. **91**, 439(A) (1953).
 Fe 54 Ferguson, Halpern, Nathans, and Yergin, Phys. Rev. **95**, 776 (1954).
 Fe 54a L. Feyvrais and T. Yuasa, Compt. rend. **239**, 1627 (1954).
 Fe 55 E. Feenberg, Phys. Rev. **99**, 71 (1955).

- Fe 56 J. M. Ferguson, M.I.T., Laboratory for Nuclear Science Progress Report, May 31 (1956).
- Fi 51 R. E. Fields and M. Walt, Phys. Rev. **83**, 479(L) (1951).
- Fi 54 G. E. Fischer, Phys. Rev. **96**, 704 (1954).
- Fl 54 Flack, Rutherford, and Grant, Proc. Phys. Soc. (London) **A67**, 973 (1954).
- Fo 52 A. Folkierski, Proc. Phys. Soc. (London) **A65**, 1006 (1952).
- Fo 54 G. N. Fowler, Proc. Phys. Soc. (London) **A67**, 1005(L) (1954).
- Fo 56 G. Ford and R. R. Lewis, Bull. Am. Phys. Soc. Ser. II, **1**, 195 (1956).
- Fr 50 J. M. Freeman, Proc. Phys. Soc. (London) **A63**, 668(L) (1950).
- Fr 50a A. P. French and P. B. Treacy, Proc. Phys. Soc. (London) **A63**, 665 (1950).
- Fr 51 J. M. Freeman and J. Seed, Proc. Phys. Soc. (London) **A64**, 313(L) (1951).
- Fr 54 Freemantle, Prowse, Hossain, and Rotblat, Phys. Rev. **96**, 1270 (1954).
- Fr 55 J. B. French and B. J. Raz, Phys. Rev. **98**, 1523(L) (1955).
- Fu 48 H. W. Fulbright and R. R. Bush, Phys. Rev. **74**, 1323 (1948).
- Fu 51 H. W. Fulbright and J. C. D. Milton, Phys. Rev. **82**, 274(L) (1951).
- Fu 54 Fujimoto, Kikuchi, and Yoshida, Progr. Theoret. Phys. (Kyoto) **11**, 264 (1954).
- Ga 53 Galonsky, Haeberli, Goldberg, and Douglas, Phys. Rev. **91**, 439(A) (1953).
- Ge 55 Gerber, Garcia, Muñoz, and Maeder, Helv. Phys. Acta **28**, 478 (1955).
- Ge 56 Gerber, Garcia, Muñoz, and Maeder, Phys. Rev. **101**, 774 (1956).
- Ge 56a Gerstein, Niederer, and Strauch, Bull. Am. Phys. Soc. Ser. II, **1**, 192 (1956).
- Ge 56b S. Geschwind (private communication).
- Gi 44 Gibert, Roggen, and Rossel, Helv. Phys. Acta **17**, 97 (1944).
- Gi 52 W. M. Gibson and E. E. Thomas, Proc. Roy. Soc. (London) **A210**, 543 (1952).
- Gi 52a D. A. Gilbert, Phys. Rev. **85**, 716(A) (1952).
- Gl 47 E. Gloditsch and F. Graf, Phys. Rev. **72**, 640(L) (1947).
- Gl 55 N. W. Glass and J. R. Richardson, Phys. Rev. **98**, 1251 (1955).
- Gl 56 R. J. Glauber and P. C. Martin, Phys. Rev. **104**, 158 (1956).
- Go 50 H. E. Gove, M.I.T., Laboratory for Nuclear Science and Engineering Progress Report, July (1950).
- Go 53 E. Goldberg, Phys. Rev. **89**, 760 (1953).
- Go 53a H. E. Gove (private communication).
- Go 54 Gove, Paul, Bartholomew, and Litherland, Phys. Rev. **94**, 749(A) (1954).
- Go 54a J. Goldemberg and L. Katz, Can. J. Phys. **32**, 49 (1954).
- Go 54b M. Goodrich and W. B. Payne, Phys. Rev. **94**, 405 (1954).
- Go 54c Goldberg, Haeberli, Galonsky, and Douglas, Phys. Rev. **93**, 799 (1954).
- Go 55 Gorodetsky, Müller, and Port, Compt. rend. **240**, 1704 and 2224 (1955).
- Go 56 Gove, Bartholomew, Paul, and Litherland, Nuclear Physics **2**, 132 (1956).
- Go 56a S. Goldstein and I. Talmi, Phys. Rev. **102**, 589(L) (1956).
- Go 56b P. Goldammer, Phys. Rev. **101**, 1375 (1956).
- Go 57 Gove, Litherland, and Paul, Bull. Am. Phys. Soc. Ser. II, **2**, 178 (1957).
- Go 57a Gove, Bartholomew, Paul, and Litherland, Nuclear Physics (erratum) (to be published).
- Go 57b H. E. Gove (private communication).
- Gr 50 Grotdal, Lönsjö, Tangen, and Bergström, Phys. Rev. **77**, 296(L) (1950).
- Gr 50a P. J. Grant, Proc. Phys. Soc. (London) **A63**, 1298 (1950).
- Gr 50b J. C. Grosskreutz and K. B. Mather, Phys. Rev. **77**, 580 (1950).
- Gr 51 G. R. Grove and J. N. Cooper, Phys. Rev. **82**, 505 (1951).
- Gr 54 Green, Harris, and Cooper, Phys. Rev. **96**, 817(A) (1954).
- Gr 54a G. W. Greenlees, Proc. Phys. Soc. (London) **A67**, 1107(L) (1954).
- Gr 55 G. W. Greenlees, Proc. Phys. Soc. (London) **A68**, 97 (1955).
- Gr 55a Groshev, Adyasevich, and Demidov, International Conference Geneva Report 8/P/651 (1955).
- Gr 55b E. R. Graves and R. W. Davis, Phys. Rev. **97**, 1205 (1955).
- Gr 55c Green, Singh, and Willmott, Phil. Mag. **46**, 982 (1955).
- Gr 55d G. L. Griffith, Phys. Rev. **98**, 579 (1955).
- Gr 55e Grant, Rutherford, Flack, and Hutchinson, Proc. Phys. Soc. (London) **A68**, 369 (1955).
- Gr 55f T. S. Green, thesis, Liverpool (1955).
- Gr 56 D. Green and J. R. Richardson, Phys. Rev. **101**, 776 (1956).
- Gr 56a W. E. Graves and S. K. Suri, Phys. Rev. **101**, 1368 (1956).
- Gr 56b J. S. Greenberg and M. Deutsch, Phys. Rev. **102**, 415 (1956).
- Gr 56c W. C. Grayson and L. W. Nordheim, Phys. Rev. **102**, 1093 (1956).
- Gr 56d H. G. Graetzer and A. B. Robbins, Bull. Am. Phys. Soc. Ser. II, **1**, 280 (1956).
- Gr 56e Green, Singh, and Willmott, Proc. Phys. Soc. (London) **A69**, 335 (1956).
- Gr 56f G. W. Greenlees and A. E. Souch, Proc. Phys. Soc. (London) **A69**, 686 (1956).
- Gu 54 P. C. Gugelot, Phys. Rev. **93**, 425 (1954).
- Gu 56 P. C. Gugelot and M. Rickey, Phys. Rev. **101**, 1613(L) (1956).
- Gu 56a P. C. Gugelot and P. R. Phillips, Phys. Rev. **101**, 1614(L) (1956).
- Ha 35 O. Haxel, Z. tech. Physik **16**, 400 (1935).
- Ha 50 Harris, Muehlhause, Rasmussen, Schroeder, and Thomas, Phys. Rev. **80**, 342 (1950).
- Ha 50a Haslam, Katz, Moody, and Skarsgard, Phys. Rev. **80**, 318 (1950).
- Ha 51 T. D. Hanscome and C. W. Malich, Phys. Rev. **82**, 304(A) (1951).
- Ha 51a W. Hägl, Helv. Phys. Acta **24**, 641(A) (1951).
- Ha 52 Hausman, Allen, Arthur, Bender, and McDole, Phys. Rev. **88**, 1296 (1952).
- Ha 52a Haslam, Summers-Gill, and Crosby, Can. J. Phys. **30**, 257 (1952).
- Ha 52b B. Hamermesh and V. Hummel, Phys. Rev. **88**, 916 (1952).
- Ha 52c J. A. Harvey, Phys. Rev. **88**, 162(A) (1952).
- Ha 53 Haeberli, Galonsky, Goldberg, and Douglas, Phys. Rev. **91**, 438(A) (1953).
- Ha 53a Hamilton, Lemonick, and Pipkin, Phys. Rev. **92**, 1191 (1953).
- Ha 54 Halpern, Nathans, and Vergin, Phys. Rev. **95**, 1529 (1954).
- Ha 54a Haslam, Roberts, and Robb, Can. J. Phys. **32**, 361 (1954).
- Ha 54b J. Haffner, M.I.T., Laboratory for Nuclear Science Progress Report, August 31, 1954.
- Ha 55 Hattori, Hisatake, Mikumo, and Momata, J. Phys. Soc. Japan **10**, 242 (1955).
- Ha 55a W. Haeberli, Phys. Rev. **99**, 640(A) (1955).
- Ha 55b T. H. Handley and W. S. Lyon, Phys. Rev. **99**, 755 (1955).
- Ha 55c D. A. Hancock and F. Verdaguer, Proc. Phys. Soc. (London) **A68**, 1080 (1955).
- Ha 56 Hausman, Monahan, Mooring, and Raboy, Bull. Am. Phys. Soc. Ser. II, **1**, 56 (1956) plus verbal report to Nuclear Data Group.
- Ha 56a R. K. Haling, Bull. Am. Phys. Soc. Ser. II, **1**, 29 (1956).
- Ha 56b Hahn, Revenhall, and Hofstadter, Phys. Rev. **101**, 1131 (1956).
- Ha 56c J. W. Haffner, Phys. Rev. **103**, 1398 (1956).
- Ha 56d H. E. Handler and J. R. Richardson, Phys. Rev. **102**, 833 (1956).
- Ha 56e Hassler, Steigert, and Pieper, Bull. Am. Phys. Soc. Ser. II, **1**, 280 (1956).
- He 47 Heitler, May, and Powell, Proc. Roy. Soc. (London) **A190**, 180 (1947).

- He 49 Herb, Snowdon, and Sala, Phys. Rev. **75**, 246 (1949).
 He 52 A. Hedgran and D. Lind, Arkiv Fysik **5**, 177 (1952).
 He 54 J. Heintze, Z. Naturforsch. **9a**, 469 (1954).
 He 54a Hee, Coche, Keller, Jarovoy, and Wack, Ann. geophys. **10**, 19 (1954).
 He 54b N. P. Heydenberg and G. M. Temmer, Phys. Rev. **94**, 1252 (1954).
 He 56 R. H. Helen, Phys. Rev. **104**, 1466 (1956).
 Hi 45 Hibdon, Pool, and Kurbatov, Phys. Rev. **67**, 289 (1945).
 Hi 54 A. Hitchcock, Phil. Mag. **45**, 379 and 385 (1954).
 Hi 54a Hird, Whitehead, Butler, and Collie, Phys. Rev. **96**, 702 (1954).
 Hi 55 N. M. Hintz, Phys. Rev. **100**, 1794(A) (1955).
 Hi 56 N. M. Hintz and R. M. Eisberg, Phys. Rev. **103**, 645 (1956).
 Hi 56a R. W. Hill, Bull. Am. Phys. Soc. **1**, 174 (1956).
 Hi 56b S. Hinds and R. Middleton, Proc. Phys. Soc. (London) **A69**, 347(L) (1956).
 Ho 40 J. B. Hoag, Phys. Rev. **57**, 937(L), 1940.
 Ho 46 N. Hole and K. Siegbahn, Arkiv Mat. Astron. Fysik **33A**, No. 9 (1946).
 Ho 50 Houtermans, Haxel, and Heintze, Z. Physik **128**, 657 (1950).
 Ho 53 J. R. Holt and T. N. Marsham, Proc. Phys. Soc. (London) **A66**, 258 (1953).
 Ho 53a J. R. Holt and T. N. Marsham, Phys. Rev. **89**, 665(L) (1953).
 Ho 53b N. F. Hornyak and T. Coor, Phys. Rev. **92**, 675 (1953).
 Ho 53c J. R. Holt and T. N. Marsham, Proc. Phys. Soc. (London) **A66**, 565 (1953).
 Ho 53d J. R. Holt and T. N. Marsham, Proc. Phys. Soc. (London) **A66**, 467 (1953).
 Ho 56 Hoyle, Fowler, Burbidge, and Burbidge, Science **124**, 611 (1956).
 Ho 57 Hoogenboom, Van Loef, and Endt (unpublished).
 Hu 41 Huber, Helv. Phys. Acta **14**, 163 (1941).
 Hu 45 Huber, Lienhard, Scherrer, and Wäffler, Helv. Phys. Acta **18**, 221 (1945).
 Hu 53 S. E. Hunt and W. M. Jones, Phys. Rev. **89**, 1283 (1953).
 Hu 54 Hunt, Kline, and Zaffarano, Phys. Rev. **95**, 611(A) (1954).
 Hu 54a W. A. Hunt and D. J. Zaffarano, U.S.A.E.C. Report ISC—469 (1954).
 Hu 54b Hunt, Jones, Churchill, and Hancock, Proc. Phys. Soc. (London) **A67**, 443 (1954).
 Hu 54c Hunt, Jones, and Churchill, Proc. Phys. Soc. (London) **A67**, 479(L) (1954).
 Hu 55 S. E. Hunt and D. A. Hancock, Phys. Rev. **97**, 567(L) (1955).
 Hu 55a T. Hürlimann and P. Huber, Helv. Phys. Acta **28**, 33 (1955).
 Hu 55b R. Huby and H. C. Newns, Appendix to El 55a.
 Hu 55c D. J. Hughes and J. A. Harvey, Brookhaven National Laboratory Report BNL 325 (1955).
 Hu 56 I. S. Hughes and D. Sinclair, Proc. Phys. Soc. (London) **A69**, 125 (1956).
 Hu 56a K. Huang, Phys. Rev. **102**, 422 (1956).
 Ig 56 Igo, Wegner, and Eisberg, Phys. Rev. **101**, 1508 (1956).
 In 50 Inghram, Brown, Patterson, and Hess, Phys. Rev. **80**, 916(L) (1950).
 In 53 D. R. Inglis, Revs. Modern Phys. **25**, 390 (1953).
 It 41 J. Itoh, Proc. Phys. Math. Soc. Japan **23**, 605 (1941).
 Iw 53 Iwersen, Koski, and Rasetti, Phys. Rev. **91**, 1229 (1953).
 Iw 55 J. E. Iwersen and W. S. Koski, Phys. Rev. **98**, 1307 (1955).
 Je 52 Jensen, Nichols, Clement, and Pohm, Phys. Rev. **85**, 112 (1952).
 Je 53 C. D. Jeffries, Phys. Rev. **90**, 1130(L) (1953).
 Jo 49 F. Johnston and J. E. Willard, Phys. Rev. **75**, 528(L) (1949).
 Jo 51 Johnson, Gordy, and Livingston, Phys. Rev. **83**, 1249(L) (1951).
 Jo 52 J. W. Jones and T. P. Kohman, Phys. Rev. **85**, 941(L) (1952).
 Jo 52a W. H. Johnson, Phys. Rev. **88**, 1213(L) (1952).
 Jo 53 J. W. Jones and T. R. Kohman, Phys. Rev. **90**, 495(L) (1953).
 Jo 54 G. A. Jones and D. H. Wilkinson, Phil. Mag. **45**, 230(L) (1954).
 Jo 55 S. A. E. Johansson, Phys. Rev. **97**, 1186(L) (1955).
 Jo 55a Joki, Miller, and Evans, Phys. Rev. **99**, 610(A) (1955).
 Jo 56 Johnson, Johnson, and Langer, Phys. Rev. **102**, 1142 (1956).
 Ju 56 A. C. Juveland and W. Jentschke, Bull. Am. Phys. Soc. Ser. II, **1**, 193 (1956).
 Ka 51 L. Katz and A. G. W. Cameron, Phys. Rev. **84**, 1115 (1951).
 Ka 51a L. Katz and A. S. Penfold, Phys. Rev. **81**, 815 (1951).
 Ka 52 Kaufmann, Goldberg, Koester, and Mooring, Phys. Rev. **88**, 673 (1952).
 Ka 52a S. Katcoff, Phys. Rev. **87**, 886 (1952).
 Ka 54 Katz, Haslam, Goldemberg, and Taylor, Can. J. Phys. **32**, 580 (1954).
 Ka 55 Kavanagh, Mills, and Sherr, Phys. Rev. **97**, 248(L) (1955).
 Ke 54 Kelley, Kuhn, and Pery, Proc. Phys. Soc. (London) **A67**, 450 (1954).
 Ke 56 O'Kelley, Lazar, and Eichler, Phys. Rev. **101**, 1059 (1956).
 Ke 56a B. D. Kern and L. W. Cochran, Phys. Rev. **104**, 711 (1956).
 Ki 42 Kikuchi, Watase, and Itoh, Z. Physik **69**, 185 (1942).
 Ki 51 Kinsey, Bartholomew, and Walker, Phys. Rev. **83**, 519 (1951).
 Ki 52 Kinsey, Bartholomew, and Walker, Phys. Rev. **85**, 1012 (1952).
 Ki 52a J. S. King and W. C. Parkinson, Phys. Rev. **88**, 141(L) (1952).
 Ki 52b B. B. Kinsey and G. A. Bartholomew, Physica **18**, 1112 (1952).
 Ki 53 Kington, Bair, Carlson, and Willard, Phys. Rev. **89**, 530(L) (1953).
 Ki 53a B. B. Kinsey and G. A. Bartholomew, Can. J. Phys. **31**, 901(L) (1953).
 Ki 53b J. S. King and E. H. Beach, Phys. Rev. **90**, 381(A) (1953).
 Ki 53c B. B. Kinsey and G. A. Bartholomew, Can. J. Phys. **31**, 537 (1953).
 Ki 54 R. M. Kiehn and C. Goodman, Phys. Rev. **95**, 989 (1954).
 Ki 54a B. B. Kinsey and G. A. Bartholomew, Phys. Rev. **93**, 1260 (1954).
 Ki 54b R. W. King, Revs. Modern Phys. **26**, 327 (1954).
 Ki 55 R. W. King, Phys. Rev. **99**, 67 (1955).
 Ki 55a Kington, Bair, Cohn, and Willard, Phys. Rev. **99**, 1393 (1955).
 Ki 56 Kistner, Schwarzschild, and Rustad, Phys. Rev. **104**, 154 (1956).
 Kl 54 Kluyver, van der Leun, and Endt, Physica **20**, 1287 (1954).
 Kl 54a Kluyver, van der Leun, and Endt, Phys. Rev. **94**, 1795(L) (1954).
 Kl 54b R. M. Kline and D. J. Zaffarano, Phys. Rev. **96**, 1620 (1954).
 Kl 55 J. C. Kluyver and C. van der Leun, Physica **21**, 604(L) (1955).
 Kl 55a J. C. Kluyver and P. M. Endt, Conference on Electromagnetically Enriched Isotopes Harwell (1955).
 Kl 57 Kloepfer, Day, and Lind, Bull. Am. Phys. Soc. Ser. II, **2**, 60 (1957).
 Ko 52 L. J. Koester, Phys. Rev. **85**, 643 (1952).
 Ko 54 Koerts, Schwarzschild, Gold, and Wu, Phys. Rev. **95**, 612(A) (1954).
 Ko 54a L. Koester, Z. Naturforsch. **9a**, 104 (1954).
 Ko 55 S. Kono, J. Phys. Soc. Japan **10**, 495 (1955).
 Kr 53 A. Z. Kranz and W. W. Watson, Phys. Rev. **91**, 1472 (1953).
 Kr 53a L. M. Khromchenko, Doklady Akad. Nauk SSSR **93**, 451 (1953).
 Kr 54 W. E. Kreger, Phys. Rev. **96**, 1554 (1954).
 Kr 54a Kraushaar, Mihelich, and Sunyar, Phys. Rev. **95**, 456 (1954).
 Kr 54b L. M. Khromchenko, Doklady Akad. Nauk SSSR **94**, 1037 (1954).

- Kr 56 R. W. Krone, A. Everett, and S. S. Hanna, Bull. Am. Phys. Soc. Ser. II, 1, 329 (1956).
 Kr 57 Kruse, Bent, and Eklund, Bull. Am. Phys. Soc. Ser. II, 2, 29 (1957).
 Ku 53 D. Kurath, Phys. Rev. 91, 1430 (1953).
 La 39 Langer, Mitchell, and McDaniel, Phys. Rev. 56, 962(L) (1939).
 La 39a J. L. Lawson, Phys. Rev. 56, 131 (1939).
 La 48 R. V. Langmuir, Phys. Rev. 74, 1559(A) (1948).
 La 49 L. M. Langer and H. C. Price, Phys. Rev. 76, 641 (1949).
 La 50 L. M. Langer, Phys. Rev. 77, 50 (1950).
 La 51 H. H. Landon, Phys. Rev. 83, 1081 (1951).
 La 54 Langevin, Yuasa, and Mérinis, J. phys. radium 15, 778 (1954).
 La 54a H. Langevin and N. Marty, J. phys. radium 15, 127 (1954).
 La 55 M. J. Laubitz, Proc. Phys. Soc. (London) A68, 1033 (1955).
 La 55a M. Langevin and P. Radvanyi, Compt. rend. 241, 33 (1955).
 La 56 R. O. Lane and J. E. Monahan, Bull. Am. Phys. Soc. Ser. II, 1, 187 (1956).
 La 56a R. O. Lane and J. E. Monahan, Bull. Am. Phys. Soc. Ser. II, 1, 346 (1956).
 La 56b Laberrigue-Frolow, Radvanyi, and Langevin, J. phys. radium 17, 530 (1956).
 La 57 Lazar, Lyon, and Macklin, Bull. Am. Phys. Soc. Ser. II, 2, 15 (1957).
 Le 54 R. D. Leamer and G. W. Hinman, Phys. Rev. 96, 1607 (1954).
 Le 55 C. Levinson and K. W. Ford, Phys. Rev. 100, 13 (1955).
 Le 56 Lewis, Olness, and Haeberli, Bull. Am. Phys. Soc. Ser. II, 1, 213 (1956).
 Le 56a H. W. Lewis and W. T. Joyner, Bull. Am. Phys. Soc. Ser. II, 1, 280 (1956).
 Le 56b L. L. Lee and F. P. Morring, Phys. Rev. 104, 1342 (1956).
 Li 37 M. S. Livingston and H. A. Bethe, Revs. Modern Phys. 9, 245 (1937).
 Li 53 M. Lindner, Phys. Rev. 89, 1150(L) (1953).
 Li 53a M. Lindner, Phys. Rev. 91, 642 (1953).
 Li 54 T. Lindqvist and A. C. G. Mitchell, Phys. Rev. 95, 1535 (1954).
 Li 54a T. Lindqvist and A. C. G. Mitchell, Phys. Rev. 95, 444 (1954).
 Li 55 K. Liden and N. Starfelt, Phys. Rev. 97, 419 (1955).
 Li 55a Little, Leonard, Prud'homme, and Vincent, Phys. Rev. 98, 634 (1955).
 Li 55b T. Lindqvist and C. S. Wu, Phys. Rev. 100, 145 (1955).
 Li 56 L. J. Lidofsky and V. K. Fischer, Phys. Rev. 104, 759 (1956).
 Li 56a Litherland, Paul, Bartholomew, and Gove, Phys. Rev. 102, 208 (1956).
 Li 57 A. E. Litherland *et al.* (private communication).
 Ly 37 E. M. Lyman, Phys. Rev. 51, 1 (1937).
 Ly 54 W. S. Lyon and J. J. Manning, Phys. Rev. 93, 501 (1954).
 Ly 55 W. S. Lyon and T. H. Handley, Phys. Rev. 100, 1280 (1955).
 Ly 56 W. S. Lyon and N. H. Lazar, Phys. Rev. 101, 1524 (1956).
 Ma 37 C. Magnan, Compt. rend. 205, 1147 (1937).
 Ma 41 C. Magnan, Ann. phys. 15, 5 (1941).
 Ma 50 J. E. Mack, Revs. Modern Phys. 22, 64 (1950).
 Ma 50a Macklin, Lidofsky, and Wu, Phys. Rev. 78, 318(A) (1950).
 Ma 52 Mandeville, Swann, Chatterjee, and Van Patter, Phys. Rev. 85, 193 (1952).
 Ma 52a W. H. Martin and S. W. Breckon, Can. J. Phys. 30, 643 (1952).
 Ma 53 L. Marquez, Phys. Rev. 92, 1511 (1953).
 Ma 53a L. Marquez, Phys. Rev. 90, 330(L) (1953).
 Ma 54 Marty, Nataf, and Prentki, J. phys. radium 15, 134 (1954).
 Ma 54a T. Mayer-Kuckuk, Z. Naturforsch. 9a, 338 (1954).
 Ma 54b J. Mattauch and R. Bieri, Z. Naturforsch. 9, 303 (1954).
 Ma 54c Maeder, Müller, and Wintersteiger, Helv. Phys. Acta 27, 3 (1954).
 Ma 55 D. Maeder and P. Stähelin, Helv. Phys. Acta 28, 193 (1955).
 Ma 55a Mazari, Alba, and Serment, Phys. Rev. 100, 972(A) (1955).
 Ma 55b P. Macq, Bull. Acad. Roy. Méd. Belg. 41, 467 (1955).
 Ma 56 Marion, Brugger, and Chapman, Phys. Rev. 101, 247 (1956).
 Ma 56a Martin, Cork, and Burson, Phys. Rev. 102, 457 (1956).
 Ma 56b Marion, Slattery, and Chapman, Phys. Rev. 103, 676 (1956).
 Mc 35 E. McMillan and E. O. Lawrence, Phys. Rev. 47, 343 (1935).
 Mc 40 McCreary, Kuerti, and Van Voorhis, Phys. Rev. 57, 351(A) (1940).
 Mc 49 McElhinney, Hanson, Becker, Duffield, and Diven, Phys. Rev. 75, 542 (1949).
 Mc 54 G. W. McClure, Phys. Rev. 94, 1637 (1954).
 Mc 54a McPherson, Pederson, and Katz, Can. J. Phys. 32, 593 (1954).
 Mc 55 J. A. McCarthy, Phys. Rev. 97, 1234 (1955).
 Mc 56 McNair, Glover, and Wilson, Phil. Mag. 1, 199 (1956).
 Me 37 A. Meye, Z. Physik. 105, 232 (1937).
 Me 48 Metzger, Alder, and Huber, Helv. Phys. Acta 21, 278 (1948).
 Me 54 W. E. Meyerhof and G. Lindstrom, Phys. Rev. 93, 949 (1954).
 Me 56 Meadows, Diamond, and Sharp, Phys. Rev. 102, 190 (1956).
 Me 57 Merritt, Campion, and Hawkings, Can. J. Phys. 35, 16 (1957).
 Mi 50 Millar, Cameron, and Glicksmann, Can. J. Research 28A, 475 (1950).
 Mi 52 C. Mileikowsky and W. Whaling, Phys. Rev. 88, 1254 (1952).
 Mi 53 Middleton, El-Bedewi, and Tai, Proc. Phys. Soc. (London) A66, 95 (1953).
 Mi 54 J. A. Miskel and M. L. Perlman, Phys. Rev. 94, 1683 (1954).
 Mi 54a A. Michalowicz, J. phys. radium 15, 156 (1954).
 Mi 55 Milani, Cooper, and Harris, Phys. Rev. 99, 645(A) (1955), plus verbal report to Nuclear Data Group.
 Mi 56 A. B. Milojević, Bull. Inst. Nuclear Sci. Boris Kidrich 6, 21 (1956).
 Mo 49 K. H. Morganstern and K. P. W. Wolf, Phys. Rev. 76, 1261 (1949).
 Mo 50 H. T. Motz and R. F. Humphreys, Phys. Rev. 80, 595 (1950).
 Mo 51 Mooring, Koester, Goldberg, Saxon, and Kaufmann, Phys. Rev. 84, 703 (1951).
 Mo 51a P. Morrison, Phys. Rev. 82, 209 (1951).
 Mo 52 H. T. Motz and D. E. Alburger, Phys. Rev. 86, 165 (1952).
 Mo 52a H. T. Motz, Phys. Rev. 85, 501(L) (1952).
 Mo 54 S. A. Moszkowski and D. C. Peaslee, Phys. Rev. 93, 455 (1954).
 Mo 54a A. Moljk and S. C. Curran, Phys. Rev. 96, 395 (1954).
 Mo 55 H. Morinaga, Phys. Rev. 97, 444 (1955).
 Mo 55a H. Morinaga, Phys. Rev. 97, 1185(L) (1955).
 Mo 55b I. L. Morgan, Phys. Rev. 99, 621(A) (1955).
 Mo 55c H. Morinaga, Phys. Rev. 100, 431(L) (1955).
 Mo 56 H. Morinaga and E. Bleuler, Bull. Am. Phys. Soc. Ser. II, 1, 30 (1956) plus verbal report to Nuclear Data Group.
 Mo 56a H. T. Motz, Phys. Rev. 104, 1353 (1956).
 Mo 56b H. Morinaga, Phys. Rev. 103, 504(L) (1956).
 Mo 56c I. L. Morgan, Phys. Rev. 103, 1031 (1956) plus verbal report to Nuclear Data Group.
 Mo 56d H. Morinaga and E. Bleuler, Phys. Rev. 103, 1423 (1956).
 Mu 56 Th. Muller, thesis, Strassbourg, Ann. Phys. (to be published).
 My 49 V. Myers and A. Wattenberg, Phys. Rev. 75, 992(L) (1949).
 Na 53 M. Nahmias and T. Yuasa, Compt. rend. 236, 2399 (1953).
 Na 53a J. Nagy, Acta Physica Acad. Sci. Hung. 3, 15 (1953).
 Na 54 R. Nathans and J. Halpern, Phys. Rev. 93, 437 (1954).
 Na 54a M. E. Nahmias, J. phys. radium 15, 568 (1954).
 Na 55 R. Nathans and P. F. Yergin, Phys. Rev. 98, 1296 (1955).

- Na 56 M. E. Nahmias and T. Yuasa, *J. phys. radium* **17**, 373(L) (1956).
- Na 56a M. E. Nahmias and T. Yuasa, *J. phys. radium* **17**, 536 (1956).
- Na 57 Nakada, Anderson, Gardner, and Wong, *Bull. Am. Phys. Soc. Ser. II*, **2**, 32 (1957).
- Ne 54 J. O. Newton, *Phys. Rev.* **96**, 241(L) (1954).
- Ne 56 Nemilov, Zherebtsova, and Funstein, *Physica* **22**, 1155(Å) (1956).
- Ne 57 J. O. Newton (private communication).
- Ni 50 A. O. Nier, *Phys. Rev.* **77**, 789 (1950).
- Ni 54 R. T. Nichols and E. N. Jensen, *Phys. Rev.* **94**, 369 (1954).
- Ni 55 R. T. Nichols and E. N. Jensen, *Phys. Rev.* **100**, 1407 (1955).
- Ny 55 K. Nybø and T. Grøtdal, *Nature* **175**, 130(L) (1955).
- Og 54 R. A. Ogg Jr. and J. D. Ray, *J. Chem. Phys.* **22**, 147 (1954).
- Ol 54 J. L. Olsen and G. D. O'Kelley, *Phys. Rev.* **93**, 1125(L) (1954).
- Ol 55 J. W. Olness and H. W. Lewis, *Phys. Rev.* **99**, 654(A) (1955).
- Ol 56 Olness, Haeberli, and Lewis, *Bull. Am. Phys. Soc. Ser. II*, **1**, 212 (1956) plus verbal report to Nuclear Data Group.
- Ov 49 Overstreet, Jacobson, and Stout, *Phys. Rev.* **75**, 231 (1949).
- Ov 56 O. E. Overseth, *Bull. Am. Phys. Soc. Ser. II*, **1**, 281 (1956).
- Pa 52 Parkinson, Beach, and King, *Phys. Rev.* **87**, 387(L) (1952).
- Pa 52a M. Paganelli and G. Quarenì, *Phys. Rev.* **86**, 423(L) (1952).
- Pa 54 Paul, Gove, Bartholomew, and Litherland, *Phys. Rev.* **749**(A) (1954).
- Pa 55 M. V. Pasechnik, International Conference Geneva Report 8/P/714 (1955).
- Pa 55a Paul, Gove, Litherland, and Bartholomew, *Phys. Rev.* **1339** (1955).
- Pa 55b Patterson, Newson, and Merzbacher, *Phys. Rev.* **99**, 1625(A) (1955).
- Pa 55c Paris, Buechner, and Endt, *Phys. Rev.* **100**, 1317 (1955).
- Pa 56 Paul, Bartholomew, Gove, and Litherland, *Bull. Am. Phys. Soc. Ser. II*, **1**, 39 (1956).
- Pa 56a S. P. Pandya, *Phys. Rev.* **103**, 956 (1956).
- Pa 57 Paris, van der Leun, and Endt, *Bull. Am. Phys. Soc. Ser. II*, **2**, 179 (1957), and unpublished work.
- Pa 57a S. P. Pandya and J. B. French, *Bull. Am. Phys. Soc. Ser. II*, **2**, 27 (1957).
- Pe 48 R. A. Peck, *Phys. Rev.* **73**, 947 (1948).
- Pe 49 R. A. Peck, *Phys. Rev.* **76**, 1279 (1949).
- Pe 50 Peterson, Barschall, and Bockelman, *Phys. Rev.* **79**, 593 (1950).
- Pe 53 D. C. Peaslee, *Nuovo cimento* **10**, 1349(L) (1953).
- Pe 56 Penning, Maltrud, Hopkins, and Schmidt, *Phys. Rev.* **104**, 740 (1956).
- Pe 57 J. R. Penning and F. H. Schmidt, *Phys. Rev.* **105**, 647 (1957).
- Pi 55 Pieper, Stanford, and Von Herrmann, *Phys. Rev.* **98**, 1185(A) (1955).
- Pl 40 Plain, Herb, Hudson, and Warren, *Phys. Rev.* **57**, 187 (1940).
- Pl 55 H. S. Plendl and F. E. Steigert, *Phys. Rev.* **98**, 1538(A) (1955) plus verbal report to Nuclear Data Group.
- Po 40 E. Pollard and W. W. Watson, *Phys. Rev.* **58**, 12 (1940).
- Po 49 Pollard, Sailor, and Wylie, *Phys. Rev.* **75**, 725 (1949).
- Po 49a Pontecorvo, Kirkwood, and Hanna, *Phys. Rev.* **75**, 982(L) (1949).
- Po 51 H. Pomerance, *Phys. Rev.* **83**, 641 (1951).
- Po 52 H. Pomerance, *Phys. Rev.* **88**, 412 (1952).
- Po 54 D. Popović, *Nuovo cimento* **12**, 143(L) (1954).
- Po 56 Pohm, Waddell, and Jensen, *Phys. Rev.* **101**, 1315 (1956).
- Pr 56 Prosser, Baumann, Brice, Read, and Krone, *Phys. Rev.* **104**, 369 (1956).
- Qu 56 A. R. Quinton and W. T. Doyle, *Phys. Rev.* **101**, 669 (1956).
- Qu 56a Quisenberry, Scolman, and Nier, *Phys. Rev.* **102**, 1071 (1956).
- Ra 53 N. F. Ramsey, *Nuclear Moments* (John Wiley and Sons, Inc., New York, 1953).
- Ra 55 Rayburn, Lafferty, and Hahn, *Phys. Rev.* **98**, 701 (1955).
- Ra 55a Ramanna, Veeraraghavan, and Iyengar, *Nuovo cimento* **1**, 623 (1955).
- Ra 56 B. J. Raz and J. B. French, *Bull. Am. Phys. Soc. Ser. II*, **1**, 223 (1956).
- Ra 56a B. J. Raz, *Bull. Am. Phys. Soc. Ser. II*, **1**, 336 (1956).
- Re 52 Reiley, Allen, Arthur, Bender, Ely, and Hausman, *Phys. Rev.* **86**, 857 (1952).
- Re 52a C. Reuterswärd, *Arkiv Fysik* **4**, 203 (1952).
- Re 53 Reardon, Krone, and Stump, *Phys. Rev.* **91**, 334 (1953).
- Re 54 A. L. Recksieler and B. Hamermesh, *Phys. Rev.* **96**, 109 (1954).
- Re 55 G. A. Renard, *J. phys. radium* **16**, 575 (1955).
- Re 56 J. B. Reynolds and K. G. Standing, *Phys. Rev.* **101**, 158 (1956).
- Re 56a C. Reuterswärd, *Arkiv Fysik* **11**, 1 (1956).
- Re 56b W. G. Read and R. W. Krone, *Phys. Rev.* **104**, 1018 (1956).
- Ri 48 H. T. Richards and R. V. Smith, *Phys. Rev.* **74**, 1870(L) (1948).
- Ri 50 Richards, Smith, and Browne, *Phys. Rev.* **80**, 524 (1950).
- Ri 55 L. S. Ring, *Phys. Rev.* **99**, 137 (1955).
- Ro 55 Roderick, Lönsjö, and Meyerhof, *Phys. Rev.* **97**, 97 (1955).
- Ro 55a Rothman, Hans, and Mandeville, *Phys. Rev.* **100**, 83 (1955).
- Ru 51 L. Ruby and J. R. Richardson, *Phys. Rev.* **83**, 698 (1951).
- Ru 52 Rudstam, Stevenson, and Folger, *Phys. Rev.* **87**, 358 (1952).
- Ru 52a Russel, Taylor, and Cooper, *Phys. Rev.* **86**, 653(A) (1952).
- Ru 53 J. G. Rutherglen and R. D. Smith, *Proc. Phys. Soc. (London)* **A66**, 800 (1953).
- Ru 54 Rutherglen, Grant, Flack, and Deuchars, *Proc. Phys. Soc. (London)* **A67**, 101 (1954).
- Ru 54a Russell, Taylor, and Cooper, *Phys. Rev.* **95**, 99 (1954).
- Ru 55 Rubin, Ajzenberg, and Reynolds, *Phys. Rev.* **98**, 1185(A) (1955).
- Ru 55a Russek, *Phys. Rev.* **99**, 834 (1955).
- Ru 55b R. A. Rubenstein and J. N. Snyder, *Phys. Rev.* **99**, 189 (1955).
- Ru 56 Rubin, Ajzenberg-Selove, and Mark, *Phys. Rev.* **104**, 727 (1956).
- Sa 49 V. L. Sailor, *Phys. Rev.* **75**, 1836 (1949).
- Sa 50 V. L. Sailor, *Phys. Rev.* **77**, 794 (1950).
- Sa 50a G. A. Sawyer and M. L. Wiedenbeck, *Phys. Rev.* **79**, 490 (1950).
- Sa 56 B. Saraf, *Phys. Rev.* **102**, 466 (1956).
- Sa 56a J. Sawicki, *Physica* **22**, 1180(A) (1956).
- Sc 48 Schelberg, Sampson, and Mitchell, *Rev. Sci. Instr.* **19**, 458 (1948).
- Sc 50 Schelberg, Sampson, and Cochran, *Phys. Rev.* **80**, 574 (1950).
- Sc 52 G. E. Schrank and J. R. Richardson, *Phys. Rev.* **86**, 248(L) (1952).
- Sc 52a Schoenfeld, Duborg, Preston, and Goodman, *Phys. Rev.* **85**, 873 (1952).
- Sc 54 G. Scharff-Goldhaber and M. McKeown, *Phys. Rev.* **95**, 613(A) (1954).
- Sc 54a C. Schwartz and A. De-Shalit, *Phys. Rev.* **94**, 1257 (1954).
- Sc 54b Schneider, Martin, Sempert, and Sutter, *Helv. Phys. Acta* **27**, 172(A) (1954).
- Sc 54c C. Schwartz, *Phys. Rev.* **94**, 95 (1954).
- Sc 54d Scherrer, Allison, and Faust, *Phys. Rev.* **96**, 386 (1954).
- Sc 55 J. P. Schiffer, *Phys. Rev.* **97**, 428 (1954).
- Sc 55a C. Schuhl and R. Basile, *Compt. rend.* **240**, 2512 (1955).
- Sc 56 Schwarzschild, Rustad, and Wu, *Phys. Rev.* **103**, 1796 (1956).
- Sc 56a M. J. Scott and R. E. Segel, *Phys. Rev.* **102**, 1557 (1956).
- Sc 56b Schwartz, Corbett, and Watson, *Phys. Rev.* **101**, 1370 (1956).

- Sc 56c Schiffer, Gossett, Phillips, and Young, Phys. Rev. **103**, 134 (1956).
 Se 49 Seidlitz, Bleuler, and Tendam, Phys. Rev. **76**, 861(L) (1949).
 Se 53 J. Seed, Phil. Mag. **44**, 921(L) (1953).
 Se 54 R. Sehr, Z. Physik **137**, 523 (1954).
 Se 55 Seiler, Cooper, and Harris, Phys. Rev. **99**, 340(A) (1955).
 Se 56 W. Selove, Phys. Rev. **101**, 231 (1956).
 Se 56a J. C. Severiens and S. S. Hanna, Phys. Rev. **104**, 1612 (1956).
 Sh 49 F. B. Shull and E. Feenberg, Phys. Rev. **75**, 1768(L) (1949).
 Sh 51 Shoemaker, Faulkner, Bouricius, Kaufmann, and Mooring, Phys. Rev. **83**, 1011 (1951).
 Sh 51a Sher, Halpern, and Mann, Phys. Rev. **84**, 387 (1951).
 Sh 51b R. K. Sheline, Phys. Rev. **82**, 954 (1951).
 Sh 51c Sheline, Holtzman, and Fan, Phys. Rev. **83**, 919 (1951).
 Sh 54 P. Shapiro, Phys. Rev. **93**, 290 (1954).
 Sh 54a H. A. Shillibeer and R. D. Russel, Can. J. Phys. **32**, 681 (1954).
 Sh 54b R. Sherr and R. H. Miller, Phys. Rev. **93**, 1076 (1954).
 Sh 54c Sherr, Li, and Christy, Phys. Rev. **96**, 1258 (1954).
 Sh 54d Sheline, Johnson, Bell, Davis, and McGowan, Phys. Rev. **94**, 1642 (1954).
 Sh 56 Shaw, Conzett, Slobodian, and Summers-Gill, Bull. Am. Phys. Soc. Ser. II, **1**, 253 (1956).
 Sh 56a R. K. Sheline, Nuclear Physics **2**, 382 (1956).
 Sh 57 H. A. Shillibeer, Geochim. Cosmochim. Acta (to be published).
 Si 46 K. Siegbahn, Phys. Rev. **70**, 127 (1946).
 Si 47 K. Siegbahn, Arkiv Mat. Astron. Fysik **34B**, No. 4 (1947).
 Si 47a K. Siegbahn and A. Johansson, Arkiv. Mat. Astron. Fysik **34A**, No. 10 (1947).
 Si 54 Simanton, Rightmire, Long, and Kohman, Phys. Rev. **96**, 1711(L) (1954).
 Si 56 R. M. Sinclair, Westinghouse Research Report 60-94511-6-R 12 (1956).
 Sm 42 G. P. Smith, Phys. Rev. **61**, 578 (1942).
 Sm 51 R. D. Smith and R. A. Anderson, Nature **168**, 429(L) (1951).
 Sm 54 Smith, Cooper, and Harris, Phys. Rev. **94**, 749(A) (1954) plus verbal report to Nuclear Data Group.
 Sm 56 R. V. Smith, Bull. Am. Phys. Soc. Ser. II, **1**, 175 (1956).
 Sm 57 R. T. Smith and D. Breitenbecher, Bull. Am. Phys. Soc. Ser. II, **2**, 59 (1957).
 Sn 55 A. H. Snell and F. Pleasonton, Phys. Rev. **100**, 1396 (1955).
 Sp 52 A. Sperduto and W. W. Buechner, Phys. Rev. **88**, 574 (1952).
 Sp 55 A. Sperduto and W. W. Buechner, Phys. Rev. **100**, 961(A) (1955).
 Sp 55a B. M. Spicer, Phys. Rev. **100**, 791 (1955).
 Sp 55b A. Sperduto and W. W. Buechner, M.I.T., Laboratory for Nuclear Science Progress Report, Nov. 30 (1955).
 St 50 R. M. Steffen, Phys. Rev. **80**, 115(L) (1950).
 St 51 Strait, Van Patter, Buechner, and Sperduto, Phys. Rev. **81**, 747 (1951).
 St 51a D. T. Stevenson and M. Deutsch, Phys. Rev. **83**, 1202 (1951).
 St 51b D. T. Stevenson and M. Deutsch, Phys. Rev. **84**, 1071(L) (1951).
 St 52 H. F. Stoddard and H. E. Gove, Phys. Rev. **87**, 262 (1952).
 St 52a P. H. Stelson and W. M. Preston, Phys. Rev. **86**, 807 (1952).
 St 53 P. Stähelin and P. Preiswerk, Nuovo cimento **10**, 1219 (1953).
 St 53a P. Stähelin, Phys. Rev. **92**, 1076(L) (1953).
 St 53b P. Stähelin, Helv. Phys. Acta **26**, 691 (1953).
 St 54 P. H. Stelson and W. M. Preston, Phys. Rev. **95**, 974 (1954).
 St 54a P. H. Stelson, Phys. Rev. **96**, 1584 (1954).
 St 56 T. Stribel, Z. Naturforsch. **11a**, 166(L) (1956).
 St 56a T. Stribel, Z. Naturforsch. **11a**, 254(L) (1956).
 St 56b G. S. Stanford and G. F. Pieper, Phys. Rev. **103**, 637 (1956).
 Su 53 Summers-Gill, Haslam, and Katz, Can. J. Phys. **31**, 70 (1953).
 Su 55 A. D. Suttle Jr. and W. F. Libby, Anal. Chem. **27**, 921 (1955).
 Sw 52 C. P. Swann and C. E. Mandeville, Phys. Rev. **87**, 215(A) (1952).
 Sw 56 C. P. Swann and W. C. Porter, Bull. Am. Phys. Soc. Ser. II, **1**, 29 (1956).
 Ta 46 R. Tangen, Det Kgl. Norske Videnskabers Selskabs Skrifter (1946).
 Ta 53 Takemoto, Dazai, and Chiba, Phys. Rev. **91**, 1024(L) (1953).
 Ta 54 G. E. Tauber and T.-Y. Wu, Phys. Rev. **93**, 295 (1954).
 Ta 54a G. E. Tauber and T.-Y. Wu, Phys. Rev. **94**, 1307 (1954).
 Ta 54b Taylor, Russell, and Cooper, Phys. Rev. **93**, 1056 (1954).
 Ta 55 Taylor, Lönsjö, and Bonner, Phys. Rev. **100**, 174 (1955).
 Ta 56 Taylor, Marshak, and Newson, Bull. Am. Phys. Soc. Ser. II, **1**, 62 (1956) plus verbal report to Nuclear Data Group.
 Te 54 G. M. Temmer and N. P. Heydenburg, Phys. Rev. **96**, 426 (1954).
 Te 54a Teener, Seagondollar, and Krone, Phys. Rev. **93**, 1035 (1954).
 Te 56 G. M. Temmer and N. P. Heydenburg, Phys. Rev. **104**, 989 (1956).
 Th 54 L. C. Thompson, Phys. Rev. **96**, 369 (1954).
 Th 56 R. Thieberger and I. Talmi, Phys. Rev. **102**, 923(L) (1956).
 Ti 51 H. K. Ticho, Phys. Rev. **84**, 847(L) (1951).
 To 49 C. H. Townes and L. C. Aamodt, Phys. Rev. **76**, 691(L) (1949).
 To 52 Toops, Sampson, and Steigert, Phys. Rev. **85**, 280 (1952).
 To 53 B. J. Toppel and S. D. Bloom, Phys. Rev. **91**, 473(A) (1953).
 To 55 Toller, Patterson, and Newson, Phys. Rev. **99**, 620(A) (1955).
 To 55a Toller, Newson, and Merzbacher, Phys. Rev. **99**, 1625(A) (1955).
 To 55b F. M. Tomonovic and C. S. Cook, Phys. Rev. **100**, 1254(A) (1955).
 To 55c J. Tobailem, J. phys. radium **16**, 48 (1955).
 To 57 Towle, Berenbaum, and Matthews, Proc. Phys. Soc. London **A70**, 84 (1957).
 Tr 56 B. Trumpy and A. Graue, Physica **22**, 1155(A) (1956).
 Tu 51 J. F. Turner and P. E. Cavanagh, Phil. Mag. **42**, 636 (1951).
 Tu 53 O. H. Turner, Australian J. Phys. **6**, 380 (1953).
 Tu 54 A. Turkevich and A. Samuels, Phys. Rev. **94**, 364 (1954).
 Ty 54 H. Tyren and P.-A. Tove, Phys. Rev. **96**, 773 (1954).
 Va 52 D. M. Van Patter and W. W. Buechner, Phys. Rev. **87**, 51 (1952).
 Va 52a Van Patter, Sperduto, Endt, Buechner, and Enge, Phys. Rev. **85**, 142(L) (1952).
 Va 52b Van Patter, Endt, Sperduto, and Buechner, Phys. Rev. **86**, 502 (1952).
 Va 53 J. J. Van Loef (private communication).
 Va 56 Van Patter, Swann, Porter, and Mandeville, Phys. Rev. **103**, 656 (1956).
 Va 56a J. J. Van Loef and D. A. Lind, Phys. Rev. **101**, 103 (1956).
 Va 56b J. Varma, Proc. Phys. Soc. (London) **A69**, 641(L) (1956).
 Va 56c J. Varma and W. Jack, Physica **22**, 1139(A) (1956).
 Va 56d Van der Leun, Endt, Kluyver, and Vrenken, Physica **22**, 1223 (1956).
 Va 56e I. J. Van Heerden and D. J. Prowse, Phil. Mag. **1**, 967(L) (1956).
 Va 56f C. van der Leun and P. M. Endt, Physica **22**, 1234(L) (1956).
 Va 57 C. van der Leun and P. M. Endt (to be published).
 Va 57a Van Patter, Rothman, Porter, and Mandeville, Phys. Rev. **107**, 171 (1957).
 Va 57b R. Van Lieshout and R. W. Hayward (private communication).

- Va 57c Van Patter, Rothman, Porter, and Mandeville, Bull. Am. Phys. Soc. Ser. II, **2**, 60 (1957).
 Va 57d Van Patter, Porter, and Rothman, Phys. Rev. **106**, 1016 (1957).
 Ve 56 S. H. Vegors and P. Axel, Phys. Rev. **101**, 1067 (1956).
 Ve 56a S. H. Vegors and R. B. Duffield, Bull. Am. Phys. Soc. Ser. II, **1**, 206 (1956).
 Ve 57 Verbinski, Hurlimann, Stephens, and Winhold, Bull. Am. Phys. Soc. Ser. II, **2**, 68 (1957).
 Vo 56 P. Von Herrmann and G. F. Pieper, Bull. Am. Phys. Soc. Ser. II, **1**, 281 (1956).
 Vo 57 Vorona, Olness, Haeberli, and Lewis, Bull. Am. Phys. Soc. Ser. II, **2**, 34 (1957).
 Wa 37 H. Walke, Phys. Rev. **52**, 663(L) (1937).
 Wa 39 Y. Watase and J. Itoh, Proc. Phys.-Math. Soc. Japan **21**, 626 (1939).
 Wa 41 Y. Watase, Proc. Phys.-Math. Soc. Japan **23**, 618 (1941).
 Wa 50 Warshaw, Chen, and Appleton, Phys. Rev. **80**, 288(L) (1950).
 Wa 52 A. H. Wapstra, Phys. Rev. **86**, 561(L) (1952).
 Wa 53 A. H. Wapstra and A. L. Veenendaal, Phys. Rev. **91**, 426(L) (1953).
 Wa 53a A. H. Wapstra, Arkiv Fysik **6**, 263 (1953).
 Wa 54 N. S. Wall, Phys. Rev. **96**, 664 (1954).
 Wa 55 Way, King, McGinnis, and Van Lieshout, Nuclear Level Schemes ($A=40-A=92$), US-AEC Report TID-5300 (1955).
 Wa 55a A. H. Wapstra, Physica **21**, 367 (1955).
 Wa 55b A. H. Wapstra, Physica **21**, 385 (1955).
 Wa 55c G. J. Wasserburg and R. J. Hayden, Phys. Rev. **97**, 86 (1955).
 Wa 56 H. Wäffler and F. Heinrich, Physica **22**, 1146(A) (1956).
 Wa 56a H. J. Watters, Phys. Rev. **103**, 1763 (1956).
 We 51 Wentink, Koski, and Cohen, Phys. Rev. **81**, 948 (1951).
 We 52 T. Westermark, Phys. Rev. **88**, 573 (1952).
 We 54 P. Weinzierl, Z. Naturforsch. **9a**, 69 (1954).
 We 56 Wetherill, Wasserburg, Aldrich, Tilton, and Hayden, Phys. Rev. **103**, 987 (1956).
 We 56a J. B. Weddell, Phys. Rev. **104**, 1069 (1956).
 Wh 39 White, Delsasso, Fox, and Creutz, Phys. Rev. **56**, 512 (1939).
 Wh 41 White, Creutz, Delsasso, and Wilson, Phys. Rev. **59**, 63 (1941).
 Wh 53 R. L. White and C. H. Townes, Phys. Rev. **92**, 1256 (1953).
 Wi 41 C. M. Witcher, Phys. Rev. **60**, 32 (1941).
 Wi 51 D. H. Wilkinson and J. H. Carver, Phys. Rev. **83**, 466(L) (1951).
 Wi 52 Willard, Kington, and Bair, Phys. Rev. **86**, 259(L) (1952).
 Wi 54 Williams, McCall, and Gutowsky, Phys. Rev. **93**, 1428 (1954).
 Wi 55 R. M. Williamson and S. A. Cox, Phys. Rev. **99**, 644(A) (1955).
 Wi 55a A. Winther, J. phys. radium **16**, 562 (1955).
 Wi 56 Willard, Bair, Cohn, and Kington, Bull. Am. Phys. Soc. Ser. II, **1**, 264 (1956).
 Wi 56a D. H. Wilkinson, Phil. Mag. **1**, 1031 (1956).
 Wo 50 D. C. Worth, Phys. Rev. **78**, 378 (1950).
 Wo 54 C. Wong, Phys. Rev. **95**, 761 (1954).
 Wo 54a M. Wolfsberg, Phys. Rev. **96**, 1712(L) (1954).
 Wo 56 E. A. Wolf, Phil. Mag. **1**, 102(L) (1956).
 Wo 56a J. L. Wolfson, Can. J. Phys. **34**, 256 (1956).
 Wr 53 B. T. Wright, Phys. Rev. **90**, 159(L) (1953).
 Wu 49 Wu, Townes, and Feldman, Phys. Rev. **76**, 692(L) (1949).
 Wu 50 C. S. Wu, Revs. Modern Phys. **22**, 386 (1950).
 Ye 56 P. F. Yergin, Phys. Rev. **104**, 1340 (1956).
 Ze 52 Zeldes, Ketelle, Brosi, Fultz, and Hibbs, Phys. Rev. **86**, 811(L) (1952).
 Zu 50 A. Zucker and W. W. Watson, Phys. Rev. **80**, 966 (1950).
 Zw 54 P. F. Zweifel, Phys. Rev. **96**, 1572 (1954) plus Erratum in Phys. Rev. **98**, 1870 (1955).